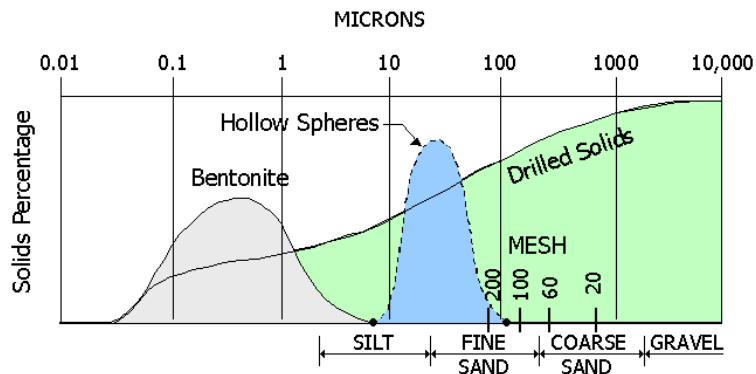


Development and Testing of Underbalanced Drilling Products

DOE Contract No. DE-AC21-94MC31197

Final Report

October 1995 – July 2001



Submitted to:

**U.S. DEPARTMENT OF ENERGY
National Energy Technology Laboratory
Attn: Roy Long
3610 Collins Ferry Road
Morgantown, West Virginia 26505**

By:

**William C. Maurer
William J. McDonald
Thomas E. Williams
John H. Cohen**

**MAURER TECHNOLOGY INC.
2916 West TC Jester
Houston, Texas 77018-7098
Tel: (713) 683-8227
Fax: (713) 683-6418**

TR01-16

July 2001

Disclaimer

This report was prepared as an account of work sponsored by an agency of the United States Government. Neither the United States Government nor any agency thereof, nor any of their employees, makes any warranty, express or implied, or assumes any legal liability or responsibility for the accuracy, completeness, or usefulness of any information, apparatus, product, or process disclosed, or represents that its use would not infringe privately owned rights. Reference herein to any specific commercial product, process, or service by trade name, trademark, manufacturer, or otherwise does not necessarily constitute or imply its endorsement, recommendation, or favoring by the United States Government or any agency thereof. The views and opinions of authors expressed herein do not necessarily state or reflect those of the United States Government or any agency thereof.

Table of Contents

DISCLAIMER	ii
ABSTRACT	xiv
EXECUTIVE SUMMARY	xvi
1. CONCLUSIONS	1-1
1.1 SIGNIFICANT FINDINGS	1-1
1.2 RECOMMENDATIONS	1-4
1.3 COMMERCIALIZATION POTENTIAL	1-4
1.3.1 Riserless Drilling	1-4
1.3.2 Underbalanced Drilling	1-4
1.3.3 FOAM Hydraulics Model	1-5
1.3.4 Formation Damage Reduction	1-5
2. INTRODUCTION	2-1
2.1 BACKGROUND	2-1
2.2 OBJECTIVES	2-6
2.3 TASK SUMMARY AND ACCOMPLISHMENTS	2-6
3. PHASE I WORK	3-1
3.1 FOAM HYDRAULICS MODEL	3-1
3.2 LIGHTWEIGHT SOLID ADDITIVE (LWSA) LABORATORY TESTING	3-1
3.3 LWSA YARD TESTS	3-1
3.4 MARKET SURVEY	3-3
3.5 PHASE I CONCLUSIONS	3-3
4. HGS CHARACTERISTICS	4-1
4.1 COMMERCIALLY AVAILABLE HOLLOW SPHERES	4-1
4.2 S38 HGS CHARACTERISTICS	4-1
4.3 S38 HGS SIZE DISTRIBUTION	4-2
4.4 EFFECT OF SPHERES ON FLUID DENSITY	4-2
4.5 SPHERE SLIP VELOCITY	4-4
4.6 HGS RECOVERY	4-4
4.7 HGS COLLAPSE PRESSURE	4-6
4.8 HGS COLLAPSE DEPTH.....	4-7
5. RHEOLOGY OF HGS FLUIDS	5-1
5.1 BASE FLUIDS TESTED	5-1
5.2 EFFECT OF HGS ON TEST FLUID DENSITY	5-2
5.3 TEST MATRIX AND PROCEDURES	5-2
5.4 NORMAL DRILLING FLUID RHEOLOGY	5-3
5.5 TEST DATA	5-3

Table of Contents (Cont'd.)

5.6	TEST RESULTS	5-8
5.6.1	PHPA Water-Base Drilling Fluid	5-8
5.6.2	Oil-Base Drilling Fluid	5-8
5.6.3	Synthetic Oil Drilling Fluid	5-8
5.6.4	3% KCl Drilling Fluid	5-8
5.6.5	Brine Fluids	5-8
5.7	CONCLUSIONS	5-9
6.	HGS BREAKAGE DURING DRILLING	6-1
6.1	TEST SETUP	6-1
6.2	TEST RESULTS	6-3
6.2.1	Effect of Nozzle Pressure	6-3
6.2.2	Effect of Standoff Distance	6-3
6.2.3	Safe Operating Range	6-3
6.3	CONCLUSIONS	6-5
7.	EFFECT OF HGS ON DRILLING RATE	7-1
7.1	LABORATORY TESTS	7-1
7.2	DIFFERENTIAL PRESSURE EFFECTS.....	7-1
7.3	BIT JET EFFECTS	7-4
7.4	PRESSURE GRADIENT EFFECTS	7-5
7.5	CONCLUSIONS	7-5
8.	EFFECT OF HGS ON FORMATION DAMAGE	8-1
8.1	FORMATION DAMAGE MECHANISMS	8-1
8.2	LABORATORY TEST PROCEDURE	8-3
8.3	LABORATORY TEST RESULTS	8-5
8.4	PHPA WATER-BASE DRILLING FLUID.....	8-5
8.5	OIL-BASE AND SYNTHETIC-OIL DRILLING FLUIDS	8-7
8.6	3% KCl DRILLING FLUID	8-9
8.7	ZnBr BRINE	8-11
8.8	HGS FOR REDUCING FORMATION DAMAGE DURING DRILLING.....	8-11
8.8.1	Review of Technology	8-12
8.8.2	Experimental Evaluation of Fluid Additives	8-13
8.9	CONCLUSIONS	8-15
9.	HGS DRILLING FLUID FIELD TESTS	9-1
9.1	MUD PIT	9-1
9.2	MUD MIXING	9-2
9.3	LIGHTWEIGHT MUD PROPERTIES	9-2
9.4	PDVSA-INTEVEP FIELD TESTS	9-3
9.5	RECYCLING HGS USING CENTRIFUGES	9-4
9.6	CONCLUSIONS	9-6

Table of Contents (Cont'd.)

10.	POTENTIAL USE OF HGS FOR DUAL-GRADIENT DRILLING	10-1
10.1	DUAL-GRADIENT DRILLING CONCEPT	10-1
10.1.1	Deep Water Drilling Problems	10-1
10.1.2	Dual-Gradient Drilling Concept	10-1
10.1.3	Seafloor Dual-Gradient Drilling Options	10-3
10.2	COMMERCIAL DUAL-GRADIENT DRILLING SYSTEMS	10-4
10.2.1	Baker/Transocean "DEEPMAN" Pump System	10-4
10.2.2	Conoco/Hydril "Mudlift" Pump System	10-6
10.2.3	Shell "SSPS" Pump System	10-8
10.2.4	Time and Cost Implementation	10-9
10.2.5	Dual-Gradient Cuttings Handling	10-9
10.2.6	Subsea Pump Project Participants	10-10
10.2.7	Subsea Pumping System Limitations	10-10
10.2.8	Subsea Pump Concerns	10-11
10.3	HOLLOW SPHERE DGD SYSTEM	10-11
10.3.1	Hollow Sphere DGD Concept	10-11
10.3.2	Sphere Requirements	10-13
10.3.3	Sphere Separation	10-13
10.3.4	Sphere Collapse Pressure	10-14
10.3.5	Hybrid Seafloor Pump/Sphere System	10-15
10.3.6	Removing Hollow Spheres from Mud	10-15
10.3.7	Large Diameter Hollow Sphere Development	10-16
10.3.8	Hollow Sphere System Applications	10-19
10.3.9	Drillstring Valve	10-20
10.3.10	Spreading Frac/Pore Pressure Curves Apart	10-20
10.3.11	Shallow Water Applications	10-20
10.3.12	Advantages of Hollow-Sphere DGD System	10-21
10.4	HOLLOW SPHERE DGD REQUIREMENTS	10-21
10.4.1	Hollow Sphere Techniques	10-21
10.4.2	Sphere Requirements (Seawater Transfer)	10-22
10.4.3	Sphere Requirements (Mud Transfer)	10-24
10.4.4	Sphere Slip Velocity	10-25
10.4.5	HGS Characteristics	10-26
10.4.6	Removing HGS from Mud	10-26
10.5	ALTERNATIVE SPHERE INJECTION SYSTEMS	10-27
10.5.1	Sphere Concentrations	10-27
10.5.2	Drillstring Sphere Injection System	10-27
10.5.3	Carrier Fluid Injection System	10-28
10.5.4	Seawater Sphere Injection System	10-29
10.5.5	Hybrid Sphere/Gas Lift Systems	10-30
10.6	SUB-SEAFLOOR SPHERE INJECTION	10-31
10.6.1	Curved-Gradient Drilling	10-31
10.6.2	Subsea Sphere Injection	10-32
10.7	EFFECT OF HOLLOW SPHERES ON MUD RHEOLOGY	10-33

Table of Contents (Cont'd.)

10.7.1	Effect of Sphere Size on Surface Area	10-33
10.7.2	Small-Diameter Hollow-Sphere Tests	10-34
10.7.3	Solid Sphere Tests	10-35
10.8	TEXAS A&M DGD STUDY	10-36
10.8.1	Hollow Sphere DGD Circulating Pressures	10-36
10.8.2	Mud Level Drop Due to U-Tubing	10-37
10.8.3	Pit Volume Gain Due to U-Tubing	10-38
10.9	SURFACE AREA OF SPHERES	10-38
10.9.1	Single Sphere	10-38
10.9.2	Multiple Spheres	10-38
10.10	BASE FLUID PROPERTIES	10-39
10.10.1	Base Drilling Fluids (Small Spheres)	10-39
10.10.2	Base Drilling Fluids (Small and Large Spheres)	10-40
10.11	CONCLUSIONS	10-40
11.	ENHANCED FOAM UNDERBALANCED DRILLING MODEL	11-1
11.1	PHASE II IMPROVEMENTS TO FOAM	11-1
11.2	IMPROVED FOAM RHEOLOGY MODEL	11-1
11.3	PRESSURE-MATCHING FEATURE	11-2
11.4	CASE STUDY	11-2
11.5	CONCLUSIONS	11-5
12.	OTHER POTENTIAL APPLICATIONS FOR HGS	12-1
12.1	FRACTURE FLUID ADDITIVE	12-1
12.2	LOW-COST EXTENDER FOR EXPENSIVE MUDS	12-1
12.3	WELLBORE STABILITY ENHANCER	12-2
12.4	ALTERNATIVE SPHERE MATERIALS	12-2
12.5	COMPLETION FLUIDS	12-2
12.6	CEMENTING ADDITIVE	12-2
12.7	CEMENT/CASING BOND IMPROVEMENT	12-3
13.	REFERENCES	13-1
APPENDIX A	— “Foam Computer Model Helps in Analysis of Underbalanced Drilling”	
APPENDIX B	— “Advanced Foam Computer Model Helps in the Design and Analysis of Underbalanced Drilling”	
APPENDIX C	— Scotchlite Product Data Sheet: Glass Bubbles, S Series	
APPENDIX D	— Final Report on Glass Spheres in Drilling Fluids	
APPENDIX E	— SPE 38637: “Field Application of Lightweight Hollow Glass Sphere	

Table of Contents (Cont'd.)

- APPENDIX F — SPE 62899: "Field Application of Glass Bubbles as a Density-Reducing Agent"
- APPENDIX G — "The Potential Use of Hollow Glass Spheres in Dual Density Drilling"
- APPENDIX H — "Impact of Hollow Glass Spheres on Wettability"

List of Figures

Figure i.	Projected Industry Use of Underbalanced Drilling	xvi
Figure ii.	FOAM "Tiled" Data Output Window.....	xvii
Figure iii.	Lightweight HGS Mud	xvii
Figure iv.	Hole Problems with Aerated Drilling Fluids	xviii
Figure v.	Dual-Gradient Drilling System	xix
Figure vi.	New Hollow-Sphere DGD System	xix
Figure vii.	Hollow Sphere Separation System	xx
Figure 1-1.	Differential Pressure and Drilling Rate	1-1
Figure 1-2.	Hollow Sphere Cleanup Mechanism	1-1
Figure 1-3.	Hollow-Sphere Dual Gradient Drilling System	1-2
Figure 1-4.	PV vs. % Sphere Concentration	1-2
Figure 1-5.	Oilfield Hydrocyclone	1-3
Figure 1-6.	FOAM Pressure-Matching Window	1-3
Figure 2-1.	Differential Pressure and Drilling Rate (Moffit, 1991)	2-2
Figure 2-2.	Hydrostatic Pressure (psi).....	2-2
Figure 2-3.	Fluid Density	2-2
Figure 2-4.	Flow Regime Types (Lorenz, 1980)	2-2
Figure 2-5.	Fluid Phase Continuity	2-5
Figure 2-6.	Foam Lifting Capacity (Beyer et al., 1972)	2-5
Figure 2-7.	Parasite Injection String	2-5
Figure 2-8.	Volume Requirement Chart (Poettman and Begman, 1955)	2-5
Figure 3-1.	FOAM Data Input Window	3-2
Figure 3-2.	FOAM Wellbore Pressure Profile	3-2
Figure 3-3.	Growth of Lightweight Fluid Use in the USA (Duda et al., 1996).....	3-2
Figure 4-1.	S38 Glass Bubble	4-3
Figure 4-2.	Solids in Unweighted Water-Base Drilling Mud (Burgoyne, et al., 1986).....	4-3
Figure 4-3.	Mud Density vs. Sphere Concentration	4-3
Figure 4-4.	Sphere Slip Velocity vs. Fluid Density	4-3
Figure 4-5.	Sphere Slip Velocity vs. Fluid Density	4-5
Figure 4-6.	Oil Field Hydrocyclone (Moore et al., 1974)	4-5
Figure 4-7.	S38 Hollow Sphere Collapse Depth	4-5
Figure 4-8.	S60 Hollow Sphere Collapse Depth	4-5
Figure 5-1.	Effect of HGS on Test Fluid Density	5-2
Figure 5-2.	Optimum Drilling Fluid PV and YP Ranges (Baroid, 1981).....	5-3
Figure 5-3.	Fluid viscosity vs. HGS Concentration	5-4
Figure 5-4.	Fluid Viscosity vs. Drill Solids Concentration	5-6

List of Figures (Cont'd.)

Figure 6-1.	HGS Breakage Test Flow Loop	6-2
Figure 6-2.	HGS Spheres Impacting Rock	6-2
Figure 6-3.	HGS Test Mud Tank	6-2
Figure 6-4.	Pressure Vessel with Stinger	6-2
Figure 6-5.	Mud Cooling Coils in Chilled Water.....	6-2
Figure 6-6.	HGS Mud Weight	6-2
Figure 6-7.	High Pressure Increases Sphere Breakage	6-4
Figure 6-8.	Sphere Breakage in Nozzle Pressure	6-4
Figure 6-9.	Sphere Breakage vs. Circulating Time	6-4
Figure 6-10.	Reduced Sphere Breakage with Increased Distance	6-4
Figure 6-11.	Sphere Breakage as a Function of Distance	6-4
Figure 6-12.	Safe Operating Zone	6-4
Figure 7-1.	DRC High Pressure Drilling Stand	7-2
Figure 7-2.	Simulated Bottom Hole Conditions	7-2
Figure 7-3.	DRC Drilling Test Data	7-2
Figure 7-4.	Drilling Rate vs. Differential Pressure (Murray & Cunningham, 1955)	7-3
Figure 7-5.	Chip Hold-Down Effects (Maurer, 1965).....	7-3
Figure 7-6.	Mud Density vs. Sphere Concentration	7-3
Figure 7-7.	Chip Hold-Down Pressure Gradients	7-3
Figure 8-1.	Formation Damage Mechanism	8-2
Figure 8-2.	Formation Pressure Gradient (Gray et al., 1980)	8-2
Figure 8-3.	Drilling Rate vs. Differential Pressure	8-2
Figure 8-4.	Water-Based Mud Particle Size (Bourgoyne et al., 1986)	8-2
Figure 8-5.	Hollow Sphere Filter Cake	8-2
Figure 8-6.	Hollow Sphere Cleanup	8-2
Figure 8-7.	Formation Damage Test Apparatus	8-3
Figure 8-8.	Formation Damage Test Cell	8-4
Figure 8-9.	Permeability Recovery with PHPA Water-Base Drilling Fluid	8-6
Figure 8-10.	Permeability Recovery with Oil-Based Drilling Fluid	8-8
Figure 8-11.	Permeability Recovery with Synthetic Oil Drilling Fluid	8-8
Figure 8-12.	Permeability Recovery with Potassium Chloride Brine	8-8
Figure 8-13.	Permeability Recovery with Zinc Bromide Brine	8-8
Figure 8-14.	Filter-Cake Thickness Contrasted with High Fluid-Loss Filter Cake	8-14
Figure 9-1.	Golden State Drilling Rig Mud System	9-1
Figure 9-2.	Theoretical and Measured Mud Weight (Well 1)	9-2

List of Figures (Cont'd.)

Figure 9-3.	Theoretical and Measured Mud Weight (Well 2)	9-3
Figure 9-4.	Baker Hughes Censor Solids-Sorting Centrifuge	9-5
Figure 9-5.	Three-Phase Centrifuge	9-6
Figure 10-1.	Dual Gradient Drilling System (Peterman, 1998)	10-1
Figure 10-2.	DGD Hydrostatic Gradients (Snyder, 1998)	10-1
Figure 10-3.	Casing Program for Conventional DGD (Snyder, 1998)	10-2
Figure 10-4.	Dual-Gradient Drilling Options	10-2
Figure 10-5.	DEEPIVISON System	10-5
Figure 10-6.	DEEPIVISON Subsea Centrifugal Pump	10-5
Figure 10-7.	DEEPIVISON Subsea Module	10-5
Figure 10-8.	Water Depth vs. Pump Units	10-5
Figure 10-9.	DEEPIVISON 4 $\frac{3}{4}$ n. Flow Stop Drillstring Valve	10-5
Figure 10-10.	Mudlift Pumping System	10-5
Figure 10-11.	MUDLIFT Subsea Pumps	10-7
Figure 10-12.	MUDLIFT Subfloor Module	10-7
Figure 10-13.	MUDLIFT Subsea Diverter	10-7
Figure 10-14.	MUDLIFT Drilling Valve	10-7
Figure 10-15.	MUDLIFT Time Schedule	10-7
Figure 10-16.	Shell SSPS System	10-7
Figure 10-17.	Shell SSPS General Configuration	10-8
Figure 10-18.	Shell SSPS Gumbo Slide & Mud/Gas Separation	10-8
Figure 10-19.	Maurer Hollow-Sphere, Dual-Gradient System	10-11
Figure 10-20.	Single Injection Point	10-12
Figure 10-21.	HGS Injection	10-12
Figure 10-22.	New Seafloor Equipment	10-12
Figure 10-23.	Photomicrograph of Glass Microspheres	10-12
Figure 10-24.	Sea Water Density Mud (50% Spheres)	10-13
Figure 10-25	Mud Density vs. Sphere Concentration	10-13
Figure 10-26.	Hollow Sphere Separation System	10-14
Figure 10-27.	Multiple Injection Points	10-14
Figure 10-28.	Combination Dual-Gradient System	10-14
Figure 10-29.	Sea Floor Pumping Power	10-14
Figure 10-30.	Oilfield Centrifuge Test	10-16
Figure 10-31.	Oilfield Hydroclone	10-16
Figure 10-32.	S38 Hollow Sphere Size	10-16

List of Figures (Cont'd)

Figure 10-33. Hollow Sphere Size	10-16
Figure 10-34. Sphere Collapse Pressure and Density	10-17
Figure 10-35. Photomicrograph of Hollow Spheres	10-17
Figure 10-36. Relative Particle Size (Microns)	10-18
Figure 10-37. Composite Hollow Spheres	10-18
Figure 10-38. Properties of Composite Spheres	10-18
Figure 10-39. Riser Buoyancy Modules	10-19
Figure 10-40. Buoyancy Manufacturing Facility	10-19
Figure 10-41. Dual-Gradient Mud Weights	10-19
Figure 10-42. Spreading Pore Pressure/Frac Curves Apart	10-19
Figure 10-43. Hollow Glass Spheres	10-22
Figure 10-44. Hollow Glass Sphere Injection Systems	10-23
Figure 10-45. Mixture Density vs. Sphere Volume	10-23
Figure 10-46. Sphere Concentration Required to Reduce Mud Weight to Seawater Density	10-23
Figure 10-47. Sphere Flow Rate Required to Produce Seawater Gradient (Seawater Transfer)	10-23
Figure 10-48. Mixture Density vs. Slurry Flow Rate (Mud Transfer; 8.34 ppg)	10-24
Figure 10-49. Mixture Density vs. Slurry Flow Rate (Mud Transfer; 10 ppg)	10-25
Figure 10-50. Mixture Density vs. Slurry Flow Rate (Mud Transfer, 14 ppg)	10-25
Figure 10-51. Sphere Slip Velocity vs. Fluid Density	10-25
Figure 10-52. Sphere Slip Velocity vs. Fluid Viscosity	10-25
Figure 10-53. Oilfield Hydroclone (Moore et al., 1974)	10-26
Figure 10-54. Hollow Sphere Size Distribution	10-27
Figure 10-55. Particle Sizes in Unweighted, Water-Based Mud (After Annis, 1974)	10-27
Figure 10-56. Drillstring Sphere Injection DGD System	10-28
Figure 10-57. Drillstring Sphere Separator	10-28
Figure 10-58. Carrier Fluid Dual-Gradient System	10-28
Figure 10-59. Carrier Fluid System Separator	10-28
Figure 10-60. Seawater Hollow Sphere Transfer System	10-30
Figure 10-61. Seafloor Screen Separation System	10-30
Figure 10-62. Seafloor Chamber Separation System	10-30
Figure 10-63. Conventional Deepwater Drilling	10-31
Figure 10-64. Dual-Gradient Deepwater Drilling	10-31
Figure 10-65. Curved-Gradient Deepwater Drilling	10-32

List of Figures (Cont'd)

Figure 10-66. Fluid Injection Techniques	10-32
Figure 10-67. Sub Seafloor Sphere Injection (4770 psi)	10-32
Figure 10-68. Sub Seafloor Sphere Injection (5410 psi)	10-32
Figure 10-69. Sub Seafloor Sphere Injection (5876 psi)	10-33
Figure 10-70. Effect of Sphere Concentration on Plastic Viscosity	10-34
Figure 10-71. Effect of Sphere Concentration on Yield Point	10-34
Figure 10-72. Effect of Sphere Size on Plastic Viscosity	10-35
Figure 10-73. Effect of Sphere Size on Yield Point	10-35
Figure 10-74. Circulating Pressure, 19.17 ppg and 10,000 ft of Water Depth	10-36
Figure 10-75. Pressure Loss and Plastic Viscosity in Riser	10-36
Figure 10-76. Drop in Mud Level vs. Time When Circulation Stops and Restarts	10-37
Figure 10-77. Fluid Level Drop vs. Time During Connections	10-37
Figure 10-78. Pit Gain and Loss During Connections	10-38
Figure 10-79. Reduction in Pressure at Mudline while Riser is Filling with HGS	10-38
Figure 11-1. FOAM 2 Factor Correlation HGS	11-3
Figure 11-2. Pressure-Matching Window	11-3
Figure 11-3. Matched Pressure Profile	11-3
Figure 11-4. FOAM 2 Predictions vs. Field Data	11-3

List of Tables

Table 2-1.	Advantages of Underbalanced Fluids	2-3
Table 2-2.	Disadvantages of Underbalanced Fluids	2-3
Table 2-3.	Russian Hollow Spheres	2-6
Table 4-1.	3M Scotchlite™ S Series Hollow Glass Spheres	4-1
Table 5-1.	Test Drilling Fluid Compositions	5-1
Table 5-2.	Effect of Hollow Spheres on Test Fluid Density (ppg)	5-2
Table 5-3.	Rheology Test Plan Matrix	5-2
Table 5-4.	Test Data Summary: PV, YP as a Function of HGS for 0% Drill Solids	5-5
Table 5-5.	Test Data Summary: PV, YP as a Function of HGS for 6% Drill Solids	5-5
Table 5-6.	Test Data Summary: PV, YP as a Function of Drill Solids for 0% HGS	5-7
Table 5-7.	Test Data Summary: PV, YP as a Function of Drill Solids for 36% HGS	5-7
Table 8-1.	Simulated Drilling Fluids Tested	8-4
Table 8-2.	Permeability Recovery with PHPA Fluid	8-6
Table 8-3.	Permeability Recovery with Oil and Synthetic Fluids	8-9
Table 8-4.	Permeability Recovery with KCl Fluid	8-10
Table 8-5.	Permeability Recovery with ZnBr ₂ Fluid	8-11
Table 10.1	Base Drilling Fluids (Small Spheres)	10-39
Table 10.2	Base Drilling Fluids (Small and Large Spheres)	10-40
Table 11-1.	Flow Properties for Foam (Okpobiri and Ikoku, 1986).....	11-1
Table 11-2.	Field Well Parameters	11-2

Abstract

Underbalanced drilling is experiencing growth at a rate that rivals that of horizontal drilling in the mid-1980s and coiled-tubing drilling in the 1990s. Problems remain, however, for applying underbalanced drilling in a wider range of geological settings and drilling environments. This report addresses developments under this DOE project to develop products aimed at overcoming these problems.

During Phase I of the DOE project, market analyses showed that up to 12,000 wells per year (i.e., 30% of all wells) will be drilled underbalanced in the U.S.A. within the next ten years.

A user-friendly foam fluid hydraulics model (FOAM) was developed for a PC Windows environment during Phase I. FOAM predicts circulating pressures and flow characteristics of foam fluids used in underbalanced drilling operations. FOAM is based on the best available mathematical models, and was validated through comparison to existing models, laboratory test data and field data. This model does not handle two-phase flow or air and mist drilling where the foam quality is above 0.97.

This FOAM model was greatly expanded during Phase II including adding an improved foam rheological model and a “matching” feature that allows the model to be field calibrated.

During Phase I, a lightweight drilling fluid was developed that uses hollow glass spheres (HGS) to reduce the density of the mud to less than that of water. HGS fluids have several advantages over aerated fluids, including they are incompressible, they reduce corrosion and vibration problems, they allow the use of mud-pulse MWD tools, and they eliminate high compressor and nitrogen costs.

Phase II tests showed that HGS significantly reduce formation damage with water-based drilling and completion fluids and thereby potentially can increase oil and gas production in wells drilled with water-based fluids.

Extensive rheological testing was conducted with HGS drilling and completion fluids during Phase II. These tests showed that the HGS fluids act similarly to conventional fluids and that they have potential application in many areas, including underbalanced drilling, completions, and riserless drilling.

Early field tests under this project are encouraging. These led to limited tests by industry (which are also described). Further field tests and cost analyses are needed to demonstrate the viability of HGS fluids in different applications. Once their effectiveness is demonstrated, they should find widespread application and should significantly reduce drilling costs and increase oil and gas production rates.

A number of important oilfield applications for HGS outside of Underbalanced Drilling were identified. One of these – Dual Gradient Drilling (DGD) for deepwater exploration and development – is very promising. Investigative work on DGD under the project is reported, along with definition of a large joint-industry project resulting from the work.

Other innovative products/applications are highlighted in the report including the use of HGS as a cement additive.

Executive Summary

INTRODUCTION

Interest in underbalanced drilling is growing worldwide at a rate not seen for a new drilling technology since the introduction of horizontal drilling in the mid-1980s and coiled-tubing drilling in the 1990s. Increasing drilling rates and reducing formation damage have been the driving forces behind the recent resurgence in underbalanced drilling. Underbalanced drilling has proven very beneficial in areas of the U.S.A. such as the Austin Chalk trend in Texas and Louisiana.

Underbalanced drilling is expected to increase significantly in the future. A DOE study showed that by the year 2005, nearly 12,000 wells will be drilled underbalanced annually in the U.S.A. (**Figure i**).

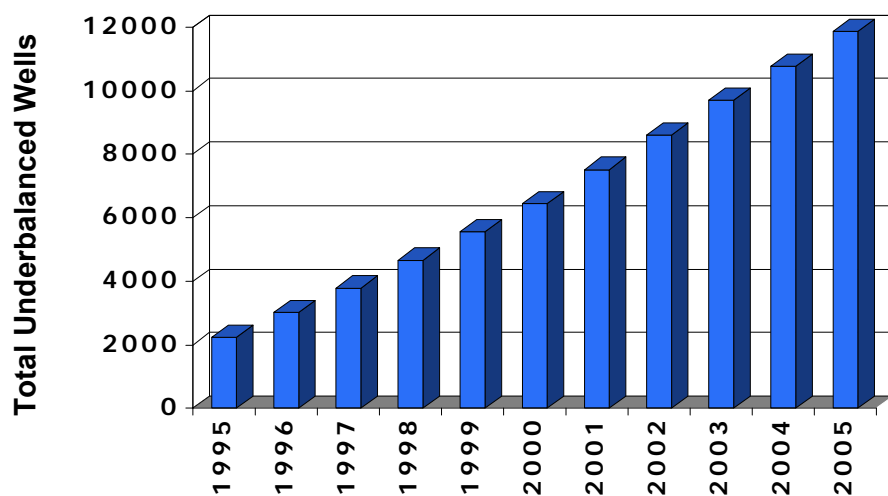


Figure i. Projected Industry Use of Underbalanced Drilling
(Duda et al., 1996)

FOAM COMPUTER MODEL

During Phase I, a user-friendly PC foam-drilling hydraulics model, FOAM, was developed that accurately predicts pressure drops, cuttings lifting velocities, foam quality, and other foam drilling variables. This model was upgraded and expanded during Phase II.

This hydraulics model runs in a Windows environment and is user-friendly and accurate. Any of three rheology models can be selected, and the model can handle any combination of gases and liquids injected while drilling. Output is generated in tabular as well as graphical form. **Figure ii** shows an example “tiled” output screen from the program.

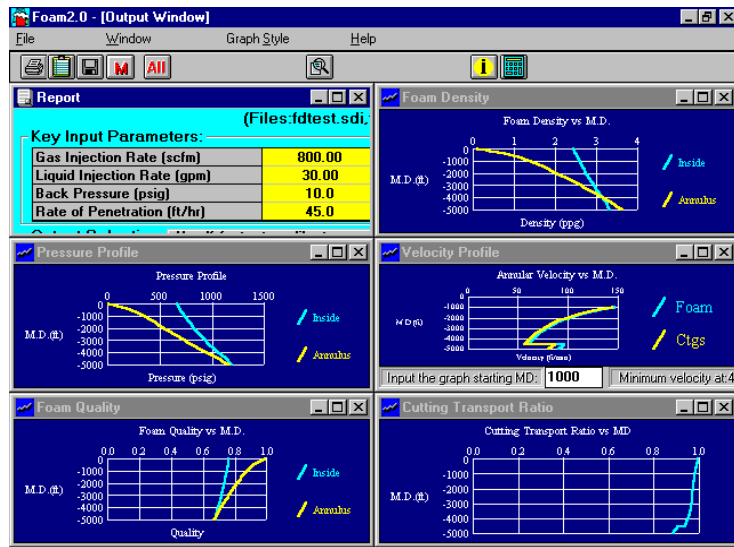


Figure ii. FOAM “Tiled” Data Output Window

Output from the FOAM model was validated by comparing it to other models, existing laboratory data, and actual field measurements. During Phase II, this model was upgraded and expanded to include an improved rheological model and a field calibration feature that allows the user to match calculated and measured standpipe pressures. These enhancements should expand use of this foam model.

LIGHTWEIGHT SOLID ADDITIVES

During Phase I, tests were conducted with a new lightweight mud that uses hollow glass spheres (HGS) to reduce the density of mud. Extensive Phase II laboratory and field tests demonstrated the high potential for HGS drilling and completion fluids.

HGS have been added in volume concentrations up to 50% to reduce the density of drilling and completion fluids. For example, adding 50% HGS to an 8.5-ppg mud, reduces its density to 5.84 ppg (**Figure iii**) without the addition of air.

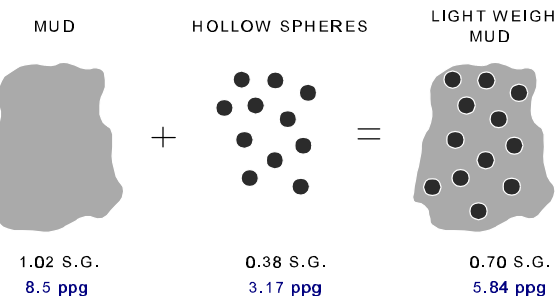


Figure iii. Lightweight HGS Mud

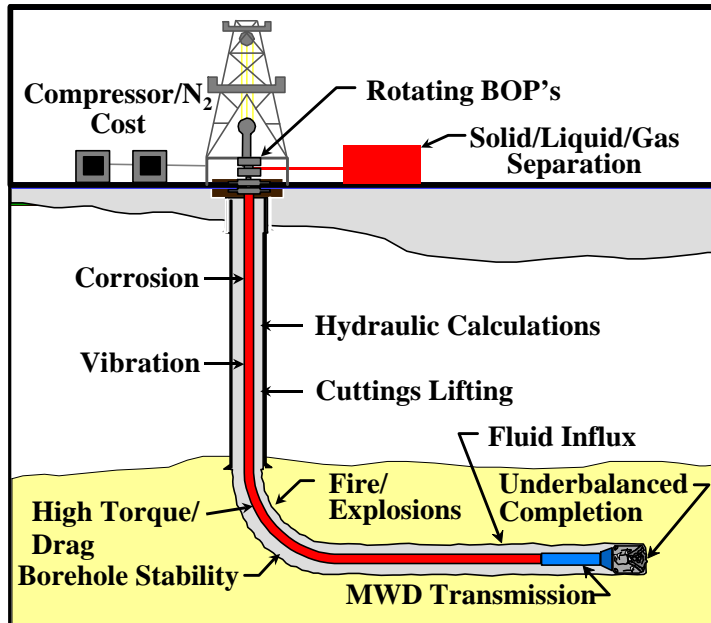


Figure iv. Hole Problems with Aerated Drilling Fluids

Figure iv shows some aerated drilling problems that are eliminated by HGS since they are chemically inert and incompressible.

Extensive laboratory tests on HGS fluids during Phase II showed the following:

1. The rheology of HGS fluids is similar to these of conventional drilling fluids.
2. HGS significantly reduce formation damage with water-base drilling fluids.
3. Breakage of HGS upon impact with the rock is not a major problem.
4. HGS have potential for eliminating seafloor pumps with riserless drilling systems.
5. HGS drilling fluids performed well in Mobil field tests in Kern County, CA.
6. HGS have potential for significantly increasing drilling rates.

The Phase II project was very successful and should lead to expanded use of the FOAM hydraulics model and HGS drilling and completion fluids in the future.

DUAL-GRADIENT DRILLING

When drilling oil and gas offshore wells in deep water, up to eight casing strings are often required due to the effect of the water pressure on the seafloor. This results in very expensive wells and long drilling times.

To reduce this problem, three industry groups are developing “dual gradient drilling” (DGD) systems that utilize seafloor pumps to reduce the fluid pressure in the wellbore annulus at the seafloor to that of seawater (**Figure v**). This DGD system can reduce the number of casing strings by 50% (e.g., from 8 to 4 casing strings) and save \$5 to \$15 million per well.

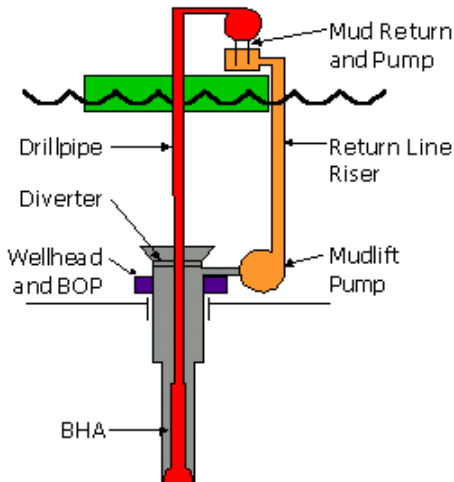


Figure v. Dual-Gradient Drilling System

Major problems with seafloor pumps include 1) they cost \$40 to \$50 million, 2) they require very large offshore rigs costing \$150,000 to \$300,000 per day, and 3) if the pumps fail, the drillstring riser must be pulled, which takes 6 to 8 days and costs \$1 to \$2 million.

During this DOE project, a new DGD concept was developed that utilizes HGS pumped to the seafloor to reduce the density of the mud in the wellbore annulus to that of seawater, thus eliminating the need for seafloor pumps (**Figure vi**).

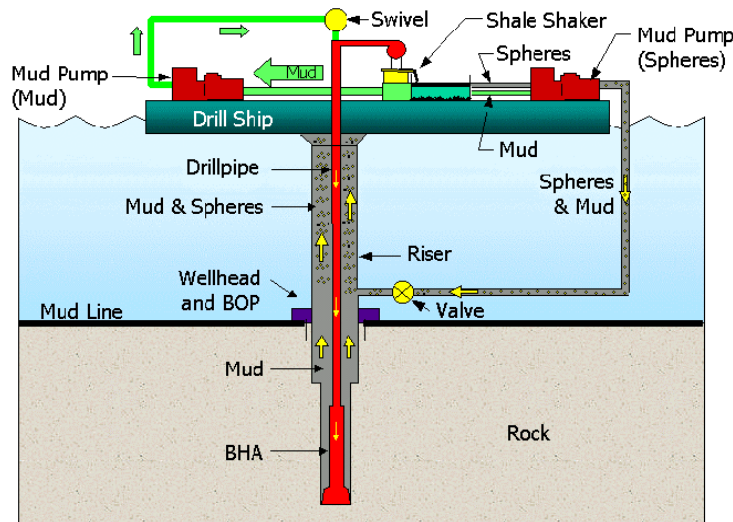


Figure vi. New Hollow-Sphere DGD System

When drilling mud containing hollow spheres is circulated back up to the drillship, the spheres are removed from the mud using shale shakers (100 mesh screens) and gravity separation since the hollow spheres will float on seawater while the heavier rock cuttings generated by the drill bit will sink (**Figure vii**).

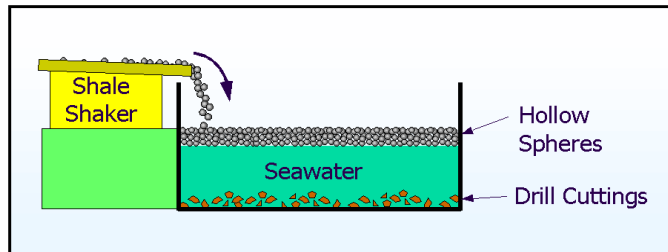


Figure vii. Hollow Sphere Separation System

This new technique will 1) reduce the cost of DGD systems from \$50 million to \$10 million, 2) significantly reduce the size and cost of drillships required, and 3) eliminate expensive delays due to seafloor pump failures.

This new technique has received widespread interest from industry and a \$1 to \$2 million joint-industry project (JIP) is now being formed by Maurer Technology to evaluate the feasibility of this system. Once feasibility is demonstrated, this system will be developed and commercialized. This DGD system has the potential to significantly reduce deep drilling costs and to make currently marginal deep water oil and gas fields economical.

1. Conclusions

1.1 SIGNIFICANT FINDINGS

Following is a list of the most significant findings resulting from the Phase II study:

1. Hollow glass spheres (HGS) can significantly increase drilling rates by reducing bottom-hole fluid pressures (**Figure 1-1**).

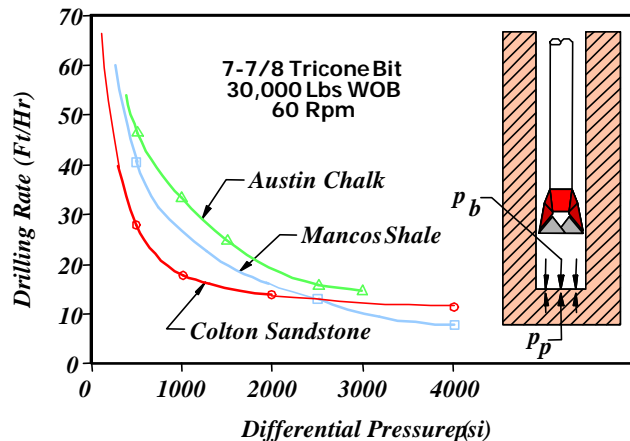


Figure 1-1. Differential Pressure and Drilling Rate

2. HGS significantly reduce formation damage with water-based drilling and completion fluids (**Figure 1-2**). In one test, a PHPA water-base mud produced 46% permeability damage without HGS, compared to no damage with 16% HGS.

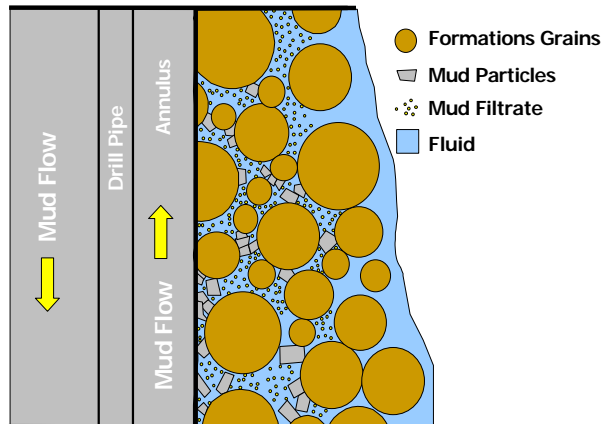


Figure 1-2. Hollow Sphere Cleanup Mechanism

3. HGS have potential application for riserless drilling since they can significantly reduce compressor and nitrogen costs, and they eliminate the need for seafloor pumps (**Figure 1-3**).

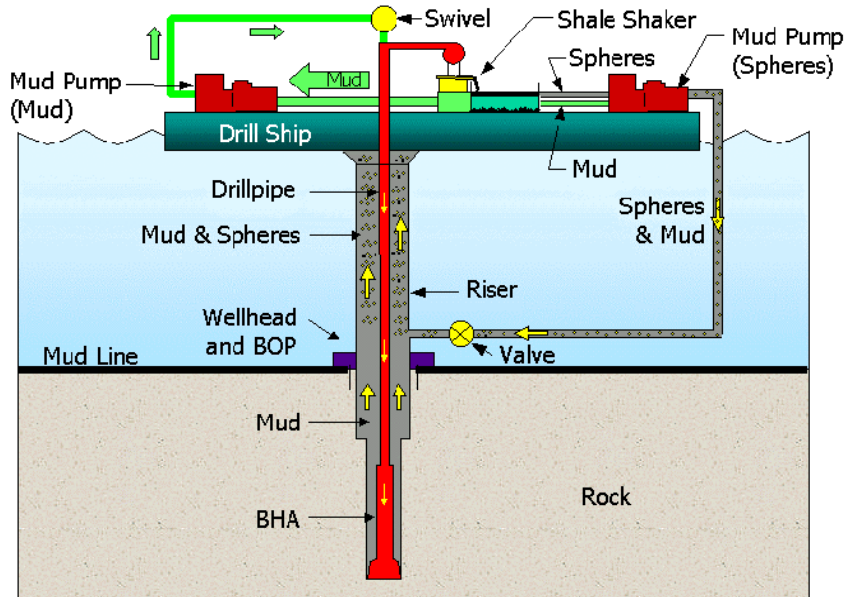


Figure 1-3. Hollow-Sphere Dual-Gradient Drilling System

4. The rheology of HGS fluids is similar to conventional drilling fluids, making them easy to run in the field (**Figure 1-4**).

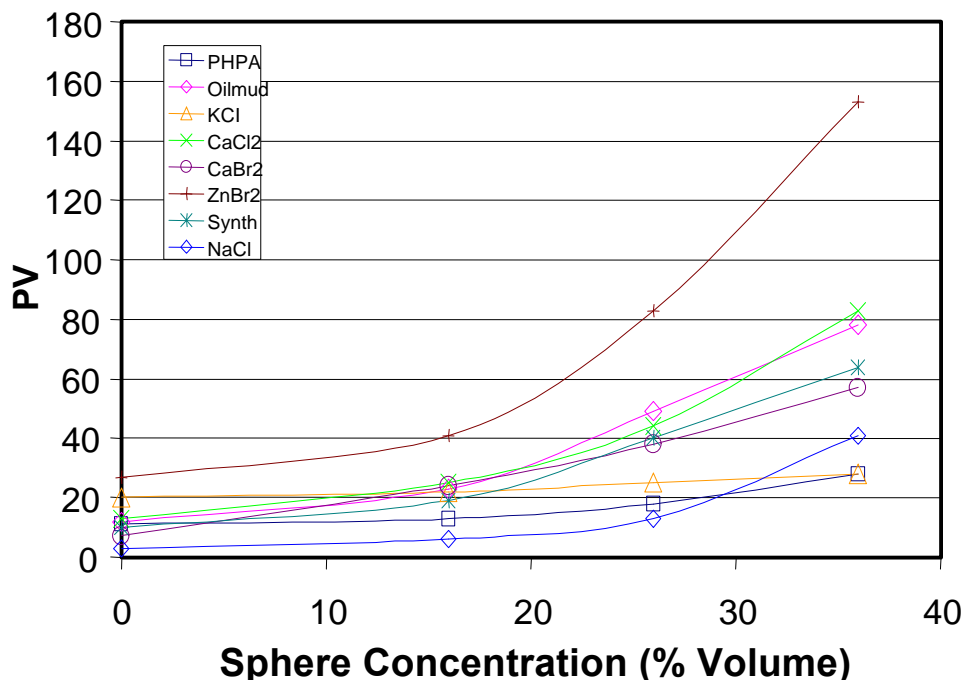


Figure 1-4. PV vs. % Sphere Concentration

5. HGS can be recovered after a well is drilled using conventional oil-field solids control equipment (**Figure 1-5**).

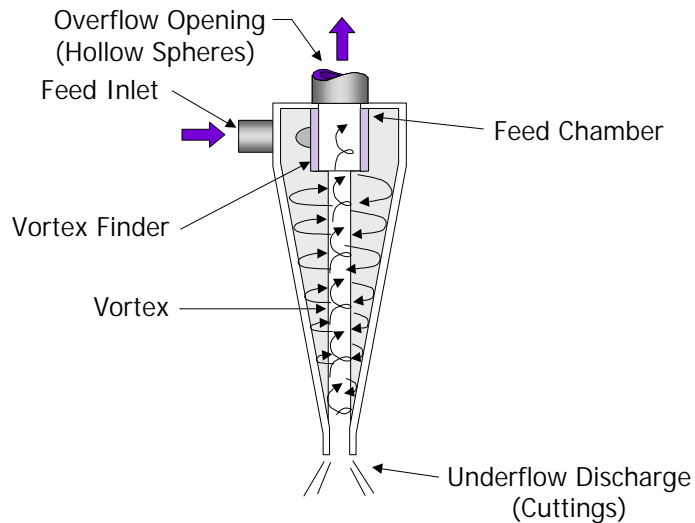


Figure 1-5. Oilfield Hydrocyclone

6. The FOAM hydraulics model can accurately predict circulating pressures and ECDs for foam drilling and thereby reduce foam drilling costs (**Figure 1-6**).

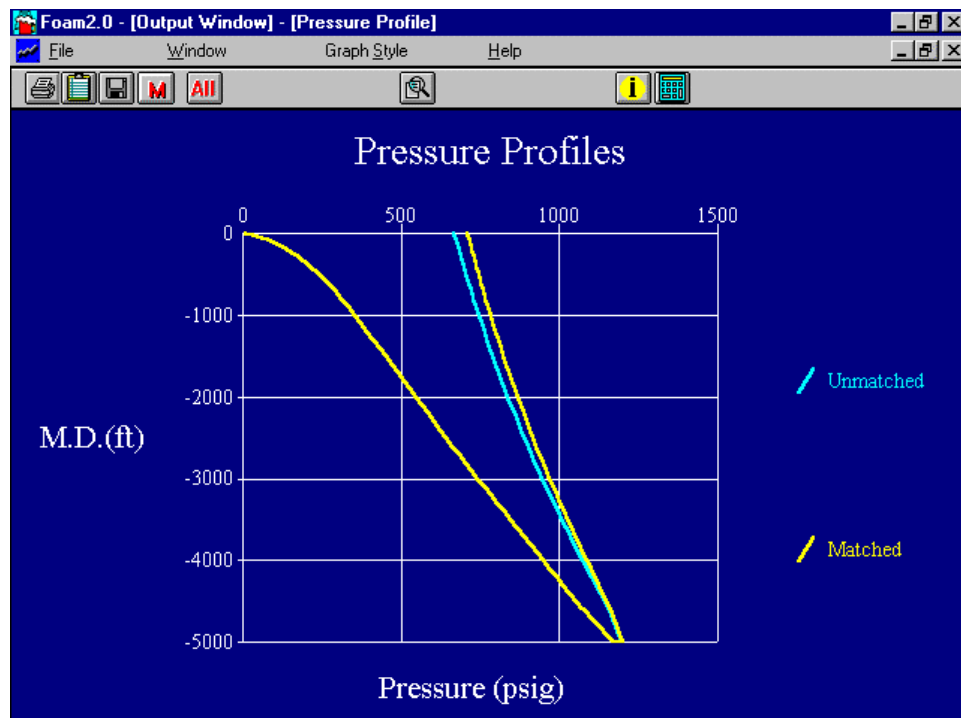


Figure 1-6. FOAM Pressure-Matching Window

1.2 RECOMMENDATIONS

The following recommendations are made as a result of the Phase II study:

1. A more detailed study of the use of HGS for riserless or “dual density” fluid drilling should be carried out in conjunction with joint-industry projects on alternative riserless drilling concepts.
2. Additional underbalanced drilling field tests should be carried out with HGS fluids to stimulate commercial implementation of this technology by service companies and operators.
3. The FOAM hydraulics model should be distributed to service companies and operators drilling underbalanced wells to determine the accuracy and usefulness of this model.
4. Laboratory formation damage and completion fluid tests strongly support the beneficial effects of HGS in water-base fluids as long as careful attention is given to fluid-loss properties. Field trials of this application should be undertaken.
5. A joint-industry project (JIP) should be formed with industry and DOE participation to develop the hollow-sphere dual-gradient drilling system since it has potential to significantly reduce deepwater drilling costs in the Gulf of Mexico.

1.3 COMMERCIALIZATION POTENTIAL

1.3.1 Riserless Drilling

HGS have significant potential for riserless Dual-Gradient Drilling. There are currently over 30 companies engaged in two JIPs led by HYDRIL/CONOCO and BAKER HUGHES INTEQ/TRANSOCEAN studying different alternatives for riserless and “dual-density” drilling. HGS are a good candidate for use on these projects. If selected as the preferred alternative, this would be a tremendous market for HGS since all wells drilled in water depths greater than 6000 ft water depth will require dual-density drilling concepts. A JIP should be formed to investigate this as a more cost-effective and reliable stand-alone system for dual-gradient drilling.

1.3.2 Underbalanced Drilling

HGS have high potential in underbalanced drilling due to their ability to significantly increase drilling rates and avoid problems encountered with aerated fluid drilling. M-I Drilling Fluids and other mud companies are reviewing the use of HGS for underbalanced drilling as a result of this DOE project. One limitation in the application of HGS has been the lack of rheological data on these

fluids. These data are now available from the Phase II study. Once released, this Phase II report should stimulate further interest and field testing of the HGS.

1.3.3 FOAM Hydraulics Model

The FOAM hydraulics model has commercial potential since it can assist drillers in calculating compressor requirements, circulation pressures, equivalent circulating densities (ECDs), and hole cleaning in directional and high-angle wells. This model can have a major impact on the foam drilling industry by allowing drillers to avoid hole problems and by significantly reducing foam drilling costs.

1.3.4 Formation Damage Reduction

The use of HGS as a drilling and completion fluid additive to reduce formation damage has considerable commercialization potential because oil and gas production is significantly reduced in many wells due to formation damage by water-base drilling fluids. Maurer Technology is in the process of filing for a patent on this concept. Once a patent is applied for, MTI will hold discussions with companies to provide this system.

2. Introduction

2.1 BACKGROUND

Oil companies first began drilling wells with air in the late 1940s. Primary motivations to use air were to increase drilling penetration rates through hard formations and to overcome severe lost-circulation problems. Increased drilling rate as a result of reduced differential pressure at the hole bottom (**Figure 2-1**) was the most important benefit of underbalanced drilling enjoyed by these operators.

The beneficial effects of reduced hydrostatic pressure with regard to increased ROP occur at all bit weights, as illustrated in **Figure 2-2**. Other benefits of air drilling include reduced formation damage, reduced lost circulation, and fewer problems with differential sticking.

Many tight gas reservoirs in the United States are attractive targets for underbalanced drilling because they are located in hard-rock country where tight (low-permeability) formations are more susceptible to formation damage from invasion of conventional drilling fluids.

Fluids lighter than water (i.e., specific gravity SG<1) are also required when drilling underbalanced in underpressured or depleted reservoirs. Many types of fluids systems are used, ranging from 100% air to 100% liquid. All fluids with densities below 6.9 ppg (SG=0.83) used to date contain gas or air in some form (**Figure 2-3**).

During the 1950s and 1960s, the variety of drilling fluids was expanded to include mist, foam, and aerated fluids. Each of the two-phase systems shown in **Figure 2-4** has been used successfully for drilling during the past four decades. However, the introduction of these two-phase fluids was accompanied by significantly increased difficulty in predicting fluid flow parameters with these compressible fluids.

The hydraulics for 100% liquid is relatively easy to predict because liquid can normally be assumed as essentially incompressible. One-hundred percent gas is harder to model, even though it is still one continuous phase, due to its compressibility. The hydraulics of mist and foam is the most difficult to model since these fluids are both compressible and two-phase. Foam is generally defined as any two-phase fluid with liquid as the continuous phase (having a gas emulsified in it), while mist is defined as a two-phase fluid having gas as the continuous phase (**Figure 2-5** on page 2-5). Gas becomes the continuous phase at gas fractions above 97-98% by volume.

Underbalanced and Foam Drilling

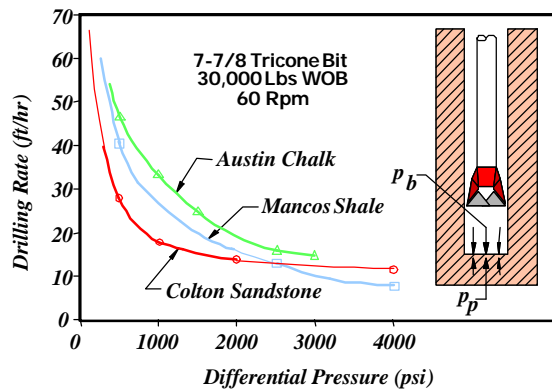


Fig. 2-1. Differential Pressure and Drilling Rate (Moffit, 1991)

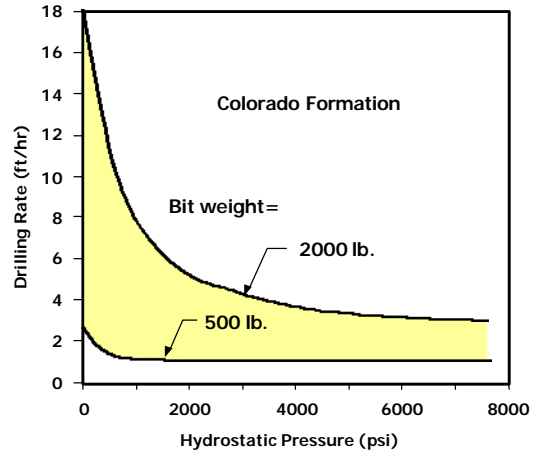


Fig. 2-2. Hydrostatic Pressure (psi)

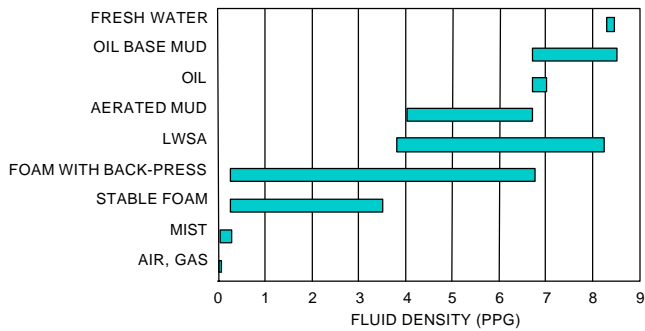


Fig. 2-3. Fluid Density

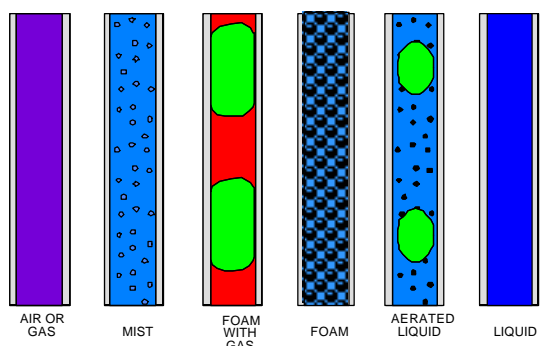


Fig. 2-4. Flow Regime Types (Lorenz, 1980)

The advantages of various lightweight fluids are summarized in **Table 2-1**. Air, gas, and mist systems are compared to foam and proposed lightweight solid additive (LWSA) systems. As stated previously, the major advantage of using underbalanced fluids is increased drilling rates.

Table 2-1. Advantages of Underbalanced Fluids

AIR/GAS/MIST	FOAM/LWSA
HIGH DRILLING RATE	HANDLES WATER INFUX
LOW CHEMICAL COSTS	IMPROVED HOLE STABILITY
EASY TO USE	EXCELLENT HOLE CLEANING
REDUCED ENVIRONMENTAL IMPACT	REDUCED COMPRESSORS
REDUCED LOST CIRCULATION	NO DOWNHOLE FIRES
LIMITS FORMATION DAMAGE	CAN USE MUD PULSE MWD (LWSA)

Fluids having gas or air as the continuous phase have the advantage of simplicity, low costs for additives, and minimal equipment requirements. These fluids also lead to less environmental risk since there is minimal liquid waste disposal. **Table 2-2** compares the disadvantages of underbalanced drilling fluids.

Table 2-2. Disadvantages of Underbalanced Fluids

AIR/GAS/MIST	FOAM/LWSA
HANDLING WATER INFUX	COST OF ADDITIVES
HOLE EROSION	MEASUREMENT/CALCULATION COMPLEXITY
DOWNHOLE FIRES	
HOLE INSTABILITY	

The primary disadvantage of air, gas or mist systems is their inability to handle formation fluid influxes. In practice, when an influx becomes too great for air or mist to handle, the fluid system must usually be switched to foam, aerated fluid, or 100% liquid.

Foams and the proposed LWSA muds (liquid muds with HGS added) eliminate many of the problems associated with air, gas, and mist drilling fluids including borehole stability problems, extensive compressor requirements, and downhole fires and explosions. The greatest advantage of foam and LWSA mud is the ability to safely handle large influxes of oil or water from the formation.

Foam has the additional advantage of increased cuttings-carrying capacity. **Figure 2-6** shows that, as the foam quality increases (i.e., the percent air increases), the lifting force increases. The maximum lifting force is achieved with 2 to 5% liquid, just within the region defined as a foam. As a foam becomes wetter, its viscosity decreases along with its ability to carry cuttings. As the fluid crosses over into a gas-continuous phase, it continues to effectively lift cuttings, but its ability to hold cuttings in suspension disappears at low velocities.

The gas phase in an aerated fluid can either be mixed with the liquid phase at the surface, or injected at some point in the drill-string casing annulus through a “parasite” string strapped to the outside of the casing (**Figure 2-7**). Air can also be injected down the annulus of dual-wall drill pipe. The injected air reduces pump pressure at the surface and lowers the hydrostatic head in the annulus.

Downhole fires and explosions are a problem when drilling with air, especially in long horizontal wells where days or weeks are spent drilling in oil or gas pay zones. If a flammable mixture of oxygen and natural gas or oil exists downhole, ignition can occur due to heat generated by friction or by sparks generated by the drill bit.

Although foam or aerated muds eliminate the potential for fires and explosions, their use is hindered by the increasingly complex hydraulics calculations and the high cost of foam chemicals. Prior to the availability of computers, it was nearly impossible to accurately calculate circulating pressures for compressible fluids. The tedious process of manually calculating hydraulics for foam systems was reduced by the development of nomographs and charts (**Figure 2-8**), rules-of-thumb, and correction factors that gave approximate answers. While these short-cut approaches allowed more broad application of foam drilling techniques, accuracy was decreased as was the engineer's ability to scientifically control these fluids.

An accurate hydraulics computer model is needed for foam drilling to allow engineers to better plan and drill wells. Chevron developed a mainframe computer model for foam circulation in the early 1970s that was state-of-the-art at that time, but its availability to the industry is limited.

Similarly, there is a need for incompressible drilling fluids that use solid additives (e.g., HGS) to lighten the fluid. This type of fluid would overcome the severe fire, explosion, and corrosion risks associated with aerated drilling fluids. Fluids successfully incorporating lightweight solid additives ($\text{SG}=0.3$ to 0.6) would have many advantages over conventional aerated fluids including:

- Allow use of MWD tools
- Eliminate expensive compressors
- Reduce corrosion problems
- Eliminate downhole fires

Underbalanced and Foam Drilling

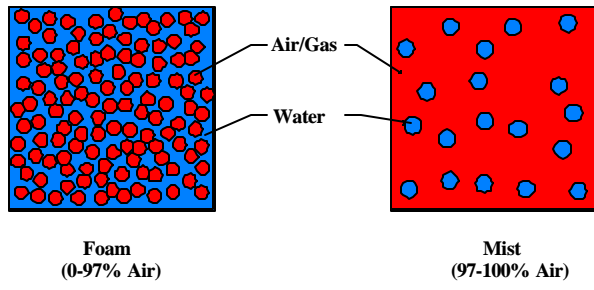


Fig. 2-5. Fluid Phase Continuity

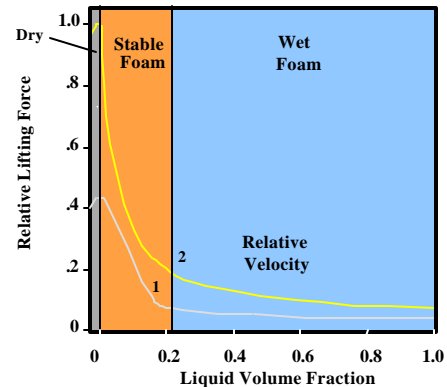


Fig. 2-6. Foam Lifting Capacity
(Beyer et al., 1972)

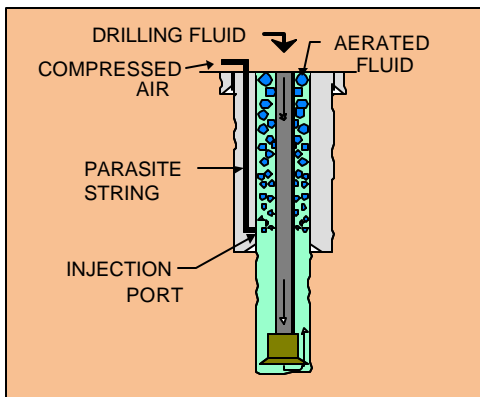


Fig. 2-7. Parasite Injection String

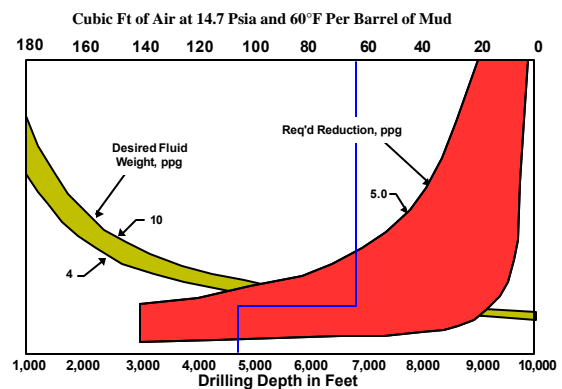


Fig. 2-8. Volume Requirement Chart
(Poettman and Begman, 1955)

- Eliminate the need for nitrogen
- Improve motor performance
- Improve hole stability
- Simplify pressure calculations
- Reduce drill-string vibration

In the late 1960s, Russian scientists tested lightweight fluids that used hollow spheres to reduce fluid density. Data available on the spheres used in the Russian development are presented in **Table 2-3**.

Table 2-3. Russian Hollow Spheres

FIRST MANUFACTURED	—	1968
FIRST USE IN DRILLING	—	1970-71
MATERIAL	—	GLASS
COMPRESSIVE STRENGTH	—	2500-3600 PSI
SPECIFIC GRAVITY	—	0.35-0.40
AVERAGE DIAMETER	—	50-70 MICRONS

Oil-field service companies have used hollow glass spheres and other lightweight additives for years to reduce the density of cements and to decrease hydrostatic head in lost-circulation situations. HGS have not been used in lightweight drilling fluids outside of Russia until this DOE project.

2.2 OBJECTIVES

The original objectives of Phase II of the project were to conduct laboratory and field testing of drilling fluids with hollow glass spheres (HGS), to transfer technology by way of DOE reports and (if possible) publications in the professional oil-industry literature, and to encourage commercial availability of materials and information for general application of this technology. The Phase II objectives were later expanded to include enhancements to the FOAM drilling computer model, conduct rheological tests on HGS drilling and completion fluids, and to study the potential application of HGS to deepwater riserless drilling.

2.3 TASK SUMMARY AND ACCOMPLISHMENTS

Phase II of this study for “Development and Testing Underbalanced Drilling Products” consisted of the three original tasks and additional tasks in the expanded program as follows:

- Prepare and receive approval of the field test plan and other required information for the National Environmental Policy Act (NEPA)
- Conduct field tests
- Technology transfer
- Expand foam underbalanced drilling model
- Conduct additional R&D on LWSA (HGS) Drilling Fluid
- Additional field tests on LWSA (HGS) Underbalanced Drilling Fluid
- Computer modeling on utilization of HGS for riserless drilling
- Additional testing of LWSA (i.e., HGS) as drilling and completion fluid additive to help mitigate formation damage
- Additional development of the Dual-Gradient Drilling (DGD) concept including co-sponsoring an industry workshop
- Investigation of additional applications for HGS

The test plan and other information for NEPA were developed and approved. Field tests were conducted as reported in this document, and technology was transferred by DOE reports and industry publications. 3M Corporation, the manufacturer of the spheres, has supplied materials to MI Drilling Fluids for use in commercial applications at an international location.

The FOAM drilling hydraulics model has been very well received in the industry, and an enhanced model has been developed. Documentation of that work is incorporated as part of this report.

After initial field tests with HGS drilling fluids, additional sites for field tests could not be located without major expenditures, which was beyond the scope of this project. Therefore, with DOE approval, funds were directed toward additional Drilling Research Center tests of 1) drilling rate tests with drilling fluids with various HGS concentrations, and 2) HGS breakage tests under a wide set of pressure, nozzle stand-off, nozzle pressure drop, and sphere concentration conditions. These are documented and analyzed in this report.

Detailed laboratory studies were conducted on the rheology of HGS drilling and completion fluids. A special test machine was developed and tests were run to measure possible formation damage caused by HGS fluids. Additional work was undertaken at the Petroleum Engineering Department Completion Fluids Laboratory at Texas A&M University.

A comprehensive study of the use of HGS for riserless drilling was conducted using the foam underbalanced drilling hydraulics model. Results of these studies are documented in this report, and have been further disseminated in information for a joint-industry project.

3. Phase I Work

3.1 FOAM HYDRAULICS MODEL

A foam hydraulics model FOAM was developed to accurately predict circulating pressures with foam. This model uses industry-accepted models including Chevron's model. **Figure 3-1** shows an input screen for FOAM and **Figure 3-2** shows wellbore circulating pressures predicted for a foam drilled well.

FOAM was expanded during Phase II by adding a hole-cleaning algorithm and a "matching" feature that allows field calibration of this model. This foam hydraulics model is described in detail in the July 1, 1996, *Oil & Gas Journal* article entitled "Foam Computer Model Helps in Analysis of Underbalanced Drilling" presented in Appendix A, and an ASME paper of the same title presented in Appendix B. A copy of FOAM version 2 is included on the electronic copy (CD) of the Final Report submitted to the DOE.

3.2 LIGHTWEIGHT SOLID ADDITIVE (LWSA) LABORATORY TESTING

Phase I laboratory tests were conducted that showed:

1. Rheology (PV, YP) and filter loss of water and oil base muds containing up to 40% hollow glass spheres (HGS) were within acceptable limits as long as the percentage of drill solids did not exceed 5 to 6%.
2. HGS can be reclaimed after a well is drilled by diluting the mud and allowing the spheres to float to the surface.
3. HGS reduce casing wear by as much as 78% by acting like ball bearings between the rotating drillpipe tool joint and the casing.

3.3 LWSA YARD TESTS

Phase I yard tests showed:

1. HGS muds can be mixed and pumped using conventional drilling rig equipment.
2. HGS can be removed from the mud while drilling using conventional oil field hydrocyclones.
3. Downhole drilling motors perform well with the hollow spheres, delivering full torque and power with no damage to the motor.

Phase I Work

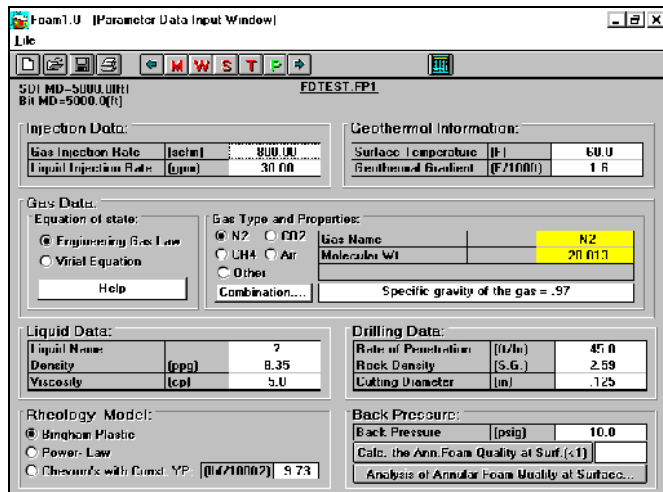


Fig. 3-1. FOAM Data Input Window

Pressure Profile

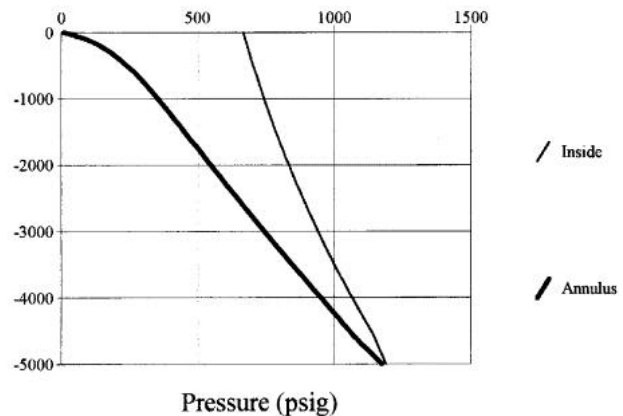


Fig. 3-2. FOAM Wellbore Pressure Profile

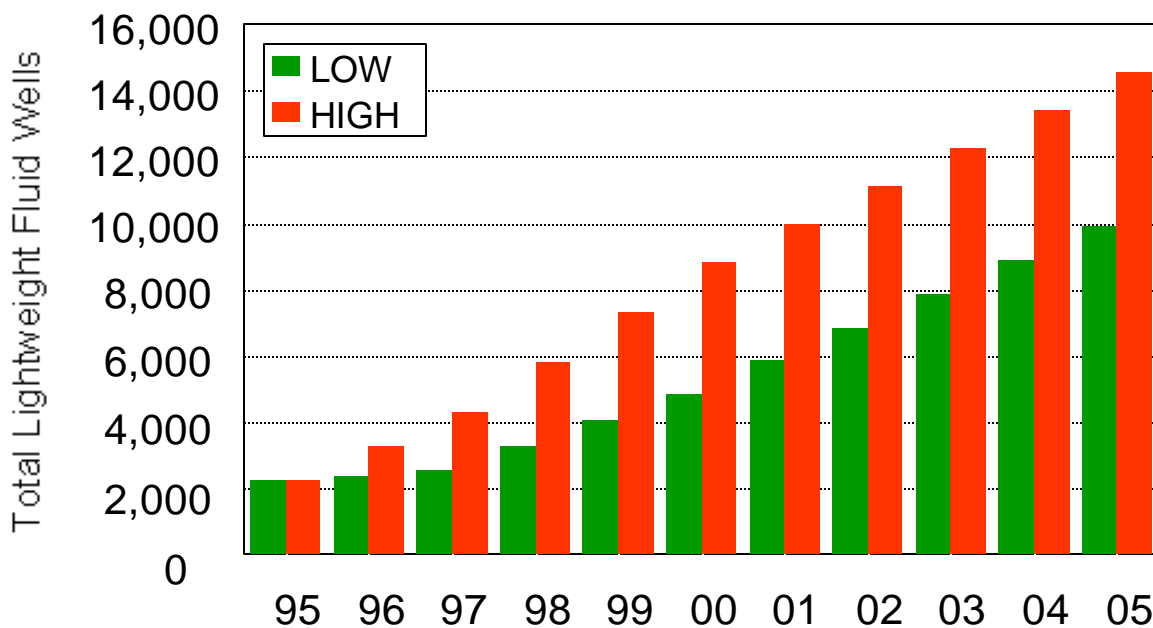


Fig. 3-3. Growth of Lightweight Fluid Use in the USA
 (Duda et al., 1996)

3.4 MARKET SURVEY

A survey of companies drilling underbalanced wells showed that:

1. Operators predict that by the year 2005, 12,000 wells (30%) will be drilled with lightweight fluids in the U.S.A. (**Figure 3-3**).
2. Operators identified reduced formation damage, increased drilling rate, and reduced lost circulation problems as the most important advantages of lightweight fluids.
3. Operators identified fluid influxes ("kicks"), the inability to transmit data with mud pulse MWD tools, and hole stability problems as the major limitations of lightweight fluids.

3.5 PHASE I CONCLUSIONS

The following conclusions were reached as a result of the Phase I study:

1. A need does exist for an easy to use personal computer model for foam drilling fluids.
2. The PC model developed in this project for calculating pressure responses and flow behavior of foam drilling fluids has been shown to be accurate by comparison with existing measurements.
3. The FOAM computer model is available for use by the oil and gas drilling industry.
4. An incompressible fluid having a density less than water would overcome many of the problems associated with aerated fluids, opening up many new areas to underbalanced drilling.
5. Lightweight incompressible drilling fluids can be constructed using commercially available hollow glass spheres (HGS). At sphere concentrations below 40% by volume, lightweight muds behave similarly to conventional drilling fluids.
6. Laboratory tests show that an HGS drilling fluid will significantly decrease casing wear caused by drill-string rotation.
7. Conventional drilling rig solids-control equipment does not damage HGS.
8. Collapse pressure of HGS (4,000 psi) will allow their use in relatively deep underbalanced wells (i.e., 9,000 to 10,000 ft depth).
9. Drill solids must be removed with large-mesh shale shaker screens and hydrocyclones. Conventional oil-field centrifuges are not effective in removing drill solids or HGS from these muds.

10. Low-cost methods of separating spheres from whole mud should be feasible using a combination of gravity segregation, conventional hydrocyclones and shale shakers.
11. The cost of HGS muds can be significantly reduced by recovering and recycling the spheres. HGS muds should be competitive with nitrogen drilling, even without recycling the spheres.
12. Underbalanced drilling has been effective in many different types of reservoirs. The technology is not limited by depth, having been used successfully at depths ranging from 200 to 20,000 ft.
13. Both operating and service companies project large growth rates for underbalanced drilling over the next decade (e.g., up to 37 % of all wells).
14. The most significant non-technical barriers to the growth of underbalanced drilling in the U.S. are limited equipment availability, lack of familiarity with lightweight fluids, and a perception of high cost.
15. The largest technical barriers to growth in underbalanced drilling are handling formation influxes, the inability to use conventional MWDs with compressible lightweight fluids, and corrosion.
16. Ninety-four percent of all operators surveyed are willing to consider using a lightweight solid additive drilling fluid such as that developed on this project.
17. By the year 2005, underbalanced drilling in the U.S. is projected to account for 10,000 to 12,000 oil and gas wells per year, depending on the growth of conventional drilling. From 2,500 to 3,600 gas wells are forecast to be drilled underbalanced per year. This activity level would result in an industry-wide improvement in Net Present Value of \$4.5 billion over the next ten years.

4. HGS Characteristics

4.1 COMMERCIALLY AVAILABLE HOLLOW SPHERES

3M manufactures Scotchlite™ S Series hollow glass spheres (HGS) with various densities and collapse pressures as described in **Table 4-1**. Further details of properties and specifications of the HGS are given in the “Scotchlite Product Data Sheet,” found in Appendix C.

Table 4-1. 3M Scotchlite™ S Series Hollow Glass Spheres

3M Product	Density (g/cc)	Collapse Pressure (psi)	Survival Rate (%)
S15	0.15	300	90
S22	0.22	400	90
S32	0.32	2,000	90
S38	0.38	4,000	90
S60	0.60	10,000	90

S38 hollow spheres were selected for testing on this project because they have the best properties for use in oil-field fluids. The S60 HGS collapse at 10,000 psi and are candidates for use in deeper wells where higher sphere collapse pressures are required.

4.2 S38 HGS CHARACTERISTICS

Manufacturer:	3M Specialty Additives (1-800-367-8905)
Product:	S38 Glass Bubbles
Material:	Water-resistant and chemically-stable unicellular soda-lime-borosilicate glass
Diameter:	8 to 125 microns (Median = 45 microns)
Density:	0.35 to 0.41 g/cc (0.38 typical)
Collapse Pressure:	4,000 psi (90% Survival Rate)
Color:	White

4.3 S38 HGS SIZE DISTRIBUTION

The diameter of commercial hollow glass S38 spheres ranges from 8 to 125 microns with a median diameter of 45 microns (**Figure 4-1**). These spheres will pass through the 20 to 80 mesh screens (762 to 177 microns) typically used on oilfield shale shakers (**Figure 4-2**).

These microspheres have small diameters because they are typically used as fillers in paints, glues and other materials to reduce their manufacturing cost. Because of the small diameter of HGS, oilfield shale shakers cannot be used to remove them from the mud when they return to the surface.

Larger diameter spheres (e.g., 1-mm diameter and larger) are needed in applications where the spheres must be removed from the mud during each circulation (e.g., riserless drilling) so they can be screened out of the mud by conventional oilfield shale shakers.

4.4 EFFECT OF SPHERES ON FLUID DENSITY

The density of fluids containing hollow glass spheres equals:

$$d = \frac{(100 - v) d_f + v d_s}{100} \quad (4-1)$$

where

- d = Fluid Density with Spheres
- d_f = Fluid Density without Spheres
- d_s = Density of Hollow Spheres
- v = Sphere Concentration (% Volume)

Figure 4-3 shows how the fluid density decreases as the sphere concentration increases. The maximum sphere concentration ranges from 35 to 50% by volume, due to increased mud viscosity with increased sphere concentration. **Figure 4-3** shows that a 50% sphere concentration can reduce the density of a 14 ppg mud to 8.6 ppg, a significant reduction.

HGS Particle Size and Slip Velocity

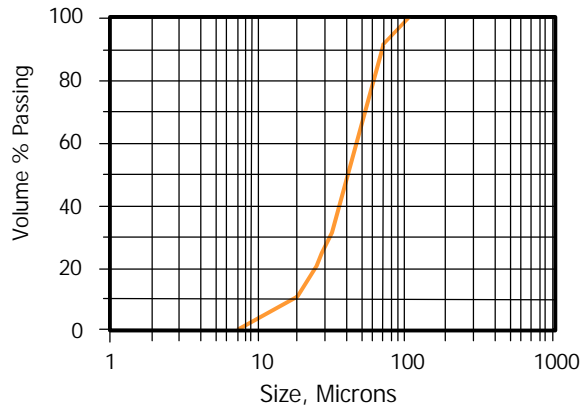


Fig. 4-1. S38 Glass Bubble

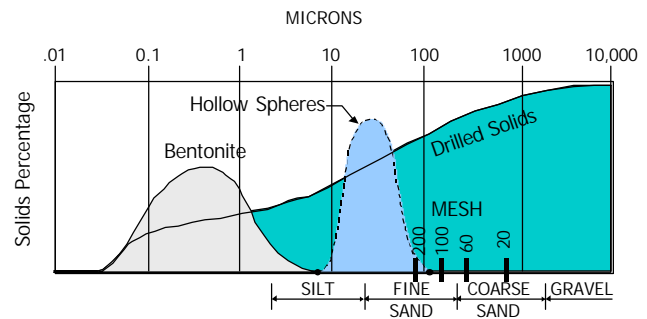


Fig. 4-2. Solids in Unweighted Water-Base Drilling Mud (Burgoyne, et al., 1986)

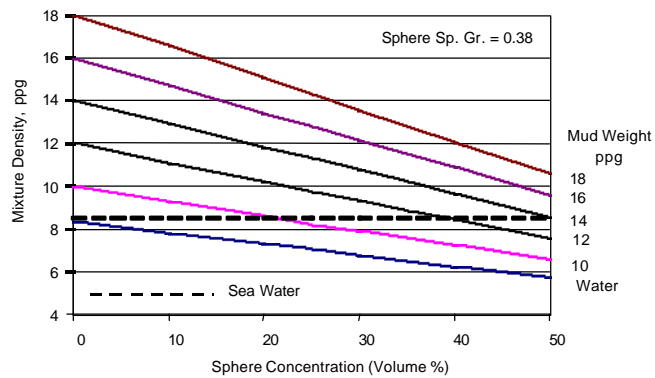


Fig. 4-3. Mud Density vs Sphere Concentration

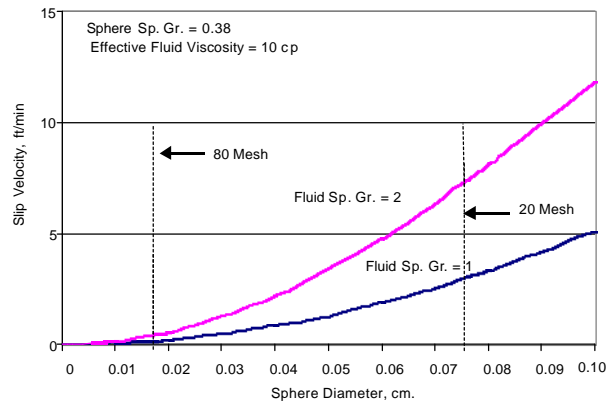


Fig. 4-4. Sphere Slip Velocity vs Fluid Density

4.5 SPHERE SLIP VELOCITY

Drill cuttings fall in the wellbore annulus because the rock cuttings are heavier than mud. Similarly, HGS float upward in mud since they are lighter than the mud.

Chien (1992) showed that the slip velocity v_s of particles in mud equals:

$$v_s^2 + 0.4458 e^{5.030 b} \left(\frac{m_e}{D d_f} \right) v_s - 19.50 e^{5.030 p} D \left(\frac{d_p}{d_f} - 1 \right) = 0 \quad (4-2)$$

where

D = Sphere Diameter (cm)

v_s = Slip Velocity (cm/sec)

d_f = Density of Fluid (g/cm^3)

d_p = Density of Particle (g/cm^3)

m_e = Effective Viscosity of Fluid (Poise)

For a sphere, $b = 1.0$ and Eq. 4-2 reduces to:

$$v_s^2 + 68.18 \left(\frac{m_e}{D d_f} \right) v_s - 2982 D \left(\frac{d_p}{d_f} - 1 \right) = 0 \quad (4-3)$$

The slip velocity increases with increased sphere diameter, increased fluid density, and with decreased fluid viscosity. **Figures 4-4 and 4-5** show that the slip velocity of spheres will be on the order of 5 to 20 ft/min, which is small compared to the fluid velocities.

4.6 HGS RECOVERY

When a well is completed, the hollow spheres can be removed and used in subsequent wells, thus significantly reducing sphere costs. The simplest way to remove the spheres is to dilute water-base muds with water and allow the spheres to float to the top of the mud tank where they can be easily recovered.

Phase I tests showed that the HGS can also be effectively removed from the mud with hydrocyclones, due to their low density. In this case, heavier rock cuttings came out the underflow at the bottom of the cone whereas the liquid mud and the hollow spheres came out the overflow (**Figure 4-6**).

HGS Particle Size and Slip Velocity

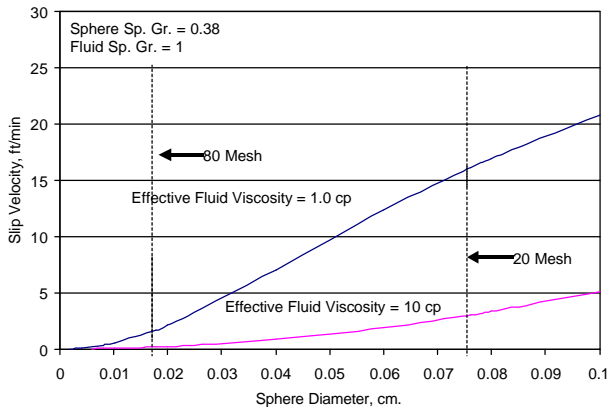


Fig. 4-5. Sphere Slip Velocity vs. Fluid Density

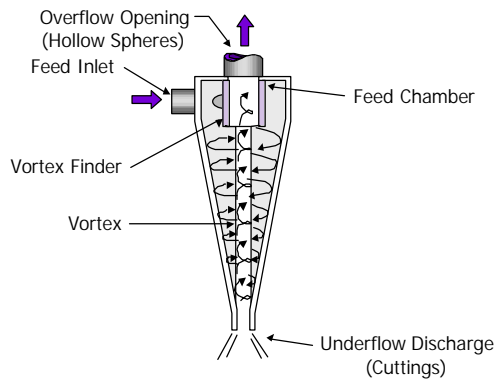


Fig. 4-6. Oilfield Hydrocyclone
(Moore et al., 1974)

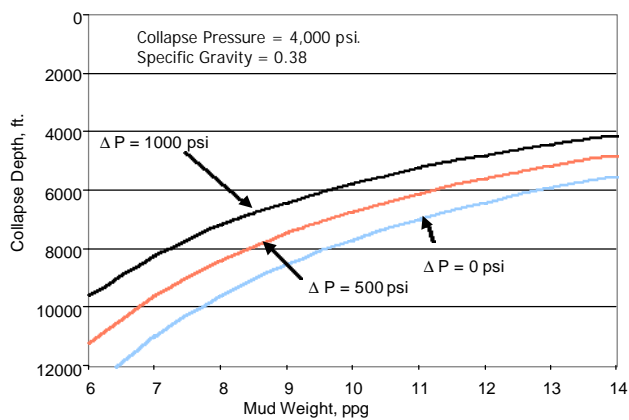


Fig. 4-7. S38 Hollow Sphere Collapse Depth

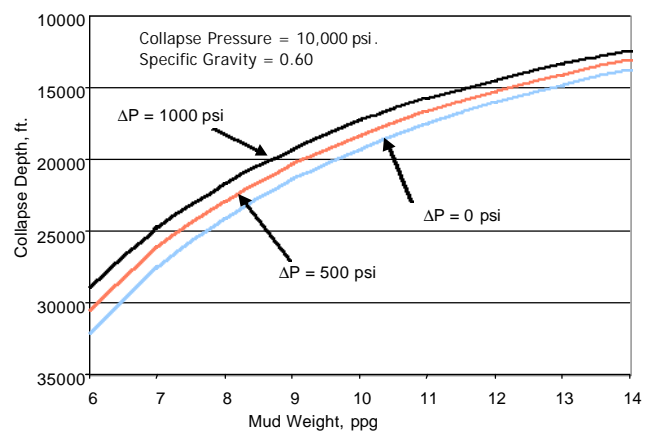


Fig. 4-8. S60 Hollow Sphere Collapse Depth

4.7 HGS COLLAPSE PRESSURE

One concern regarding the use of using larger diameter spheres to facilitate their removal from the mud with oilfield shale shakers is the collapse pressure of the larger spheres.

Timoshenko (1951) showed that the collapse pressure of a sphere, p_c , due to external pressure equals:

$$p_c = \frac{2s_f (b^3 - a^3)}{3b^3} \quad (4-4)$$

Density of a sphere equals:

$$d_s = d_g \left(\frac{b^3 - a^3}{b^3} \right) \quad (4-5)$$

Substituting **Eq. 4-5** into **Eq. 4-4** and rearranging, thus yields:

$$p_c = \frac{2s_f d_s}{3d_g} \quad (4-6)$$

where

- a = Sphere Inner Diameter (inches)
- b = Sphere Outer Diameter (inches)
- p_c = Collapse Pressure (psi)
- s_f = Glass Shear Strength (psi)
- d_g = Density of Glass (lb/in^3)
- d_s = Density of Hollow Sphere (lb/in^3)

Eq. 4-6 shows that, for a given glass (s_f and $d_g = \text{constant}$), HGS of the same density will collapse at the same external pressure. This is significant, because it shows that it is possible to significantly increase the diameter of the spheres without affecting their collapse pressure.

4.8 HGS COLLAPSE DEPTH

S38 spheres will collapse if subjected to pressures in excess of 4,000 psi. The highest fluid pressure occurs at the bottom of the well due to the weight of the column of fluid in the well. If fluid is circulating, the highest pressure exists inside the drillstring, just above the drilling motor and bit.

The depth at which the HGS will collapse equals:

$$\text{Collapse Depth} = \frac{p_c - d(p)}{0.052 d_m} \quad (\text{feet}) \quad (4-7)$$

where

p_c = Sphere Collapse Pressure (psi)

$d(p)$ = Frictional Pressure Drop Across Motor, Bit and Wellbore Annulus

d_m = Mud Density (ppg)

Typically $d(p)$ ranges from 500 to 1000 psi.

Figure 4-7 shows that with no flow ($d(p) = 0$), the S38 spheres (4,000 psi collapse pressure) will collapse at a well depth of 12,800 ft with a 6 ppg mud and at 5500 ft with a 14 ppg mud. With $d(p) = 1000$ psi, the S38 spheres will collapse at 9600 ft with a 6 ppg mud and at 4100 ft with a 14 ppg mud.

The spheres will typically be used in lightweight muds (less than 7 ppg) in which case the S38 spheres can be used to depths of 8000 to 11,000 feet.

The S60 spheres can be used at depths in excess of 12,000 to 30,000 ft as shown in **Figure 4-8** due to their higher collapse pressure (10,000 psi).

5. Rheology of HGS Fluids

5.1 BASE FLUIDS TESTED

Rheological tests were conducted at Mudtech Laboratories, Inc. in Houston on the eight drilling and completion fluids shown in **Table 5-1** with a range of concentrations of Hollow Glass Spheres (HGS).

Table 5-1. Test Drilling Fluid Compositions

PHPA Water-Base Drilling Fluid		3% KCl Drilling Fluid	
Houston Tap Water, bbl	1	Houston Tap Water, bbl	1
API Bentonite, ppb	10	API Bentonite, ppb	10
PHPA, ppb	1	KCl, ppb	10.5
Caustic Soda, ppb	0.25	Xanthan Gum, ppb	1
Density, ppg	9.87	Density, ppg	8.55

Oil-Base Drilling Fluid		CaBr₂ Brine	
No. 2 Diesel, bbl	0.67	15.6 ppg Brine, bbl	1
Organoclay, ppb	5	HEC, ppb	0.5
Primary Emulsifier, ppb	8	Density, ppg	15.60
Secondary Emulsifier, ppb	5		
Lime, ppb	5		
30% CaCl ₂ , bbl	0.22		
Amine Lignite, ppb	8		
Barite, ppb	150		
Density, ppg	10.71		

Synthetic Oil Drilling Fluid		CaCl₂ Brine	
Polyalphaolefin, bbl	0.67	11.7 ppg Brine, bbl	1
Organoclay, ppb	5	HEC, ppb	0.5
Primary Emulsifier, ppb	8	Density, ppg	11.70
Secondary Emulsifier, ppb	5		
Lime, ppb	5		
30% CaCl ₂ , bbl	0.22		
Amine Lignite, ppb	8		
Barite, ppb	150		
Density, ppg	10.75		

NaCl Brine	
10.0 ppg Brine, bbl	1
HEC, ppb	0.5
Density, ppg	9.96

ZnBr₂ Brine	
19.2 ppb Brine, bbl	1
HEC, ppb	0.5
Density, ppg	19.17

5.2 EFFECT OF HGS ON TEST FLUID DENSITY

Table 5-2 and **Figure 5-1** show that the densities of the test fluids were decreased 2 to 6 pounds per gallon (ppg) by the addition of 36% spheres.

Table 5-2. Effect of Hollow Spheres on Test Fluid Density (ppg)

Test Fluid	HGS Concentration (%)			
	0	16	26	36
Water base (PHPA) Mud	9.87	7.66	7.11	6.62
Oil Mud	10.71	9.56	8.84	8.14
Synthetic Oil Mud	10.75	9.56	8.84	8.14
KCl Mud	8.55	7.76	7.20	6.70
NaCl Brine	9.96	8.88	8.18	7.57
ZnBr ₂ Brine	19.17	16.64	14.99	13.55
CaBr ₂ Brine	15.60	13.63	12.35	11.23
CaCl ₂ Brine	11.70	10.35	9.47	8.70

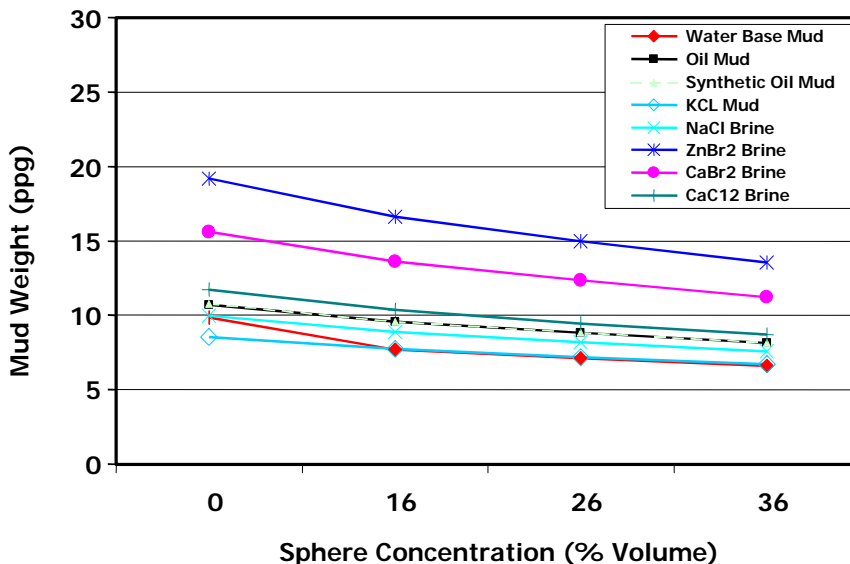


Figure 5-1. Effect of HGS on Test Fluid Density

5.3 TEST MATRIX AND PROCEDURES

Each of the eight test fluids was tested with sphere concentrations of 0 to 36% and simulated drill solids concentrations of 0 to 10% as shown in **Table 5-3**.

Table 5-3. Rheology Test Plan Matrix

HGS (% mud)	Drill Solids (% wt.)					
	0	2	4	6	8	10
0	x	x	x	x	x	x
16	x	x	x	x	x	x
26	x	x	x	x	x	x
36	x	x	x	x	x	x

Standard oil-field drilling fluid mixing and testing procedures were used including blending and shearing preparations and Fann rheometer tests.

A 6-speed Fann 35A rheometer was used to measure Plastic Viscosity, Yield Point, and initial, 10-second, and 30-minute gel strengths. API filtrate was measured for 30 minutes at 100 psi differential for the water-base fluids and HPHT filtrate (250EF, 500 psi) was measured for 30 minutes for the oil-base and synthetic oil drilling fluids. Electrical stabilities were also determined for the oil-base and synthetic drilling fluids. Filtration rates were not measured on the brine fluids.

5.4 NORMAL DRILLING FLUID RHEOLOGY

Figure 5-2 shows that the optimum operating range for plastic viscosity (PV) for drilling fluids ranges from 3 to 55 cp and the optimum range for yield point (YP) ranges from 10 to 32 lb/100 sq ft.

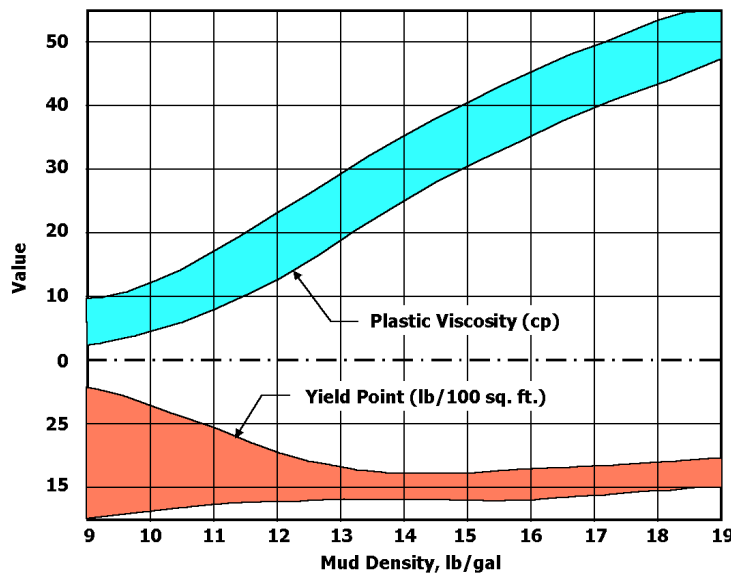


Figure 5-2. Optimum Drilling Fluid PV and YP Ranges (Baroid, 1981)

5.5 TEST DATA

PV and YP data are summarized in **Figure 5-3** and **Tables 5-4** and **5-5** as a function of sphere concentration and in **Figure 5-4** and **Tables 5-6** and **5-7** as a function of drill solids concentration.

A complete set of original data is contained in Appendix D, MEI Report TR98-25, "Final Report on Glass Spheres in Drilling Fluids."

Fluid Viscosity vs HGS Concentration

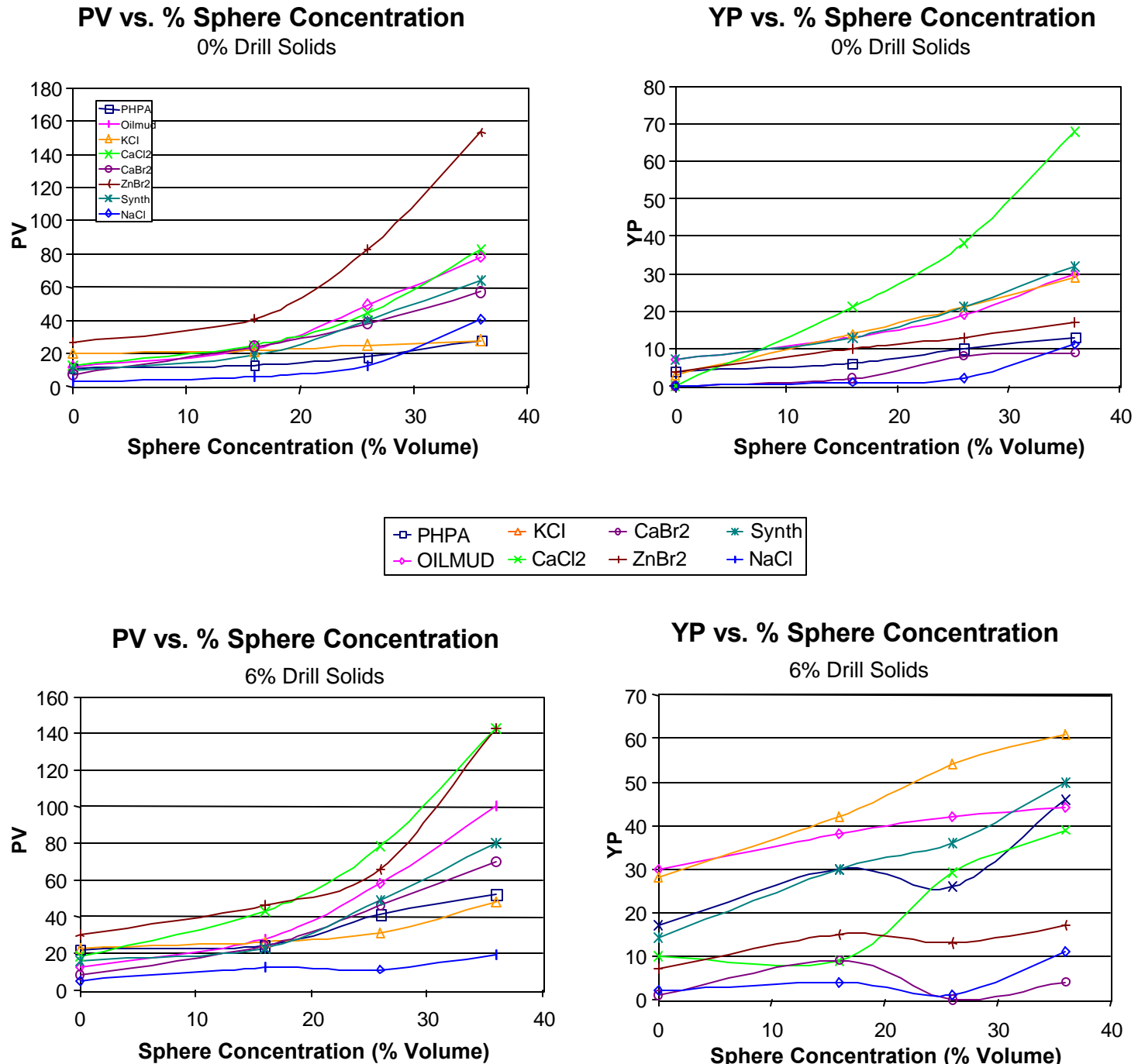


Fig. 5-3. Fluid Viscosity vs. HGS Concentration

Table 5-4. Test Data Summary: PV, YP as a Function of HGS for 0% Drill Solids

PV								
% HGS	PHPA	Oil Mud	Synth	KCl	CaCl ₂	CaBr ₂	ZnBr ₂	NaCl
0	11	12	10	20	13	7	27	3
16	13	23	19	22	25	24	41	6
26	18	49	40	25	44	38	83	13
36	28	78	64	28	83	57	153	41

YP								
% HGS	PHPA	Oil Mud	Synth	KCl	CaCl ₂	CaBr ₂	ZnBr ₂	NaCl
0	4	7	7	3	0	0	4	0
16	6	13	13	14	21	2	10	1
26	10	19	21	21	38	8	13	2
36	13	30	32	29	68	9	17	11

Table 5-5. Test Data Summary: PV, YP as a Function of HGS for 6% Drill Solids

PV								
% HGS	PHPA	Synth	Oil Mud	KCl	CaCl ₂	CaBr ₂	ZnBr ₂	NaCl
0	22	16	12	23	18	8	30	5
16	24	23	28	26	43	24	46	12
26	41	49	58	31	78	46	66	11
36	52	80	100	48	143	70	143	19

YP								
% HGS	PHPA	Synth	Oil Mud	KCl	CaCl ₂	CaBr ₂	ZnBr ₂	NaCl
0	17	14	30	28	10	1	7	2
16	30	30	38	42	9	9	15	4
26	26	36	42	54	29	0	13	1
36	46	50	44	61	39	4	17	11

Fluid Viscosity vs Drill Solids Concentration

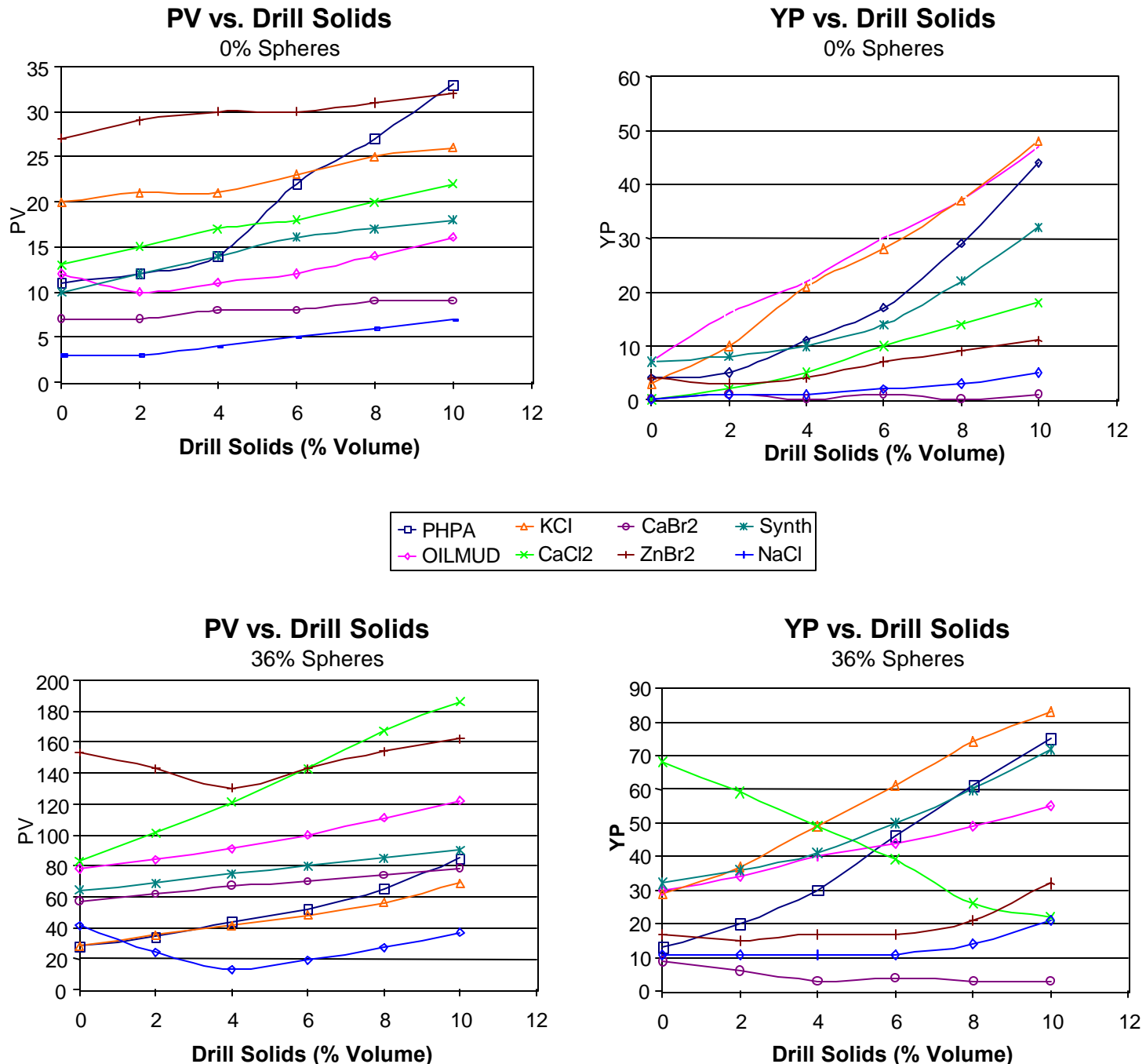


Fig. 5-4. Fluid Viscosity vs. Drill Solids Concentration

Table 5-6. Test Data Summary: PV, YP as a Function of Drill Solids for 0% HGS

PV for 0% HGS								
% Drill Solids	PHPA	Synth	Oil Mud	KCl	CaCl ₂	CaBr ₂	ZnBr ₂	NaCl
0	11	10	12	20	13	7	27	3
2	12	12	10	21	15	7	29	3
4	14	14	11	21	17	8	30	4
6	22	16	12	23	18	8	30	5
8	27	17	14	25	20	9	31	6
10	33	18	16	26	22	9	32	7

YP for 0% HGS								
% Drill Solids	PHPA	Synth	Oil Mud	KCl	CaCl ₂	CaBr ₂	ZnBr ₂	NaCl
0	4	7	7	3	0	0	4	0
2	5	8	16	10	2	1	3	1
4	11	10	22	21	5	0	4	1
6	17	14	30	28	10	1	7	2
8	29	22	37	37	14	0	9	3
10	44	32	47	48	18	1	11	5

Table 5-7. Test Data Summary: PV, YP as a Function of Drill Solids for 36% HGS

PV for 36% HGS								
% Drill Solids	PHPA	Synth	Oil Mud	KCl	CaCl ₂	CaBr ₂	ZnBr ₂	NaCl
0	28	64	78	28	83	57	153	41
2	34	69	84	35	101	62	143	24
4	44	75	91	41	121	67	130	13
6	52	80	100	48	143	70	143	19
8	65	85	111	56	167	74	154	27
10	85	90	122	69	186	78	162	37

YP for 36% HGS								
% Drill Solids	PHPA	Synth	Oil Mud	KCl	CaCl ₂	CaBr ₂	ZnBr ₂	NaCl
0	13	32	30	29	68	9	17	11
2	20	36	34	37	59	6	15	11
4	30	41	40	49	49	3	17	11
6	46	50	44	61	39	4	17	11
8	61	60	49	74	26	3	21	14
10	75	72	55	83	22	3	32	21

5.6 TEST RESULTS

Most of the HGS test fluids behaved like standard fluids with fluid viscosity increasing with increased HGS and drill solids content.

With higher HGS and drill solids concentrations, some of the brines (e.g., CaCl_2 and CaBr_2) exhibited unusual rheological behaviors. Repeat tests on these brines also showed inconsistent results that could have been caused by variations in fluid properties or by the test procedures.

5.6.1 PHPA Water-Base Drilling Fluid

Partially Hydrolyzed Polyacrylate Polymer (PHPA) acted like a normal drilling fluid. Plastic viscosities, yield points, and gel strengths increased with increasing concentrations of HGS and drill solids. With 16 to 26% HGS, fluid viscosity became excessive with 8% drill solids, whereas with 36% HGS, the viscosity became excessive with 6% drill solids. API filtration rates remained fairly constant with little variation observed.

5.6.2 Oil-Base Drilling Fluid

Viscosity of the oil-base drilling fluid also increased with increased HGS and drill solids concentrations. With 0 to 26% HGS concentration, viscosity increased as expected, whereas with 36% HGS, the yield points were lower than expected with 8 to 10% drill solids. Electrical stabilities were dramatically lower at the 8% and 10% simulated drill solids concentration, which may be associated with this unexpected behavior.

5.6.3 Synthetic Oil Drilling Fluid

Synthetic oil drilling fluid was prepared using a C16/18 polyalphaolefin (PAO) as the base oil. This drilling fluid performed similarly to the oil base mud except that the viscosity of the synthetic-oil mud was slightly lower because PAO has a lower viscosity than No. 2 diesel.

5.6.4 3% KCl Drilling Fluid

Viscosity of the 3% KCl drilling fluid increased with increased additions of HGS and drill solids as expected. KCl fluids containing 26% or more HGS became very viscous with more than 8% drill solids.

5.6.5 Brine Fluids

Viscosity of the ZnBr_2 brine increased in a predictable manner when HGS and drill solids were added, but this brine did not exhibit the viscosity decrease seen with the other three brines. The NaCl , CaCl_2 and CaBr_2 brines without HGS additive, were virtually unaffected by increased drill solids, indicating that these brines have an inhibiting effect on the drill solids.

With HGS, these three brines initially thinned when drill solids were added and then thickened as the concentration of drill solids increased. This behavior, which was duplicated in repeat tests, is unusual. The reason for this behavior is unknown. The HGS additive should be inert in these brines with no chemical reactions occurring. It is possible that the HGS additive, which dramatically increases the volume of the system, reduced the concentration of HEC and viscosity until a concentration of drill solids was attained that caused the viscosity to increase. Future testing should be conducted to test this premise.

5.7 CONCLUSIONS

The following conclusions were reached as a result of these rheological tests:

1. Viscosity of HGS drilling fluids and brines increase with increased HGS and drill solid concentrations.
2. Viscosity of some of these HGS fluids became excessive with HGS concentrations in excess of 25% and drill solid concentrations in excess of 6%.
3. When HGS and drill-solids concentrations are kept within acceptable limits, HGS fluids are rheologically similar to conventional fluids.

6. HGS Breakage During Drilling

Phase I tests showed that hollow glass spheres (HGS) were not damaged by conventional mud pumps or surface mud handling equipment.

Phase II laboratory tests were conducted at the Drilling Research Center (DRC) in Houston, Texas, to determine if the hollow spheres will break when they exit bit nozzles and impact the rock. These tests showed that with proper nozzle selection and standoff, sphere breakage can be minimized once malformed spheres (typically 5 to 10%) break during their initial pass through the nozzles.

6.1 TEST SETUP

The test loop shown in **Figure 6-1** was used to test the survivability of HGS jetted from bit nozzles. Mud containing HGS is pumped from a 50-gallon mud tank through a nozzle at the end of an adjustable stinger inserted into a pressure vessel. The stinger can be moved to adjust the standoff distance from the nozzle to a Texas Pink granite rock sample in the pressure vessel.

Figure 6-2 shows mud containing HGS impacting the rock and breaking the spheres. **Figure 6-3** shows the HGS test mud in the 50-gallon mud mixing tank.

Figure 6-4 shows the pressure vessel with the stinger. After exiting the nozzle, the fluid exits the chamber through a choke that holds back pressure on the pressure chamber and keeps the chamber full of fluid.

To measure the rate of sphere breakage, mud was circulated for 3 hours at 10 gal/min. At this flow rate, the mud recirculated through the nozzle every five minutes, or 36 times in the 3-hour test. This is equivalent to flowing a 400-barrel system at 200 gal/min for 2 days (50.4 hours). To keep the mud from heating, the mud was circulated through a cooling coil immersed in chilled water (**Figure 6-5**).

The pressure drop across the nozzle was varied from 0 to 500 psi by varying the nozzle diameter. The standoff distance between the nozzle and the rock was varied from 0.5 to 6 inches by use of the stinger.

Sphere breakage was monitored by taking fluid samples at 15-minute intervals and weighing these samples in a 500 ml Erlenmeyer flask to measure mud density as shown in **Figure 6-6**. To reduce possible errors, 3 samples were weighed and averaged for each measurement. A mud mixer on the mud tank ensured that HGS material was well mixed into the water.

HGS Breakage During Drilling

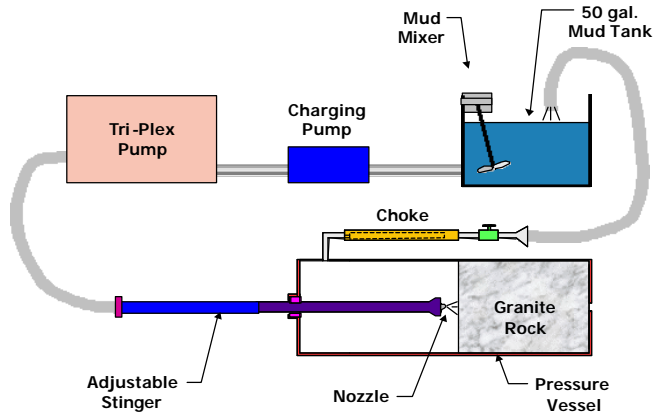


Fig. 6-1. HGS Breakage Test Flow Loop

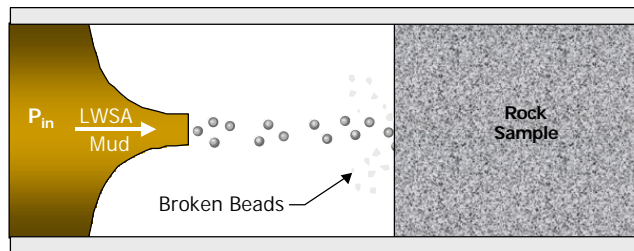


Fig. 6-2. HGS Spheres Impacting Rock



Fig. 6-3. HGS Test Mud Tank



Fig. 6-4. Pressure Vessel with Stinger



Fig. 6-5. Mud Cooling Coils in Chilled Water



Fig. 6-6. HGS Mud Weight

6.2 TEST RESULTS

6.2.1 Effect of Nozzle Pressure

The force with which the spheres impact the hole bottom is crucial to their survival. Selecting a nozzle size that produces a lower pressure drop allows the spheres to be used with all types of bits. **Figure 6-7** shows that at high pressures, some of the spheres break as they impact the bottom of the hole, whereas at lower pressures, they bounce off the bottom undamaged.

Figure 6-8 shows how mud weight (i.e., sphere breakage) increases as a function of nozzle pressure and circulation time for different nozzles with 0.5 inch standoff distance. The data show that the rate of breakage increases (i.e., mud weight increase more) with increased pressure.

Figure 6-9 shows the percentage of broken spheres at 1 to 3 hours circulation time for nozzle pressures of 0 to 500 psi. The breakage rate without a nozzle (0 psi) is approximately 3%. This breakage is independent of pressure and impact velocity, indicating that it is due to breakage of malformed spheres. The graph shows that most of the spheres break in the first hour and that the breakage rate decreases with time once the weaker spheres are broken. This shows that a reused HGS mud should perform better than a new HGS mud since the weaker spheres will already have been broken.

The data show that breakage increases with increased pressure. After 3 hours at 500 psi, 35% of the spheres were broken. However, this raises the mud weight only from 6.5 lb/gal to 7.3 lb/gal — a 12% increase. The mud weight can be held constant by continually adding spheres to make up for the broken spheres.

6.2.2 Effect of Standoff Distance

The standoff distance between the nozzle and rock has a significant effect on sphere breakage since sphere breakage decreases with increased standoff distance (**Figure 6-10**).

Figure 6-11 shows how sphere breakage decreases as the nozzle standoff distance is increased from 0.5 to 6 inches for nozzles operating at 500 psi pressure.

The 1.5- and 3-inch standoff tests were stopped after 2 hours because of pump failures. These data show that for 3 hours circulation, the breakage decreases from 35% to 13% as the standoff distance is increased from 0.5 in. to 6 in. This corresponds to a mud weight change of only about 0.3 pounds per gallon.

6.2.3 Safe Operating Range

Figure 6-12 shows the safe operating zone where less than 15% of the spheres were broken after the equivalent of two days circulating time.

HGS Breakage During Drilling

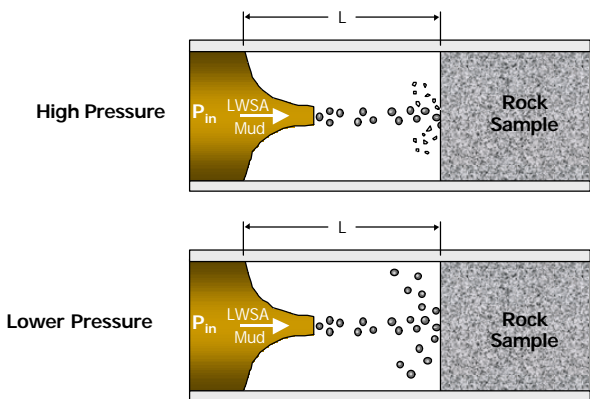


Fig. 6-7. High Pressure Increases Sphere Breakage

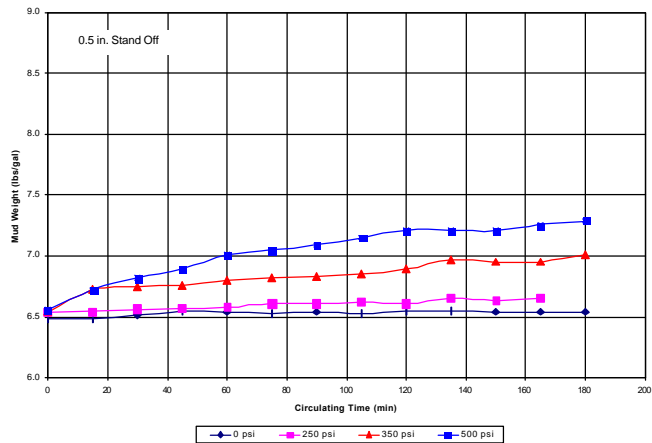


Fig. 6-8. Sphere Breakage in Nozzle Pressure

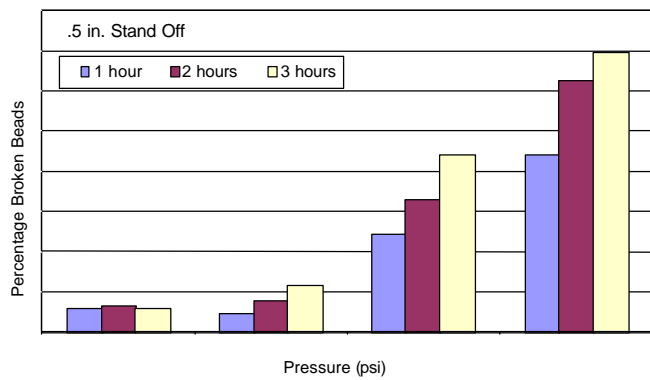


Fig. 6-9. Sphere Breakage vs Circulating Time

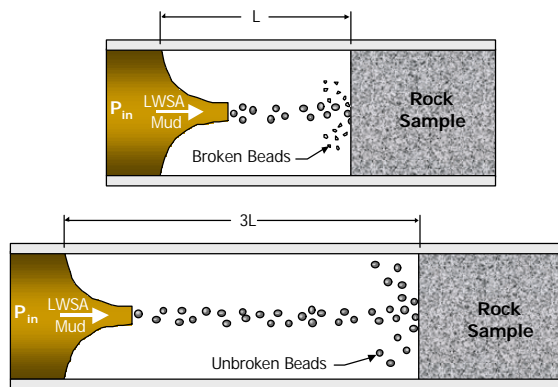


Fig. 6-10. Reduced Sphere Breakage with Increased Distance

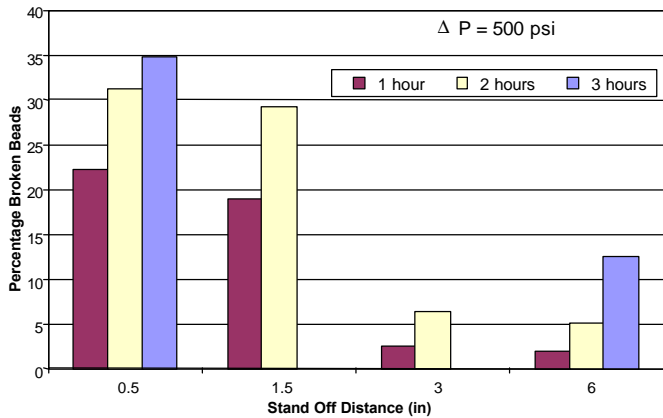


Fig. 6-11. Sphere Breakage as a Function of Distance

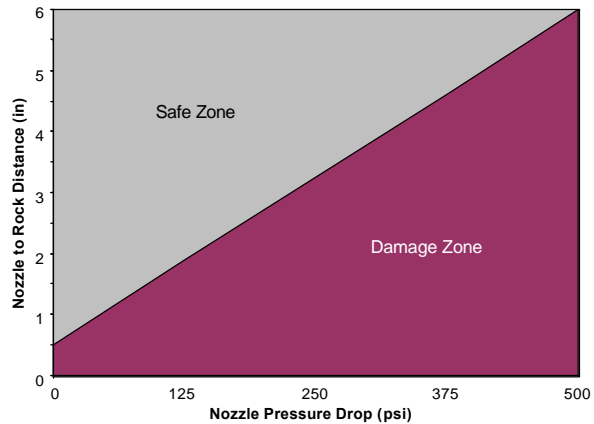


Fig. 6-12. Safe Operating Zone

6.3 CONCLUSIONS

1. HGS breakage during impact with the rock is not a major problem.
2. Sphere breakage increases with increased nozzle pressure and decreased nozzle standoff distance.
3. Weak, malformed spheres (5 to 10%) tend to break on their first pass through the nozzles.
4. Once the weak spheres are broken, there is minimal breakage unless very short standoffs (less than 0.5 inch) or high nozzle pressures (over 500 psi) are used.

7. Effect of HGS on Drilling Rate

7.1 LABORATORY TESTS

Drilling tests were conducted in the Drilling Research Center (DRC) high-pressure drilling stand in Houston to determine the effect of the HGS on drilling rate (**Figure 7-1**).

This drilling stand simulates deep oil-well drilling by applying higher fluid pressure in the wellbore than in the formation ($P_w > P_f$) to create a differential pressure across the hole bottom (**Figure 7-2**).

Drilling tests were conducted in sandstone and limestone at differential pressures of 0, 750 and 1500 psi with PDC and roller bits (**Figure 7-3**).

The drilling tests showed the following:

1. PDC bits drill sandstone and limestone much faster than roller bits.
2. Drilling rates decreased 50 to 90% as the differential pressure was increased from 0 to 1500 psi.
3. Differential pressure decreased drilling rates more with PDC bits than with roller bits.
4. At atmospheric pressure (0 psi), drilling rates were identical with and without HGS.
5. At higher differential pressures (750 and 1500 psi), HGS reduced drilling rates slightly in three of the four tests, possibly due to reduced jet impact and increased chip hold-down effects.

7.2 DIFFERENTIAL PRESSURE EFFECTS

Differential pressure between the wellbore and formation fluids has a major effect on drilling rate. **Figure 7-4** shows that drilling rate in Indiana limestone decreased from 10.4 to 1.04 ft/hr as differential pressure was increased from 0 to 2,000 psi. Similar decreases in drilling rate are observed in other sedimentary rocks (e.g., sandstone, shale and marble).

This reduction in drilling rate is due to poor hole cleaning caused by a “chip hold-down” effect which prevents rock cuttings from being removed from the craters between bit tooth impacts (**Figure 7-5**).

Drilling Tests

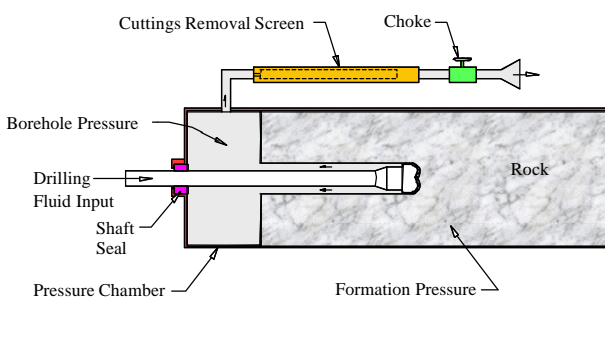


Fig. 7-1. DRC High Pressure Drilling Stand

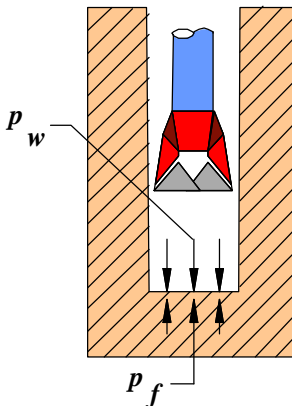


Fig. 7-2. Simulated Bottom Hole Conditions

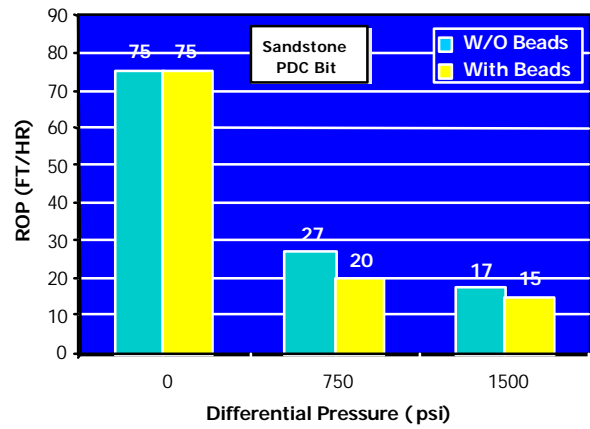
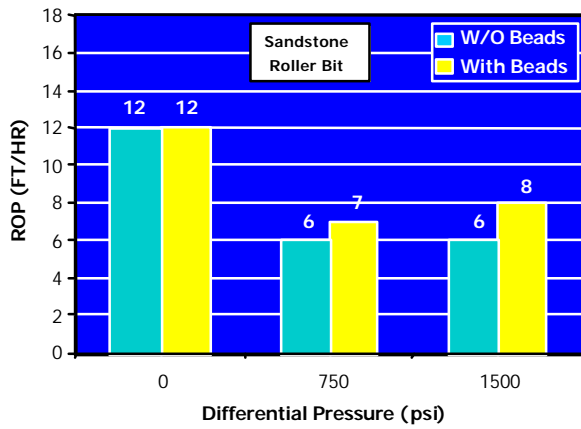
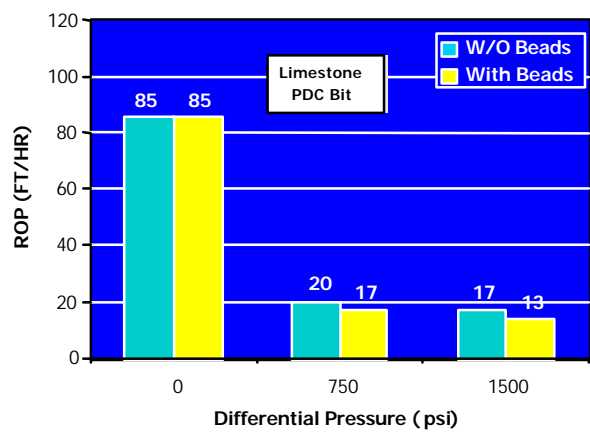
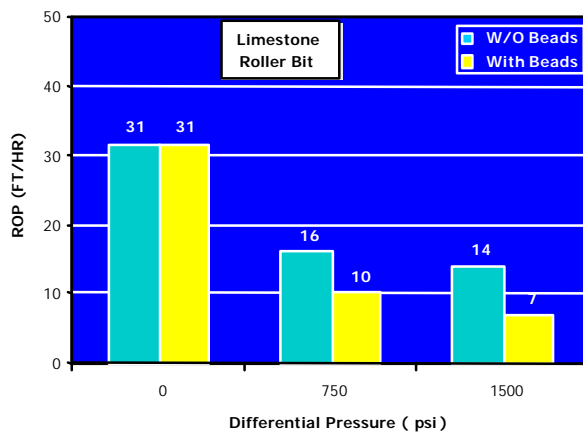


Figure 7-3. DRC Drilling Test Data

Drilling Mechanisms

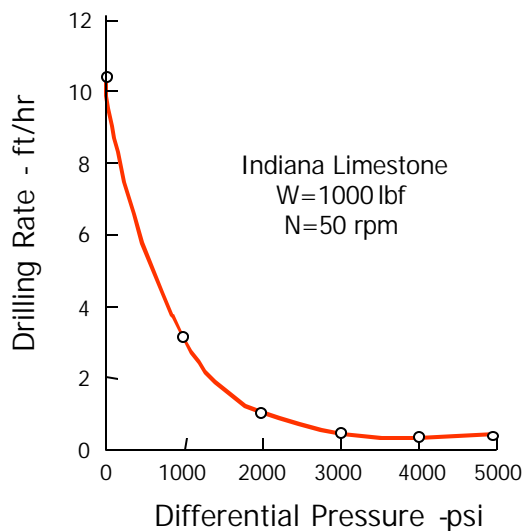


Fig. 7-4. Drilling Rate vs. Differential Pressure (Murray & Cunningham, 1955)

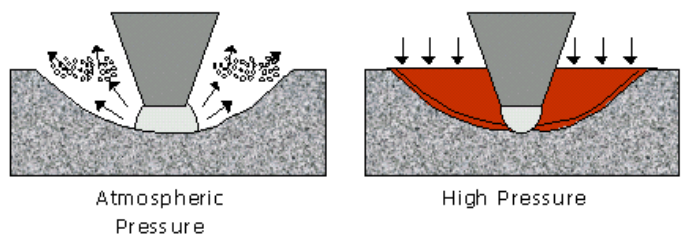


Fig. 7-5. Chip Hold-Down Effects (Maurer, 1965)

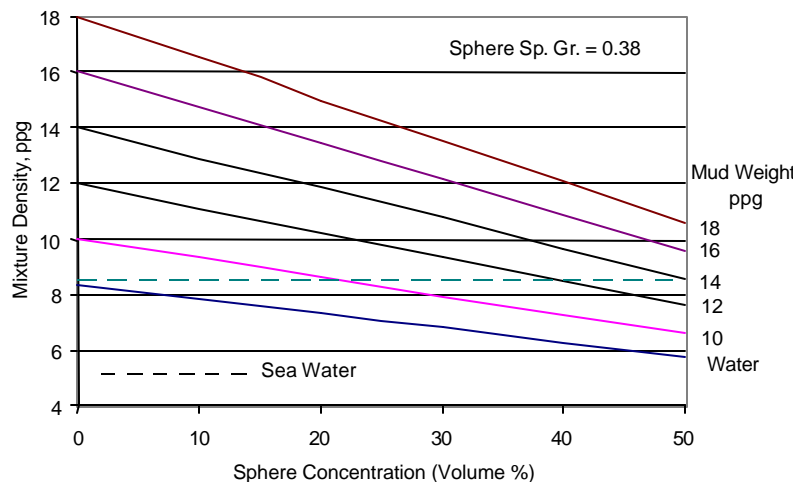


Fig. 7-6. Mud Density vs. Sphere Concentration

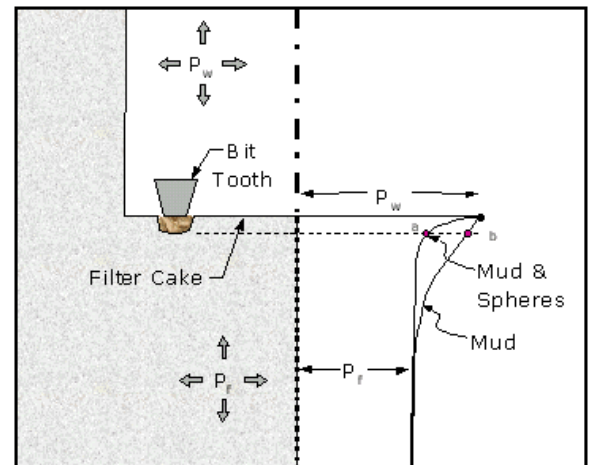


Fig. 7-7. Chip Hold-Down Pressure Gradients

A crushed zone is formed beneath a roller bit tooth as load is applied to the drill bit. At a critical bit load, curved fractures propagate to the surface of the rock. At atmospheric pressure, cuttings fly from the center when these fractures are formed, providing “perfect” cleaning and no regrinding of cuttings. In deep wells, high pressures hold the cuttings in the crater causing regrinding of the cuttings and reduced drilling rates.

In a normally-pressured formation, fluid pressure in the pore spaces equals the pressure exerted by a column of water extending to the surface. At a depth of 10,000 feet, a 10-ppg mud exerts a pressure of 5200 psi in the wellbore compared to 4330 psi for a column of water (8.34 ppg), corresponding to a differential pressure of 870 psi. **Figure 7-4** shows that 870-psi differential pressure would decrease the drilling rate in Indiana limestone from 10.4 to 3.5 ft/hr, a 66% reduction.

Figure 7-6 shows that 21% hollow spheres reduce the density of a 10-ppg mud to 8.34, resulting in no differential pressure and a drilling rate increase from 3.5 to 10.2 ft/hr.

Drilling rate increases of 1.5- to 3-fold are typically observed with foam drilling and 2- to 5-fold increases are observed with air drilling due to reduction in differential pressure at the hole bottom.

7.3 BIT JET EFFECTS

Drill cuttings are removed from the hole bottom by fluid jets on the drill bits. The jet impact force, F , tending to remove the rock cuttings from the hole bottom equals (Bourgoyn et al., 1986).

$$F = 0.01823 c_d q \sqrt{\rho \Delta p} \quad \text{lbs} \quad (7-1)$$

where

c_d = Nozzle Coefficient (0.94)

q = Flow Rate (gpm)

ρ = Fluid Density (ppg)

Δp = Pressure Drop (psi)

Eq. 7-1 shows that the jet impact force varies as the square root of the fluid density $\tilde{\rho}$. The 36% sphere concentration used in these tests reduced the density of the water (plus polymer) from 8.34 to 6.41 ppg which reduced the jet impact force by a factor of

$$\frac{F_2}{F_1} = \sqrt{6.41/8.34} = 0.87 \quad (7-2)$$

This reduction in jet impact force may account for some reduction in drilling rate, in addition to changes in pressure gradients at the hole bottom.

7.4 PRESSURE GRADIENT EFFECTS

The hollow spheres plug the rock pore spaces at the rock surface, causing a much steeper pressure gradient at the rock surface ($P_w - a$) than caused by mud particles which move deeper into the rock ($P_w - b$). This high differential pressure causes increased chip hold-down and slightly more reduction in drilling rate than conventional muds without the spheres (**Figure 7-7**).

Reduction in drilling rate due to this pressure gradient effect is usually more than offset by the large drilling rate increase due to reduction in mud density and differential pressure produced by the HGS.

7.5 CONCLUSIONS

The following conclusions were reached as a result of these tests:

1. Reducing bottom-hole pressure by the use of HGS can significantly increase drilling rates with both roller and PDC bits.
2. HGS have no effect on drilling rate at atmospheric pressure.
3. At high differential pressures, HGS reduce drilling rates slightly.

8. Effect of HGS on Formation Damage

To address concern that hollow glass spheres (HGS) could cause excessive formation damage due to their small size (8 to 100 microns), laboratory tests were conducted. The first series of laboratory tests showed that HGS would cause less formation damage than water-base muds without spheres. These tests are described in Sections 8.1 to 8.7.

The application of HGS in fluids used for drilling into producing formations (“drill-in fluids”) was investigated with a second series of tests. These results are described in Section 8.9. A separate Topical Report (McDonald et al., 2001) describing this work was also prepared by MEI, Texas A&M and DCFT. These tests showed that drilling and drill-in fluids properly designed with HGS would not cause additional formation damage as compared to fluids with other additives, and in certain cases could be an overall enhancing additive.

8.1 FORMATION DAMAGE MECHANISMS

When a well is drilled with water-base mud, bentonite and drill solids in the mud flow into the rock pore spaces and partially plug the formation, causing “skin damage” near the rock surface (**Figure 8-1**).

The “skin” or damaged zone has higher permeability than the virgin rock, causing a high pressure drop across the damaged zone which can significantly reduce oil and gas production rates (**Figure 8-2**).

The production rate for a vertical well with Darcy flow equals:

$$Q = \frac{2\pi K H [P_e - P_w]}{B \mu [\ln(R_e/R_w) + S]} \quad (8-1)$$

where

Q	= Production Rate (cm^3/sec)	P_w	= Bottom-Hole Flowing Pressure (atm)
K	= Rock Permeability (md)	μ	= Fluid Viscosity (cp)
H	= Formation Thickness (cm)	R_e	= Drainage Radius (cm)
B	= Formation Volume Factor (RB/STB)	R_w	= Wellbore Radius (cm)
P_e	= Reservoir Pressure (atm)	S	= Skin Factor (Dimensionless)

The ratio of well productivity with and without formation damage equals:

$$\frac{Q_d}{Q_i} = \frac{\ln(R_e/R_w)}{\ln(R_e/R_w) + S} \quad (8-2)$$

Formation Damage Mechanisms

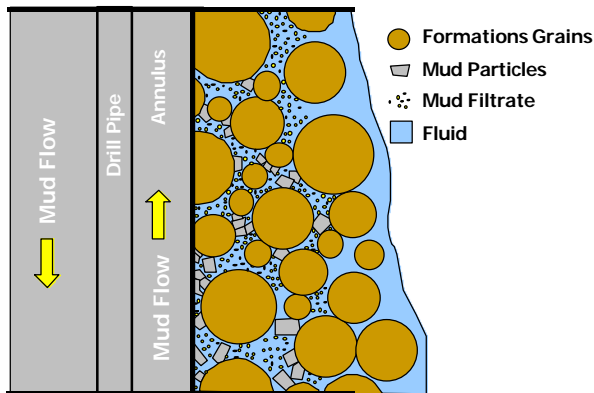


Fig. 8-1. Formation Damage Mechanism

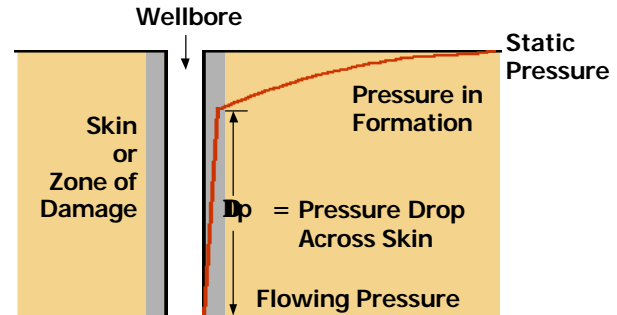


Fig. 8-2. Formation Pressure Gradient
(Gray et al., 1980)

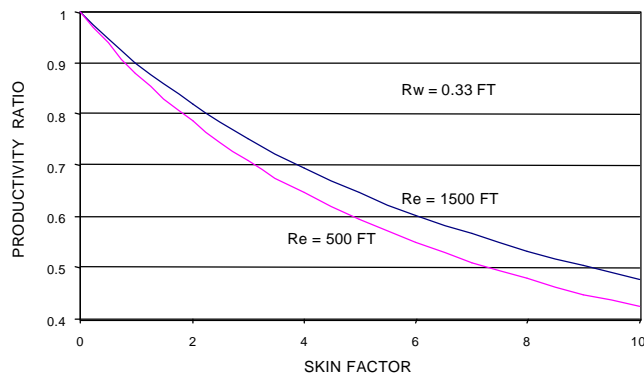


Fig. 8-3. Drilling Rate vs. Differential Pressure

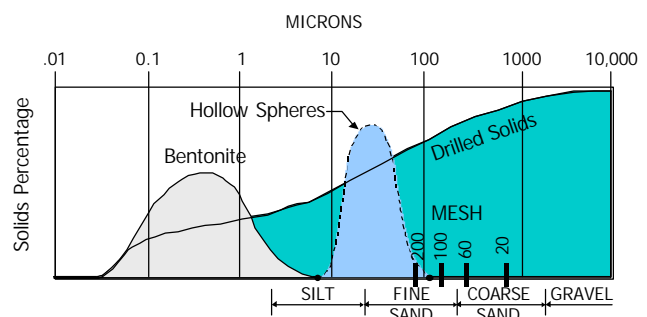


Fig. 8-4. Water-Based Mud Particle Size
(Bourgoyn et al., 1986)

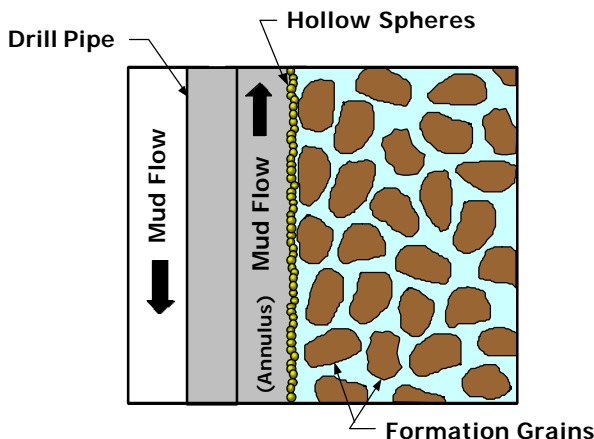


Fig. 8-5. Hollow Sphere Filter Cake

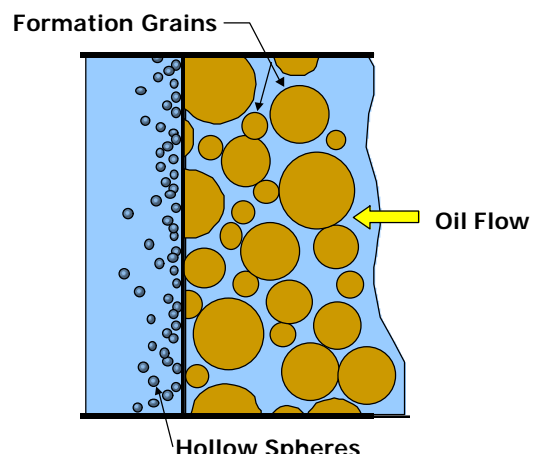


Fig. 8-6. Hollow Sphere Cleanup

where

$$Q_d = \text{Flow Rate with Formation Damage} \quad (\text{cm}^3/\text{sec})$$

$$Q_i = \text{Flow Rate without Formation Damage} \quad (\text{cm}^3/\text{sec})$$

Eq. 8-2 shows that the productivity ratio is a function of reservoir drainage radius, R_e , wellbore radius, R_w , and skin factor, S . **Figure 8-3** shows that with a 1,500-foot drainage radius ($R_e = 1,500$), the well productivity ratio for an 8-inch diameter well ($R_w = 0.333$ ft) decreases from 1.0 to 0.48 as the skin factor increases from 0 to 10, whereas with a 500-foot drainage radius, the productivity ratio decreases from 1.0 to 0.43. Skin factors of 3 to 5 are common, which shows that formation damage can reduce well productivity by 30 to 40%, demonstrating the benefits of underbalanced drilling.

HGS are considerably larger than bentonite particles and most of the drill solids (**Figure 8-4**). As a result, the hollow spheres form a “filter cake” at the surface of the rock and do not migrate deep into the rock like bentonite particles or drill cuttings (**Figure 8-5**). When reverse flow occurs (i.e., the well is produced), the glass spheres are flushed from the rock surface and there is no permanent formation damage or skin effect (**Figure 8-6**). As a result, wells drilled with water-base muds containing HGS produce oil and gas at much higher rates than those drilled without spheres.

8.2 LABORATORY TEST PROCEDURE

A series of tests was conducted at MUDTECH Laboratories, Inc., in Houston to determine if HGS cause serious damage to potential producing formations. These tests were conducted using the formation damage test apparatus shown in **Figures 8-7 and 8-8**.

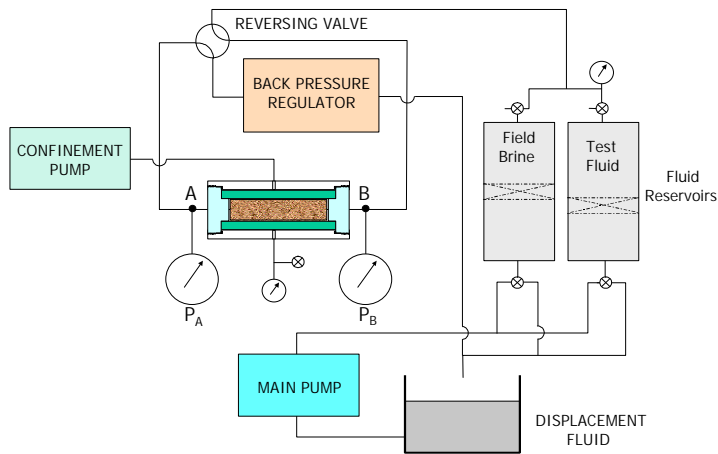


Figure 8-7. Formation Damage Test Apparatus

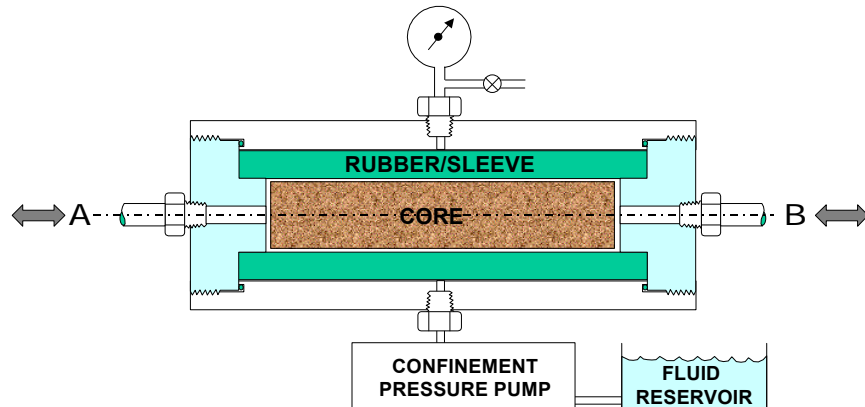


Figure 8-8. Formation Damage Test Cell

Tests were conducted with HGS concentrations of 0 to 36% in five different fluids with 2,500 psi confining pressure (**Table 8-1**). The chemistry of these fluids is given in Chapter 5.

Table 8-1. Simulated Drilling Fluids Tested

Fluid	HGS Concentration (%)			
	0	16	26	36
PHPA Drilling Fluid	x	x	x	x
Oil Base Drilling Fluid	x	x	x	x
Synthetic Drilling Fluid	x			x
3% KCl Drilling Fluid	x			x
ZnBr ₂ Brine	x			x

The formation damage tests were conducted in Berea Sandstone cores (15 to 20 md) saturated with field brine. Cores were prepared as follows:

- Fourteen 1" diameter x 2" long cores were drilled from a block of Berea sandstone. The cores were cleaned with methanol, dried at 65EC for 16 hours, measured, and weighed.
- The cores were then saturated with simulated field brine under 20 inches of mercury vacuum, allowed to equilibrate for at least 24 hours, and then reweighed.
- Porosity was determined by subtracting the dried weight from the saturated weight and dividing by the specific gravity of the field brine.

The following procedure was used for each test:

Step 1: Install and Pressurize Core:

A fresh core was installed in the test cell and the confining pressure was raised to 2,500 psi.

Step 2: Determine Initial Core Permeability:

Flow was established with the field brine in the normal production direction, from A to B in **Figure 8-8**. Pressures were measured and initial core permeability calculated.

Step 3: Drilling Fluid Testing:

A test fluid (mud or brine) was then flowed through the core in the opposite direction (B to A) to simulate flow from the wellbore into the rock during drilling. A pressure of 500 psi was maintained across the core for four hours to allow solids to flow into (and damage) the core.

Step 4: Simulated Production Cleanup:

Field brine was then flowed in the producing direction (A to B) to simulate well cleanup (i.e., removal of plugging particles). A maximum of 100 pore volumes was flowed, with measurements made and return permeabilities calculated at 10 pore-volume increments.

Step 5: Core Shaving:

After the cleanup flow period, the system was depressured, disassembled, and 1/8" was carefully shaved from the wellbore exposed end (B) of the core.

Step 6: Core Permeability Retest:

The core was retested and the permeability calculated in the producing direction (A to B) to determine how deep the damage had penetrated into the core.

8.3 LABORATORY TEST RESULTS

Formation damage tests were conducted with four drilling fluids:

- PHPA Water-Base Drilling Fluid
- Oil-Base Drilling Fluid
- Synthetic Oil Drilling Fluid
- KCl Drilling Fluid

and one completion brine (no solids):

- KCl Brine

with 0 to 36% HGS.

8.4 PHPA WATER-BASE DRILLING FLUID

With a PHPA water-base drilling fluid with no spheres, the mud produced a permanent permeability reduction of 43%, whereas with 16 to 36% spheres, there was no permanent damage (**Figure 8-9**). This shows that production from a well drilled with a water-base drilling fluid containing HGS would be significantly higher than a well drilled with a water-base drilling fluid containing no spheres.

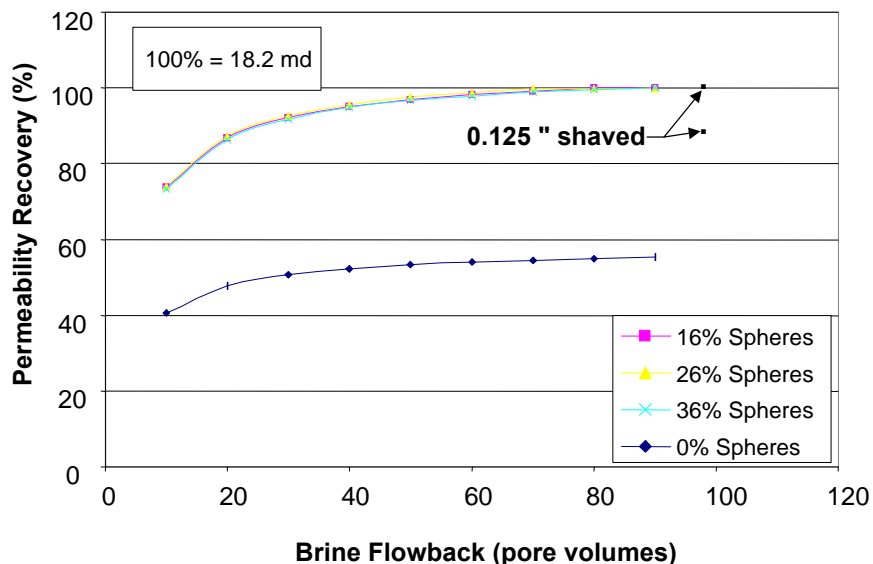


Figure 8-9. Permeability Recovery with PHPA Water-Base Drilling Fluid

Shaving off 0.125 inch of the damaged surface increased the permeability recovery for the water-based mud without spheres from 47 to 87.5%, showing that most of the damage was in the top 0.125 inch layer.

Table 8-2 shows how the core permeability changed during cleanup.

Table 8-2. Permeability Recovery with PHPA Fluid

	PHPA w/0% HGS		PHPA w/16% HGS	
	Permeability (md)	Recovery (%)	Permeability (md)	Recovery (%)
Initial Brine Permeability	18.2	100.0	18.2	100.0
Permeability with Test Fluid	5.7	31.3	4.8	26.4
Return Permeability				
10 pore volumes	7.4	40.5	13.4	73.7
20 pore volumes	8.7	47.7	15.8	86.7
30 pore volumes	9.2	50.7	16.7	92.1
40 pore volumes	9.5	52.3	17.3	95.1
50 pore volumes	9.7	53.3	17.6	96.9
60 pore volumes	9.8	54.0	17.9	98.2
70 pore volumes	9.9	54.6	18.0	99.2
80 pore volumes	10.0	55.9	18.2	100.0
90 pore volumes	10.0	55.3	—	100.0
100 pore volumes	10.1	55.5	—	100.0
(1/8" shaved)	15.9	87.4	18.2	100.0
	PHPA w/26% HGS		PHPA w/36% HGS	
	Permeability (md)	Recovery (%)	Permeability (md)	Recovery (%)
Initial Brine Permeability	18.2	100.0	18.2	100.0
Permeability with Test Fluid	3.4	18.7	3.1	17.0
Return Permeability				
10 pore volumes	13.5	74.1	13.3	73.4
20 pore volumes	15.8	87.2	15.7	86.4
30 pore volumes	16.8	92.6	16.7	91.8
40 pore volumes	17.4	95.6	17.2	94.8
50 pore volumes	17.7	97.5	17.6	96.7
60 pore volumes	18.0	98.8	17.8	97.9
70 pore volumes	18.2	100.0	18.0	98.9
80 pore volumes	—	100.0	18.1	99.6
90 pore volumes	—	100.0	18.2	100.0
100 pore volumes	—	100.0	—	100.0
(1/8" shaved)	18.2	100.0	18.2	100.0

After four hours exposure, the water-base PHPA drilling fluid without spheres reduced the permeability of the core from 18.2 to 5.7 md and then recovered to 10.1 md after 100 pore volumes of cleanup. After shaving 1/8" from the core, the permeability increased to 15.9 md showing that the PHPA drilling fluid invaded the core and caused damage.

When 16 to 36% spheres were added to the PHPA drilling fluid, the permeabilities were reduced to 3.1 to 4.8 md, but cleaned up to 100% after 70 to 90 pore volumes of backflow. Shaving 1/8" from the core confirmed that the permeability had returned to its original value. The reduction in

permeability and subsequent recovery with the HGS indicate that the spheres form a filter cake and do not enter the formation, and clean up rapidly with backflow.

THESE TEST RESULTS SHOW THAT HOLLOW GLASS SPHERES CAN SIGNIFICANTLY REDUCE FORMATION DAMAGE WHEN DRILLING WITH WATER-BASE MUDS. THIS FINDING COULD HAVE A SIGNIFICANT IMPACT ON UNDERBALANCED DRILLING AND SHOULD BE PURSUED EITHER AS A PHASE III OR A NEW PROJECT. THIS CONCEPT MAY BE PATENTABLE AND POSSIBLY HAS COMMERCIAL VALUE.

8.5 OIL-BASE AND SYNTHETIC-OIL DRILLING FLUIDS

Tests showed that with oil-base and synthetic-oil fluids, the reduction in permeability was identical with and without spheres and in both cases all of the damage was removed (100% recovery) after 100 pore volume backflow of the brine (**Figures 8-10 and 8-11 and Table 8-3**).

Effect of HGS on Formation Damage

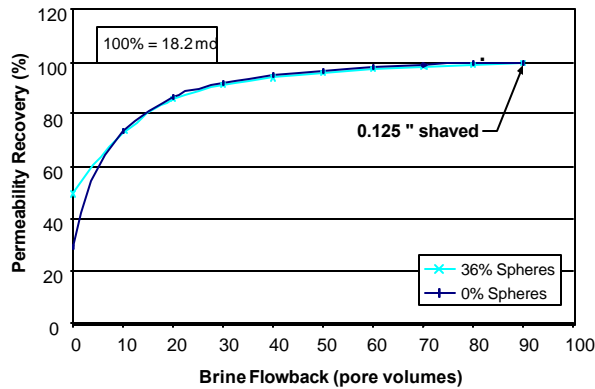


Fig. 8-10. Permeability Recovery with Oil-Based Drilling Fluid

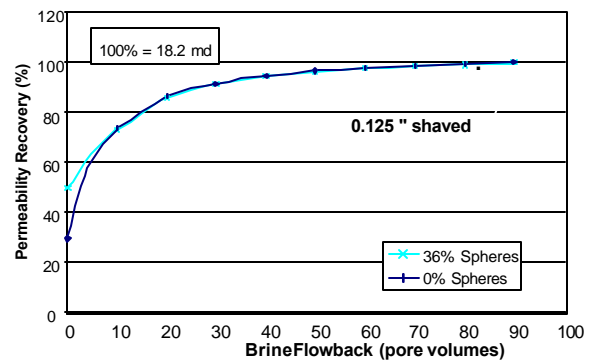


Fig. 8-11. Permeability Recovery with Synthetic Oil Drilling Fluid

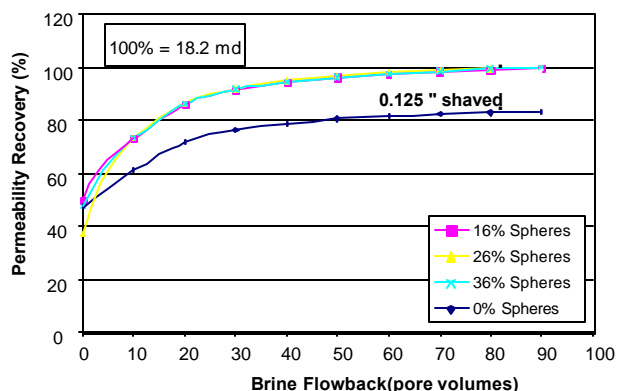


Fig. 8-12. Permeability Recovery with Potassium Chloride Brine

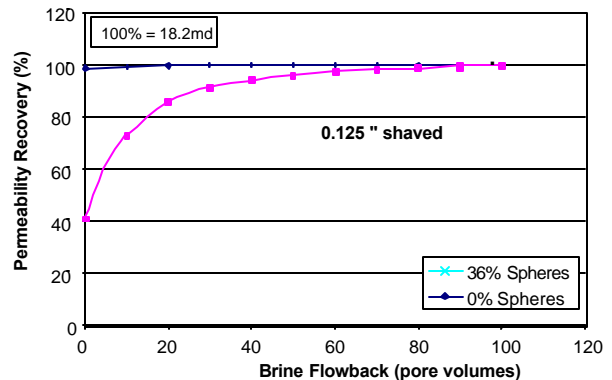


Fig. 8-13. Permeability Recovery with Zinc Bromide Brine

Table 8-3. Permeability Recovery with Oil and Synthetic Fluids

	OIL BASE		OIL BASE w/36% LWSA	
	Permeability (md)	Recovery (%)	Permeability (md)	Recovery (%)
Initial Brine Permeability	18.2	100.0	18.2	100.0
Permeability with Test Fluid	5.8	31.9	7.0	47.8
Return Permeability				
10 pore volumes	13.4	73.6	13.2	72.8
20 pore volumes	15.7	86.6	15.6	85.7
30 pore volumes	16.7	92.0	16.5	91.0
40 pore volumes	17.3	94.9	17.1	93.9
50 pore volumes	17.6	96.9	17.4	95.8
60 pore volumes	17.8	98.2	17.6	97.1
70 pore volumes	18.0	99.1	17.8	98.0
80 pore volumes	18.1	99.8	17.9	98.7
90 pore volumes	18.2	100.0	18.0	99.3
100 pore volumes	—	—	18.1	99.7
(1/8" shaved)	18.2	100.0	18.2	100.0
Initial Brine Permeability	17.7	100.0	17.7	100.0
Permeability with Test Fluid	5.0	28.2	4.7	47.8
Return Permeability				
10 pore volumes	12.9	73.1	12.9	73.0
20 pore volumes	15.2	86.0	15.2	85.8
30 pore volumes	16.2	91.4	16.1	91.2
40 pore volumes	16.7	94.3	16.7	94.1
50 pore volumes	17.0	96.2	17.0	96.0
60 pore volumes	17.2	97.5	17.2	97.3
70 pore volumes	17.4	98.4	17.4	98.2
80 pore volumes	17.5	99.1	17.5	98.9
90 pore volumes	17.6	99.7	17.6	99.5
100 pore volumes	17.7	100.0	17.7	100.0
(1/8" shaved)	17.7	100.0	17.7	100.0

Neither the oil base nor the synthetic base drilling fluids, with or without HGS, caused any permanent damage to the cores. After an initial permeability reduction, the permeabilities returned to their original values after 100 pore volumes of clean up flow.

8.6 3% KCl DRILLING FLUID

Potassium Chloride (3% KCl) drilling fluid with no HGS provided a permanent permeability reduction of 17% (83% recovery) that could not be cleaned up by backflow, whereas with the HGS (16 to 36%), no permanent damage was done to the cores (**Figure 8-12** and **Table 8-4**).

These tests show that the addition of 16% or more spheres in Potassium Chloride drilling fluid can significantly reduce formation damage and thereby significantly increase oil and gas production rates.

Table 8-4. Permeability Recovery with KCl Fluid

	3% KCl HGS		3% KCl w/16% HGS	
	Permeability (md)	Recovery (%)	Permeability (md)	Recovery (%)
Initial Brine Permeability	18.2	100.0	18.2	100.0
Permeability with Test Fluid	8.7	47.8	9.1	50.0
Return Permeability				
10 pore volumes	11.1	61.1	13.3	73.1
20 pore volumes	13.1	71.9	15.6	86.1
30 pore volumes	13.9	76.4	16.6	91.4
40 pore volumes	14.3	78.9	17.1	94.4
50 pore volumes	14.6	80.5	17.5	96.2
60 pore volumes	14.8	81.5	17.7	97.5
70 pore volumes	15.0	82.3	17.9	98.5
80 pore volumes	15.1	82.9	18.0	99.2
90 pore volumes	15.2	83.4	18.1	99.7
100 pore volumes	15.2	83.7	18.2	100.0
(1/8" shaved)	17.2	94.5	18.2	100.0
Initial Brine Permeability	18.2	100.0	18.2	100.0
Permeability with Test Fluid	7.0	38.5	3.1	47.8
Return Permeability				
10 pore volumes	13.4	73.5	13.3	73.4
20 pore volumes	15.7	86.5	15.7	86.4
30 pore volumes	16.7	91.9	16.7	91.8
40 pore volumes	17.2	94.8	17.2	94.8
50 pore volumes	17.6	96.7	17.6	96.7
60 pore volumes	17.8	97.9	17.8	97.9
70 pore volumes	18.0	98.9	18.0	98.9
80 pore volumes	18.1	99.6	18.1	99.6
90 pore volumes	18.2	100.0	18.2	100.0
100 pore volumes	—	—	—	—
(1/8" shaved)	18.2	100.0	18.2	100.0

The 3% KCL drilling fluid without HGS reduced the permeability of the core from 18.2 to 8.7 md and then recovered to 15.2 md after 90 pore volume backflow. After shaving 1/8" from the core, the permeability increased to 17.2 md. This indicates that the 3% KCL drilling fluid caused internal damage to the core.

With 16 to 36% spheres, the 3% KCL drilling fluid reduced the permeability to 3.1 to 9.1 md, with all the damage being cleaned up after 90 to 100 pore volume backflow in all cases. Shaving 1/8" from the core confirmed that the permeabilities had returned to their original values. The reduction in permeability and subsequent recovery with spheres indicates that the spheres form a filter cake on the rock surface, but do not permanently damage the formation.

THESE TESTS SHOW THAT THE HOLLOW SPHERES CAN REDUCE FORMATION DAMAGE WITH KCI DRILLING FLUIDS AND THEREFORE INCREASE OIL AND GAS PRODUCTION IN WELLS DRILLED WITH THESE FLUIDS.

8.7 ZnBr BRINE

Zinc Bromide brine with HGS produced slightly more damage than the brine without the spheres, but with 100 pore volumes of backflow all of the damage was removed in both cases and there was 100% recovery (**Figure 8-13** and **Table 8-5**).

Table 8-5. Permeability Recovery with ZnBr₂ Fluid

	ZnBr ₂		ZnBr ₂ w/36% HGS	
	Permeability (md)	Recovery (%)	Permeability (md)	Recovery (%)
Initial Brine Permeability	18.0	100.0	17.7	100.0
Permeability with Test Fluid	17.7	98.3	7.5	42.4
Return Permeability				
10 pore volumes	17.8	99.1	12.9	72.9
20 pore volumes	17.9	99.7	15.2	85.8
30 pore volumes	18.0	100.0	16.1	91.2
40 pore volumes	—	—	16.7	94.1
50 pore volumes	—	—	17.0	95.9
60 pore volumes	—	—	17.2	97.3
70 pore volumes	—	—	17.4	98.2
80 pore volumes	—	—	17.5	98.9
90 pore volumes	—	—	17.6	99.5
100 pore volumes	—	—	17.7	100.0
(1/8" shaved)	18.0	100.0	17.7	100.0

The ZnBr₂ brine fluid without spheres initially reduced the permeability by only 1.7%. This damage was removed after only 30 pore volumes of backflow. The ZnBr₂ brine with 36% HGS reduced permeability to 7.5 md, but the original permeability was completely recovered after 100 pore volumes of backflow.

8.8 HGS FOR REDUCING FORMATION DAMAGE DURING DRILLING

As a further study of the results described above, work was conducted at the Completions Technology Laboratory of the Petroleum Engineering Department at Texas A&M University to evaluate the performance of HGS materials to mitigate formation damage in drilling fluids, completion fluids, and drill-in fluids (DIFs). Formation damage was of special concern. Formation damage is not generally considered an attribute of drilling fluids. Nonetheless, since drilling fluids are often employed in drilling productive zones and DIFs must exhibit acceptable drilling fluid characteristics, both families of materials were considered. A separate Topical Report (McDonald et al., 2001) was prepared with detailed results from the analysis and experimental investigation. The report was written to provide a basis for the evaluation of fluid additives – in this case, HGS – as beneficial materials in well construction fluids. A summary of the Topical Report is presented below along with conclusions from that study.

8.8.1 Review of Technology

To establish a clear context for use of HGS as an additive in well-construction fluids, the Topical Report first presents a review of fluid technology used in drilling fluids, DIFs and completion fluids. It defines the terminology used by specialists in each part of this industry activity. Special attention is given to the chemical and other materials that constitute these increasingly complex fluids.

New demands are constantly being placed on well-construction fluids. Ten years ago, the industry had not yet drilled a subsalt well or completed a horizontal well in the Gulf of Mexico. Today these and other technologies are provided as standard services by drilling contractors and service companies. This report highlights these new technologies, compares fluid performance, and attempts to evaluate the role of new additives in well-construction fluids.

New lightweight HGS additives have been investigated for lowering the density of drilling fluids. This type of fluid can overcome the disadvantages from which conventional underbalanced drilling fluids suffer. However, before engineers can incorporate these materials into new drilling, completion, and DIFs, data must be developed on the new systems and their performance in a number of areas. Section 1 of the report reviews the functions of wellbore construction fluids, and "sets the table" for the experimental tests described in Section 2.

S38 HGS materials were used for laboratory tests performed at Texas A&M. The density of this product is 0.38 g/cc and it exhibits a burst strength of 4000 psi. Diameter of the HGS ranges from 8 to 125 microns, with a median of 45 microns. The material is borosilicate glass and is chemically stable under most conditions found in oil and gas applications. HGS will pass through 20 to 80 mesh screens typically used on oil-field shakers. These microspheres are widely used as extenders in paints, adhesives, and other materials to reduce costs.

The particle size of HGS materials lies between fine sand and silt. The major effect of HGS on drilling fluids is to reduce density. HGS are reported to be employed in fluids at concentrations up to 50% by volume with corresponding reductions in density of typically 30% or more.

In recent years, the industry has come to understand that most formation damage is the result of wellbore wall damage at the surface of the formation rather than from internal formation blocking. Results from previous studies suggested that HGS were effective at reducing formation damage. However, this interpretation does not describe the conditions fully. Section 2 of the Topical Report discusses formation damage in a more complete fashion. Included in this section are experimental data collected at Texas A&M in the Department of Petroleum Engineering's Completions Laboratory on "baseline fluids" for illustrating the difference between typical drilling fluids and those containing HGS. This study also complements previous work conducted on this project (see Sections 8.1 to 8.7) as well as previous laboratory studies conducted by Texas A&M on formation damage in producing zones.

Texas A&M investigators examined the role of drill solids in causing formation and completion damage in horizontal open-hole completions. A variety of core flow techniques were employed to simulate DIF filter-cake deposition and well production in horizontal open-hole completions. The wellbore flow equipment was designed to emulate conditions in either completely open holes without sand-control screens or unconsolidated open-hole sections with sand-control screens.

One of the most important observations derived from this recent work indicates that the filter cakes developed by the DIFs tested formed on the surface of the formation rather than within the pore space. Therefore, the impairment of permeability was attributed completely to the external filter cake.

8.8.2 Experimental Evaluation of Fluid Additives

Advancements in the performance of well construction fluids have been most successful in 1) shale stability (wellbore) enhancement, 2) ROP increases, and 3) meeting environmental requirements. Superior filter cakes that isolate wellbore fluids from the formation improve wellbore stability. However, fluids and additives used to impart stability also have to meet the other criteria. HGS materials, being inert, do not interfere with chemical interactions and benefits of fluids, but rather make their presence felt by their bulk.

Two representative drilling fluids were chosen for evaluating rheology of HGS: PHPA fluids and KCL polymer muds. The former material has a higher solids content than the latter. Fluids with different concentrations of HGS were subjected to basic mud tests. Results were compared with the same systems without HGS.

Fluid system densities ranged from 8.35 ppg (no HGS) to 5.99 ppg (35% HGS). The system studied was the PHPA mud with bentonite solids, drill solids, and HGS solids. The data from the viscosity measurements are similar to that reported previously. As the solids content of the system was increased above about 15% HGS solids, the rheology began to deteriorate.

The high concentrations of solids in the test samples caused erratic rheology and poor API filter-loss control, greater than 45 ml in some cases. High fluid loss signifies thick filter-cake tendencies. Normal API data should be less than 10 ml. Larger values are significant, indicating poor fluid-loss control. Drilling fluids with poor fluid-loss control generally exhibit differential sticking characteristics unacceptable in most circumstances. Two of these filter cakes are shown in **Figure 8-14**.



Figure 8-14. Filter-Cake Thickness Contrasted with High Fluid-Loss Filter Cake

Fluid-loss additives (FLA) were added to KCL polymer low-solids drilling fluid. These materials are generally colloidal size such as modified starches and micronized cellulosics. Results showed the new samples had acceptable API fluid-loss test results and filter cakes typical of systems without HGS.

Analysis of the basics of drilling fluids, completion fluids, and DIFs, supported by experimental evidence obtained on different fluids using HGS, indicates that these materials impart new properties to their parent systems. Density of the fluids can be lowered significantly. Samples of HGS (5%) in a PHPA lowered density from 8.34 ppg to 7.35 ppg with little change in rheology. The HGS systems also behave as inert solids in these systems. PV change in a PHPA system for a 16% HGS system was roughly the same as addition of 6% drill solids (13 vs. 22). In water-base systems designed for drilling in depleted reservoirs or for drilling through formation with low parting pressures, HGS systems offer attractive alternates to other systems. **Best performance is achieved when HGS concentrations are less than 20% volume.**

The addition of HGS solids altered performance of drilling fluids and DIFs in the same manner as other inert solids. For example, API fluid loss increased from 8 ml to 45 ml when HGS concentration reached 15% in a PHPA system. This behavior in a drilling fluid would increase the tendency of the fluid to cause differential sticking. The cause for the alteration in filter-cake performance can be attributed to the narrow MW range of the HGS and its tendency to disrupt the

packing of particulates. Additional tests with added FLA (fluid-loss additives) reversed this tendency. Again, HGS systems with less than 20% microspheres offered best results.

Special core flow permeability tests were performed to determine if lift-off pressure and regain permeability would be affected by HGS. The low-solids KCL polymer DIF was specially formulated with FLA to ensure good filtrate control. Tests using the fluid indicated that there was essentially no difference in permeability regain with and without HGS (5.5 psi vs 5.0 psi and 1130 md vs. 1250 md). Comparison of these results with prior data from earlier tests by MEI shows that fluids designed for low fluid loss are not adversely affected by HGS while other types of fluids may be affected adversely.

8.9 CONCLUSIONS

1. There was no difference in formation damage by adding HGS to oil-base and synthetic-oil fluids.
2. $ZnBr_2$ brine without spheres produced essentially no formation damage (2%), whereas $ZnBr_2$ brine with spheres produced some damage. However, this damage was completely cleaned up with backflow.
3. A 3% KCl mud with spheres produced minor damage that was cleaned up with 100 pore volumes of backflow, whereas without the spheres, the 3% KCl mud produced permanent damage (16.3%) that could not be cleaned up with backflow.
4. The PHPA water-based mud with spheres produced minor damage that completely cleaned up (100% recovery) with 90 pore volumes of backflow. Without HGS, the PHPA mud caused considerable permanent damage (44.5%) that could not be cleaned up with backflow.
5. HGS can significantly reduce or eliminate formation damage with water-base and KCl drilling fluids and thereby significantly increase oil and gas production rates.
6. The use of hollow spheres to reduce formation damage may be patentable and may have commercial application.
7. The addition of HGS solids altered performance of special drill-in fluids in the same manner as other inert solids.
8. API fluid loss in drill-in fluids was increased by HGS, a behavior that increases the tendency of the fluid to cause differential sticking.
9. The best performance of HGS fluids with respect to formation damage was observed when HGS concentrations are less than 20% volume.

10. HGS materials impart unique density lowering characteristics to drilling fluids. However, these fluids must be specially tailored to avoid deterioration of basic drilling fluid properties typical of systems with high solids content. Accordingly, it is recommended that additional studies be performed if HGS materials are to be commercially employed in underbalanced-drilling applications. Well-construction fluids should be formulated "from the ground up" to take advantage of the properties of HGS materials.

9. HGS Drilling Fluid Field Tests

Several field tests have been conducted using HGS since this project was initiated. MEI conducted two successful field tests with HGS muds in Mobil Oil Corporation (now ExxonMobil) wells in Kern County, California in September 1996. These tests, described in Sections 9.1 to 9.3, showed that the hollow spheres can be easily mixed into the mud and that rheological properties of the lightweight mud were similar to conventional muds. No problems were encountered on these tests. The success of these tests demonstrate the high potential of using HGS for underbalanced drilling. An SPE paper was presented in 1997 to document this work and help transfer this technology (see **Appendix E**).

Another field application test was conducted by PDVSA-INTEVEP in Venezuela. This test is described in Section 9.4. An SPE paper describing this test is included in **Appendix F**.

To assure HGS drilling fluids are cost-effective, the HGS must be separated from the returning drilling mud and cuttings, and recycled into the cleaned drilling mud to maintain the proper fluid density. Section 9.5 describes work by others using centrifuging for effective separation of HGS for re-use.

9.1 MUD PIT

Figure 9-1 shows the mud pit system used in the 1700-ft Mobil wells for the initial field tests.



Figure 9-1. Golden State Drilling Rig Mud System

Two to four hundred barrels of mud containing 10 to 20% HGS were used on these wells.

9.2 MUD MIXING

A conventional diaphragm pump was used to transfer the HGS from 640 lb boxes into the fluid. Diaphragm pumps, also called cellar or trash pumps, are commonly found on most rigs. In fact, an identical pump was available on the test rig.

The diaphragm pump was capable of transferring 640 lbs of dry HGS to the mud per hour. The highest rate achieved was 640 lbs in 30 minutes. Air fluidization is typically used to inject the hollow spheres into fluids. If air fluidization had been used, 640-lb boxes of HGS could have been transferred to the mud in 5 to 10 minutes. None of the HGS became airborne during these mixing operations because they were injected through a hose placed in the hopper.

9.3 LIGHTWEIGHT MUD PROPERTIES

The rheological properties were kept within acceptable limits ($PV = 10$ to 25 cp; $YP = 5$ to 10 lb/100 sf) throughout the tests. The theoretical and actual mud weights were close in both wells showing that there was minimal breakage of the hollow spheres (**Figures 9-2 and 9-3**).

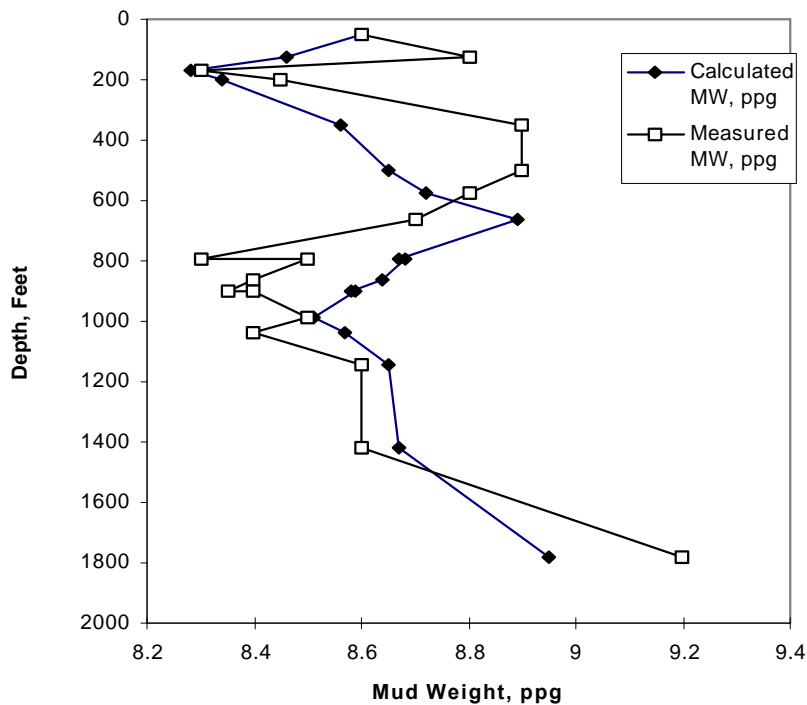


Figure 9-2. Theoretical and Measured Mud Weight (Well 1)

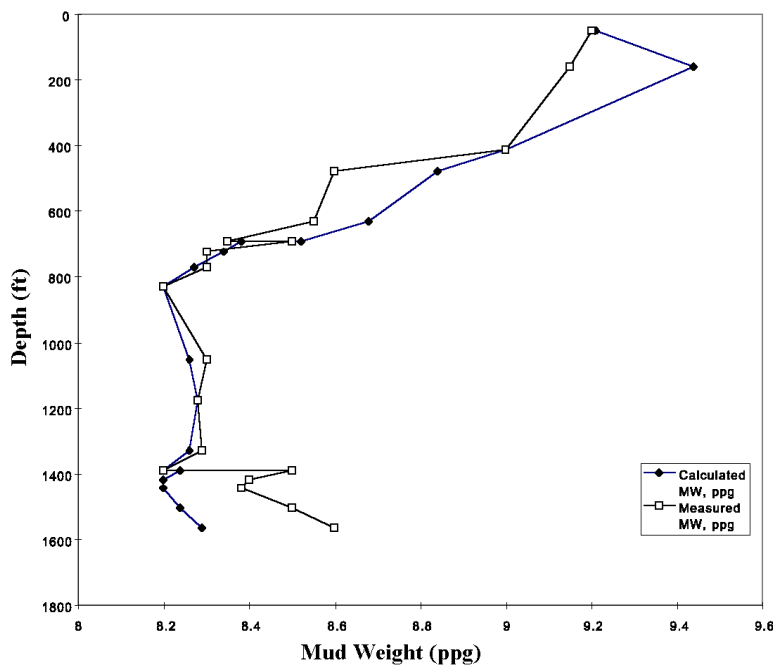


Figure 9-3. Theoretical and Measured Mud Weight (Well 2)

An indeterminate amount of water was added near the bottom of both wells, accounting for the measured differences between the calculated and measured values at the bottom of the well. In Well 1, the HGS reduced frictional drag and eliminated reaming usually required in these wells.

9.4 PDVSA-INTEVEP FIELD TESTS

Since this project was initiated, over 25 wells have been drilled with HGS drilling fluids around the world including: re-entry angled wells in Brazil, a horizontal well in Venezuela, and vertical wells in Italy.

A study by Intevep for PDVSA of re-entry and horizontal wells in the Guafita area of Venezuela indicated opportunity for improvement in several areas including: drilling fluids, geomechanics, and drilling mechanics. It was recommended to utilize a lower density fluid to avoid previous overbalanced conditions. Specifically, it was proposed to use a fluid density between 6.8 and 7.1 ppg until an operational window was determined.

Interflow® (a drilling, completion and workover fluid developed by PDVSA-Intevep) was designed and developed for use in low-pressure zones like those existing in the Guafita area. This fluid met

the requirements. HGS were added to the fluid to reduce density instead of compressible aerated fluids. This provided the lowest surface to volume ratio for any geometry considered (lowest viscosity).

In conjunction with 3-M, Intevep was able to lower the density of an emulsion drilling fluid by adding HGS to the base fluid. The fluid was stable, homogenous, single-phased, non-compressible and had useful rheological and filtrate properties when used in high-permeability, low-pressure producing zones. Field mixing was easily accomplished.

From this Intevep/PDVSA well it was learned that:

- > Conventional solids-control equipment can be utilized with this type of fluid.
- > The well did not experience any differential sticking.
- > A hole in-gauge was observed, suggesting the fulfillment of the well drilling plan.
- > A relative improvement in productivity was observed.

More details from these field trials are presented in Appendix F.

9.5 RECYCLING HGS USING CENTRIFUGES

The most economical utilization of HGS requires recycling. The only HGS recycle approach that has been field tested on a reasonable scale is one that involves a centrifuge. It is known that, with a small amount of dilution and in low gel-point fluids, glass bubbles segregate and float to the top. This flotation concept can easily be demonstrated on a small scale in the laboratory.

Prior work by others indicates that normal two-port centrifuges could not be used on-line to remove colloidal heavy cuttings from drilling fluids during drilling while in glass bubbles are present. This finding has been verified with equipment from Brandt and from Baker Process at the rig site while conducting drilling operations.

While making this determination, 3-M found that, depending on the rotary speed of the centrifuge, differential speed, and flow, a conventional two-port centrifuge could separate glass bubbles very well. But under this configuration, the possibility also exists for HGS to accumulate on the auger (if HGS are present in high concentrations in the fluid) and block the outlet ports. The problem is basically that much higher volume percent is being occupied by HGS versus drilled solids. Either the combination of high- and low-density solids came out together or they overwhelmed the capacity of the centrifuge and plugged it.

However, a successful test on a centrifuge from Baker Process in Germany (three exit ports) has worked very well with a three component fluid consisting of cuttings, glass bubbles, and the liquid portion of an aqueous-base drilling fluid. All components were successfully separated.

This centrifuge, a Censor model, is a “solids-sorting centrifuge” made by BIRD HUMBOLDT, BAKER PROCESS, a part of Baker Hughes Company (**Figure 9-4**). It is normally used for sorting solids, mainly recycling plastics of different densities at very sharp cuts. The particulate shape and size are not significant. In principle, left and right hand screw flights are fitted to a screw body; this ensures material transportation in opposite directions. The screw rotates inside the centrifuge at a speed varying slightly from that of the centrifuge bowl. Due to this effect the two products are transported to opposite ends of the centrifuge where they are lifted beyond the liquid ring and discharged.

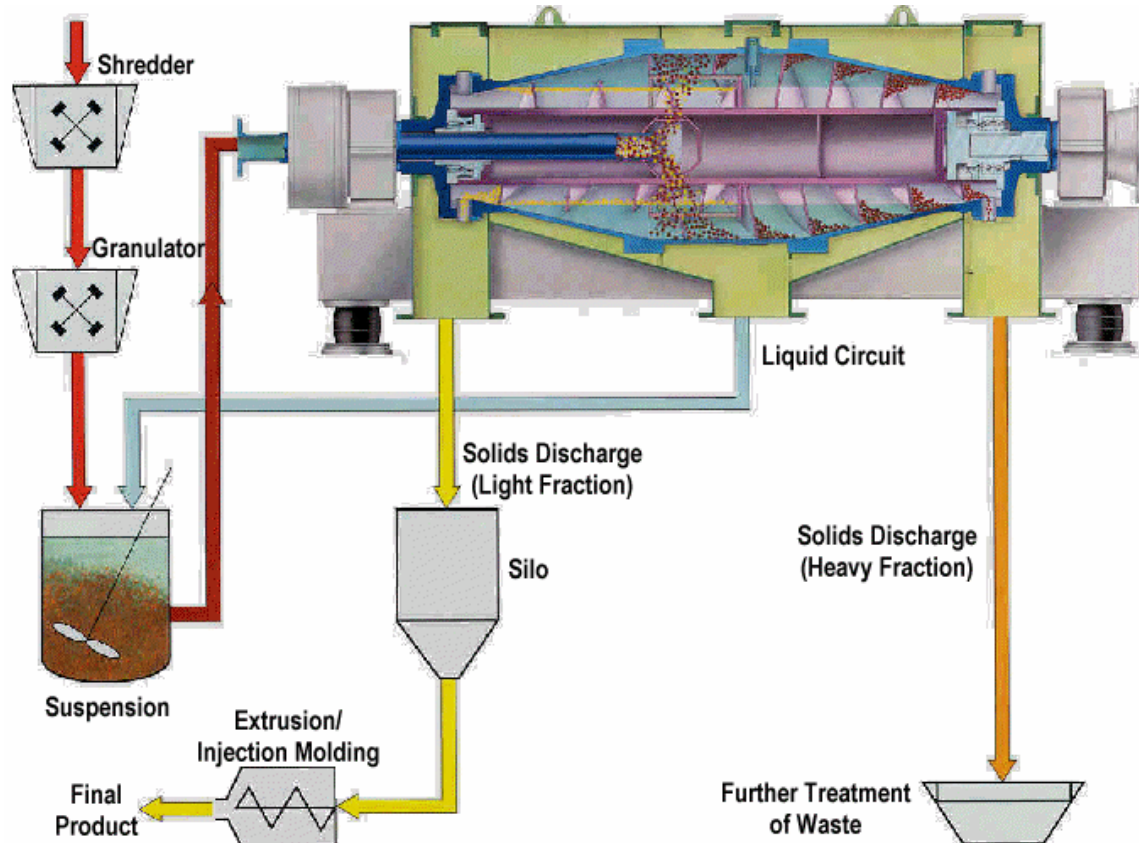


Figure 9-4. Baker Hughes Censor Solids-Sorting Centrifuge

In 1999, Baker ran an extended test for about 10 hours using a Censor, and no problems occurred. HGS recovery was termed excellent. Drill solids were also separated. The liquid stream had a minuscule amount of HGS, about 1.3% by volume.

Another centrifuge manufacturer, Brandt Tuboscope, has a high-speed centrifuge with an axial flow conveyor (model HS3400). With minor retrofitting of the liquid ports, this system could separate the HGS from heavy solids and from liquid. This concept would also be similar to the multiple ports

on a three-phase centrifuge (**Figure 9-5**) which is used to simultaneously separate solids, water, and oil layers from drilling mud or the above mentioned three-port solid-sorting centrifuge.

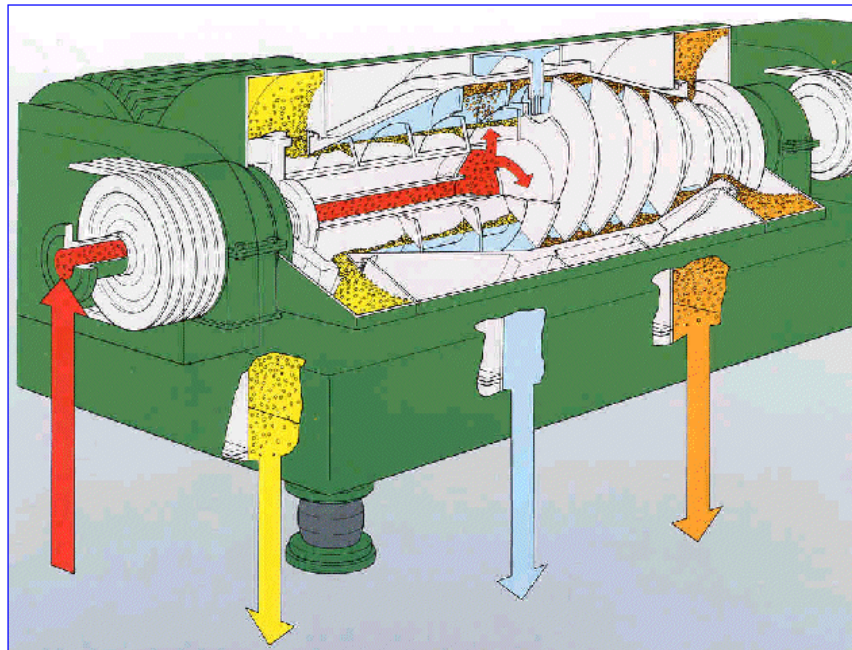


Figure 9-5. Three-Phase Centrifuge

9.6 CONCLUSIONS

The following conclusions were reached as result of HGS field tests:

1. These field tests were very successful and demonstrated the potential of using HGS fluids for underbalanced drilling.
2. The hollow spheres can be easily and safely mixed into drilling fluid during field operations.
3. New mud containing HGS can be built in the field.
4. The HGS are compatible with conventional field drilling fluids.
5. HGS can be circulated through conventional roller cone or PDC bits with little or no destruction of the spheres.
6. HGS can be circulated through conventional downhole mud motors with no detrimental effect on the spheres or the motors.
7. The survival rate of the spheres was within acceptable limits.
8. The environmental effect of using HGS was minimal.

9. The HGS had no detrimental effect on the drilling rig equipment.
10. The drilling fluid systems on these field tests were very small (<200 barrel active volume), allowing accurate monitoring and measurement of the sphere concentrations.
11. HGS muds are an economic alternative to aerated drilling fluid and should find increased use in the future.
12. HGS can be recycled to reduce costs.

Additional details from the Mobil/MEI field tests can be found in the technical paper SPE 38637, "Field Application of Light Weight Hollow Glass Sphere Drilling Fluid," contained in **Appendix A**.

Additional details from PDVSA-INTEVEP's tests can be found in the technical paper SPE 62899, "Field Application of Glass Bubbles as a Density-Reducing Agent," contained in **Appendix F**.

10. Potential Use of HGS for Dual-Gradient Drilling

10.1 DUAL-GRADIENT DRILLING CONCEPT

10.1.1 Deep Water Drilling Problems

A major problem with offshore drilling is maintaining wellbore annulus pressure above pore pressure so that the well does not “kick,” and below fracture pressure so that the well does not hydraulically fracture and lose circulation. In deep water, pore and fracture pressure gradients are typically close together, making drilling very difficult.

10.1.2 Dual-Gradient Drilling Concept

With conventional offshore drilling, a riser extends from the seafloor to the drillship. Fluid is circulated down the drillstring and up the riser back to the drillship. The column of mud in the riser annulus exerts high pressure at the seafloor, making drilling difficult.

To overcome this problem, several companies are developing **Dual-Gradient Drilling (DGD)** systems where subsea pumps will be placed on the seafloor to reduce the wellbore annulus pressure at that depth (**Figure 10-1**). The seafloor pumps pump mud back to the surface up risers or up smaller return riser lines (riserless drilling).

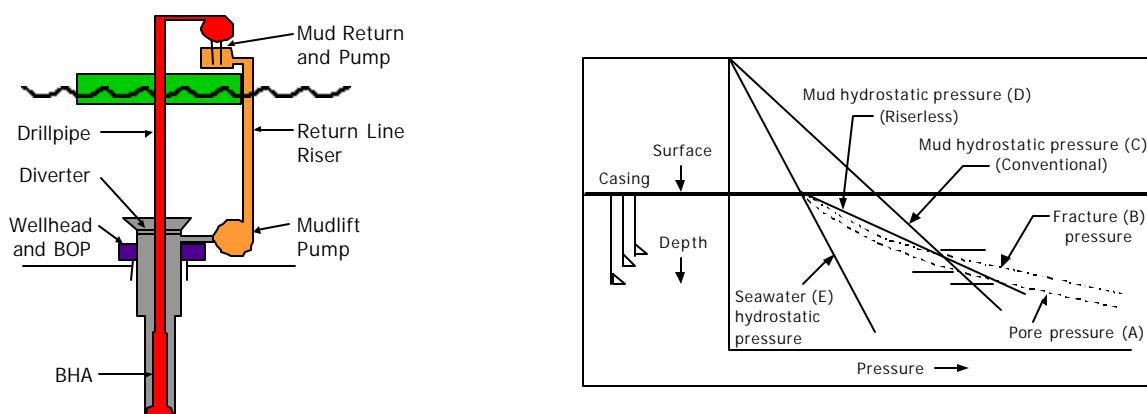


Figure 10-1. Dual Gradient Drilling System
(Peterman, 1998)

Figure 10-2. DGD Hydrostatic Gradients
(Snyder, 1998)

Figure 10-2 shows mud hydrostatic pressure gradients for conventional and riserless drilling. Because of the seawater column, and the unconsolidated nature of the sediments near the seafloor, the pore pressure (A) and fracture pressure (B) curves are often close together, making it difficult to maintain wellbore annulus pressure between these curves.

With conventional riser drilling, the mud hydrostatic pressure gradient (C) is a straight line extending from the floating drillship, as shown in **Figure 10-2**. This hydrostatic gradient line traverses the pore and fracture gradients over a short vertical distance, requiring numerous casing strings.

If the annular pressure at the seafloor is reduced to that of seawater by a DGD system, the hydrostatic curve (D) is a straight line that extends from the seafloor. The slope of this line is significantly reduced, allowing a much greater vertical distance to be drilled while staying between the pore and fracture gradient curves. This allows fewer casing strings, smaller drillships, and reduced drilling costs.

Figure 10-3 shows conventional and riserless casing programs for a Gulf of Mexico well where riserless drilling reduces the number of casing strings from 8 to 5, saving \$3 million, since each casing string costs \$1 million (Gault, 1996).

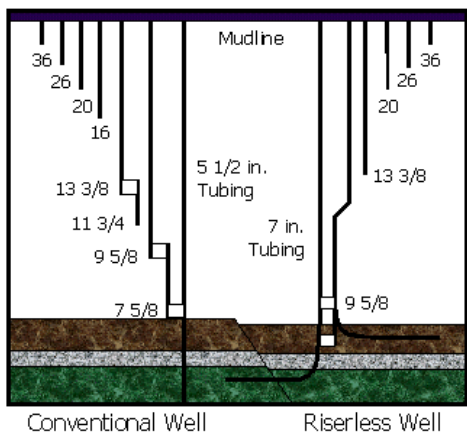


Figure 10-3. Casing Program for Conventional DGD (Snyder, 1998)

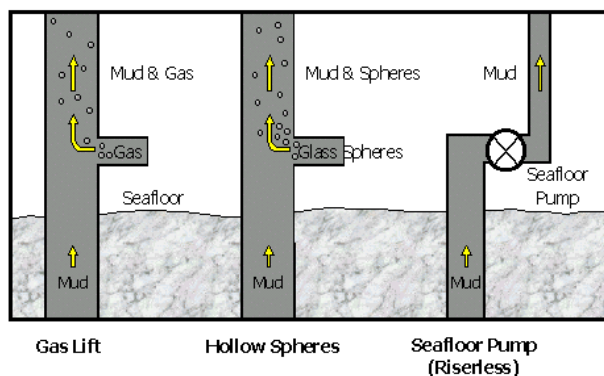


Figure 10-4. Dual-Gradient Drilling Options

In this example, DGD allows running 7-inch instead of 5 1/4 inch production tubing, resulting in higher well productivity due to the large flow area. In addition, larger casing (9 vs. 7 inch) allows the use of multilateral drilling, which can further increase production. This shows that in addition to significantly reducing drilling costs, DGD has the potential to significantly increase oil and gas production in deepwater wells.

In addition to reducing the number of casing strings required, as described in the next section, DGD reduces tension load requirements on the riser and mud storage requirements on the drilling vessel, which will reduce the size of drillships or increase the depth capability of these drillships.

10.1.3 Seafloor Dual-Gradient Drilling Options

Figure 10-4 shows three options for DGD including: 1) seafloor pumps, 2) gas lift, and 3) hollow spheres. These systems can also be used in conjunction with each other.

Although the gas-lift and hollow-sphere systems are shown with risers, they can also be used with return flow lines and riserless systems. These systems eliminate the requirement for seafloor pumps, thus significantly reducing the amount of equipment on the seafloor.

Subsea pumps (centrifugal, electric submersible, and diaphragm) located on the seafloor provide all the flexibility needed to handle any drilling situation. However, they have the disadvantage of high cost and reliability problems associated with keeping complex pumping systems operating on the seafloor. A major concern with DGD systems are problems associated with operating and maintaining pumps on the seafloor.

With gas-lift systems, gas is pumped to the seafloor and injected into the bottom of the riser to reduce the density of the mud in the riser. Problems associated with gas lift include 1) high compressor costs, 2) high nitrogen costs, 3) corrosion problems, 4) compressibility of gas causing nonlinear pressure gradients, and 5) difficulties degassing the mud before it is re-injected into the well.

With the hollow sphere system, spheres (glass, plastic, composites, metal, etc.) would be injected into the riser at the seafloor to reduce the density of the mud returning up the riser. This technique is similar to the gas lift system except that the hollow spheres are incompressible and therefore require less horsepower, they produce linear pressure gradients and they do not require expensive compressors or nitrogen.

10.2 COMMERCIAL DUAL -GRADIENT DRILLING SYSTEMS

10.2.1 Baker/Transocean “DEEPIVISON” Pump System

Baker Hughes/Transocean Sedco Forex (Sjoberg, 2000) are developing a “DEEPIVISON” dual gradient drilling (DGD) system that utilizes electrically-powered centrifugal subsea pumps manufactured by National Oilwell (Figure 10-5). Figure 10-6 shows a 6-stage, 1250-hp DEEPIVISON pump/motor module. The centrifugal pumps use “chomper” impellers that can handle gumbo, sand, gravel-sized pieces of hard limestone, and large pieces of aluminum, cement, and rubber without damage to the pumps.

Figure 10-6 shows a 10,000-foot water depth DEEPIVISON subsea assembly with five centrifugal pumps (4050 total horsepower) and weighs 350,000 pounds. The DEEPIVISON is modular and can include from one to five centrifugal pumps, depending on water depth and the pump head required (Figure 10-7).

DEEPIVISON uses a “Flow Stop Sub” in the drillstring to prevent U-tubing when circulation is stopped (Figure 10-8). The DEEPIVISON system initially being developed for use in the Gulf of Mexico has the following characteristics (Sjoberg, 2000):

Water Depths:	4,000-7,500 ft (10,000 ft with min. modifications)
Well Depths:	28,000 ft TVD (45,000 ft TD)
Number of Depths:	5 (10,000 ft water)
Weight:	350,000 lbs
Size:	15 ft x 17 ft x 40 ft
Wells:	9-in. casing to TD
Drillstring:	Jointed, conventional drill pipe
Well Profile:	Including complex directional
Mud Weights:	Maximum 19.2 ppg
Rig Specification:	Discover Enterprise; Ocean Confidence; others later

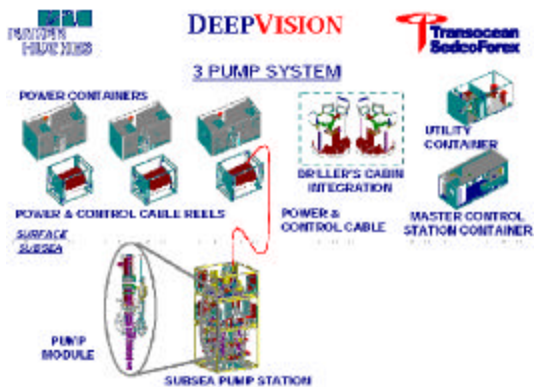


Figure 10-5. DEEPIVISON System

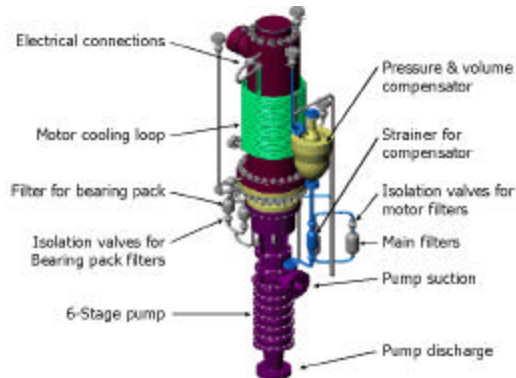


Figure 10-6. DEEPIVISON Subsea Centrifugal Pump

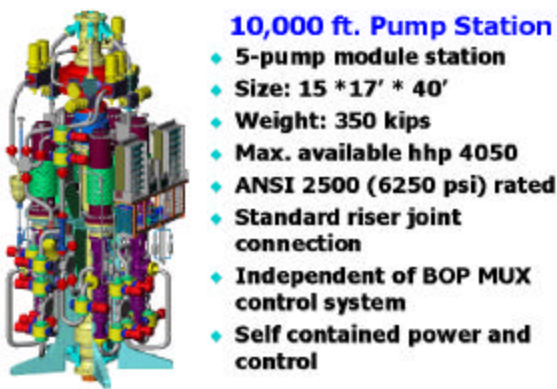


Figure 10-7. DEEPIVISON Subsea Module

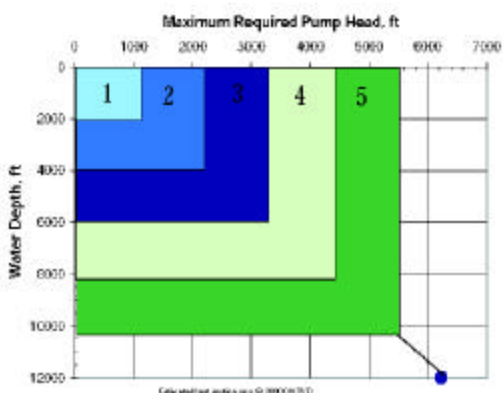


Figure 10-8. Water Depth vs. Pump Units

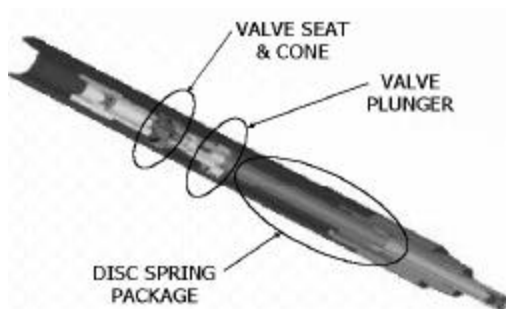


Figure 10-9. DEEPIVISON 4 3/4-in. Flow Stop Drillstring Valve

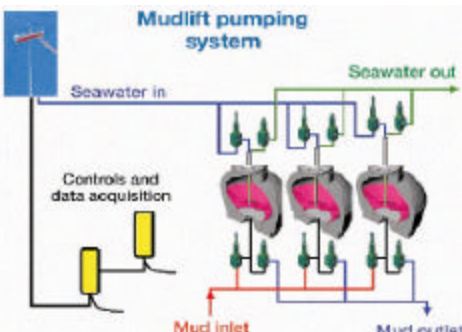


Figure 10-10. Mudlift Pumping System

The DEEPIVISON JIP was initiated by Baker-Hughes and Transocean Sedco Forex in 1997. The Phase III commercialized project currently underway is being

funded by Baker, Transocean, BP, and Chevron. Phase III includes component testing in the second quarter of 2001 to provide proof-of-concept in November of 2001. The system should be ready for commercialization at that time (Neil Forrest, 2000).

10.2.2 Conoco/Hydril “Mudlift” Pump System

The Conoco/HYDRIL “MUDLIFT” System (Smith et al., 2000) utilizes three to six 80-gallon seafloor positive-displacement diaphragm pumps that are powered by seawater pumped to the seafloor through a 5 to 6-inch I.D. line on the riser (**Figures 10-9 and 10-10**). Once the seawater passes through the pump, it is dumped into the ocean at the seafloor. This three-pump package is being manufactured for upcoming field trials.

The seawater power system eliminates the need for electric cables, surface mounted reels, subsea electric motors and subsea hydraulic systems. The slow-speed diaphragm pumps contain large valves that allow them to pump large cuttings without breaking down. The seafloor unit includes a “rock crusher” to mechanically crush large cuttings, gumbo, float equipment, cement, etc., to less than 1.5-inch particles so that they will pass through the diaphragm pumps without damaging them.

Figure 10-11 shows a MUDLIFT subsea assembly containing six diaphragm pumps, two solid control units, and electric control equipment. This unit is designed for 10,000-foot water depth.

The MUDLIFT System uses a subsea rotating diverter (**Figure 10-12**) to divert mud to the subsea pumps. This diverter uses a rotating rubber element to seal against the drillstring and rotating seals that allow the bearings to operate in oil.

This system utilizes a special drillstring valve (**Figure 10-13**) that prevents U-tubing of the mud in the drill pipe when circulation is stopped. The basic function of this valve is to close when circulation stops and to open when circulation starts.

A prototype system has been successfully field tested on a jack-up rig. A “marinized” system will be tested in 1150 feet of water in mid-March 2001. The system will be commercialized in 2002 (**Figure 10-14**).

Conoco and HYDRIL have spent a “major effort” on developing well control procedures and training modules for this system, because they recognize that retaining experienced deepwater drilling personnel would be the biggest challenge with this system.



Figure 10-11. MUDI IFT Subsea Pumps

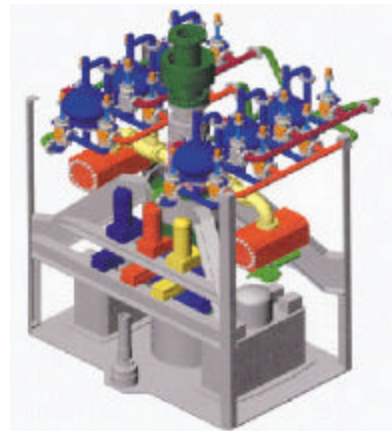


Figure 10-12. MUDLIFT Subfloor Module

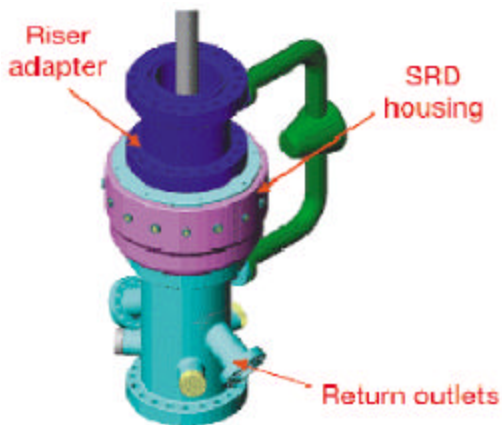


Fig 10-13. MUDI IFT Subsea Diverter

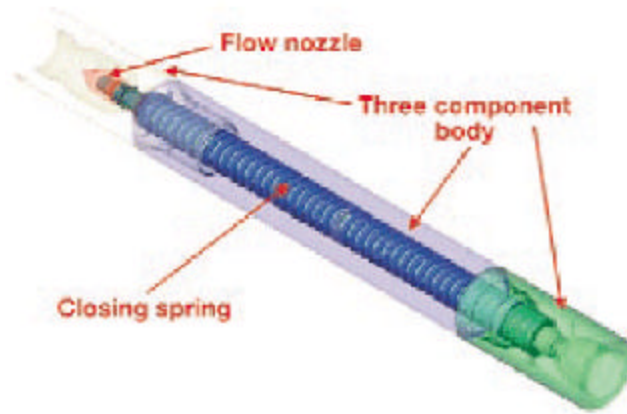


Figure 10-14. MUDLIFT Drilling Valve

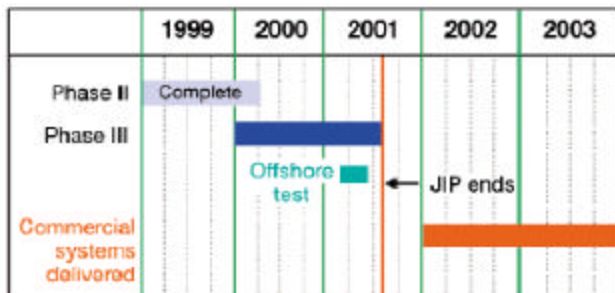


Figure 10-15. MUDLIFT Time Schedule

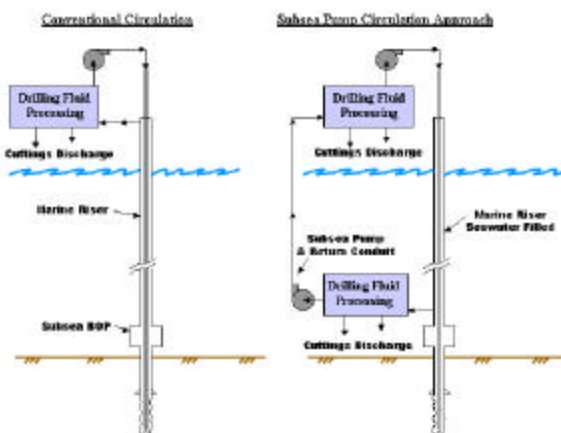


Figure 10-16. Shell SSPS System

An earlier version of this MUDLIFT system used electric motors to power the diaphragm seafloor pumps, but the electric motors were eliminated in a later design due to concerns about the reliability of the subsea electric motors and cables.

Conoco manages this project and HYDRIL manufactures the subsea diaphragm pumps. Other industry partners include BP, Chevron, Texaco, Diamond Offshore, Global Marine, and Schlumberger.

10.2.3 Shell “SSPS” Pump System

The Shell “Subsea Pumping System” (SSPS) (Gonzalez, 2000) uses seafloor electric-submersible pumps (ESPs) to reduce wellbore pressure at the seafloor (**Figure 10-15**). The SSPS pumps are similar to oilfield ESPs used to pump oil and water from oil wells (**Figure 10-16**).

A nitrogen-filled chamber (**Figure 10-17**) at the seafloor “decouples” the wellbore from the seafloor pumps to ensure that the pressure in the wellbore at the seafloor always equals seawater pressure. This nitrogen-filled chamber, which is located above the BOP, uses nitrogen tanks to maintain pressure inside the chamber equal to seawater pressure outside the chamber.

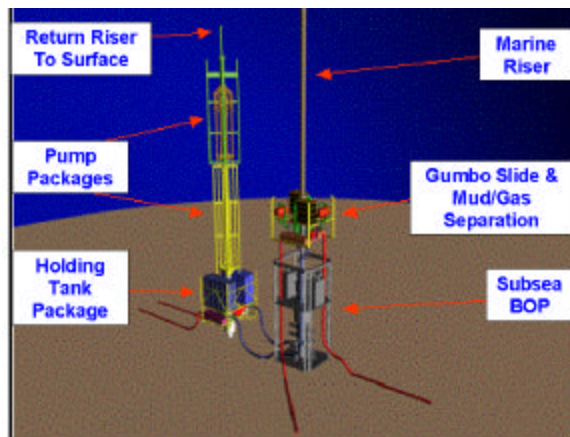


Figure 10-17. Shell SSPS General Configuration

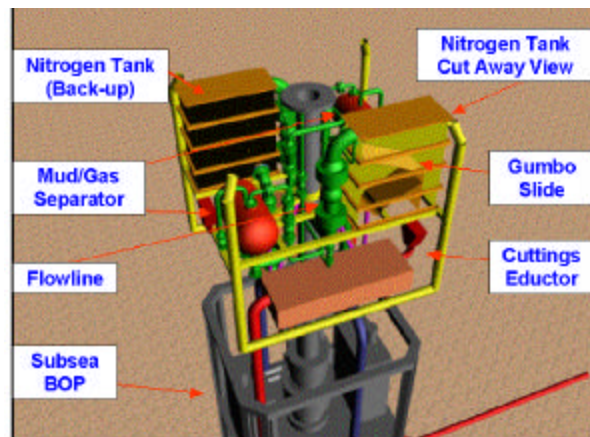


Figure 10-18. Shell SSPS Gumbo Slide & Mud/Gas Separation

The nitrogen chamber uses a 20° internal “gumbo slide” to remove gumbo, cuttings and other debris larger than 0.25 inches from the mud before the mud enters the seafloor electric-submersible pumps. Large cuttings coming across the top of the gumbo slide are discharged to the seafloor. This gumbo slide increases the reliability of the system because large cuttings do not pass through the pumps and other subsea equipment and therefore do not have to be crushed at the seafloor.

This seawater ambient pressure chamber allows easy detection of kicks compared to other DGD systems where kick detection is a problem. When a kick occurs, it is detected in a conventional manner and the BOPs are closed. Mud is then circulated to a nitrogen-filled subsea mud/gas separator/gas buster chamber where the gas is separated from the mud and vented to the seawater (**Figure 10-18**). The mud goes to a “holding tank” where it is pumped to the surface.

Environmental concerns in discharging large cuttings to the seafloor are a major limitation of this system since some major operators are adopting “zero discharge” offshore drilling operations. These operators have stated they cannot use the SSPS due to this policy.

10.2.4 Time and Cost Implementation

BP (Frazelle, 2001) states that the cost of implementing a DGD system is \$40 to \$70 million (depending on the rig modifications required), and that the delivery time for a system is 18 months. BP stated that it plans to place an order for a DGD system at the end of the second quarter of 2001.

10.2.5 Dual-Gradient Cuttings Handling

A major concern of drilling engineers is how subsea pumping systems will handle large bit cuttings and large hole sloughing particles so that these rock fragments will not plug the pumps. These subsea pumping systems handle large cuttings as follows:

Mudlift (Diaphragm pumps)

“Rock crusher” crushes particles to less than 1.5 inch before they pass through the pump.

DeepVision (Centrifugal pumps)

“Chomper” blades crush particles to less than 0.5 inch before they pass through the pump.

Shell SSPS (Turbine pumps)

“Gumbo slide” screens out particles larger than 0.25 inch and dumps them to the seafloor.

10.2.6 Subsea Pump Project Participants

Participants on the latest phase of the subsea pump projects are as follows:

Mudlift

Conoco	Texaco
Hydril*	Diamond Offshore
BP	Global Marine
Chevron	Schlumberger

Deepvision

Baker Hughes*	BP
Transocean Sedco Forex*	Chevron

SSPS

Shell

**Project Manager*

10.2.7 Subsea DGD System Limitations

Following are concerns that drilling engineers have expressed about DGD subsea pumping systems:

1. Very expensive
2. Very complex
3. Potential low reliability
4. Must pull riser to repair pumps
5. Rock cuttings must pass through seafloor pumps
6. Difficulty in detecting kicks
7. Handling large volume kicks
8. Requires large, expensive Generation-5 rigs
9. 5 year rig commitment
10. \$40 to \$70 million cost
11. High daily operating cost
12. Too expensive for shallow water
13. Cannot implement quickly

10.2.8 Subsea Pump Concerns

Drilling engineers have the following concerns about subsea pumps:

1. Subsea pump failures
2. Power transmission failures
3. Pump degradation (erosion)
4. Insufficient power during emergencies
5. “Gas Locking” pumps
6. Rock cuttings and debris plugging pumps
7. Handling large volume gas kicks
8. Making connections
9. Handling complex emergencies

10.3 HOLLOW SPHERE DGD SYSTEM

10.3.1 Hollow Sphere DGD Concept

With the lightweight hollow-sphere dual-gradient drilling (DGD) system, hollow spheres (glass (HGS), plastic, composite, metal, etc.) are pumped to the seafloor and injected into the bottom of the riser to reduce the density of the mud in the riser to that of seawater (**Figure 10-19**).

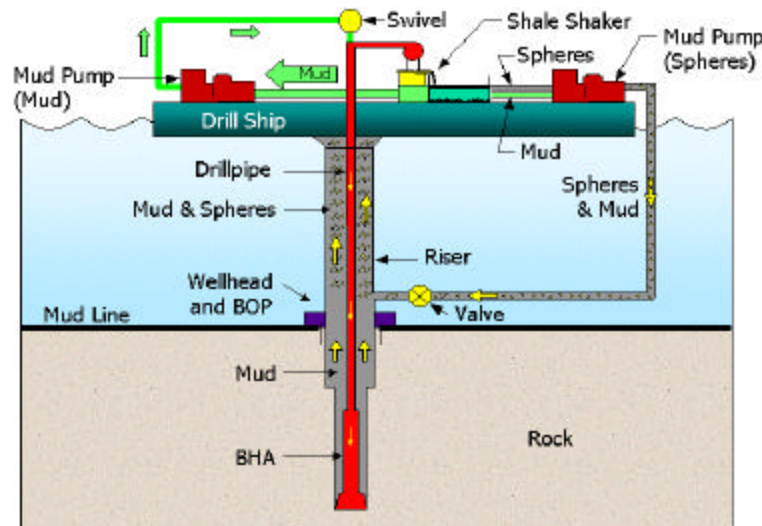


Figure 10-19. Maurer Hollow-Sphere, Dual-Gradient System

The mud and spheres are mixed together at the surface, pumped to the seafloor as a slurry and injected into the riser to reduce the density of the mud (**Figures 10-20 and 10-21**). A major advantage of this system is that no new equipment is needed on the seafloor except a remotely controlled valve (**Figure 10-22**).

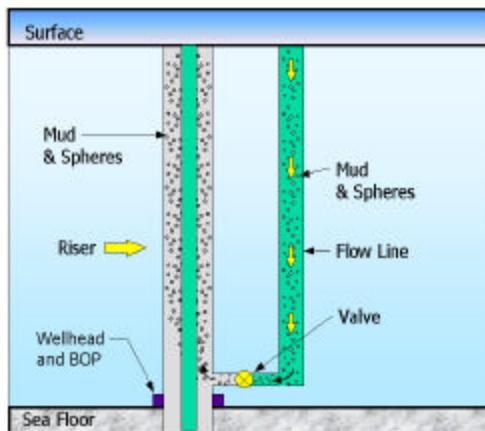
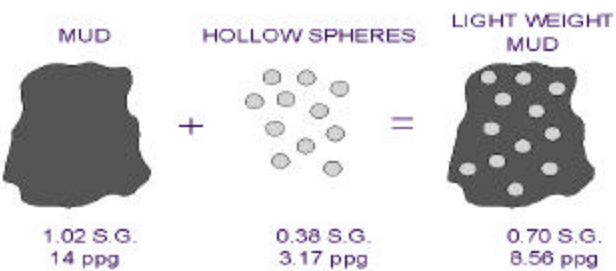


Figure 10-20. Single Injection Point

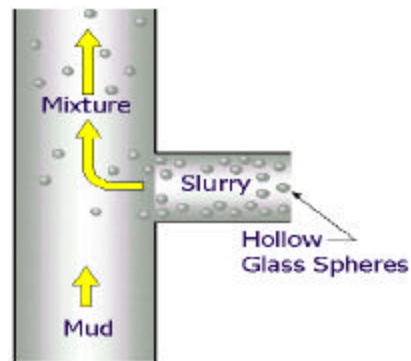


Figure 10-21. HGS Injection

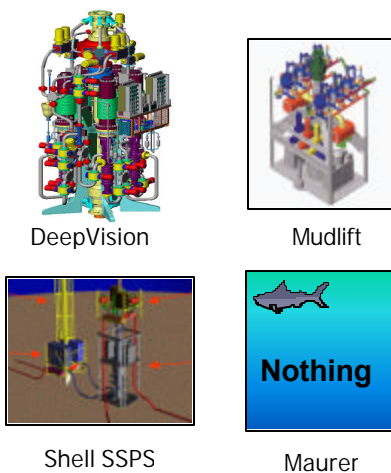


Figure 10-22. New Seafloor Equipment



Figure 10-23. Photomicrograph of Glass Microspheres

10.3.2 Sphere Requirements

The hollow spheres can be made of glass, composites, plastics, or other materials. **Figure 10-23** shows hollow glass microspheres (10- to 100-micron diameter) manufactured by 3M that have a specific gravity of 0.38 g/cc (i.e., HGS as described elsewhere in this report). Adding 50% by volume of these microspheres to a 14-ppg mud will reduce the density of the mud to that of seawater (8.56 ppg) as shown in **Figure 10-24**.

Figure 10-25 shows how the density of a mud decreases as the percentage of spheres increases. This shows that 21% spheres are required to reduce the density of a 10-ppg mud to that of seawater compared to 50% with a 14-ppg mud.

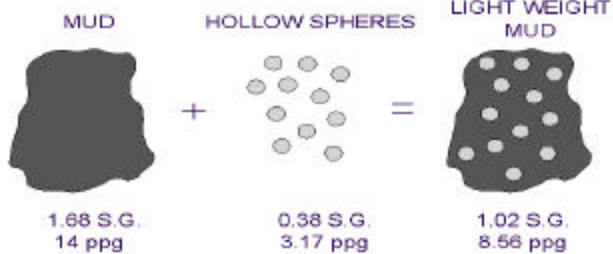


Figure 10-24. Sea Water Density Mud
(50% Spheres)

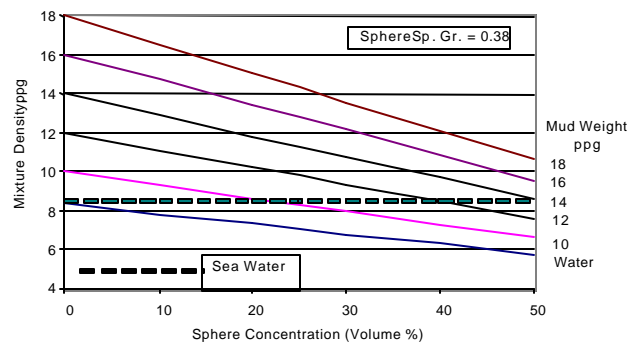


Figure 10-25. Mud Density vs. Sphere Concentration

10.3.3 Sphere Separation

All of the hollow spheres must be removed from the low density mud when it returns up the riser to the drill rig. Heavy mud (without spheres) is then circulated down the drillpipe to the hole bottom while the hollow spheres are circulated to the seafloor and injected into the riser.

Extensive tests conducted by Maurer, Baker-Hughes, and others have shown that 100% sphere recovery from the mud is not possible with centrifuges or hydrocyclones at high circulation rates required with DGD drilling (800 to 1400 gpm). To overcome sphere recovery limits, Maurer has a patent pending on the concept of using large-diameter hollow spheres (>100 microns) that can be removed from the mud with conventional oilfield shale shakers (**Figure 10-26**). This allows 100% separation and ensures that no spheres will be recirculated down the drillpipe and cause well control problems. Drill cuttings and spheres can be easily separated in a seawater tank since hollow spheres will float and rock cuttings will sink.

10.3.4 Sphere Collapse Pressure

Density of hollow spheres increases with increased collapse strength due to thicker walls. Consequently, it is beneficial to use the lowest strength spheres (i.e., lowest density) possible.

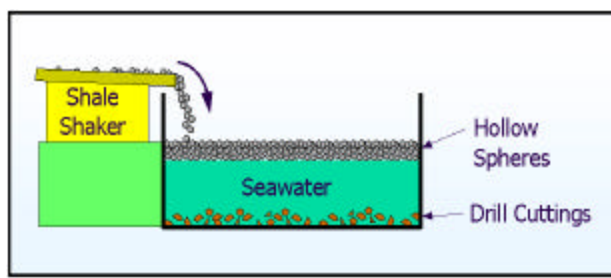


Figure 10-26. Hollow Sphere Separation System

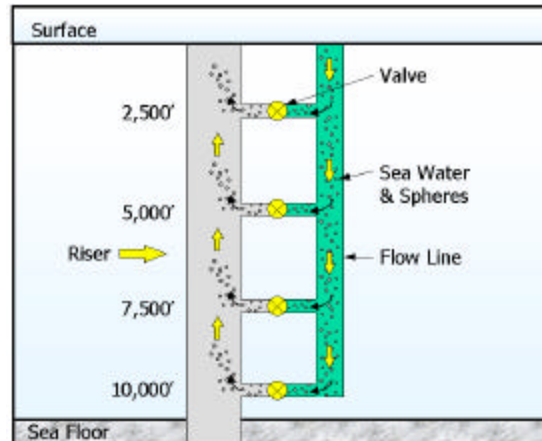


Figure 10-27. Multiple Injection Points

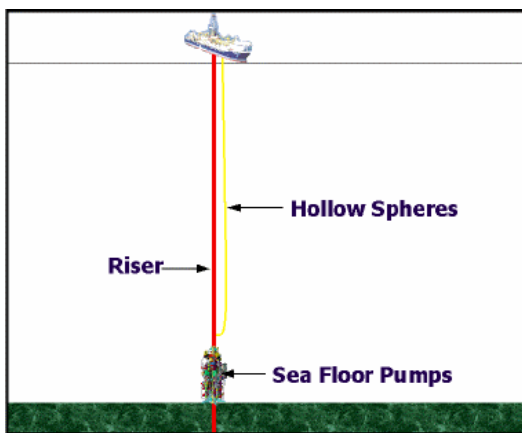


Figure 10-28. Combination Dual-Gradient System

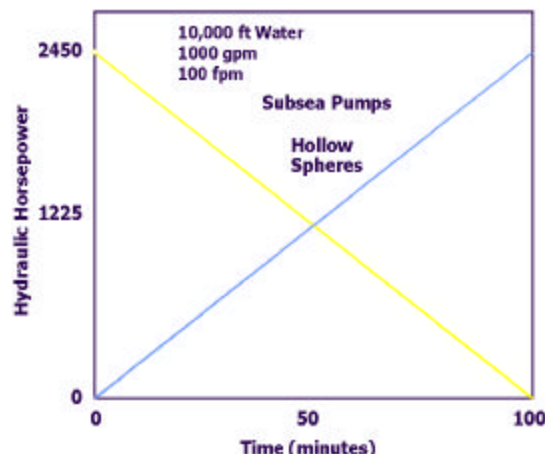


Figure 10-29. Sea Floor Pumping Power

The spheres encounter the highest hydrostatic pressure when drilling is initiated and the riser is full of heavy mud (without spheres). To reduce this problem, heavier spheres with higher collapse pressures can initially be injected into the bottom of the riser and then replaced with lighter, lower-collapse-pressure spheres once the riser is full of spheres. Another possibility is to initially inject spheres near the top of the riser and then sequentially inject spheres at lower points in the riser, an approach similar to initiating a gas-lift system (**Figure 10-27**).

Another problem with the spheres is that it takes 60 to 90 minutes for the spheres to reach the surface when drilling is initiated. This time delay can be reduced by simultaneously injecting spheres into the riser at multiple depths when drilling is initiated as shown in **Figure 10-27**.

10.3.5 Hybrid Seafloor Pump/Sphere System

Hollow spheres can be used in conjunction with seafloor pumps as shown in **Figure 10-28** to provide extra pumping capabilities during emergencies, or to act as a back-up system if the seafloor pumps fail. With this hybrid system, seafloor pumps would provide 100% of the pumping capacity when the spheres are first injected into the riser, and then the seafloor pump power can be decreased to zero as the spheres are circulated to the surface (**Figure 10-29**).

10.3.6 Removing Hollow Spheres From Mud

During DGD drilling, the spheres must be removed from the mud when the mud returns to the surface so that heavier mud (without spheres) can be recirculated through the drill string to the hole bottom and hollow spheres reinjected into the bottom of the riser. Tests show that centrifuges (**Figure 10-30**) and hydrocyclones (**Figure 10-31**) cannot remove 100% of the spheres at the high flow rates (800 to 1,400 gpm) used with DGD. Therefore, they are not suitable for use with hollow sphere DGD drilling systems.



Figure 10-30. Oilfield Centrifuge Test

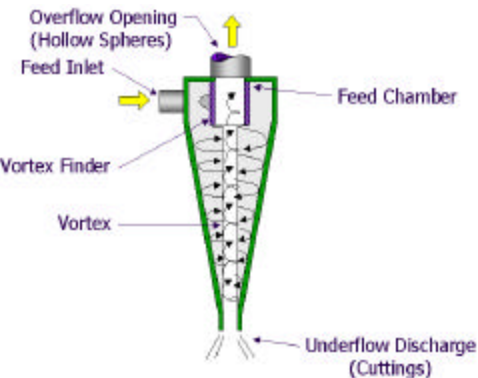


Figure 10-31. Oilfield Hydroclone

The diameter of commercial small hollow glass microspheres (HGS) ranges from 8 to 125 microns with a median of 45 microns (**Figure 10-32**). They will therefore pass through the 20 to 80 mesh (762 to 177 microns) screens typically used on oilfield shale shakers (**Figure 10-33**). Conventional shale shakers cannot be used to remove the small hollow spheres currently available. Because of this limitation, Maurer has a patent pending on the use of large-diameter hollow spheres (>100 microns) that can be removed from the mud by conventional oilfield shale shakers.

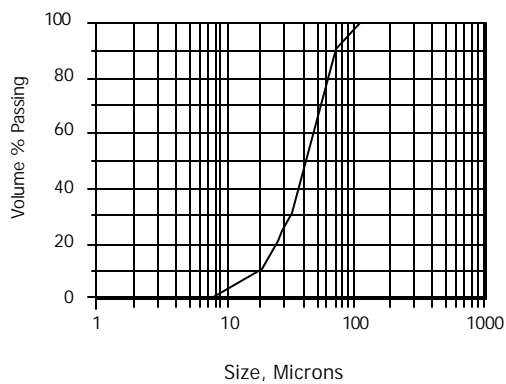


Figure 10-32. S38 Hollow Sphere Size

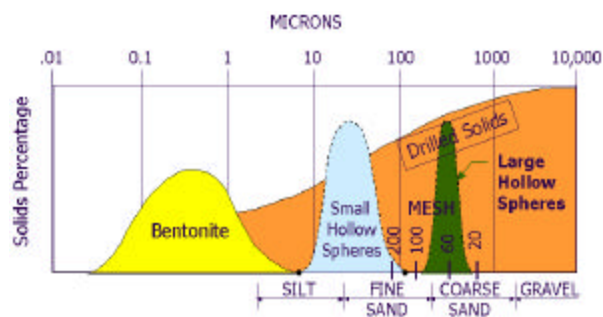


Figure 10-33. Hollow Sphere Size

10.3.7 Large-Diameter Hollow Sphere Development

Because of the difficulties of removing small-diameter hollow spheres from mud, Maurer developed the concept of using large-diameter hollow spheres (>100 microns) for DGD drilling to allow the spheres to be removed with conventional oilfield shale shakers. Large hollow spheres (>100 microns) have several advantages over smaller hollow spheres

(10 to 100 microns) including: 1) lower mud viscosities; and 2) easily screened from the mud with conventional oilfield shale shakers.

One concern regarding the use of large-diameter spheres was that their collapse pressure might not be adequate. **Figure 10-34** shows collapse pressure and density equations for hollow spheres. When the collapse pressure equation is divided by the density equation, sphere diameters (a and b) disappear. This indicates that for a given material with fixed shear strength σ_m and fixed density D_m , collapse pressure is independent of sphere diameter. Therefore, for a given material and a given sphere density, spheres can be made any diameter and the collapse pressure will remain constant.

Sphere Density (ρ)

$$\rho = \rho_m \left\{ \frac{b^3 - a^3}{b^3} \right\}$$

Sphere collapse pressure (p) - (Timoshenko, 1950)

$$p = \frac{2\sigma_m}{3} \left\{ \frac{b^3 - a^3}{b^3} \right\}$$

$$p = \frac{2\sigma_m \rho}{3\rho_m} = k\rho$$



Figure 10-34. Sphere Collapse Pressure and Density

Figure 10.35. Photomicrograph of Hollow Spheres

This analysis led to the manufacture of large prototype hollow glass spheres that have diameters of 200 to 800 microns, compared to 10 to 100 microns for the smaller commercial hollow glass spheres (**Figure 10-35**). These larger spheres can be screened out of the mud using conventional shale shaker screens (100 to 200 mesh) as shown in Figure 10-33.

Figure 10-36 shows that the *small* hollow spheres are much smaller than the openings in a 100 mesh screen and that the *larger* hollow glass spheres are much larger than these openings, so screening the larger hollow spheres from the mud should not be a problem. This figure also shows that the 12-mesh frac sand commonly pumped with high-pressure oilfield frac pumps is over five times larger than the large hollow glass spheres, so pumping these large hollow glass spheres should not be a major problem.

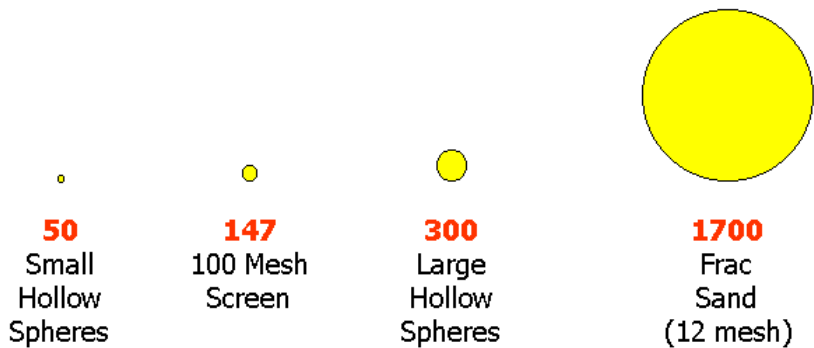


Figure 10-36. Relative Particle Size (Microns)

Large carbon-fiber composite hollow spheres (10 mm diameter) are also being evaluated for use with this DGD system (**Figure 10-37**). These have diameters of 10 mm (0.39 inch) and densities of 0.43 to 0.66 g/cc and can be used at water depths to 15,000 ft (6,500 psi) (**Figure 10-38**).



Figure 10-37. Composite Hollow Spheres

Water Depth (ft)	Foam System Density (g/cc)			
	PVC	Thermoplastic Macrospheres	GRE Minispheres	Carbon Fibre Minispheres
1000	0.25	0.28		
2000	0.36	0.34	0.40	
3000		0.36	0.41	
4000		0.39	0.45	
5000		0.43	0.48	0.43
6000		0.44	0.51	0.45
7000		0.48	0.55	0.46
8000		0.53	0.60	0.48
9000		0.53	0.62	0.50
10000			0.65	0.53
11000				0.56
12000				0.59
13000				0.61
15000				0.66

Figure 10-38. Properties of Composite Spheres

These composite spheres are used in offshore riser buoyancy materials and have very uniform composition and properties (**Figure 10-39**).

A schematic of the facility used to manufacture hollow composite spheres and buoyancy material is shown in **Figure 10-40**. These composite spheres can be made in different diameters, so optimum diameters will need to be determined.



Figure 10-39. Riser Buoyancy Modules

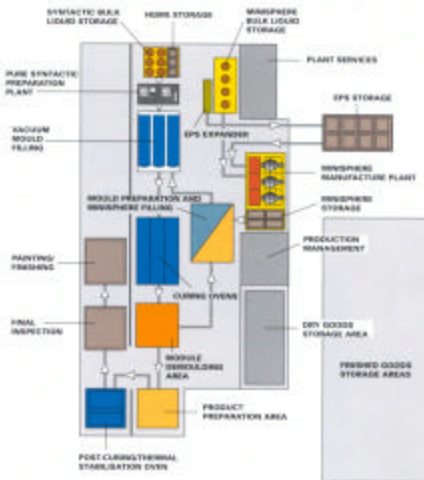


Figure 10-40. Buoyancy Manufacturing Facility

10.3.8 Hollow Sphere System Applications

The mud weight required with the DGD drilling system increases with each casing string as shown in **Figure 10-41**. In most areas, mud weights higher than 14 ppg will not be required with DGD drilling systems. An exception is BP's Crazy Horse field in the GOM where mud weights up to 18 ppg will be required.

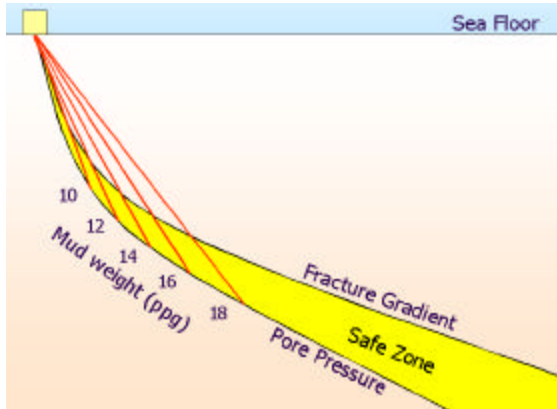


Figure 10-41. Dual-Gradient Mud Weights

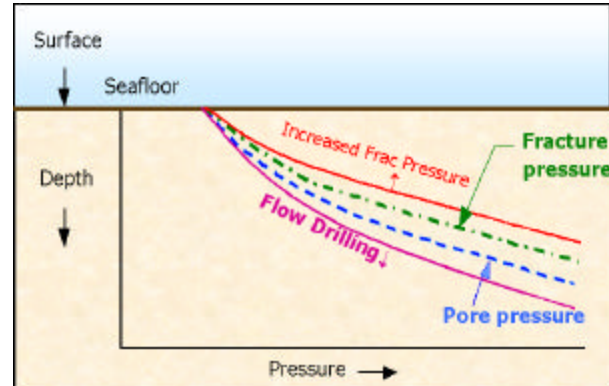


Figure 10-42. Spreading Pore Pressure/Frac Curves Apart

Most drilling engineers believe that the major benefit of DGD drilling systems will be realized with the first two casing strings below the mud line since the greatest problems occur in these upper sections of the well where DGD mud weights are typically less than 14 ppg. They also believe that mud weight reductions of 3 to 5 ppg in the

lower casing strings will be adequate and that seawater density will not require the heavier muds (14 to 18 ppg) in the deeper sections of the well.

10.3.9 Drillstring Valve

All DGD drilling systems, including the hollow sphere system, require drillstring valves that can be closed when circulation is stopped (e.g., during connections) to prevent U-tubing of drilling mud in the well.

10.3.10 Spreading Frac/Pore Pressure Curves Apart

The need for a DGD system arises because the frac and pore pressure curves near the seafloor are close together, thereby making drilling difficult and necessitating numerous casing strings (see Figure 10-2). The concept of DGD drilling is designed to keep the wellbore pressure within these curves.

An alternative method to reduce the number of casing strings is to spread these curves further apart as shown in **Figure 10-42**. It may be possible to increase the frac pressure by 1) injecting chemicals to consolidate a zone around the wellbore, 2) utilizing special mud chemicals, 3) compacting a zone around the wellbore, 4) sealing microfractures around the wellbore, or 5) building an impermeable filter cake on the wellbore walls.

Flow drilling will allow drilling at pressures below the pore pressure curve, thus effectively spreading the curves apart. Wellbore-stability experts from several major operators have stated that they believe it may be possible to spread these curves apart using these techniques.

10.3.11 Shallow Water Applications

DGD drilling has considerable potential application for drilling at water depths of 2000 to 5000 ft where wellbore stability, shallow water flows, and lost circulation are major problems. Seafloor pumping systems are too expensive for these shallow applications, so the proposed low-cost hollow sphere system should be an attractive alternative. Shallow-water applications for this DGD system will probably be much larger than deepwater applications since there are significantly more wells drilled at shallow water depths than at water depths greater than 5000 ft.

10.3.12 Advantages of Hollow-Sphere DGD System

Advantages of the hollow-sphere DGD drilling system include:

1. Complements existing seafloor pumping systems
2. Reduces the use of or eliminates seafloor pumps
3. Increases life and reliability of seafloor pumps
4. Provides contingency for seafloor pump failures
5. Utilizes conventional rig pumps
6. Easier to operate than seafloor pumps
7. Cuttings and debris do not pass through the DGD pumps
8. Handles any size cuttings or debris
9. Easy kick detection and well control
10. Handles large volume kicks
11. Eliminates “gas locking” of seafloor pumps
12. Maintains seawater gradient during connections
13. Eliminates electric and hydraulic power lines to seafloor
14. Spheres produce linear pressure gradients

10.4 HOLLOW SPHERE DGD REQUIREMENTS

10.4.1 Hollow Sphere Techniques

There are two basic techniques for pumping HGS to the sea floor: *mud transfer* and *seawater transfer* (**Figure 10-43**). With *mud transfer*, mud and spheres are mixed together at the surface and pumped to the sea floor as slurry and injected directly into the riser. The major advantage of this system is that there is no complicated seafloor equipment, while the major disadvantage is that the mud pumped with the slurry dilutes the mud in the well, making high sphere concentrations impossible.

With *seawater transfer*, spheres are pumped to the seafloor with seawater, separated from the seawater using a seafloor separator (screen) and injector (e.g., Moineau

pump), and then injected into the riser. Mud can be diverted from the annulus to the injector if needed, to facilitate injecting the spheres into the riser. Major advantages of this technique are 1) the seawater transfer fluid can be injected into the surrounding water and 2) high sphere concentrations are possible.

The seawater transfer system requires a seafloor separator/injector and is therefore more complicated than the mud transfer system. Consequently, the mud transfer system is preferred with mud weights less than 10 ppg, whereas the seawater transfer system is preferred for mud weights above 10 ppg.

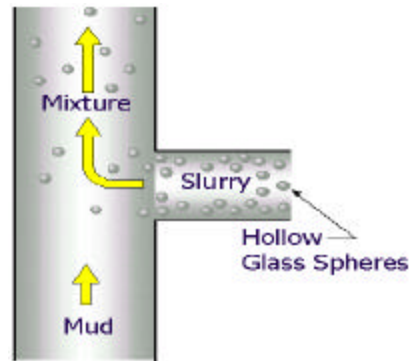


Figure 10-43. Hollow Glass Spheres

10.4.2 Sphere Requirements (Seawater Transfer)

If HGS are pumped directly (spheres only) into the mud stream (seawater transfer), density of the mud in the riser is:

$$P_r = \frac{(100 - v)p_m + vp_s}{100} \quad (10-1)$$

where

p_r = Mud Density in Riser

p_m = Mud Density without Spheres

p_s = Density of Hollow Spheres

v = Sphere Concentration (% Volume)

Figure 10-44 shows how mud density decreases as sphere concentration increases. The maximum sphere concentration ranges from 35 to 50% by volume, due to increased mud viscosity with increased sphere concentration. **Figure 10-45** shows that 50% sphere concentration can reduce mud weight from 14 to 8.6 ppg, a significant reduction.

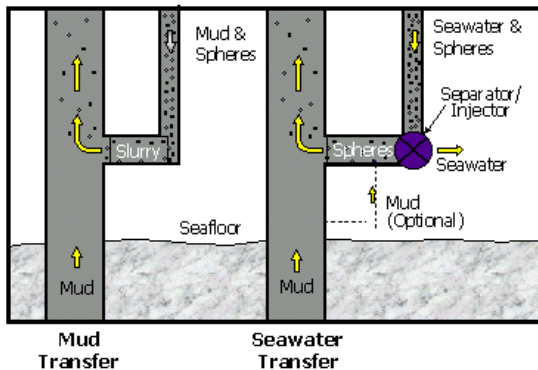


Fig. 10-44. Hollow Glass Sphere Injection Systems

The goal of riserless drilling is to reduce the effective mud weight to that of seawater. **Figure 10-46** shows that a sphere concentration of 18% reduces the density of a 10-ppg mud to that of seawater whereas a 52% concentration is required with 14-ppg mud. This shows that it is feasible to use HGS as an alternative to riserless drilling for a wide range of mud weights.

Figure 10-47 shows that a sphere flow rate equal to the mud flow rate (50% sphere concentration) will reduce the density of a 13.8-ppg mud to that of seawater (8.56 ppg). This shows that the seawater transfer technique could be effective with most muds.

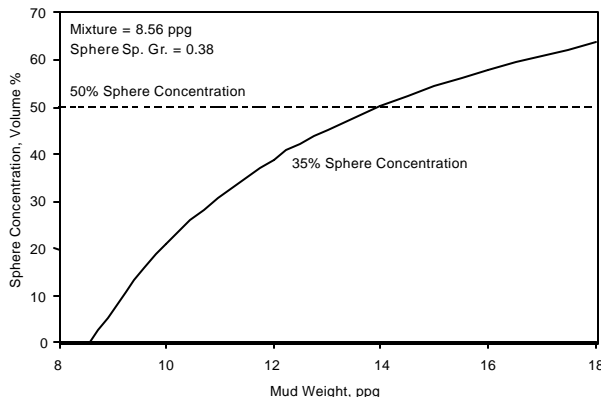


Fig. 10-46. Sphere Concentration Required to Reduce Mud Weight to Seawater Density

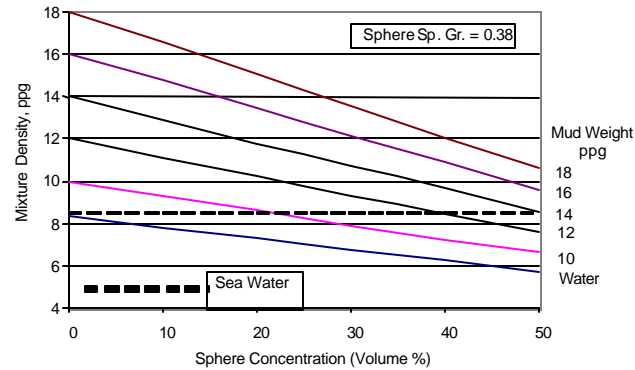


Fig. 10-45. Mixture Density vs. Sphere Volume

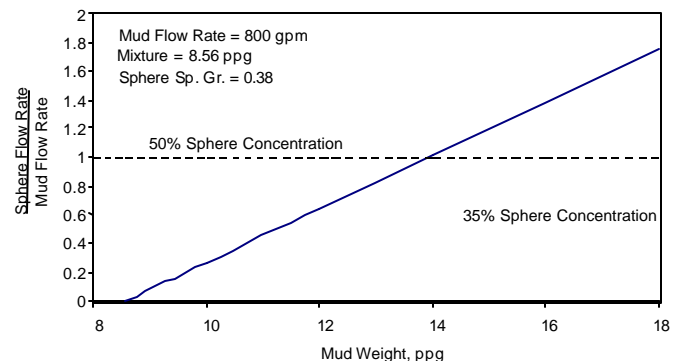


Fig. 10-47. Sphere Flow Rate Required to Produce Seawater Gradient (Seawater Transfer)

10.4.3 Sphere Requirements (Mud Transfer)

If HGS are pumped into the mud stream in the form of a slurry (mud and spheres), the density of the mud in the riser, p_r , equals:

$$p_r = \frac{p_m Q_m + p_s Q_s}{Q_m + Q_s} \quad (10-2)$$

and the flow rate of the mixture in the riser equals:

$$Q_{mix} = Q_m + Q_s \quad (10-3)$$

where

- p_r = Mud Density in Riser
- p_m = Mud Density without Spheres
- p_s = Slurry Density (Mud and Spheres)
- Q_m = Mud Flow Rate
- Q_{mix} = Mixture Flow Rate
- Q_s = Slurry Flow Rate

With *mud transfer*, spheres are pumped from the drill rig to the sea floor in a mud slurry (up to 50% concentration) and this slurry is injected directly into the mud in the riser. The mud pumped to the sea floor mixes with the mud in the riser, thus increasing the mud flow rate and diluting the sphere concentration. For example, when pumping 800 gpm of slurry (50% spheres) into well mud flowing at 800 gpm, the flow rate in the riser increases to 1,600 gpm and the sphere concentration decreases to 25%. Therefore, the maximum sphere concentration that can be achieved with the *mud transfer* system is about 25%, compared to about 50% with the *seawater transfer* system.

Figure 10-48 shows

how the density of water (8.34 ppg) decreases with increased slurry flow rate for different sphere concentrations (water and spheres). These calculations ignore slip velocities of the spheres which are typically on the order of 5 to 20 ft/min (as described in the next section).

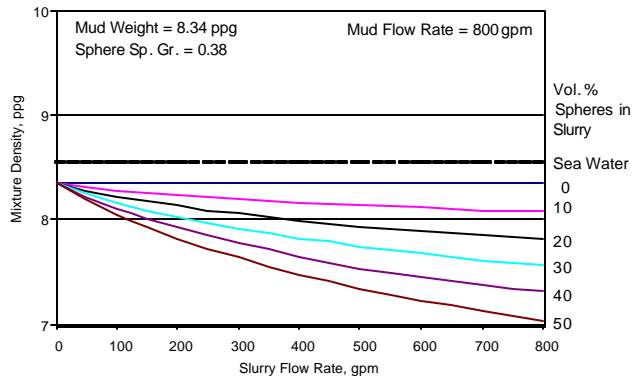


Fig. 10-48. Mixture Density vs. Slurry Flow Rate

Figures 10-49 and 10-50 show how the densities of 10 and 14 ppg muds decrease as the slurry flow rate and sphere concentration increases. With higher mud weights, the *mud transfer* system cannot reduce the mud density to that of seawater, so the *seawater transfer* system must be used.

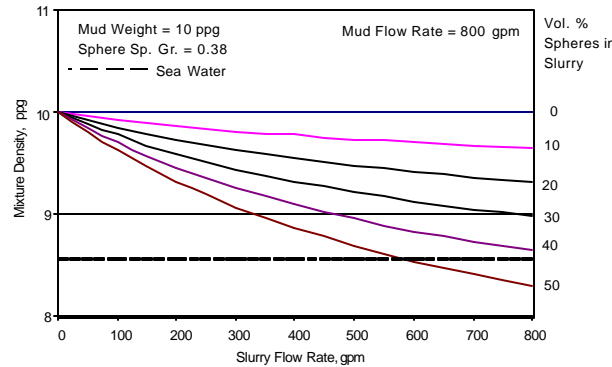


Fig. 10-49. Mixture Density vs. Slurry Flow Rate (Mud Transfer; 10 ppg)

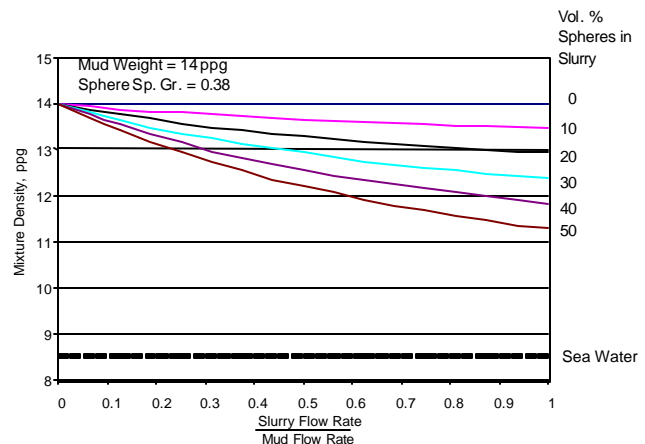


Fig. 10-50. Mixture Density vs. Slurry Flow Rate (Mud Transfer; 14 ppg)

10.4.4 Sphere Slip Velocity

Drill cuttings fall in the wellbore annulus because the rock cuttings are heavier than mud. Similarly, HGS float upward in mud since they are lighter than the mud.

Chapter 4 shows that the slip velocity of HGS increases with increased sphere diameter, increased fluid density, and decreased fluid viscosity (**Figures 10-51 and 10-52**). These figures show that the slip velocities of the spheres will be on the order of 5 to 20 ft/min, which is small compared to the fluid velocities riser or return flow line.

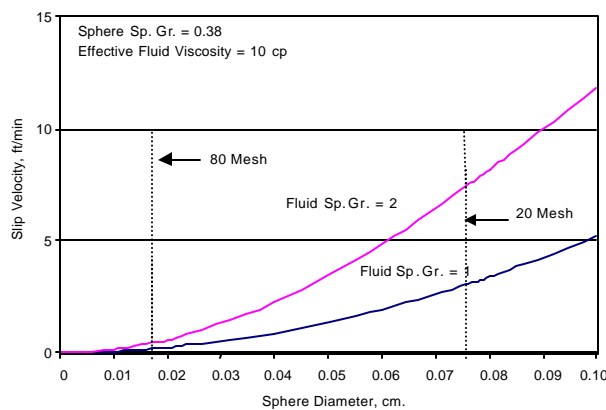


Fig. 10-51. Sphere Slip Velocity vs. Fluid Density

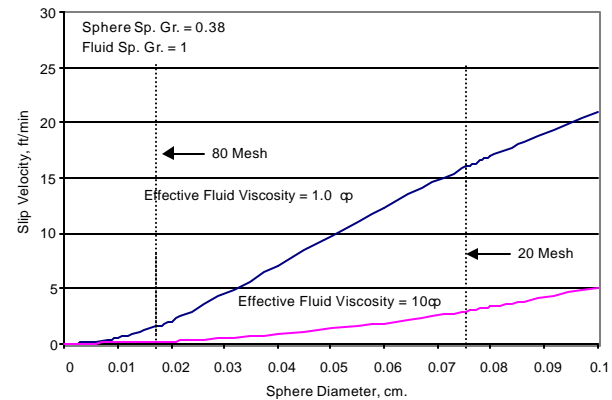


Fig. 10-52. Sphere Slip Velocity vs. Fluid Viscosity

10.4.5 HGS Characteristics

Manufacturer:	3M Specialty Additives (1-800-367-8905)
Product:	S38 Glass Bubbles
Material:	Water-resistant and chemically-stable unicellular soda-lime-borosilicate glass
Diameter:	8 to 125 microns (Median = 45 microns)
Density:	0.35 to 0.41 g/cc (0.38 typical)
Collapse Pressure:	4000 psi (90% Survival Rate)
Color:	White

10.4.6 Removing HGS From Mud

During riserless drilling, the spheres must be removed from the mud when it returns to the surface so that the heavier mud (without the spheres) can be recirculated to the bottom of the well and the HGS recirculated to the riser or return flow line. Tests showed that hollow spheres can be effectively removed from the mud with hydrocyclones (**Figure 10-53**), due to their low density. With the hydrocyclone, the heavier rock cuttings came out the underflow at the bottom of the cone, whereas the liquid mud and the HGS came out the overflow. These tests showed that hydrocyclones can effectively remove the hollow spheres from the mud, but not at the high flow rates (800 to 1200 gpm) required with offshore rigs.

The diameter of commercial HGS ranges for 8 to 125 microns with a median of 45 microns (**Figure 10-54**) and therefore pass through the 20 to 80 mesh (762 to 177 microns) screen typically used on oilfield shale shakers.

These microspheres have small diameters because they are typically used as fillers in paints, glues and other materials to reduce manufacturing costs. Oilfield shale shakers therefore cannot be used to remove the spheres from the mud when they return to

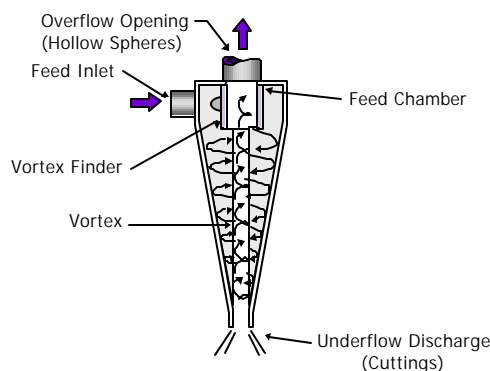


Figure 10-53. Oilfield Hydroclone
(Moore et al., 1974)

the surface. Larger diameter spheres (e.g., 1 mm and larger) are needed so that they can be screened out of the mud by conventional oilfield shale shakers (**Figure 10-55**).

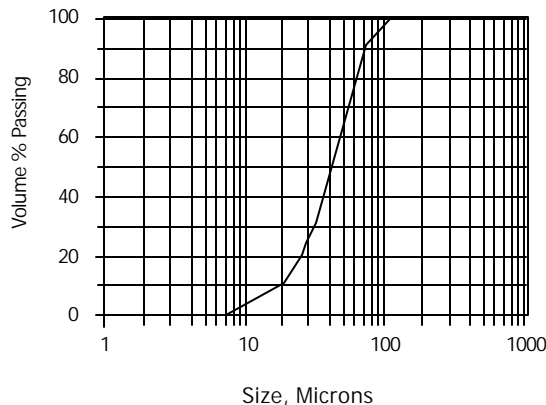


Fig. 10-54. Hollow Sphere Size Distribution

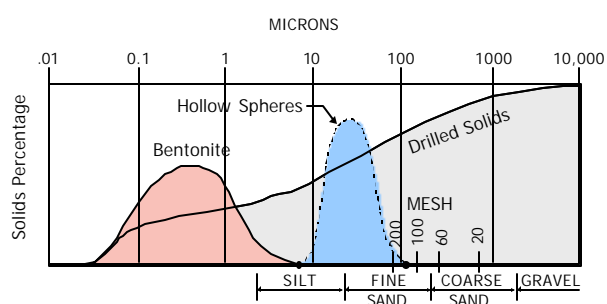


Fig. 10-55. Particle Sizes in Unweighted Water-Based Mud (After Annis, 1974)

10.5 ALTERNATIVE SPHERE INJECTION SYSTEMS

10.5.1 Sphere Concentrations

Sphere concentrations of 25 to 35% should be easily achievable with the DGD system shown in Figure 10-19, whereas sphere concentrations of 40 to 60% may be difficult to achieve. Following are three alternative sphere injection techniques that may allow sphere concentrations of 50 to 60%.

10.5.2 Drillstring Sphere Injection System

Figure 10-56 shows a Drillstring Sphere Injection system where hollow spheres are 1) pumped down the drillstring to the seafloor, 2) separated from the mud using a downhole sphere separator drillstring, and 3) injected into the bottom of the riser (**Figure 10-57**).

The mud containing no spheres then passes through the drill bit and into the wellbore annulus. Mud density in the riser is equal to that in the drillpipe so there is no “U-tubing” except for the weight of the cuttings in the wellbore annulus.

Major advantages of this system are that 1) high sphere concentrations (50 to 60%) can be achieved since there is no mud dilution, 2) the spheres do not have to be

separated from the mud when they return to the surface, 3) less deck space is required on the drill rig, and 4) this is a simple system to operate.

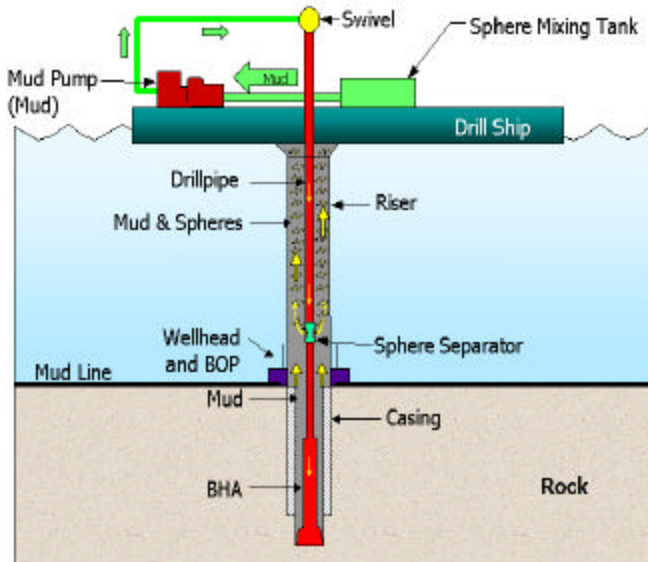


Figure 10-56. Drillstring Sphere
Injection DGD System

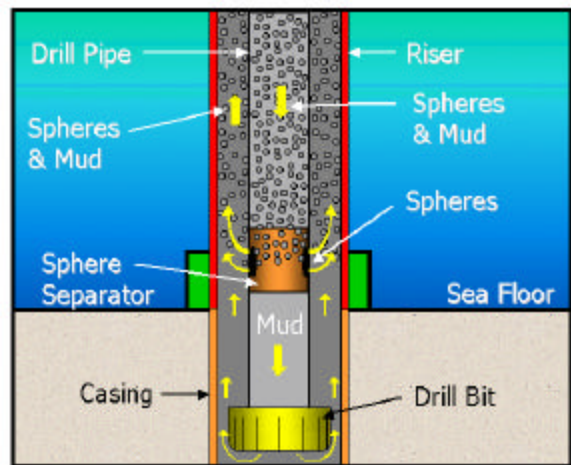


Figure 10-57. Drill String Sphere Separator

10.5.3 Carrier Fluid Injection System

With the Carrier Fluid Injection system shown in **Figures 10-58 and 10-59**, a lightweight “carrier” fluid circulates the spheres to the hole bottom where the spheres are removed from the slurry (carrier fluid & spheres) and injected into the bottom of the riser. The carrier fluid then flows up a separate flow line to the drill rig.

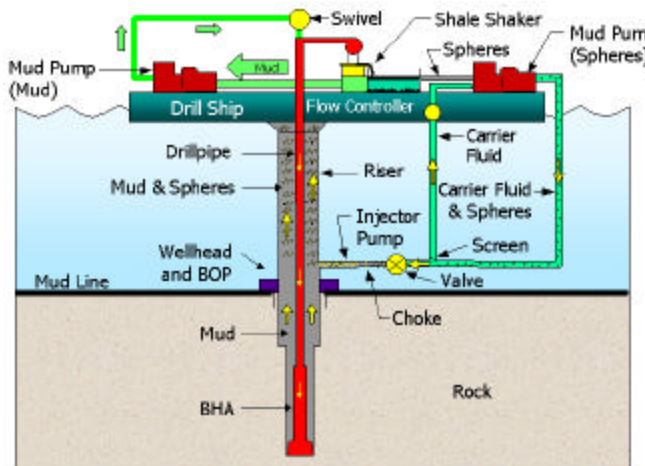


Figure 10-58. Carrier Fluid Dual-Gradient
System

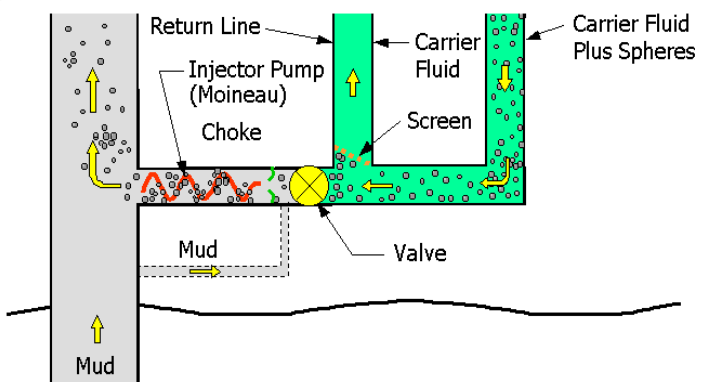


Figure 10-59. Carrier Fluid System Separator

If the density of the carrier fluid is less than seawater (8.6 ppg), U-tubing will lift the carrier fluid back to the rig so no seafloor pumps will be required. For example, with 10,000 feet water depth, a 7.6-ppg carrier fluid will produce a pumping pressure p , equal to:

$$p = 0.052 \times 10,000 \times (8.6 - 7.6) = 520 \text{ psi}$$

which will be adequate to overcome friction losses and pump the carrier fluid up to the surface.

When the spheres are injected into the riser, the void space between the spheres must be filled with fluid. This is accomplished by diverting part of the heavy drilling mud coming up the wellbore into the void spaces between the spheres as shown in **Figure 10-59**.

A “flow controller” at the top of the carrier fluid return line will regulate flow so that the flow rate of the carrier fluid (excluding spheres) going down the first flow line to the seafloor will exactly equal the flow rate of the carrier fluid returning up the second flow line to the drill rig, so that no carrier fluid will flow into the riser.

The ideal carrier fluid is the base fluid in the mud (e.g. water or synthetic oil) since these base fluids will not contaminate the mud in the riser if small amounts of the base fluid flow into the riser. A small amount of the base fluid might be allowed to flow into the riser to offset the volume of hole being drilled.

If the carrier fluid is slightly heavier than the seawater gradient in the riser, a small 100- to 200-hp seafloor pump can be used at the seafloor to lift the carrier fluid in the return line. A choke can also be used at the seafloor to force carrier fluid up the return flow line to the surface. The major advantage of this system is that high sphere concentrations (40 to 60%) should be achievable.

10.5.4 Seawater Sphere Injection System

Another option for sphere injection is the Seawater Sphere Injection system. For this case seawater will transfer the hollow spheres to the seafloor (**Figure 10-60**) where the spheres will be separated from the seawater using screens (**Figure 10-61**) or nitrogen filled chambers (**Figure 10-62**) and then injected into the riser, while the seawater is dumped into the ocean.

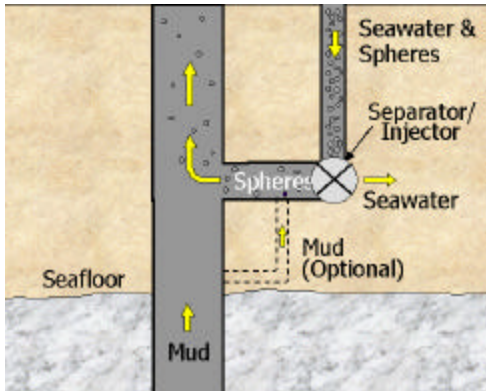


Figure 10-60. Seawater Hollow Sphere Transfer System

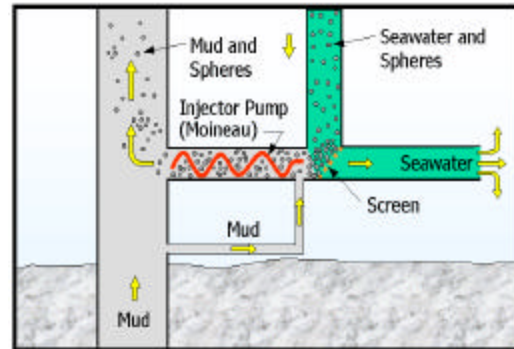


Figure 10-61. Seafloor Screen Separation System

The major advantage of this seawater transfer DGD system is that high sphere concentrations (40 to 50%) can be achieved since the seawater is dumped into the ocean and does not dilute the mud in the riser.

The major disadvantage of this system is that all residue mud must be removed from the spheres before they are pumped to the seafloor, otherwise, this mud will pollute the seawater being dumped into the ocean. It may be difficult to adequately clean the spheres at circulation rates (e.g. 500 to 1500 gpm).

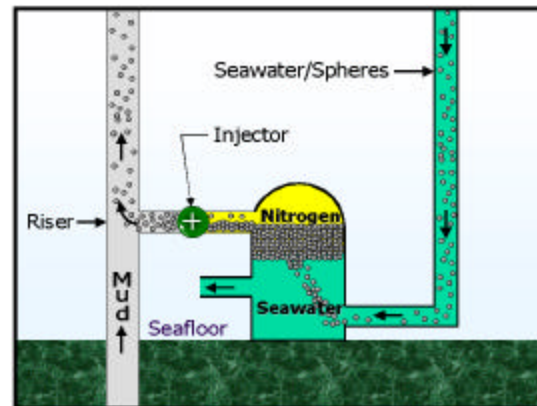


Figure 10-62. Seafloor Chamber Separation System

10.5.5 Hybrid Sphere/Gas-Lift Systems

Gas lift could be used in combination with the hollow spheres with a sphere/gas hybrid system to produce extra lift in the riser. Gas would be injected high into the riser where the nitrogen bubbles are more effective and where the compressor pressures and nitrogen requirements would be lower. Injecting nitrogen into the riser could be equivalent to increasing the sphere concentration by 10 to 25%.

10.6 SUB-SEAFLOOR SPHERE INJECTION

10.6.1 Curved-Gradient Drilling

The major problem with deepwater drilling is that the frac and pore pressure curves are close together and it is difficult to keep the wellbore pressure between these curves. With conventional drilling, the pressure curves are straight lines drawn from the drill rig, so eight casing strings are required for the example well shown in **Figure 10-63**. With DGD, the pressure curves are straight lines drawn from the seafloor so only four casing strings are required for the example well shown in **Figure 10-64**.

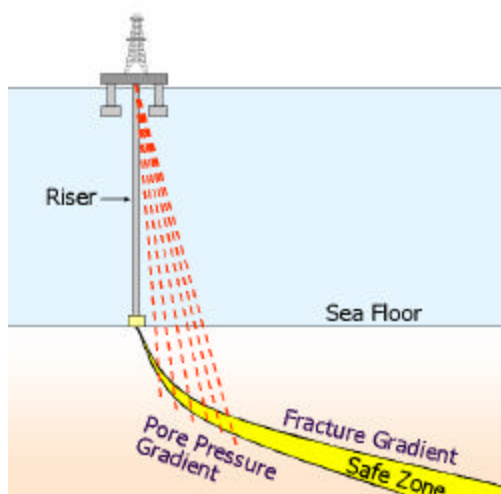


Figure 10-63. Conventional Deepwater Drilling

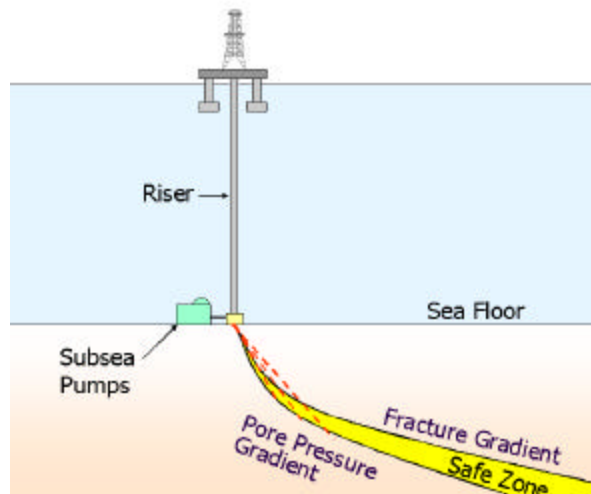


Figure 10-64. Dual-Gradient Deepwater Drilling

Maurer has developed a new concept called '**Curved-Gradient Drilling**' where lightweight materials (e.g., hollow spheres, lightweight solids, gases, etc.) are injected at one or more points below the seafloor to produce a "curved" gradient as shown in **Figure 10-65**. This technique allows wellbore pressure to remain between the frac and pore pressure curves for greater distances, thus reducing the number of casing strings required.

Hollow spheres or other lightweight materials can be injected into the wellbore annulus below the seafloor by different methods including 1) dual-wall drillpipe, 2) parasite strings outside of the casing, 3) tieback casing strings, 4) jet subs, or 5) combinations of these techniques as shown in **Figure 10-66**.

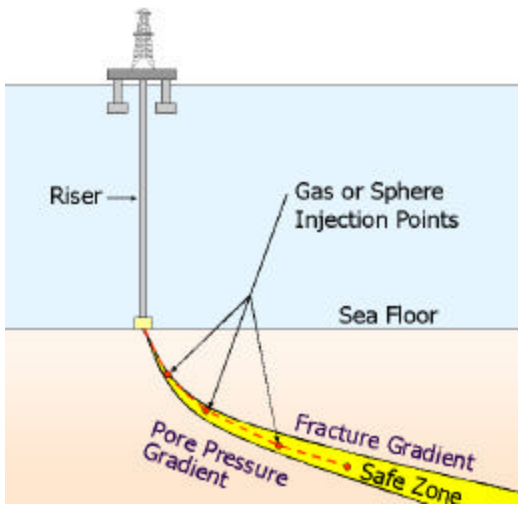


Figure 10-65. Curved-Gradient Deepwater Drilling

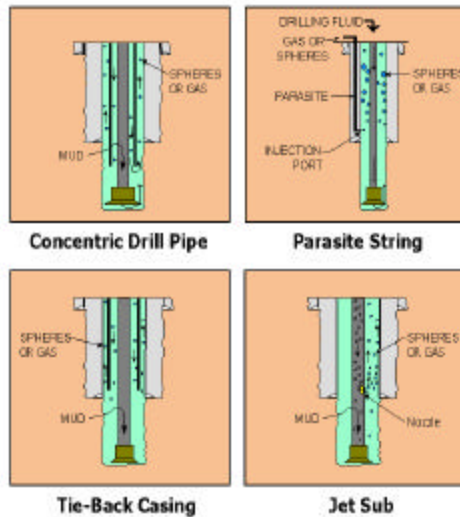


Figure 10-66. Fluid Injection Techniques

This curved-gradient technique could be used with “drilling-with-casing” systems to eliminate casing running problems once the section is drilled.

10.6.2 Subsea Sphere Injection

Figure 10-67 shows pressure gradients for a well drilled in 10,000 ft of water with 14-ppg mud where hollow spheres or seafloor pumps are used to produce a seawater gradient at the bottom of the riser. Pressure is 4470 psi at the seafloor, 8,110 psi at 15,000 ft, and 11,750 psi at 20,000 ft.

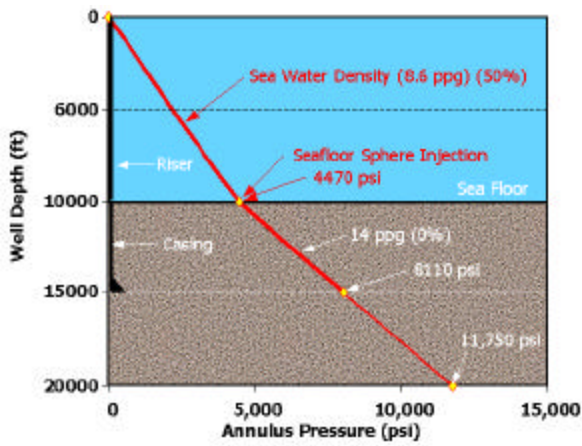


Figure 10-67. Sub Seafloor Sphere Injection (4770 psi)

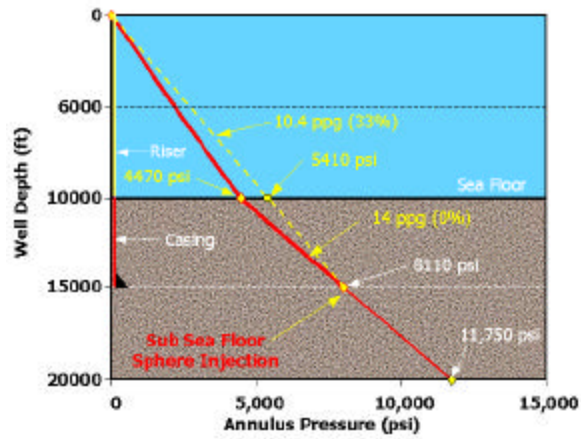


Figure 10-68. Sub Seafloor Sphere Injection (5410 psi)

A 50% sphere concentration (0.38 g/cc HGS) is required to produce a seawater gradient at the seafloor with a 14-ppg mud (Figure 10-67). A seawater gradient is

required when drilling into the seafloor, but higher gradients (i.e., heavier muds) can be used if the hollow spheres are injected below the seafloor.

For instance, if the hollow spheres are injected into the wellbore annulus at the bottom of casing set at 15,000 ft, a mud weight of 10.4 ppg will produce the required 8110 psi wellbore pressure at this depth (**Figure 10-68**). The 10.4-ppg mud requires a sphere concentration of only 33%, which is much easier to achieve than the 50% concentration required with sphere at the seafloor.

Similarly, if spheres were injected into 14-ppg at 20,000 ft, 11.3-ppg mud will produce the necessary 11,750 psi pressure. This situation will require a sphere concentration of only 25% (**Figure 10-69**).

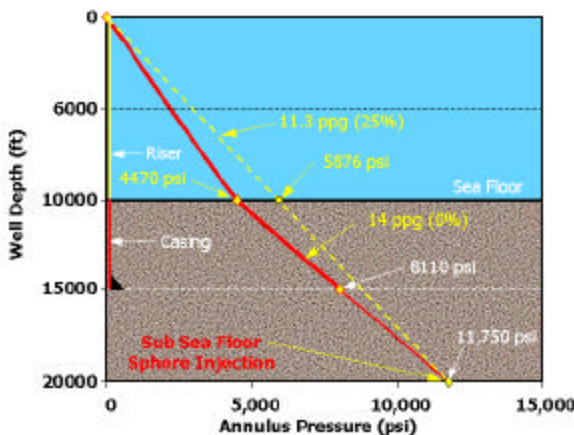


Figure 10-69. Sub-Seafloor Sphere Injection (5876 psi)

Sphere injection below the seafloor therefore has the advantage that it allows curved gradients to be used and significantly reduces sphere concentrations required at greater well depths.

10.7 EFFECT OF HOLLOW SPHERES ON MUD RHEOLOGY

10.7.1 Effect of Sphere Size on Surface Area

Oilfield mud engineers are aware that the viscosity of a mud increases as the percentage of fine solids (drill solids, barite, etc.) in the mud is increased because of the large surface area of the fine solids. For a given volume of cuttings V , the total surface area of the hollow spheres equals (Section 10.9).

$$A = \frac{3V}{R} \quad (10-4)$$

where R is the radius of the spheres.

Equation 10-4 shows that for a given volume of spheres, the surface area of the spheres is inversely proportional to the radius of the spheres. A 100-fold increase in sphere radius will therefore reduce the surface area by 99%, which will significantly reduce the impact on viscosity due to the reduction in surface area of the spheres.

10.7.2 Small-Diameter Hollow-Sphere Tests

The effect of small-diameter HGS (10 to 100 microns) on mud rheology was tested with three muds ranging in density from 8.55 to 10.75 ppg. (Compositions presented in Section 10.10) (see Table 10-1). **Figures 10-70 and 10-71** show how plastic viscosity (PV) and yield point (YP) of these fluids increase with increased sphere concentrations, respectively. Although these values are high, they are within acceptable limits for oilfield muds.

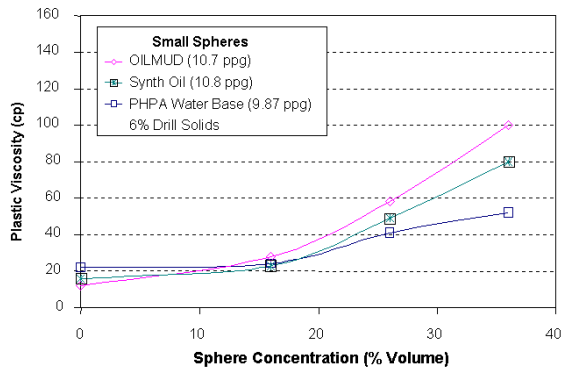


Figure 10-70. Effect of Sphere Concentration on Plastic Viscosity

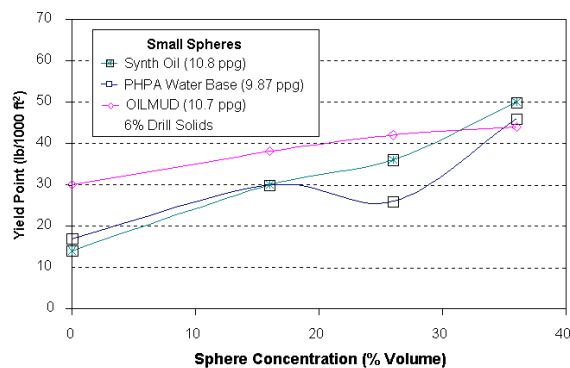


Figure 10-71. Effect of Sphere Concentration on Yield Point

Mud weights as high as 15 to 18 ppg will be used with DGD. These heavier muds contain considerable solids (bentonite, barite, drill solids, etc.), and therefore have high viscosities, so sphere concentrations of 30 to 50% may result in excessive mud viscosity when using small hollow spheres. To overcome this problem, the concept of using larger diameter hollow spheres was developed (see Section 10.3.7).

10.7.3 Solid Sphere Tests

Laboratory tests were conducted with solid glass 90-micron (170 mesh) diameter spheres (small spheres) and 850-micron (20 mesh) diameter spheres (large spheres) to determine if larger spheres would reduce viscosity. Although solid spheres were heavier than hollow spheres (2.5 vs. 0.4 g/cc), and somewhat larger, they were suitable for testing this concept. The tests were conducted with an 8.8-ppg water-based PHPA mud containing 6% fine drill solids.

With a 36%-by-volume sphere concentration, large solid glass spheres increased plastic viscosity of the mud from 13.5 to 16 cp (18.5%), while small spheres increased plastic viscosity from 13.5 to 22 (63%), showing that larger spheres significantly reduced the impact on mud viscosity.

With water-base mud with no drill solids, larger spheres produced no increase in plastic viscosity whereas small spheres increased plastic viscosity from 12.5 to 22.5 cp (80% increase). This also shows that increasing the size of the hollow spheres should significantly reduce the viscosity of the mud (as compared to mud with small spheres).

Both small and large spheres reduced the yield point of the mud containing 6% drill solids, showing that excessive yield point should not be a problem with the spheres (**Figures 10-72 and 10-73**).

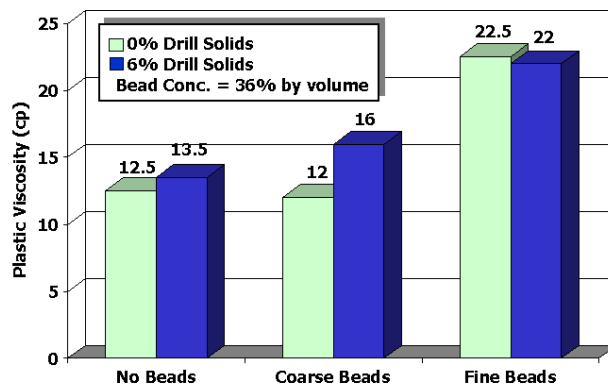


Figure 10-72. Effect of Sphere Size on Plastic Viscosity

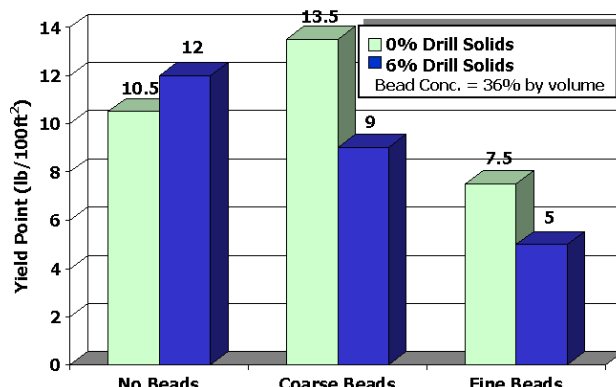


Figure 10-73. Effect of Sphere Size on Yield Point

10.8 TEXAS A&M DGD STUDY

10.8.1 Hollow Sphere DGD Circulating Pressures

As part of this DOE project, Dr. Hans Juvkam-Wold and Liliana Vera with Texas A&M reviewed wellbore hydraulics of the hollow sphere DGD drilling system (complete report in **Appendix G**). **Figure 10-74** shows the circulating pressure with 0, 36, 50, and 66% by volume HGS (0.38 g/cc) concentrations and a 19.17-ppg mud.

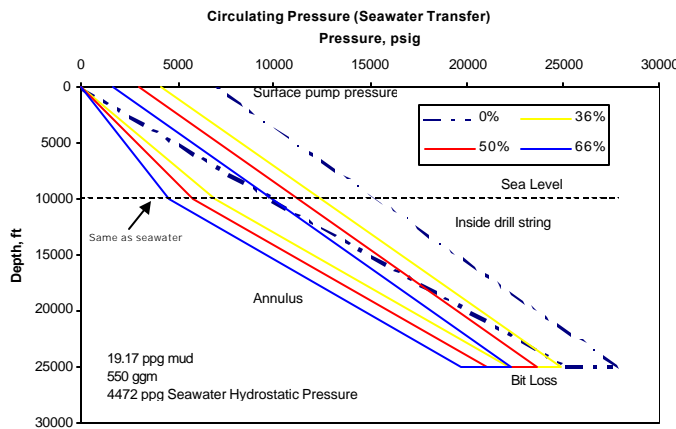


Figure 10-74. Circulating Pressure, 19.17 ppg and 10,000 ft Water Depth

Figure 10-75 shows how the plastic viscosity and pressure losses increase with increased sphere concentration.

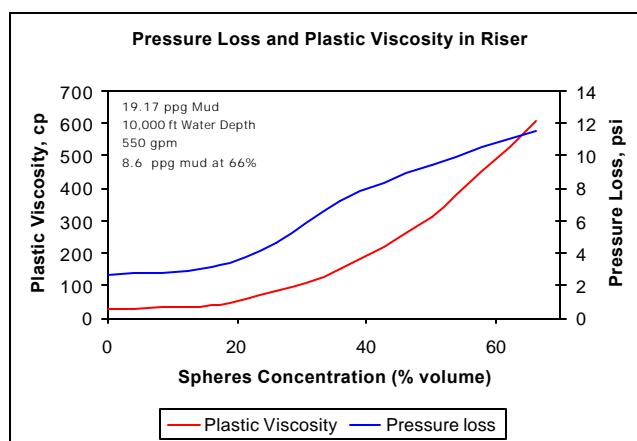


Figure 10-75. Pressure Loss and Plastic Viscosity in Riser

10.8.2 Mud Level Drop Due to U-Tubing

Figure 10-76 shows how the mud level drops in the drillstring due to “U-tubing” when circulation is stopped with 9.87 and 10.75 ppg muds.

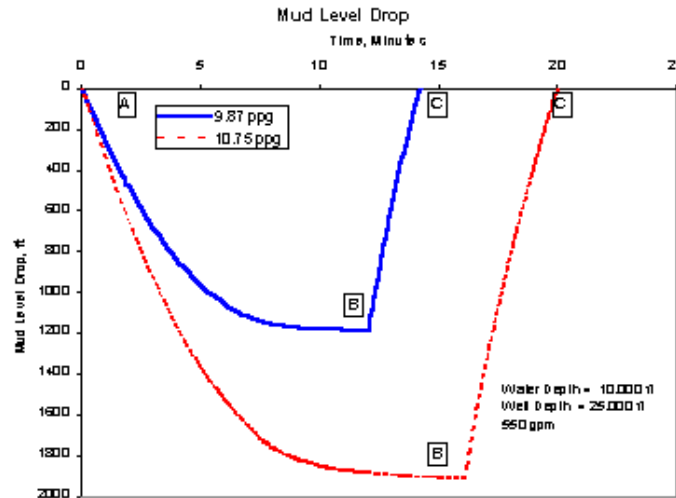


Figure 10-76. Drop in Mud Level vs. Time When Circulation Stops and Restarts

Figure 10-77 shows how the mud level in the drillstring drops during a connection if a drillstring mud valve is not used, and how fast it starts up when circulation is resumed.

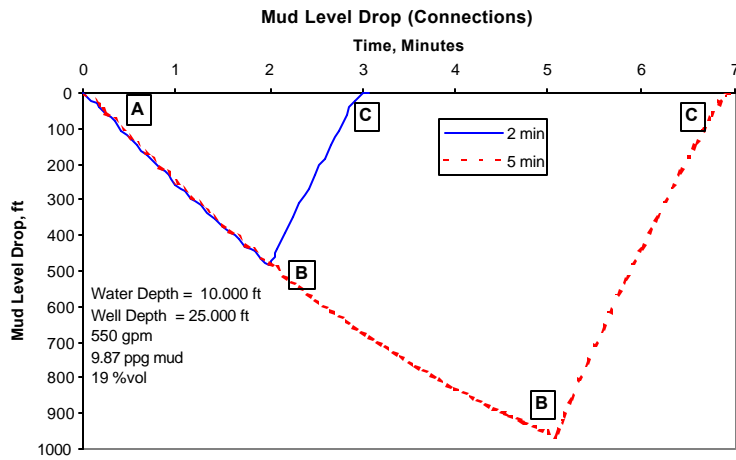


Figure 10-77. Fluid Level Drop vs. Time During Connections

10.8.3 Pit Volume Gain Due to U-Tubing

Figure 10-78 shows pit gain due to U-tubing during connections (with no drillstring valve) and **Figure 10-79** shows the reduction in pressure at the mudline with various sphere concentrations when circulation is first initiated and then as hollow spheres fill the riser.

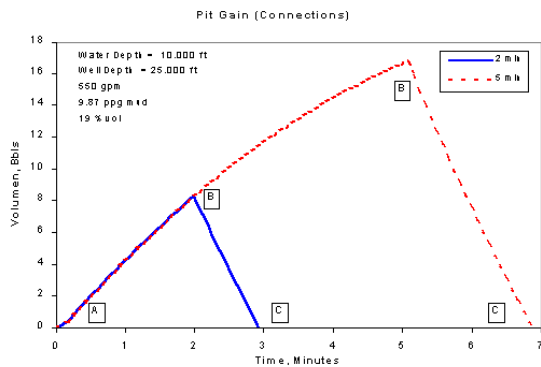


Figure 10-78. Pit Gain and Loss During Connections

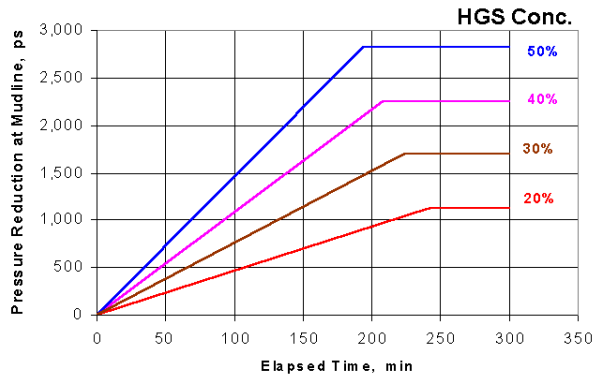


Figure 10-79. Reduction in Pressure at Mudline while Riser is Filling with HGS

10.9 SURFACE AREA OF SPHERES

10.9.1 Single Sphere

The volume v and the surface area of a sphere equal:

$$v = \frac{4}{3} \pi R^3 \quad (10-5)$$

$$a = 4\pi R^2 \quad (10-6)$$

where R is the sphere radius.

10.9.2 Multiple Spheres

For a given volume of spheres V , the number of spheres required equals:

$$n = \frac{V}{v} = \frac{3V}{4\pi R^3} \quad (10-7)$$

The total surface area A for n spheres therefore equals:

$$A = n4\pi R^2 = \frac{3V}{R} \quad (10-8)$$

Equation 10-8 shows that for a given volume of spheres, surface area of the spheres is inversely proportional to the radius of the spheres. A 100-fold increase in radius will reduce surface area by 99%. Thus, sphere size will significantly impact the viscosity of drilling fluids since viscosity is directly related to the surface area of the solids in the mud. This relationship indicates that large hollow spheres should result in much lower mud viscosities than smaller spheres.

10.10 BASE FLUID PROPERTIES

10.10.1 Base Drilling Fluids (Small Spheres)

Table 10-1. Base Drilling Fluids (Small Spheres)

PHPA WATER-BASE DRILLING FLUID		SYNTHETIC OIL DRILLING FLUID	
Houston Tap Water	1	Polyalphaolefin, bbl	0.67
API Bentonite, ppb	10	Organoclay, ppb	5
PHPA, ppb	1	Primary Emulsifier, ppb	8
Caustic Soda, ppb	0.25	Secondary Emulsifier, ppb	5
Density, ppg	9.87	Lime, ppb	5
		30% CaCl ₂ , bbl	0.22
		Amine Lignite, ppb	8
		Barite, ppb	150
		Density (ppg)	10.75

OIL-BASE DRILLING FLUID	
No. 2 Diesel, bbl	0.67
Organoclay, ppb	5
Primary Emulsifier, ppb	8
Secondary Emulsifier, ppb	5
Lime, ppb	5
30% CaCl ₂ , bbl	0.22
Amine Lignite, ppb	8
Barite, ppb	150
Density (ppg)	10.71

10.10.2 Base Drilling Fluids (Small and Large Spheres)

Table 10-2. Base Drilling Fluids (Small and Large Spheres)

WATER-BASE DRILLING FLUID		OIL-BASE FLUID	
Tap water, bbl	0.84	Diesel Oil, bbl	0.63
Bentonite, ppb	20	Organoclay, ppb	5
Lignosulfonate, ppb	2	Primary Emulsifier, ppb	9
Lignite, ppb	2	Secondary Emulsifier, ppb	6
Caustic Soda, ppb	1	Lime, ppb	8
XCD Polymer, ppb	0.5	25% CaCl ₂ , bbl	0.21
Barite, ppb	185	Barite, ppb	240
Density (ppg)	12.0	Density (ppg)	12.0

10.11 CONCLUSIONS

1. HGS have potential application with dual-gradient drilling (DGD).
2. Spheres for DGD may be constructed of any material including glass, ceramics, metals, etc. Solid spheres made of lightweight materials (e.g., plastics) can also be used.
3. Hollow spheres eliminate the need for seafloor pumps which can be expensive and difficult to operate.
4. Hollow spheres can be pumped with conventional mud pumps, thus eliminating expensive compressors, and nitrogen required with gas-lift systems.
5. Increasing the diameter of commercial hollow spheres to 1 mm will allow them to be screened out of mud using oilfield shale shakers (20 to 80 mesh).
6. Commercially available hollow spheres (0.38 g/cc) have collapse pressures of 4000 psi, which will allow their use to depths of 9000 ft. Heavier-wall spheres can be used for greater water depths.
7. Additional R&D is needed to fully evaluate the potential of using hollow spheres for deepwater drilling and DGD systems.

11. Enhanced Foam Underbalanced Drilling Model

11.1 PHASE II IMPROVEMENTS TO FOAM

Several modifications have been made to the Phase I Underbalanced Drilling Model, FOAM 1, resulting in a new version, FOAM 2, which is ready for distribution:

1. Improved foam rheology model
2. A pressure-matching feature that allows field calibration by matching measured and calculated standpipe pressure has been added

A copy of FOAM version 2 is included on the electronic copy (CD) of the Final Report submitted to the DOE.

11.2 IMPROVED FOAM RHEOLOGY MODEL

To predict pressure drops for foam flow, foam rheological parameters must be determined for the foam mixture. During Phase I, Bingham plastic and power-law models were used in FOAM 1.

Okpobiri and Ikoku (1986) experimentally studied foam rheology with a concentric annular viscometer that closely simulated actual hole conditions. They concluded that foam is a power-law pseudoplastic fluid with a flow behavior index n' and flow consistency K , both of which are functions of foam quality. Fluid properties for different foam qualities are listed in **Table 11-1**.

Table 11-1. Flow Properties for Foam (Okpobiri and Ikoku, 1986)

Quality		K_s' (lbf sec $^{n'}$ /sq ft)	Flow Consistency Index, K (lbf sec $^{n'-2}$ /ft)	n'
Range	Average			
0.96 to 0.977	0.97	0.0946	2.566	0.326
0.94 to 0.96	0.95	0.1228	3.323	0.290
0.91 to 0.92	0.915	0.2262	6.155	0.187
0.89 to 0.91	0.90	0.2079	5.647	0.200
0.84 to 0.86	0.85	0.1828	4.958	0.214
0.79 to 0.81	0.80	0.1344	3.635	0.262
0.77 to 0.78	0.775	0.1236	3.343	0.273
0.74 to 0.76	0.75	0.1078	2.918	0.295
0.72 to 0.73	0.715	0.1061	2.8716	0.293
0.69 to 0.71	0.70	0.1026	2.777	0.295
0.65 to 0.69	0.67	0.1022	2.766	0.290

Based on their results, a subroutine calculating flow behavior index n and consistency index K of foam was added to FOAM 2. The new correlation for K as function of foam quality is shown in **Figure 11-1**.

Many companies found that FOAM pressure predictions correlate well with field measured volumes. The foam rheological model has been fine-tuned using DEA-101 Participant field data to make the model more accurate. The fine-tuned rheological parameters are implemented in FOAM 2 which significantly increases the accuracy of this model.

The FOAM model contains a rheology model only for foam whereas the DEA-101 MUDLITE model contains rheological models for two-phase flow, mist, air and the same foam model used in FOAM 2.

11.3 PRESSURE-MATCHING FEATURE

A pressure-matching feature was added to FOAM 2 that applies a “K factor” to adjust predicted standpipe pressures so they match measured standpipe pressures for specific field conditions. In the pressure matching window, K_m factor is calculated as:

$$K_m = \frac{(\text{Measured Standpipe Pressure} & \text{ Calculated Standpipe Pressure})}{\text{Calculated Standpipe Pressure}} \quad (11-1)$$

Once this pressure matching feature is used, it matches the predicted and measured standpipe pressures and then uses the K factor to adjust the pressure profile throughout the well as shown in **Figures 11-2** and **11-3**.

11.4 CASE STUDY

A well was recently drilled with foam where MUDLITE predictions were compared to real-time, bottom-hole annular pressure data (**Table 11-2**).

Table 11-2. Field Well Parameters

Fluid:	Aerated Foam	Water:	130 - 150 gpm
MW:	9.3 ppg	Soap:	50 gal/hr (max)
SPP:	1,000 psi	Air:	650 - 700 scfm
BHT:	74EF	ROP:	3.1 - 8 ft/hr

MUDLITE pressure predictions correlated well with measured values on this well (**Figure 11-4**). The well was drilled near balance with air to lower the hydrostatic head to overcome lost circulation problems. No severe fluid losses occurred while drilling this well.

FOAM Hydraulics Model

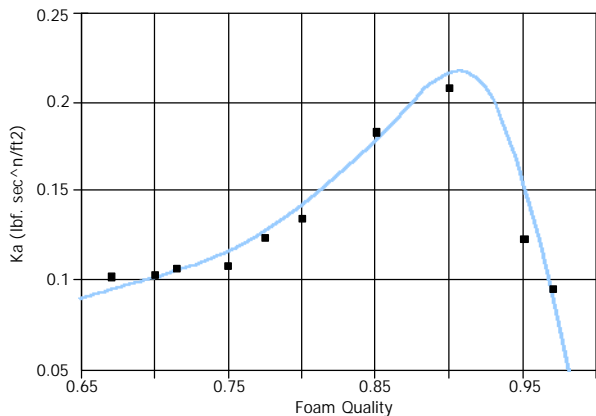


Fig. 11-1. FOAM 2 K Factor Correlation

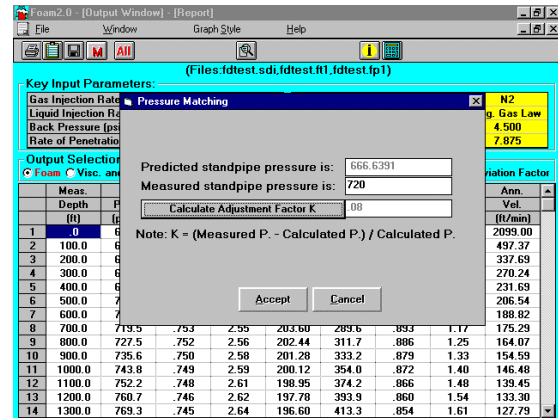


Fig. 11-2. Pressure Matching Window

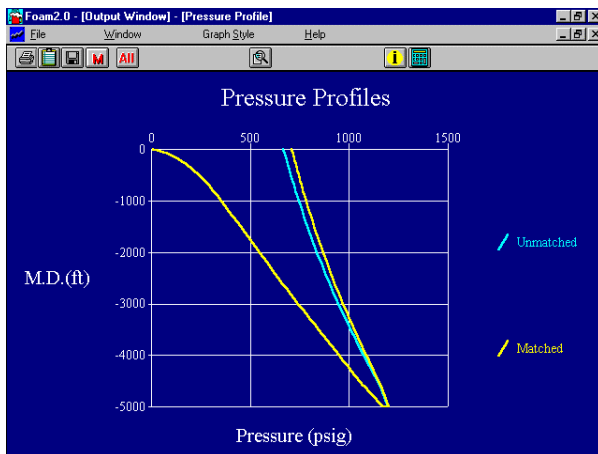


Fig. 11-3. Matched Pressure Profile

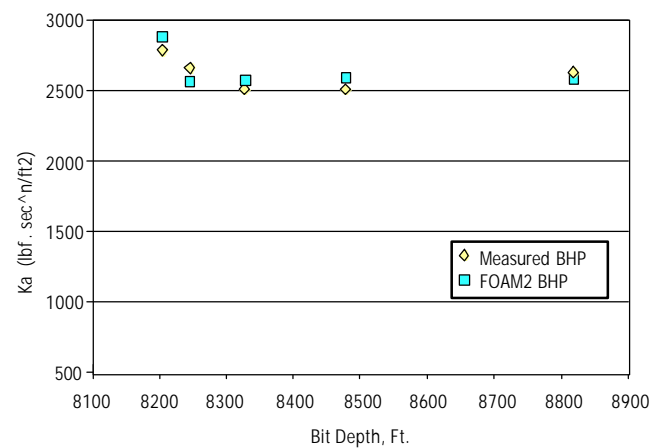


Fig. 11-4. FOAM 2 Predictions vs Field Data

The rheological field foam model (power-law) used in MUDLITE 2 has been fine-tuned to make it more accurate. Following are cases that demonstrate that the new foam rheological model used in FOAM 2 and MUDLITE 2 is very accurate.

Case 1:

MD = 8,202 ft
 Gas Q = 650 scfm
 Liquid Q = 190 gpm
 ROP = 8.0 ft/hr

Field Data	FOAM Predictions	
	Version 1.0	Version 2.0
Surface 1,000 psi	1,626.9	1,099.2
BHP (psi) 2,750-2,800	3,226.9	2,866.6

Case 2:

MD = 8,243 ft
 Gas Q = 650 scfm
 Liquid Q = 140 gpm
 ROP = 3.1 ft/hr

Field Data	FOAM Predictions	
	Version 1.0	Version 2.0
Surface ?	1,059.1	672.8
BHP (psi) 2,600-2,700	2,967.7	2,557.6

Case 3:

MD = 8,324 ft
 Gas Q = 650 scfm
 Liquid Q = 140 gpm
 ROP = 6.8 ft/hr

Field Data	FOAM Predictions	
	Version 1.0	Version 2.0
Surface ?	1,070	679
BHP (psi) 2,500	2,974	2,562.6

Case 4:

MD = 8,474 ft
 Gas Q = 650 scfm
 Liquid Q = 140 gpm
 ROP = 6.8 ft/hr

Field Data	FOAM Predictions	
	Version 1.0	Version 2.0
Surface ?	1,085.6	687.3
BHP (psi) 2,500	2,982.2	2,568.3

Case 5:

MD = 8,818 ft
 Gas Q = 650 scfm
 Liquid Q = 140 gpm
 ROP = 6.8 ft/hr

Field Data	FOAM Predictions	
	Version 1.0	Version 2.0
Surface ?	1,122.1	706
BHP (psi) 2,600	2,992.4	2,572.8

11.5 CONCLUSIONS

The following conclusions were reached as a result of this work on the model FOAM:

1. The Phase I FOAM 1 foam hydraulics model has been upgraded to FOAM 2.
2. An improved foam rheology model has been added that significantly improves circulating pressure predictions.
3. A high-angle (55E to 90E) cuttings transport model has been added to allow hole-cleaning calculations with extended-reach and horizontal wells.
4. A “pressure-matching” feature has been added that field calibrates the model so predicted and measured standpipe pressures are equal.
5. FOAM version 2 is ready for distribution and should significantly improve foam drilling operations.

12. Other Potential Applications for HGS

In addition to underbalanced and riserless drilling, other potential uses of Hollow Glass Spheres (HGS) were identified which were beyond the scope of this Phase II study. Additional work needs to be done to evaluate these other promising HGS applications.

12.1 FRACTURE FLUID ADDITIVE

During the mid-1980s, Dowell and other service companies studied the use of HGS and other buoyant additives in prepad frac fluids. The concept was that these lightweight additives would rise in the fractures and “screen out,” thus limiting upward growth and increasing fracture horizontal length.

The Phase II study showed that in addition to their low density, HGS have other properties that may be beneficial in frac fluids including:

1. Reduced fluid leakoff
2. Form low-permeability filter cake
3. Reduced formation damage
4. Increased fluid viscosity
5. Non-reactive with formation
6. High temperature stability
7. Stabilize temperature-dependent fluids
8. Incompressible

Additional work needs to be done to fully evaluate use of HGS with frac fluids.

12.2 LOW-COST EXTENDER FOR EXPENSIVE MUDS

HGS are commonly used as inexpensive fill material in paints, glues, and other materials to reduce manufacturing costs. Oil-base and synthetic-oil drilling muds are very expensive (\$200 to \$1000 per barrel) so HGS may have application as extenders in these expensive fluids. The density of the spheres could be adjusted by varying the wall thickness for use in different density muds.

A feasibility study could quickly evaluate the benefits and possible limitations of this concept.

12.3 WELLBORE-STABILITY ENHANCER

Wellbore-stability problems are much greater with water-base muds than with oil-base muds because of shale hydration caused by water movement into the shale. HGS fluids form low-permeability filter cakes which may reduce movement of water into the shale and thereby improve wellbore stability.

12.4 ALTERNATIVE SPHERE MATERIALS

The S38 hollow glass spheres tested on this project have a specific gravity of 0.38. Hollow spheres can be purchased with specific gravities ranging from 0.15 to 0.60 as shown in Chapter 4. This will allow matching the density of the spheres to that of the base fluid when HGS are used solely as filler material. Solid spheres have a specific gravity of approximately 2.2, and may have application with heavy muds.

Materials such as ceramics, metals, and plastics could be used as alternatives to glass in the manufacture of the hollow spheres. These materials may have application in deeper wells where higher collapse pressures are required.

12.5 COMPLETION FLUIDS

HGS could be used to reduce the density of completion fluids to allow completions in depleted reservoirs, and as filler material in expensive brines (\$500 to \$1500 per barrel) to reduce their cost. HGS could also be used to reduce loss of these expensive brines due to leakoff.

12.6 CEMENTING ADDITIVE

HGS have application for improving primary cementing of gas and oil wells, and may also be of benefit for improving cementing of production casing in geothermal environments. The Department of Energy is co-funding a project entitled "Ultra-Lightweight Cement" (DE-FC26-O0NT40919). The objective of this project is to develop an improved ultra-lightweight cement using a novel additive: ultralight hollow glass spheres (ULHS).

The new ULHS cement systems will allow wells to be successfully completed with less formation damage while still providing effective formation isolation. These strong, ULHS cements will be especially beneficial in low-pressure reservoirs. This project will be completed in 2002.

12.7 CEMENT/CASING BOND IMPROVEMENT

An additional application of HGS is as an additive for drilling-fluid flushes prior to cementing. Oil-base and synthetic-base muds are difficult to remove from the pipe, which is critical for obtaining a good cement bond to prevent gas or fluid migration.

Until recently, there was no method to dynamically measure the effectiveness of the flush (referred to by the oil and gas industry as “wettability determination”). A new test apparatus was developed by Cementing Solutions, Inc. and Chandler Instruments to gauge this procedure.

A short series of tests was conducted by Cementing Solutions, Inc. to measure the impact of HGS fluids on mud removal. HGS were first added to the drilling fluid. With normal spacer or flush fluids, there was no significant improvement in clean-up of the mud. Next, HGS were added to the spacer fluids and the removal of synthetic-base mud was measured. Results were markedly improved.

This improvement in mud clean-up prior to cementing could save valuable rig time and help prevent gas migration in many wells. A summary of the test results from Cementing Solutions is presented in **Appendix H**. Additional testing is warranted and could lead to a significant improvement in primary cementing, as well as cost reductions in chemical additives and rig time.

13. References

- Annis, M.R., 1974: *Drilling Fluids Technology*, Exxon Co. U.S.A., Houston, Texas.
- Arco, Manuel J. et al., 2000: "Field Application of Glass Bubbles as a Density-Reducing Agent," SPE 62899, presented at 2000 SPE Annual Technical Conference and Exhibition, Dallas, Texas, October 1-4.
- Baroid, 1981: "Drilling Fluid Technology," NL Industries, Inc., in-house publication.
- Beyer, A.H., Millhone, R.S., and Foote, R.W., 1972: "Flow Behavior of Foam as a Well Circulating Fluid," SPE 3986, presented at the SPE 47th Annual Fall Meeting, San Antonio, Texas, October 2-5.
- Bourgoyne Jr., Adam T., Millheim, Keith K., Chenevert, Martin E., and Young Jr., F.S., 1986: *Applied Drilling Engineering*, 1st Printing, Society of Petroleum Engineers, Richardson, Texas.
- Duda, John R., and Medley Jr., George H., 1996: "Strong Growth Projected for Underbalanced Drilling," *Oil & Gas Journal Special*, September 23.
- Frazelle, Andy, 2001: "Dual Gradient Drilling," *Well-Connected*.
- Gault, Allen, 1996: "Riserless Drilling: Circumventing the Size/Cost Cycle in Deepwater," *Offshore*, May.
- Goldsmith, Riley, 1998: "MudLift Drilling System Operations," OTC 8751, presented at the 1998 Offshore Technology Conference, held in Houston, Texas, May 4-7.
- Goldsmith, Riley, 2000: "Dual Gradient Drilling Opportunities and Challenges," presented at the DOE/MMS Deepwater Dual-Density Drilling Workshop, September 28.
- Gonzalez, Rome, 2000: "Subsea Pumping, a Dual Gradient Approach to Deepwater Drilling," presented at the DOE/MMS Deepwater Dual-Density Drilling Workshop, Houston, Texas, September 28.
- Gonzalez, Rome, Shaughnessy, John and Grindle, W.D. (Dave), 2000: "Industry Leaders Shed Light on Drilling Riser Gas Effects," *Oil & Gas Journal*, July 17.
- Jorden, James R. and Campbell, Frank L., 1984: "Well Logging I — Rock Properties, Borehole Environment, Mud and Temperature Logging," Monograph Vol. 9, SPE Henry L. Doherty Series, Henry L. Doherty Memorial Fund of AIME, SPE of AIME, New York-Dallas.
- Larsen, T.I., et al., 1997: "Development of a New Cuttings-Transfer Model for High-Angle Wellbores Including Horizontal Wells," *SPE Drilling and Completion*, June.

- Liu, Gefei, 1996: "Advanced Foam Computer Model Helps in Analysis of Underbalanced Drilling," API/ASME Energy Week '96 Conference and Exposition, Houston, Texas, January 29-31.
- Lorenz, Howard, 1980: "Field Experience Pins Down Uses for Air Drilling Fluids," *Oil & Gas Journal*, May 12.
- McDonald, William J. et al., 2001: "Hollow Glass Spheres (HGS) to Reduce Formation Damage During Drilling," Topical Report for U.S. Department of Energy, Morgantown, West Virginia, July.
- Medley, Jr., George H., Maurer, William C., Liu, Gefei, and Garkasi, Ali Y., 1995: "Development and Testing of Underbalanced Drilling Products," report DOE/MC/31197-5129, Topical Report for U.S. Department of Energy, Morgantown, West Virginia, September.
- Moffitt, Stan, 1991: Personal Communication, Reed Tool Company Data, Houston, Texas, September 5.
- Moore, Preston L. Ormsby, George S., Grace, Robert D., Patton, Charles C., and Smith, Dwight K., 1974: *Drilling Practices Manual*, The Petroleum Publishing Co., Tulsa, Oklahoma.
- Murray, A.S. and Cunningham, R.A., 1955: "Effect of Mud Column Pressure on Drilling Rates," AIME Paper No. 505-G, *Transactions*, Vol. 204, October.
- Okpobiri, G.A. and Ikoku, C.U., 1986: "Volumetric Requirements for Foam and Mist Drilling Operations," *SPE Drilling Engineering*, February.
- Peterman, Charles P., 1998: "Riserless and Mudlift Drilling - The Next Steps in Deepwater Drilling," OTC 8752, presented at the 1998 Offshore Technology Conference, Houston, Texas, May 4-7.
- Poettman, F.H. and Begman, W.E., 1955: "Density of Drilling Muds Reduced by Air Injection," *World Oil*, August 1.
- Sanghani, V. and Ikoku, C.U., 1983: "Rheology of Foam and Its Implications in Drilling and Cleanout Operations," ASME AO-203, presented at the 1983 Energy-Sources Technology Conference and Exhibition, Houston, Texas, January 30-February 3.
- Sjoberg, Geir, 2000: "Deep Vision," presented at the AADE Technical Conference on Dual Gradient Drilling Systems held in Houston, Texas, February 8-10, 2000.
- Sjoberg, Geir, 2000: "Deep Vision, " presented at the DOE/MMS Deepwater Dual-Density Drilling Workshop held at the Red Lion Hotel in Houston, Texas, September 28.
- Snyder, Robert E., 1998: "Riserless Drilling Project Develops Critical New Technology," *World Oil*, January.

Smith, Kenneth L, and Weddle Curtis E. III, 2000: "Dual-Gradient Drilling Nearly Ready for Field Test," *World Oil*, October.

Smith, Ken, 2000: "Best Available Practical Drilling Technology—The Search Continues" SubSea MudLift Drilling presentation, presented at the AADE Technical Conference on Dual Gradient Drilling Systems held in Houston, Texas, February 8-10, 2000.

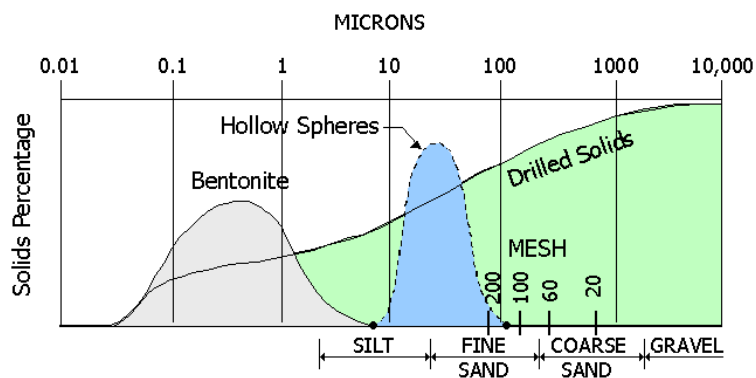
Smith, Ken and Weddle, Curtis, 2000: "SubSea MudLift Drilling Joint Industry Project," presented at the DOE/MMS Deepwater Dual-Density Drilling Workshop held at the Red Lion Hotel in Houston, Texas, September 28.

Development and Testing of Underbalanced Drilling Products

DOE Contract No. DE-AC21-94MC31197

Final Report October 1995 – July 2001

Appendices



Submitted to:

**U.S. DEPARTMENT OF ENERGY
National Energy Technology Laboratory
Attn: Roy Long
3610 Collins Ferry Road
Morgantown, West Virginia 26505**

By:

**William C. Maurer
William J. McDonald
Thomas E. Williams
John H. Cohen**

**MAURER TECHNOLOGY INC.
2916 West TC Jester
Houston, Texas 77018-7098
Tel: (713) 683-8227
Fax: (713) 683-6418**

TR01-16

July 2001

Appendix A

**“Foam Computer Model Helps in Analysis of
Underbalanced Drilling”**

by

**Gefei Liu & George Medley
MAURER ENGINEERING INC.**

Oil & Gas Journal
July 1, 1996

TECHNOLOGY

Foam computer model helps in analysis of underbalanced drilling

Gefei Liu, George H. Medley Jr. Maurer Engineering Inc. Houston

A new mechanistic model attempts to overcome many of the problems associated with existing foam flow analyses. The model calculates varying Fanning friction factors, rather than assumed constant factors, along the flow path. Foam generated by mixing gas and liquid for underbalanced drilling has unique rheological characteristics, making it very difficult to accurately predict the pressure profile.

A user-friendly personal-computer program was developed to solve the mechanical energy balance equation for compressible foam flow. The program takes into account influxes of gas, liquid, and oil from formations. The pressure profile, foam quality, density, and cuttings transport are predicted by the model.

A sensitivity analysis window allows the user to quickly optimize the hydraulics program by selecting the best combination of injection pressure, back pressure, and gas/liquid injection rates.

This new model handles inclined and horizontal well bores and provides handy engineering and design tools

Based on a presentation at Energy Week Conference & Exhibition, Houston, Jan. 29-Feb. 2.

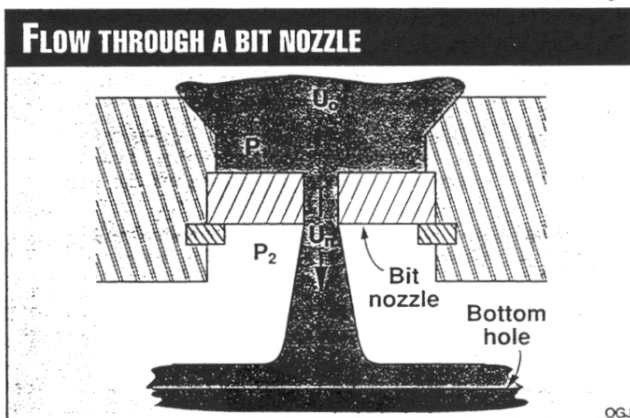


Fig. 1

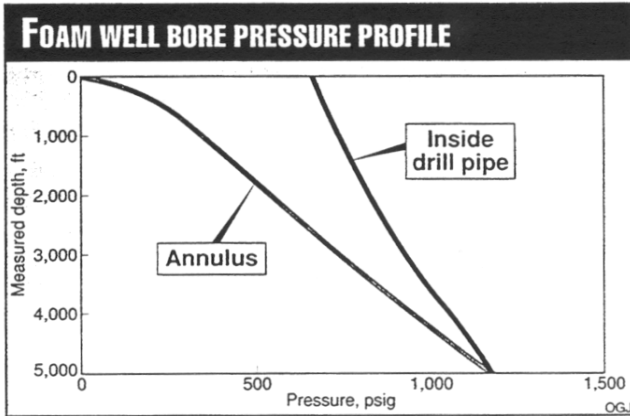


Fig. 2

tages of foam drilling over conventional mud drilling include high penetration rates, a high cuttings transport ratio, and less formation damage. In areas with low bottom hole pressures, the use of a lighter fluid, such as foam, is required.

The complex and unique flow mechanism involved in foam operations often confuses drilling operators about the optimum combination of liquid and gas injection rates. Other questions remain, such as how to predict the bottom hole pressure and how to combine different controllable variables to optimize results. Existing foam drilling design methods largely depend on field operation charts or on calculations using a mainframe computer. During the past 20 years, extensive study of foam rheological behavior and factors affecting foam circulation in oil wells has made it possible to develop a comprehensive computer program to meet the demands of foam drilling design and analysis.

From existing foam rheology models and the steady-state mechanical energy balance equation, Maurer Engineering Inc. has developed a Windows-styled computer model (FOAM) to help oper-

for underbalanced drilling, well bore cleanout, and other foam operations.

Foam has been used extensively in the petroleum

industry for decades. It has been proven effective and economic as a circulating fluid in hole cleanout and drilling operations. Advan-

EQUATIONS

$$V_g = \frac{ZRT}{M_g P}$$

$$V = \frac{a}{P} + b$$

$$\frac{u du}{g_c} - \frac{g d(VD)}{g_c} + V dP + \frac{2u^2 f d(MD)}{g_c D} = 0$$

$$u = cV = \frac{ac}{P} + bc$$

$$\frac{dP}{d(MD)} = F_p (MD, VD, P)$$

$$\frac{u dv}{g_c} - \frac{g d(VD)}{g_c} + V dP + \frac{2u^2 f d(MD)}{g_c (D_h - D_p)} = 0$$

$$\frac{dP}{d(MD)} = F_A (MD, VD, P)$$

$$\frac{u du}{g_c} + V dP = 0$$

$$b(P_2 - P_1) + (a) \ln \left(\frac{P_2}{P_1} \right) + 8.1 \times 10^{-4} U_n^2 = 0$$

$$U_n = \frac{ac'}{P_2} + bc'$$

$$\rho_L = \rho_o f_o + \sum_i \rho_i f_i$$

$$f_o = \frac{q_o}{q_o + \sum_{i=1}^N q_i}$$

$$f_i = \frac{q_i}{q_o + \sum_{i=1}^N q_i}$$

$$(1) M_g = M_{go} f_o + \sum_{i=1}^N M_{gi} f_i \quad (13)$$

$$(2) f_o = \frac{m_{go}}{m_{go} + \sum_{i=1}^N m_{gi}}$$

$$(3) f_i = \frac{m_{gi}}{m_{go} + \sum_{i=1}^N m_{gi}} \quad (14)$$

NOMENCLATURE

D	= Drill pipe ID, in.
D _h	= Open hole diameter, in.
D _p	= Drill pipe OD, in.
f	= Fanning friction factor
g	= Acceleration due to gravity
g _c	= 32.2 (ft-lbm) / (lbf - sq ft)
m _g	= Mass rate of gas
m _l	= Mass rate of liquid
m _s	= Mass rate of cuttings
m _{gi}	= Mass rate of influx gas
m _{gi}	= Mass rate of inlet gas
MD	= Measured depth, ft
M _g	= Molecular weight of gas, lb/lb-mole
M _{gl}	= Molecular weight of influx gas
M _{gi}	= Molecular weight of inlet gas
N	= Number of influxes
P	= Absolute pressure, psia
P ₁	= Pressure upstream of the nozzle
P ₂	= Bottom hole pressure
q _o	= Liquid injection rate
q _w	= Water/oil influx rate
ρ _o	= Density of inlet liquid
R	= Gas constant, 10.73 (psi cu ft)/(lb-mole °R)
T	= Absolute temperature, °R
u	= Average velocity of the foam, fpm
U _n	= Nozzle velocity
V	= Specific volume of foam
V _g	= Specific volume of gas
V _l	= Specific volume fluid
VD	= Vertical depth, ft
Z	= Gas compressibility factor

ators with the design and analysis of underbalanced drilling. The program simulates underbalanced drilling operations using foam as a circulating medium and can be used to evaluate and develop operational guidelines.

This article presents the foam flow equations and explains how to numerically solve compressible non-Newtonian flow in a three-dimensional well bore. Equations of state describing pressure, volume, and temperature interactions of compressible foam are presented. Flow regimes ranging from laminar to turbulent are covered.

Rheological models

Foam can be treated as a homogeneous fluid with

variable density and viscosity. During foam operations, foam quality depends on the pressure and temperature in the tubing or annulus. The pressure has to be determined through the mechanical energy balance equation, in which the frictional pressure drop term relies on the foam rheological model. It is therefore important to have an accurate rheological model describing dynamic foam behavior.

Theoretical approaches to the rheology of foam were presented by researchers in the early 1900s.^{1,2} Mitchell demonstrated that foam behaves as a Bingham plastic fluid, based on his experimental work in capillary tubes, and he empirically derived a set of equations for foam viscosity.³ It should be

noted that these equations do not apply at the limiting case of 100% foam quality.

Krug presented plastic viscosities and yield strengths of foam as a function of foam quality.⁵ Beyer, et al., first formulated a foam rheological model from laboratory and pilot-scale experimental data.⁶ Their observations suggested that foam behaves as a Bingham plastic fluid. Their study did not demonstrate a dependence of yield point on liquid volume fraction or foam quality.

Sanghani and Ikoku experimentally studied foam rheology with a concentric annular viscometer that closely simulated actual hole conditions.⁷ They concluded that foam is a power-law pseudoplastic fluid with flow behavior index n and flow

consistency K, both functions of foam quality.

A review of the literature shows varied opinions on foam rheological models. Some researchers found that the power-law model was statistically superior to the Bingham plastic model in correlating data, while others found that foam more closely obeys the Bingham plastic model. The computer model described here includes both power-law and Bingham plastic models and allows the user to choose which one to use.

Foam flow equations

In the special case of a two-phase system such as foam, where gas is finely and uniformly dispersed in the liquid phase, homogeneous

Fig. 3

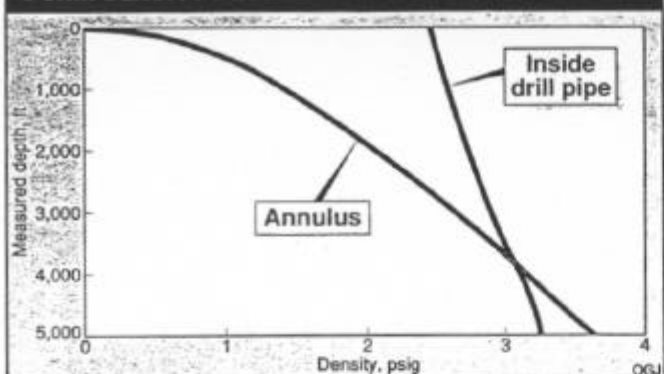
FOAM DENSITY PROFILE

Fig. 3

Fig. 4

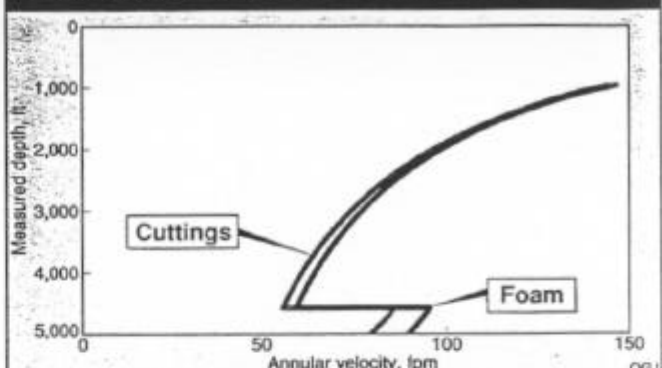
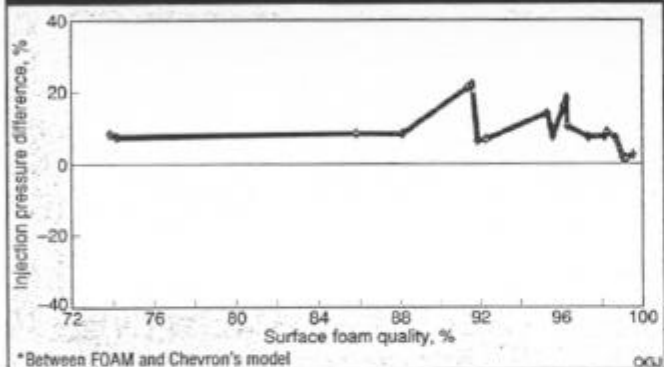
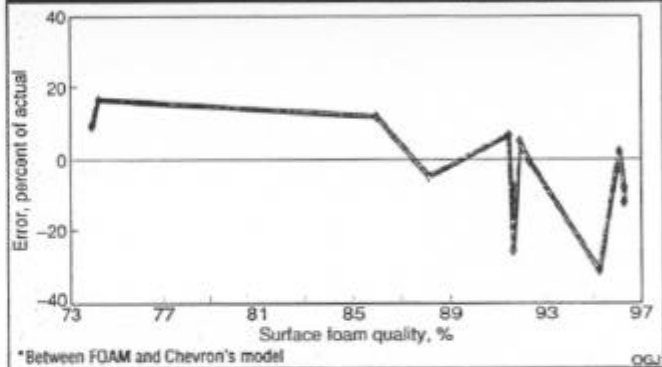
CUTTINGS LIFTING VELOCITY NEAR BOTTOM

Fig. 5

Fig. 6

SURFACE INJECTION PRESSURE COMPARISON*

*Between FOAM and Chevron's model

SURFACE PRESSURE COMPARISON*

*Between FOAM and Chevron's model

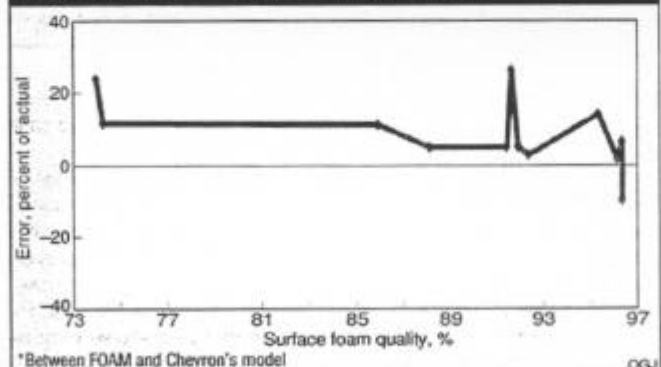
fluid can be assumed, and no equation is required for the phase interface.

Foam consists of a compressible component (gas) and an incompressible component (liquid). The incompressible component is easier to handle because of its constant density. The compressible gas requires much more attention because its density depends on temperature and pressure.

Pressure is coupled with gas volume fractions through a friction factor. An improved version of Lord's pressure drop equation and Spoerker's method are used in the following equation derivation.¹⁰ The friction factor is calculated along the well bore rather than assumed constant.

Equations of state

The relationship between the variation of density of a fluid with pressure and temperature is termed the equation of state. For engineering

BOTTOM HOLE PRESSURE COMPARISON*

purposes, the most practical form of the equation of state for a real gas is given by Equation 1.¹⁰

Equations of state for both downward and upward foam flow can be expressed as Equation 2. The coefficients a and b are defined in the accompanying box and Table 1.

The expressions of a and b take different forms for downward flow inside drill

pipe and upward flow in the annulus. For upward flow in the annulus, the foam is mixed with rock cuttings. There are three phases present in the annular mixture in which liquid and cuttings are incompressible, whereas the gas phase is compressible.

Mechanical energy equations

Once the equations of state for foam have been

established, the next step is to use the momentum and energy equations to analyze the dynamic foam behavior. The mechanical energy equation may be considered either a consequence of the momentum equation or a reduced form of the total energy equation.

For downward flow inside the drill pipe, the differential mechanical energy balance equation is given by Equation 3.

The average velocity of the foam, u , can be obtained using the continuity equation. In terms of specific volume, it can be expressed as Equation 4. The coefficient c is defined in the accompanying box.

After substituting Equation 4 into Equation 3, the differential mechanical energy balance takes the form in Equation 5. For upward flow in the annulus, the differential mechanical energy balance equation takes the form in Equation 6.

EQUATIONS OF STATE AND COEFFICIENTS

For downward flow inside the drill pipe, the mass fraction of gas is defined as:

$$W_g = \frac{P_{g,z} M_g V_g}{m_g + m_l} \quad (A-1)$$

Then the specific volume of foam mixture can be expressed as:

$$V = W_g V_g + (1 - W_g) V_l \quad (A-2)$$

Therefore, combining Equations A-1 and A-2 will lead to the equation of state for the downward foam flow inside drill pipe:

$$V = \frac{a}{P} + b \quad (A-3)$$

The coefficients a and b are defined in Table 1.

For upward flow in the annulus, the foam is mixed with rock cuttings. Three phases are present in the mixture. The mass fractions of the three components are:

$$\begin{aligned} W_g &= \frac{m_g}{m_g + m_l + m_s} \\ W_l &= \frac{m_l}{m_g + m_l + m_s} \\ W_s &= \frac{m_s}{m_g + m_l + m_s} \end{aligned} \quad (A-4)$$

The specific volume of the foam/cuttings mixture can be expressed as:

$$V = W_g V_g + W_l V_l + W_s V_s \quad (A-5)$$

Combining Equations A-4 and A-5 will lead to the equation of state for the upward foam flow in the annulus:

$$V = \frac{a}{P} + b \quad (A-6)$$

The functions of different mechanical energy balance inside drill pipe and the annulus:

$$F_p (MD, VD, P) =$$

$$\frac{S_p P^3 + \frac{2f abc^2}{25.8} P^2 + \frac{f}{25.8} a^2 c^2 P}{bP^3 + aP^2 - abc^2 P - a^2 c^2} \frac{1}{D} \quad (A-7)$$

where

$$S_p = \frac{f}{25.8} b^2 c^2 - D \frac{d(VD)}{d(MD)} \quad (A-8)$$

$$F_A (MD, VD, P) =$$

$$\frac{S_A P^3 + \frac{2f abc^2}{21.1} P^2 + \frac{f}{21.1} a^2 c^2 P}{bP^3 + aP^2 - abc^2 P - a^2 c^2} \frac{1}{D_h - D_p} \quad (A-9)$$

and where

$$S_A = \frac{f}{21.1} b^2 c^2 + (D_h - D_p) \frac{d(VD)}{d(MD)} \quad (A-10)$$

Table 1

COEFFICIENTS IN EQUATION OF STATE FOR FOAM

Coefficients	Inside drill pipe	In the annulus	Cross bit (c)
a	$\frac{W_g ZRT}{M_g}$	$\frac{W_g ZRT}{M_g}$	N/A
b	$(1 - W_g) V_l$	$W_l V_l + W_s V_s$	N/A
c or c'	$\frac{4}{\pi D^2 (m_g + m_l)}$	$\frac{4}{\pi (D_h^2 - D_p^2) (m_g + m_l + m_s)}$	Total flow area

The average velocity of the foam in the annulus is also described by Equation 4. The variable c for upward annular flow is different, however (see accompanying box).

Substituting annular velocity into Equation 6 will yield the differential mechanical energy balance in upward annular flow (Equation 7).

Equations 5 and 7 can be solved numerically. The back pressure, which is known, serves as a boundary condition for Equation 7. Numerical techniques are used to calculate a sequence of pressure values corresponding to dis-

crete values of the measured depth. The expressions of F_p and F_a are given in the accompanying box.

Pressure drop across nozzles

To calculate the pressure drop through a short constriction such as a bit nozzle, it generally is assumed that the change in elevation, the velocity upstream of the nozzle, and the frictional pressure loss across the nozzle are negligible (Fig. 1). Thus, Equation 3 becomes Equation 8.

Substituting Equations 2 and 4 into Equation 8 and integrating yields Equation 9

in field units. Nozzle velocity U_n is defined by Equation 10.

Equation 9 can be solved numerically to obtain the pressure upstream of nozzle P_1 . The bottom hole pressure P_2 is calculated from Equation 7 beforehand.

Influx modeling

One advantage of foam drilling is a lower bottom hole pressure, which helps increase the rate of penetration. Influxes of gas, water, or oil can occur as a result of low bottom hole pressure, however. These influxes will change the existing foam system, resulting in a change in the pressure profile inside

the drill pipe as well as in the annulus.

The total liquid density can be calculated from the rates and densities of the injected liquid and those of water/oil influxes (Equations 11 and 12).

The final liquid viscosity can be calculated in a similar fashion.

The molecular weight of the mixture of injected gas and influx gas can be calculated using weighting factors similar to those used for calculating liquid density and viscosity (Equations 13 and 14).

Equations of state for gas and upward annular foam

flow should use these adjusted parameters for annular positions above the influx points.

Program operation

The FOAM model uses four sets of input data to organize well and drilling data and rheological parameters. Each of the four sets of input data is stored in a separate file. The well data input file stores well and field names and other documentation to identify the specific case being calculated. The well bore directional profile is described in the survey data input file. Inclination and azimuth are recorded at the corresponding survey point measured depth.

The third FOAM input file, tubular data input, includes information on the drillstring, casing, hole size, and bit nozzles. Additionally, locations and rates of influxes of gas, water, and oil from one or more zones can be specified. The final input is the parameter data input file, in which the user specifies gas and liquid injection rates and properties, drilling rate, cuttings size, rock density, temperature gradients, back pressure, and gas and fluid rheological data.

After the four data input files are completed, the calculations are performed. FOAM then tiles up the output screens, allowing the user to click on the individual output screens of interest.

Fig. 2 shows a foam pressure profile where the pressure increases from 665 psi at the compressor to 1,180 psi at the hole bottom and then decreases as aerated fluid flows up the annulus and expands. This pressure profile is useful in ensuring that pressures do not exceed frac pressure and formation pressure.

Fig. 3 shows that foam density for this example increases from 2.4 ppg at the surface to 3.3 ppg at the hole bottom, then increases to 3.7 ppg from the addition of cuttings at the bit and then decreases to air density as the

gas expands in the annulus.

Accurate calculation of cuttings lifting velocity is critical for conducting safe and efficient drilling operations because poor hole cleaning is a major problem with air, gas, and mist drilling. Cuttings lifting problems are most critical at the top of the drill collars where the velocities are lowest.

Fig. 4 shows an example where the cuttings lifting velocity is only 56 fpm at the top of the drill collars because of the reduction in pipe diameter at this point. Large cuttings often cannot be lifted beyond this point and remain there until they are reground to a smaller size. This explains why air cuttings are often fine powder, while foam cuttings are much larger ($\frac{1}{4}$ in. diameter) because of the better lifting capacity of foams.

FOAM's output section also includes a sensitivity analysis feature that allows drilling engineers to observe the effects of changes in air and liquid injection rates and choke pressure on various downhole parameters. These variables, which can be adjusted in the field if problems occur, have been combined into a separate screen for ease of use in planning and troubleshooting wells. As changes are made in these variables, the effects of those changes can be viewed immediately, allowing quick optimization of the variables.

Comparison to other models

The FOAM computer model was validated by comparing it to existing test-well measurements and field measurements.

Comparisons were initially made with Chevron Petroleum Technology Co.'s Foamup computer program. Foamup output was derived from data provided by Chevron. In 1972, Chevron ran extensive laboratory tests for developing its model using a test well.

Foamup serves as the current industry standard for

foam predictive models, even though it was developed in the early 1970s. The model runs in a mainframe environment.

Foamup is based on Bingham plastic fluid rheology, with a constant set value for fluid yield point. A constant yield point may not accurately model the rheology of foam fluids because, as the pressure changes at different depths, the foam quality also changes, resulting in changes in fluid viscosity and yield point. However, good results have been obtained with the Chevron model over the years.

The FOAM computer model includes the option of using the same basic fluid rheology model used by Chevron. FOAM also includes an option to change the initial yield point of the fluid used in the calculations. The Chevron rheology option was used as the basis of comparison between FOAM and Foamup. Twenty-three different cases were run to compare FOAM and Foamup using data from Chevron's tests.

Fig. 5 shows that the difference in the surface injection pressures predicted by the two programs was 0.7–21.2% for foam qualities of 74–100%. Foam qualities were all calculated at the surface in the annulus. The average difference in calculated injection pressure is 8.2%. This level of agreement is acceptable, assuming that one of the models can be demonstrated to be accurate.

The FOAM program, as currently designed, is based on theoretical assumptions that are valid for true foams only. If foam quality is greater than 96–97%, the calculations are not necessarily valid. Fig. 5 shows that FOAM agrees best with Chevron's Foamup at foam qualities of 99% and higher, however.

The average difference in bottom hole pressure predicted by the two programs in the true foam region (i.e., <97% foam quality) is only 9.9%. This level of agreement

is acceptable, again assuming that either model is capable of accurate pressure prediction. FOAM is designed just for this application.

Two other models were identified in the available technical literature. The first of these was a Bingham plastic model developed by Krug and Mitchell.¹¹ The other is a power-law model developed by Okpobiri and Ikoku.¹²

A comparison of FOAM's Bingham plastic model with the Krug/Mitchell model shows that the difference in predicted surface pressures between the two models ranges 10.3–18.2%. The average difference for the 11 test cases was 13.9%. In every case, the FOAM computer model predicted surface pressures lower than those predicted by the Krug/Mitchell model.

The bottom hole pressures predicted by the models differed from 4 to 16.2%. The average difference for all 11 cases was 9.5%. Again, all predictions by FOAM were lower than those made by the Krug/Mitchell model. A difference of less than 10% is acceptable, again assuming that either model is accurate.

A comparison of results from FOAM's power law fluid model option with the Okpobiri/Ikoku model found the closest agreement of any model considered. The differences in surface pressure predictions range from 1.3 to 13.6%. Predicted bottom hole pressures differed by 8.5–18.8% for the cases shown.

The average difference in surface pressures predicted by FOAM and Okpobiri/Ikoku for all 11 cases run was only 5.2%; the average difference for bottom hole pressures was 8.6%. Both of these differences indicate acceptable agreement between these models.

Comparison to lab data

Results made available by Chevron from 1972 unpublished test well measurements were the best source of data available to gauge the accuracy of

FOAM. Chevron's test well had a plugged-back total depth of 2,904 ft with 9%-in. casing from surface to total depth. A string of 2%-in. tubing was run to 2,809 ft. There were recording pressure gauges installed behind the tubing in the tubing-by-casing annulus at depths of 2,809 ft, 1,887 ft, and 953 ft.

Air and liquid (i.e., foam) were injected at 23 different rates and mixtures, and pressures were recorded by the gauges and at the surface. Each of these 23 data points was used to validate the FOAM model up to a foam quality of 97% because foams become unstable above this value. The pressures predicted by the model at each gauge depth and at the surface injection point were all compared to the measured pressures. All results were plotted as a function of foam quality at the surface.

Pressures predicted at the surface matched the measured pressures more closely than at any other location. The error in the surface pressure predictions made by FOAM ranged from 0.3% to a maximum of 30.3% (Fig. 6). The average error was 11.1%.

This level of agreement (11.1%) is an acceptable level of accuracy. The measured data may have been no more accurate. None of the tests was repeated to gauge repeatability or precision of the measurements.

The pressures predicted at the bottom of the hole by FOAM were in close agreement with the measurements (Fig. 7). The error ranged 1.1–25.8%.

The average disagreement between FOAM and the measurements for bottom hole pressure was 10.0%.

Comparison to field data

To collect field data under specific conditions, Maurer Engineering personnel visited a drilling location while foam drilling was under way. The operation was a horizontal reentry, and the visit occurred during the kickoff

THE AUTHORS



Liu



Medley

Gefei Liu is a senior mechanical engineer with Maurer Engineering Inc. in Houston. He develops computer modeling and software while providing technical support for horizontal well, coiled tubing and slim hole, underbalanced drilling, and other specialized drilling and completion projects. He has done research in areas of well bore stability, drilling hydraulics, casing wear, and underbalanced (air/mist/foam) drilling. Liu has an MS in engineering mechanics from the University of Texas at Austin.

George H. Medley Jr. is a senior petroleum engineer with Maurer Engineering Inc. in Houston. He is in charge of underbalanced drilling and well design for Maurer Engineering. Medley previously worked for Exxon for 17 years, 11 of those years as a senior drilling engineer. He has extensive experience in applying new technology to field operations, including horizontal wells, slim hole drilling, aerated and low-solids drilling fluids, advanced PDC bits, turbodrills, and thermal treatment of oil-based drill cuttings. He designed operational procedures for multiple remote wildcats and large scale development drilling programs. Medley has a BS in civil engineering from Texas A&M University.

operation.

Accurate data were collected for two separate sets of conditions. One set of data was recorded when the bit was at the kickoff point; another set of measurements was taken when the hole was about 130 ft deeper at an inclination of 28°. At both depths, surface pressure and liquid and gas injection rates were recorded.

The accuracy of the FOAM program ranged from +3.1 to -4.8%. Foam qualities for the two cases, calculated at a depth of 100 ft in the annulus, were 95.1 and 96.0%, respectively. The most accurate prediction was made at the lower foam quality.

The calculated surface pressures differed from actual measured pressures by only 20–40 psi.

In the first case, actual injection pressure was 610 psi with 800 scfm of air and 31 gpm of foamer solution. The second data point was measured with an injection pressure of 750 psi with 800 scfm

of air and 24 gpm of foamer. The FOAM model predicted injection pressures of 629 psi and 714 psi, respectively, for the two cases.

Results

The FOAM model predictions compared favorably with Chevron's and other published foam models.

The model predictions also correlated well with field data from Chevron well data and a foam-drilled well in Kansas.

FOAM handles only foam fluids and will not handle cases where the foam quality is larger than 0.97.

The FOAM model is being expanded to include the transition from foam to air/mist in the annulus. This expanded model called Mudlite, being developed on the Drilling Engineering Association DEA-101 project, handles all cases from pure air to pure foam drilling.

Acknowledgment

The authors thank Harry Dearing of Chevron Petrole-

um Technology Co. for his advice and help in comparing the FOAM model to existing data. The authors also thank John Duda of the U.S. Department of Energy for his support and project guidance in developing the model.

References

1. Einstein, A., "Eine Neue Bestimmung der Molekulardimensionen," Annalen der Physik, Vol. 19, No. 5, 1906, p. 289.
2. Hatschek, E., "Die Viskosität der Dispersoide. I. Suspensioide," Kolloid Z., Vol. 7, 1910, p. 301.
3. Hatschek, E., "Die Viskosität der Dispersoide. II. Suspensioide," Kolloid Z., Vol. 8, 1910, p. 34.
4. Mitchell, B.J., "Viscosity of Foam," PhD dissertation, University of Oklahoma, 1969.
5. Krug, J.A., "Air and Water Requirements for Foam Drilling Operations," MS thesis, Colorado School of Mines, 1971.
6. Beyer, A.H., Millhone, R.S., and Foote, R.W., "Flow Behavior of Foam as a Well Circulating Fluid," Society of Petroleum Engineers paper 3986, presented at the SPE 47th Annual Fall Meeting, San Antonio, Oct. 2–5, 1972.
7. Sanghani, V., and Ikoku, C.U., "Rheology of Foam and Its Implications in Drilling and Cleanout Operations," American Society of Mechanical Engineers paper AO-203, presented at the Energy-Sources Technology Conference and Exhibition, Houston, Jan. 30–Feb. 3, 1983.
8. Lord, D.L., "Analysis of Dynamic and Static Foam Behavior," Journal of Petroleum Technology, January 1981.
9. Spoerker, H.F., Trepess, P., Valkó, P., and Economides, M.J., "System Design for the Measurement of Downhole Dynamic Rheology for Foam Fracturing Fluid," SPE paper 22840, presented at the SPE 66th Annual Meeting, Dallas, Oct. 6–9, 1991.
10. Grovier, G.W., and Aziz, K., The Flow of Complex Mixtures in Pipes, Robert E. Krieger Publishing Co., Malabar, Fla., 1987.
11. Krug, J.A., and Mitchell, B.J., "Charts help find volume pressure needed for foam drilling," OGJ, Feb. 7, 1972, pp. 61–64.
12. Okpobiri, G.A., and Ikoku, C.U., "Volumetric Requirements for Foam and Mist Drilling Operations," SPE Drilling Engineering, February 1986.
13. Graham, R.L., "Air Drilling Technology Needs Assessment," Final Report under Contract No. GRI-95/0039 for the Gas Research Institute, Chicago, Reuben L. Graham Inc., October 1995.
14. Mitchell, B.J., "Test data fill theory gap on using foam as a drilling fluid," OGJ, Sept. 6, 1971, pp. 96–100.

Appendix B

**"Advanced Foam Computer Model Helps in the
Design and Analysis of Underbalanced Drilling"**

by

**Gefei Liu & George Medley
MAURER ENGINEERING INC.**

**API/ASME Energy Week '96
Conference & Exhibition**

Advanced Foam Computer Model Helps in the Design and Analysis of Underbalanced Drilling

Gefei Liu and George H. Medley, Jr., Maurer Engineering Inc., 2916 West T.C. Jester, Houston, Texas U.S.A., PH: 713/683-8227; FAX 713/683-6418; e-mail mei@maureng.com.

ABSTRACT

Foam generated by mixing gas and liquid for underbalanced drilling has unique rheological characteristics, making it very difficult to accurately predict the pressure profile. A new mechanistic model attempts to overcome many of the problems associated with existing foam flow analyses. Varying Fanning friction factors, rather than assumed constants, are calculated along the flow path.

A user-friendly PC computer program was developed to numerically solve the mechanical energy balance equation for compressible foam flow, taking into account influxes of gas, liquid, and oil from formations. The pressure profile, foam quality, density, and cuttings transport are predicted by the model.

A Sensitivity Analysis Window allows the user to quickly optimize the hydraulics program by selecting the best combination of injection pressure, back pressure, and gas/liquid injection rates.

This new model handles inclined and horizontal wellbores, and provides handy engineering and design tools for underbalanced drilling, wellbore clean-out, and other foam operations.

INTRODUCTION

Foam has been used extensively in the petroleum industry for decades. It has proven effective and economic as a circulating fluid in hole clean-out and drilling operations.

Advantages of foam drilling over conventional mud drilling include high penetration rates, a high cuttings transport ratio, and less formation damage. In areas with low bottom-hole pressures, the use of a lighter fluid, such as foam, is required.

The complex and unique flow mechanism involved in foam operations often confuses drilling operators concerning the optimum combination of liquid and gas injection rates. Other questions remain, such as how to predict the bottom-hole pressure and how to combine different controllable variables to obtain optimized results. Existing foam drilling design methods largely depend on field operation charts or on calculations using a mainframe computer. Over the last 20 years, extensive study of foam rheological behavior and factors affecting foam circulation in oil wells has made it possible to develop a comprehensive computer program to meet the demands of foam drilling design and analysis.

Based on existing foam rheology models and the steady-state mechanical energy balance equation, Maurer Engineering Inc. (MEI) has developed a Windows-styled computer model (FOAM) to help operators with the design and analysis of underbalanced drilling. The program simulates underbalanced drilling operations using foam as a circulating medium and can be used to evaluate and develop operational guidelines.

The objective of this paper is to present foam flow equations and explain how to numerically solve compressible non-Newtonian flow in a three-dimensional wellbore.

Equations of state describing pressure, volume, and temperature interactions of compressible foam are presented. Flow regimes ranging from laminar to turbulent are covered.

RHEOLOGICAL MODELS

Foam can be treated as a homogeneous fluid with variable density and viscosity. During foam operations, foam quality depends on the pressure and temperature in the tubing or annulus. The pressure has to be determined through the mechanical energy balance equation in which the frictional pressure drop term relies on the foam rheological model. It is therefore important to have an accurate rheological model describing dynamic foam behavior.

Theoretical approaches to the rheology of foam were presented by researchers such as Einstein (1906) and Hatschek (1910A & B). Mitchell (1969) demonstrated that foam behaves as a Bingham plastic fluid, based on his experimental work in capillary tubes, and he empirically derived a set of equations for foam viscosity. It should be noted that these equations do not apply at the limiting case of 100 percent foam quality.

Krug (1971) presented plastic viscosities and yield strengths of foam as a function of foam quality. Beyer et al. (1972) first formulated a foam rheological model from laboratory and pilot-scale experimental data. Their observations suggested that foam behaves as a Bingham plastic fluid. Their study did not demonstrate a dependence of yield point on liquid volume fraction or foam quality.

Sanghani and Ikoku (1983) experimentally studied foam rheology with a concentric annular viscometer that closely simulated actual hole conditions. They concluded that foam is a power-law pseudoplastic fluid with flow behavior index n and flow consistency K , both functions of foam quality.

A review of the literature shows diversified opinions on foam rheological models. Some researchers found that the power-law model was statistically superior to the Bingham plastic model in correlating data, while others found that foam more closely obeys the Bingham plastic model. The computer model described here includes both power-law and Bingham plastic models and allows the user to choose which one to use.

FOAM FLOW EQUATIONS

In the special case of a two-phase system such as foam, where gas is finely and uniformly dispersed in the liquid phase, homogeneous fluid can be assumed and no equation is required for the phase interface.

Foam consists of a compressible component (gas) and an incompressible component (liquid). The incompressible component is easier to handle because of its constant density. The compressible gas requires much more attention, since its density depends on temperature and pressure.

Pressure is coupled with gas volume fractions through a friction factor. An improved version of Lord's (1981) pressure drop equation and Spoerker et al.'s (1991) method are used in the following equation derivation. Friction factor is calculated along the wellbore rather than assumed constant.

EQUATIONS OF STATE

The relationship between the variation of density of a fluid with pressure and temperature is termed the equation of state. For engineering purposes, the most practical form of the equation of state for a real gas is given by (Grovier and Aziz, 1987):

$$V_g = \frac{ZRT}{M_g P} \quad (1)$$

where	V_g	=	Specific volume of gas
	Z	=	Gas compressibility factor
	M_g	=	Molecular weight of gas (lbm/lb-mole)
	R	=	Gas constant, $10.73 \frac{\text{(psia)} \cdot (\text{ft}^3)}{(\text{lb-mole})(^\circ\text{R})}$
	T	=	Absolute temperature, ($^\circ\text{R}$)
	P	=	Absolute pressure, (psia)

Equations of state for both downward and upward foam flow can be expressed as:

$$V = \frac{a}{P} + b \quad (2)$$

where	V	=	Specific volume of foam
-------	-----	---	-------------------------

The coefficients a and b are defined in Appendix A. The expressions of a and b take different forms for downward flow inside drill pipe and upward flow in the annulus, because for upward flow in the annulus, the foam is mixed with rock cuttings. There are three phases present in the annular mixture in which liquid and cuttings are incompressible, while the gas phase is compressible.

MECHANICAL ENERGY EQUATIONS

Once the equations of state for foam have been established, the next step is to use the momentum and energy equations to analyze the dynamic foam behavior. The mechanical energy equation may be considered either a consequence of the momentum equation or a reduced form of the total energy equation.

For downward flow inside the drill pipe, the differential mechanical energy balance equation is:

$$\frac{u}{g_c} \frac{du}{dL} - \frac{g}{g_c} \frac{d(VD)}{dL} + VdP + \frac{2u^2 f}{g_c D} \frac{d(MD)}{dL} = 0 \quad (3)$$

where	u	=	Average velocity of the foam, ft/s
	f	=	Fanning friction factor
	g	=	Acceleration due to gravity
	g_c	=	$32.2 \text{ (ft-lbm)/(lbf-s}^2)$

- MD = Measured depth, ft
 VD = Vertical depth, ft
 D = Drill pipe ID, in.

The average velocity of the foam, u , can be obtained using the continuity equation. In terms of specific volume, it can be expressed as:

$$u = cV = \frac{ac}{P} + bc \quad (4)$$

where the coefficient, c , is defined in Appendix A.

After substituting Eq. 4 into Eq. 3, the differential mechanical energy balance takes the form:

$$\frac{dP}{d(MD)} = F_p(MD, VD, P) \quad (5)$$

For upward flow in the annulus, the differential mechanical energy balance equation takes the form:

$$\frac{u \ du}{g_c} - \frac{g \ d(VD)}{g_c} + VdP - \frac{2u^2 f \ d(MD)}{g_c(D_h - D_p)} = 0 \quad (6)$$

where D_h = Open-hole diameter, in.
 D_p = Drill-pipe OD, in.

The average velocity of the foam in the annulus is also described by Eq. 4. However, the variable c for upward annular flow is different (see Appendix A).

Substituting annular velocity into Eq. 6 will yield the following differential mechanical energy balance in upward annular flow:

$$\frac{dP}{d(MD)} = F_a(MD, VD, P) \quad (7)$$

Eqs. 5 and 7 can be solved numerically. The back pressure, which is known, serves as a boundary condition for Eq. 7. Numerical techniques are used to calculate a sequence of pressure values corresponding to discrete values of the measured depth. The expressions of F_p and F_a are given in Appendix A.

PRESSURE DROP ACROSS NOZZLES

To calculate the pressure drop through a short constriction such as a bit nozzle (Figure 1), it generally is assumed that the change in elevation, the velocity upstream of the nozzle, and the frictional pressure loss across the nozzle are negligible. Thus, Eq. 3 becomes

$$\frac{u \ du}{g_c} + VdP = 0 \quad (8)$$

Substituting Eq. 2 and Eq. 4 into Eq. 8 and integrating yields the following expression in field units:

$$b(P_2 - P_1) + a \ln\left(\frac{P_2}{P_1}\right) + 8.1 \times 10^{-4} U_n^2 = 0 \quad (9)$$

where P_1 = Pressure upstream of the nozzle
 P_2 = Bottom-hole pressure
 U_n = Nozzle velocity

Nozzle velocity U_n is defined as

$$U_n = \frac{ac'}{P_2} + bc' \quad (10)$$

Eq. 9 can be solved numerically to obtain the pressure upstream of nozzle P_1 . The bottom-hole pressure P_2 is calculated from Eq. 7 beforehand; c' in Eq. 10 is explained in Appendix A.

INFLUX MODELING

One advantage of foam drilling is a lower bottom-hole pressure, which increases the rate of penetration. However, influxes of gas, water or oil can occur as a result of low bottom-hole pressure. These influxes will change the existing foam system, resulting in a change in the pressure profile inside the drill pipe as well as in the annulus.

The total liquid density can be calculated from the rates and densities of the injected liquid and those of water/oil influxes.

$$\rho_L = \rho_o f_o + \sum_i^N \rho_i f_i \quad (11)$$

$$\begin{aligned} \text{where } \rho_o &= \text{Density of inlet liquid} \\ f_o &= \frac{q_o}{q_o + \sum_{i=1}^N q_i} \\ f_i &= \frac{q_i}{q_o + \sum_{i=1}^N q_i} \end{aligned} \quad (12)$$

q_o = Liquid injection rate
 q_i = Water/oil influx rate
 N = Number of water/oil influxes

The final liquid viscosity can be calculated in a similar fashion.

Molecular weight of the mixture of injected gas and influx gas can be calculated using weighting factors similar to those used for calculating liquid density and viscosity:

$$M_g = M_{go}f_o + \sum_{i=1}^N M_{gi}f_i \quad (13)$$

where M_{go} = Molecular weight of inlet gas
 M_{gi} = Molecular weight of influx gas

$$f_o = \frac{m_{go}}{m_{go} + \sum_{i=1}^N m_{gi}}$$

$$f_i = \frac{m_{gi}}{m_{go} + \sum_{i=1}^N m_{gi}} \quad (14)$$

m_{go} = Mass rate of inlet gas
 m_{gi} = Mass rate of influx gas
 N = Number of gas influxes

Equations of state for gas and upward annular foam flow should use these adjusted parameters for annular positions above the influx points.

PROGRAM OPERATION

The FOAM model uses four sets of input data to better organize well and drilling data and rheological parameters. Each of the four sets of input data is stored in a separate file. The Well Data Input file stores well and field names, and other documentation to identify the specific case being calculated. The wellbore directional profile is described in the Survey Data Input file. Inclination and azimuth are recorded at the corresponding survey point measured depth.

The third FOAM input file, Tubular Data Input, includes information on the drill string, casing, hole size, and bit nozzles. Additionally, locations and rates of influxes of gas, water, and/or oil from one or more zones can be specified. The final input is the Parameter Data Input file where the user specifies gas and liquid injection rates and properties, drilling rate, cuttings size, rock density, temperature gradients, backpressure, and gas and fluid rheological data.

After the four data input files are completed, the calculations are performed. FOAM then "tiles" up the output screens, allowing the user to click on the individual output screen(s) of interest.

Figure 2 shows an example of output data for a 7½-in. well drilled with foam to a depth of 5000 feet. A full screen version of each profile or a full report can be generated and printed.

Figure 3 shows a foam pressure profile where the pressure increases from 665 psi at the compressor to 1180 psi at the hole bottom and then decreases as aerated fluid flows up the annulus and expands. This pressure profile is useful in ensuring that pressures do not exceed frac pressure and formation pressure.

Figure 4 shows that foam density for this example increases from 2.4 ppg at the surface to 3.3 ppg at the hole bottom, then increases to 3.7 ppg due to the addition of cuttings at the bit, and decreases to air density as the gas expands in the annulus.

Accurate calculation of cuttings lifting velocity is critical for conducting safe and efficient drilling operations since poor hole cleaning is a major problem with air, gas, and mist drilling. Cuttings lifting problems are most critical at the top of the collar where the velocities are lowest.

Figure 5 shows an example where the cuttings lifting velocity is only 56 ft/min at the top of the drill collars due to the reduction in pipe diameter at this point. Large cuttings often cannot be lifted beyond this point, remaining there until they are reground to a smaller size. This explains why air cuttings are often fine powder, while foam cuttings are much larger (e.g., ¼- to ½-in. diameter) due to better lifting capacity of foams.

FOAM's output section also includes a sensitivity analysis feature that allows drilling engineers to observe the effects of changes in air and liquid injection rates and choke pressure on various downhole parameters (Figure 6). These variables, which can be adjusted in the field if problems occur, have been combined into a separate screen for ease of use in planning and troubleshooting wells. As changes are made in these variables, impacts of those changes can be viewed immediately, allowing quick optimization of the variables.

COMPARISON TO OTHER MODELS

The FOAM computer models was validated by comparing it to existing test-well measurements and field measurements.

Comparisons were initially made with Chevron's FOAMUP computer program. FOAMUP output was derived from data provided by Chevron. In 1972, Chevron ran extensive laboratory tests for developing their model using a test well.

FOAMUP serves as the current industry standard for foam predictive models, even though it was developed in the early 1970s. The model runs in a mainframe environment.

FOAMUP is based on Bingham plastic fluid rheology, with a constant set value for fluid yield point. A constant yield point may not accurately model the rheology of foam fluids

because, as the pressure changes at different depths, the foam quality also changes, resulting in changes in fluid viscosity and yield point. However, good results have been obtained with the Chevron model over the years.

The FOAM computer model includes the option of using the same basic fluid rheology model used by Chevron. FOAM also includes an option to change the initial yield point of the fluid used in the calculations. The Chevron rheology option was used as the basis of comparison between FOAM and FOAMUP.

Twenty-three different cases were run to compare FOAM and FOAMUP using data from Chevron's tests.

Figure 7 shows that the difference in the surface injection pressures predicted by the two programs ranges from 0.7 to 21.2 percent for foam qualities of 74 to 100 percent. Foam qualities were all calculated at the surface in the annulus. The average difference in calculated injection pressure is 8.2 percent. This level of agreement is acceptable, assuming that one of the models can be demonstrated to be accurate.

The FOAM program, as currently designed, is based on theoretical assumptions that are valid for true foams only. If foam quality is greater than 96-97 percent, the calculations are not necessarily valid. However, Figure 7 shows that FOAM agrees best with Chevron's FOAMUP at foam qualities of 99 percent and higher.

The average difference in bottom-hole pressure predicted by the two programs in the true foam region (i.e., < 97 percent foam quality) is only 9.9 percent. This level of agreement is acceptable, again assuming that either model is capable of accurate pressure prediction. FOAM is designed just for this application.

Two other models were identified in the available technical literature. The first of these was a Bingham plastic model developed by Krug and Mitchell (1972). The other is a power-law model developed by Okpobiri and Ikoku (1986).

A comparison of FOAM's Bingham-plastic model with the Krug/Mitchell model (Figure 8) shows that the difference in predicted surface pressures between the two models ranges from 10.3 to 18.2 percent. The average difference for the eleven test cases was 13.9 percent. In every case, the FOAM computer model predicted surface pressures lower than those predicted by the Krug/Mitchell model.

The bottom-hole pressures predicted by the models differed from 4 to 16.2 percent (see Figure 8). The average difference for all eleven cases was 9.5 percent. Again, all predictions by FOAM were lower than those made by the Krug/Mitchell model. A difference of less than 10 percent is acceptable, again assuming that either model is accurate.

A comparison of results from FOAM's power-law fluid model option with the Okpobiri/Ikoku model found the closest

agreement of any model considered. Figure 9 shows that the differences in surface pressure predictions range from 1.3 to 13.6 percent. Predicted bottom-hole pressures differed by 8.5 to 18.8 percent for the cases shown.

The average difference in surface pressures predicted by FOAM and Okpobiri/Ikoku for all eleven cases run was only 5.2 percent; the average difference for bottom-hole pressures was 8.6 percent. Both of these differences indicate acceptable agreement between these models.

COMPARISON TO LABORATORY DATA

Results made available by Chevron from their 1972 unpublished test well measurements were the best source of data available to gauge the accuracy of FOAM. Chevron's test well had a plugged-back total depth of 2904 ft with 9½-in. casing from surface to total depth. A string of 2½-in. tubing was run to 2809 ft. There were recording pressure gauges installed behind the tubing in the tubing-by-casing annulus at depths of 2809 ft, 1887 ft, and 953 ft.

Air and liquid (i.e., foam) were injected at twenty-three different rates and mixtures, and pressures were recorded by the gauges and at the surface. Each of these twenty-three data points was used to validate the FOAM model up to a foam quality of 97 percent since foams become unstable above this value. The pressures predicted by the model at each gauge depth and at the surface injection point were all compared to the measured pressures. All results were plotted as a function of foam quality at the surface.

Pressures predicted at the surface matched the measured pressures more closely than at any other location. Figure 10 shows the error in the surface pressure predictions made by FOAM ranged from 0.3 percent to a maximum of 30.3 percent. The average error was 11.1 percent.

This level of agreement (11.1 percent) is an acceptable level of accuracy. The measured data may have been no more accurate. None of the tests was repeated to gauge repeatability or precision of the measurements.

Figure 11 shows that the pressures predicted at the bottom of the hole by FOAM were in close agreement with the measurements. The error ranges from 1.1 to 25.8 percent.

The average disagreement between FOAM and the measurements for bottom-hole pressure is 10.0 percent.

COMPARISON TO FIELD DATA

To collect field data under specific conditions, Maurer Engineering personnel visited a drilling location while foam drilling was underway. The operation was a horizontal re-entry, and the visit occurred during the kick-off operation.

Accurate data were collected for two separate sets of conditions. One set of data was recorded when the bit was at the kick-off point; another set of measurements was taken when the hole was about 130 ft deeper at an inclination of 28°. At both depths, surface pressure and liquid and gas injection rates were recorded.

The accuracy of the FOAM program ranged from +3.1 to -4.8 percent. Foam qualities for the two cases, calculated at a depth of 100 ft in the annulus, were 95.1 and 96.0 percent, respectively. The most accurate prediction was made at the lower foam quality.

Figure 12 shows that the calculated surface pressures differed from actual measured pressures by only 20-40 psi.

In the first case, actual injection pressure was 610 psi with 800 scfm of air and 31 gpm of foamer solution. The second data point was measured with an injection pressure of 750 psi with 800 scfm of air and 24 gpm of foamer. The FOAM model predicted injection pressures of 629 psi and 714 psi, respectively, for the two cases.

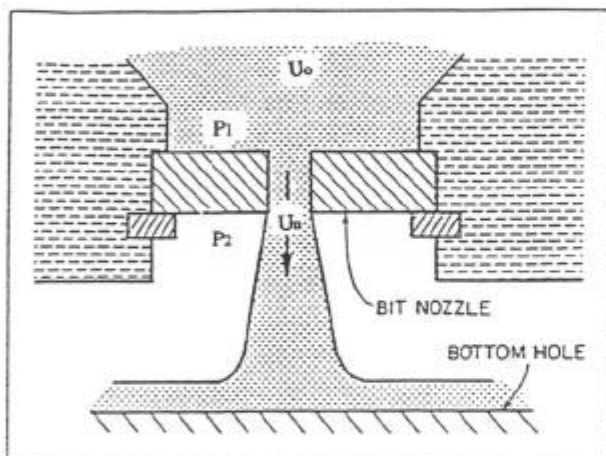


Figure 1. Flow through a bit nozzle.
(Okpobiri & Ikoku, 1986)

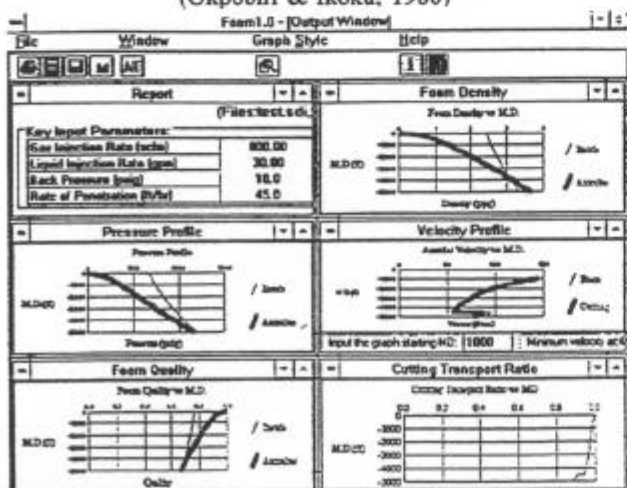


Figure 2. FOAM "tiled" output window.

ADDITIONAL WORK

The FOAM model is being expanded to include the transition from foam to air/mist in the annulus. This expanded model called MUDLITE, being developed on the DEA-101 project, handles all cases from pure air to pure foam drilling.

CONCLUSIONS

1. The FOAM model predictions compared favorably with Chevron and other published foam models.
2. The model predictions also correlated well with field data from Chevron well data and a foam-drilled well in Kansas.
3. FOAM handles only foam fluids and will not handle cases where the foam quality is larger than 0.97.
4. A new MUDLITE model, covering air, mist, and foam drilling, is being developed.

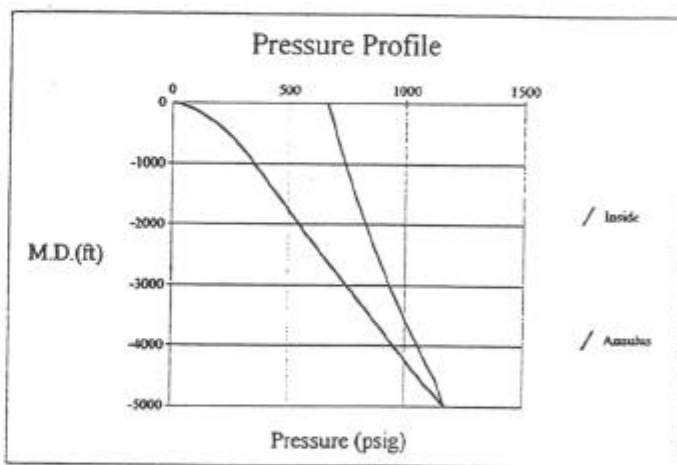


Figure 3. FOAM Wellbore Pressure Profile

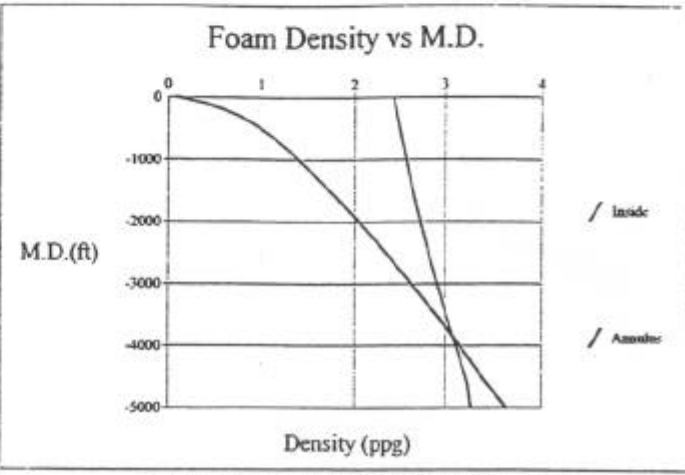


Figure 4. FOAM Foam Density Profile

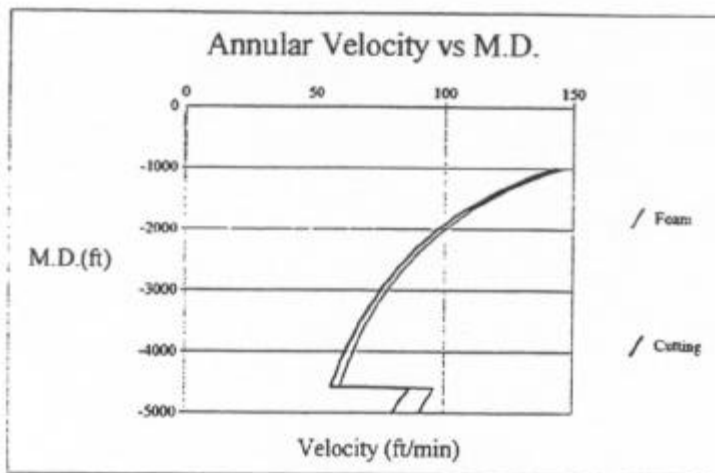


Figure 5. Cuttings Lifting Velocities Near Bottom

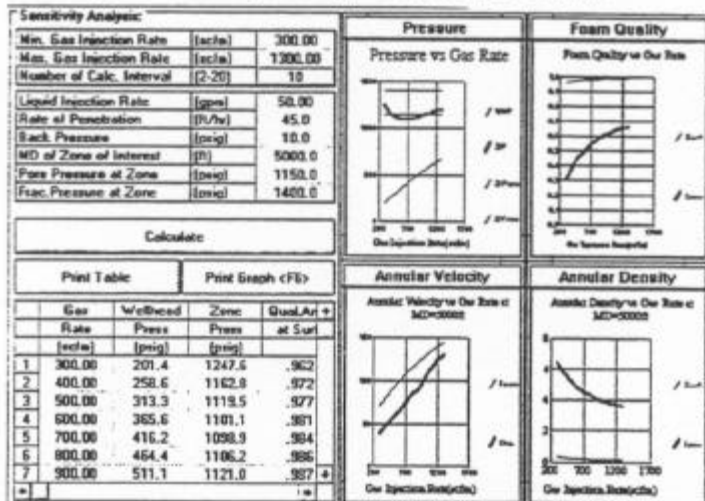


Figure 6. FOAM Sensitivity Analysis Screen

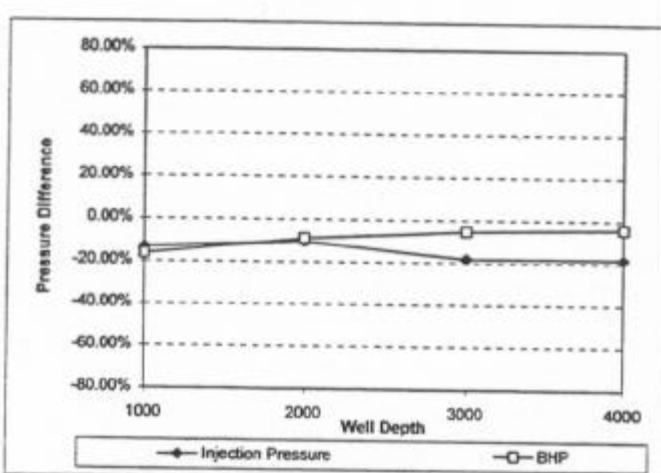


Figure 8. Comparison of FOAM and Krug/Mitchell model.

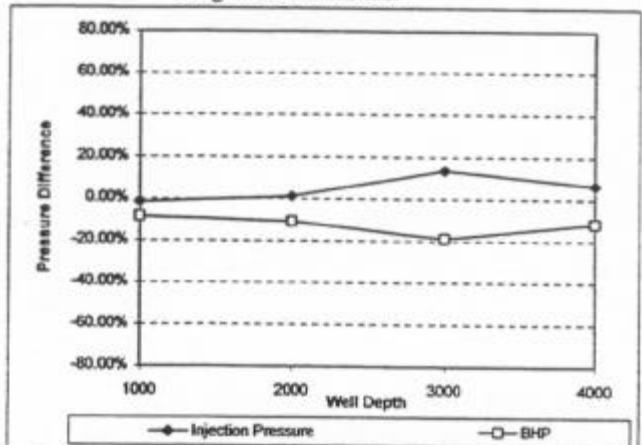


Figure 9. Comparison of FOAM and Okpobiri/Ikoku model.

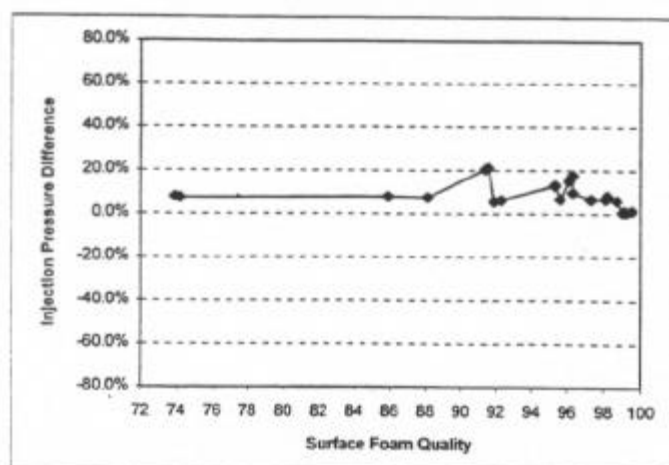


Figure 7. Surface injection pressures predicted by FOAM and Chevron's model.

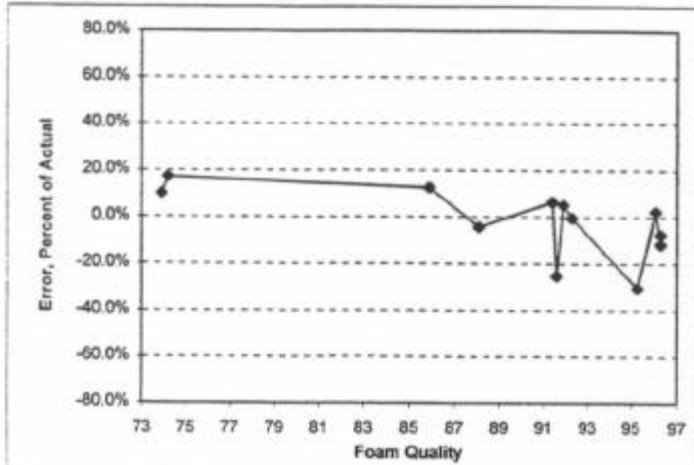


Figure 10. Comparison of FOAM to Chevron laboratory data (surface pressure).

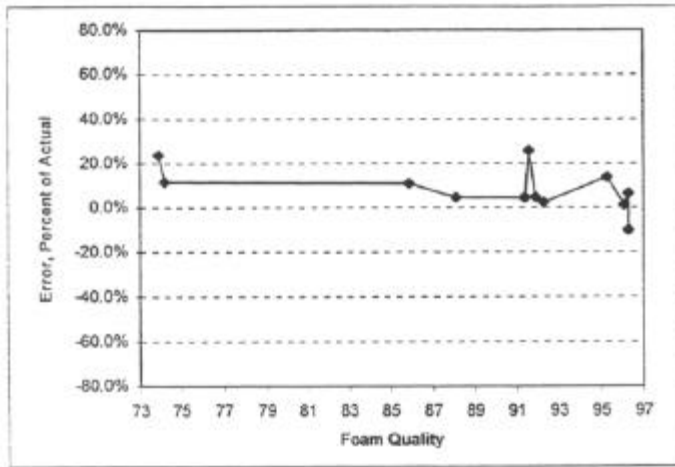


Figure 11. Comparison of FOAM to Chevron laboratory data (bottom-hole pressure).

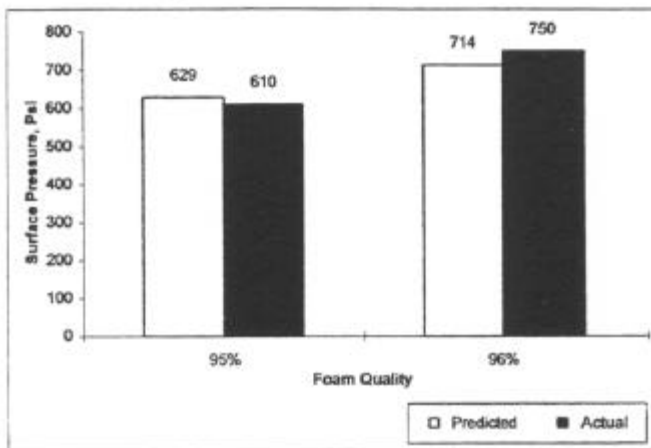


Figure 12. Comparison of FOAM to MEI field data (injection pressure)

ACKNOWLEDGEMENTS

We wish to thank Harry Dearing of Chevron Petroleum Technology Company for his advice and help in comparing the FOAM model to existing data. We also thank John Duda of the U.S. DOE for his support and project guidance in developing the model.

REFERENCES

- Beyer, A.H., Millhone, R.S. and Foote, R.W., 1972: "Flow Behavior of Foam as a Well Circulating Fluid," SPE 3986, presented at the SPE 47th Annual Fall Meeting, San Antonio, Texas, October 2-5.
- Einstein, A., 1906: "Eine Neue Bestimmung der Molekuldimensionen," *Annalen der Physik* 19, Ser. 5, 289.
- Graham, R.L., 1995: *Air Drilling Technology Needs Assessment*, Final Report under Contract No. GRI-95/0039 for the Gas Research Institute, Chicago, Illinois, Reuben L. Graham, Inc., October.
- Grovier, G.W. and Aziz, K., 1987: *The Flow of Complex Mixtures in Pipes*, Robert E. Krieger Publishing Company, Malabar, Florida.
- Hatschek, E., 1910: "Die Viskosität der Dispersoide. I. Suspensoide," *Kolloid Z* 7, 301.
- Hatschek, E., 1910: "Die Viskosität der Dispersoide. II. Suspensoide," *Kolloid Z* 8, 34.
- Krug, J.A. and Mitchell, B.J., 1972: "Charts Help Find Volume Pressure Needed for Foam Drilling," *Oil & Gas Journal*, February 7.
- Krug, Jack A., 1971: *Air and Water Requirements for Foam Drilling Operations*, Master of Science thesis, Colorado School of Mines.
- Lord, D.L., 1981: "Analysis of Dynamic and Static Foam Behavior," *Journal of Petroleum Technology*, January.
- Mitchell, B.J., 1971: "Test Data Fill Theory Gap on Using Foam as a Drilling Fluid," *Oil & Gas Journal*, September 6.
- Mitchell, B.J., 1969: "Viscosity of Foam," Ph.D. dissertation, University of Oklahoma.
- Okpobiri, Godwin A. and Ikoku, Chi U., 1986: "Volumetric Requirements for Foam and Mist Drilling Operations," *SPE Drilling Engineering*, February.
- Sanghani, V. and Ikoku, C.U., 1983: "Rheology of Foam and Its Implications in Drilling and Cleanout Operations," ASME AO-203, presented at the 1983 Energy-Sources Technology Conference and Exhibition held in Houston, Texas, January 30-February 3.
- Spoerker, H.F., Trepess, P., Valkó, P. and Economides, M.J., 1991: "System Design for the Measurement of Downhole Dynamic Rheology for Foam Fracturing Fluid," SPE 22840, presented at the SPE 66th Annual Meeting held in Dallas, Texas, October 6-9.

APPENDIX A

For downward flow inside the drill pipe, the mass fraction of gas is defined as:

$$W_g = \frac{m_g}{m_g + m_l} \quad (A-1)$$

where m_g = Mass rate of gas
 m_l = Mass rate of liquid

Then the specific volume of foam mixture can be expressed as

$$V = W_g V_g + (1 - W_g) V_l \quad (A-2)$$

where V = Specific volume of foam
 V_g = Specific volume of gas
 V_l = Specific volume of fluid

Therefore, combining Eq. A-1 and A-2 will lead to the equation of state for the downward foam flow inside drill pipe:

$$V = \frac{a}{P} + b \quad (A-3)$$

The coefficients a , b in Eq. A-3 are defined in Table A-1.

For upward flow outside in the annulus, the foam is mixed with rock cuttings. Three phases are present in the mixture. The mass fractions of the three components are

$$\begin{aligned} W_g &= \frac{m_g}{m_g + m_l + m_s} \\ W_l &= \frac{m_l}{m_g + m_l + m_s} \\ W_s &= \frac{m_s}{m_g + m_l + m_s} \end{aligned} \quad (A-4)$$

where m_s = Mass rate of cutting

The specific volume of foam/cutting mixture can be expressed as

$$V = W_g V_g + W_l V_l + W_s V_s \quad (A-5)$$

Combining Eqs. A-4 and A-5 will lead to the equation of state for the upward foam flow in the annulus.

$$V = \frac{a}{P} + b \quad (A-6)$$

The coefficients a , b in Eq. A-6 are defined in Table A-1.

The functions of differential mechanical energy balance inside drill pipe and in the annulus are:

$$\frac{F_p(MD, VD, P)}{S_p P^3 + \frac{2f abc^2}{25.8} P^2 + \frac{f}{25.8} a^2 c^2 P} \cdot \frac{1}{b P^3 + a P^2 - abc^2 P - a^2 c^2} \cdot \frac{1}{D} \quad (A-7)$$

where

$$S_p = \frac{f}{25.8} b^2 c^2 - D \frac{d(VD)}{d(MD)} \quad (A-8)$$

$$\frac{F_A(MD, VD, P)}{S_A P^3 + \frac{2f abc^2}{21.1} P^2 + \frac{f}{21.1} a^2 c^2 P} \cdot \frac{1}{b P^3 + a P^2 - abc^2 P - a^2 c^2} \cdot \frac{1}{D_h - D_p} \quad (A-9)$$

and where

$$S_A = \frac{f}{21.1} b^2 c^2 + (D_h - D_p) \frac{d(VD)}{d(MD)} \quad (A-10)$$

TABLE A-1. Coefficients in Equation of State for Foam

Coefficients	Inside Drill Pipe	In the Annulus	Cross Bit (c')
a	$\frac{W_g ZRT}{M_g}$	$\frac{W_g ZRT}{M_g}$	N/A
b	$(1-W_g) V_1$	$W_1 V_1 + W_s V_s$	N/A
c or c'	$\frac{4}{\pi D^2} (m_g + m_l)$	$\frac{4}{\pi(D_h^2 - D_p^2)} (m_g + m_l + m_z)$	$\frac{m_g + m_l}{\text{Total Flow Area}}$

Appendix C

Scotchlite Product Data Sheet:

Glass Bubbles, S Series

January 1995



ScotchliteTM Glass Bubbles S Series



Product Data

January, 1995

Supersedes all previous Data Pages

Features, Advantages, and Benefits

Feature	Advantage	Benefit
Published Product Specification	Measurable and consistent product parameters	Predictable performance
Low Density	Reduced composite weight	Potential freight savings
Spherical Shape <small>(minimum surface area to volume ratio)</small>	Low resin demand	Lower viscosity at equal volume loading
		Potential for more filler at equal viscosity
		Reduced resin usage may result in reduced shrinkage
		Sprayable, castable and moldable
		Blends readily into compounds
Chemically Stable Glass	Low alkalinity	Compatible with most resins
		Stable shelf life and viscosity
	Non-combustible	Reduced Fire Hazard
	Non-porous	Does not absorb resin
Variety of Product Types	Flexibility to meet varied product/processing requirements	Can be formulated to make stable emulsions
		Can select Glass Bubbles to meet many required parameters
Specially Formulated Hollow Glass Spheres	High strength to weight ratio	Able to survive processing
	Stable voids	Low thermal conductivity
		Low dielectric constant

Scotchlite™ Glass Bubbles S Series

Typical Properties

Note: The following product information and data should be considered representative or typical only and should not be used for specification purposes.

Isostatic Crush Strength: See Product Specifications, paragraph B.

Density: See Product Specifications, paragraph C.

Chemical Resistance: In general, the chemical properties of Scotchlite Glass Bubbles resemble those of a soda-lime borosilicate glass.

Packing Factor: Varies from 55% to 68%
(Ratio of bulk density to true particle density.)

Oil Absorption: 31-36 g oil/100 cc of Glass Bubbles, per ASTM D1483.

Thermal Properties:

A. Conductivity: 0.6 to 1.8 (Btu x in.) / (hr. x ft.² x °F) at 32°F (0°C), based on theoretical calculations. Conductivity increases with temperature and product density. The thermal conductivity of a composite will depend on the matrix material and volume loading of glass bubbles.

B. Stability: Appreciable changes in bubble properties may occur above 600°C depending on temperature and duration of exposure.

Flotation: See Product Specifications, paragraph F.

Volatile Content: See Product Specifications, paragraph G.

Alkalinity: See Product Specifications, paragraph E.

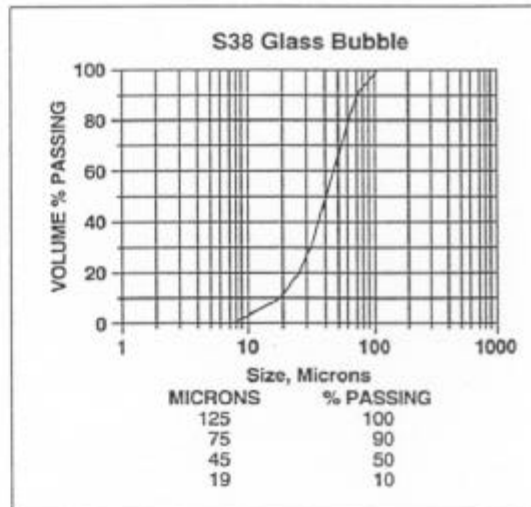
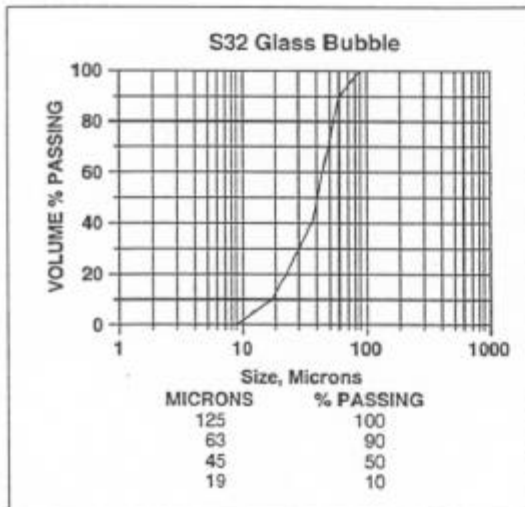
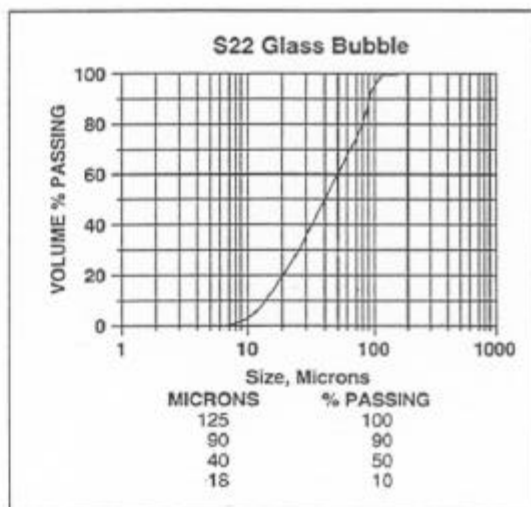
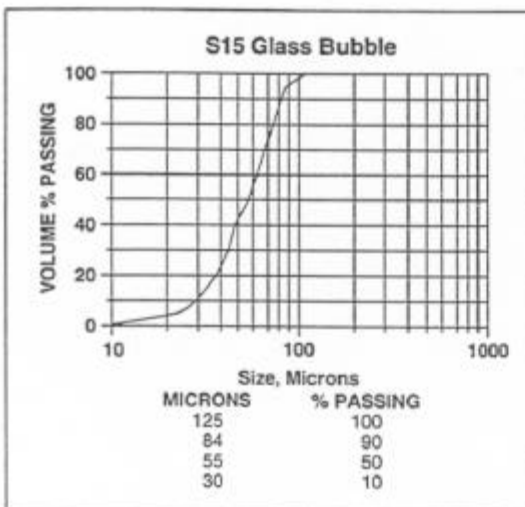
pH: Since Glass Bubbles are a dry powder, pH is not defined. The pH effect will be determined by the alkalinity as specified in paragraph E of the Specification. When glass bubbles are mixed with de-ionized water at 5 volume percent loading, the resulting pH of the slurry is typically 9.1 to 9.9, as measured by a pH meter.

Dielectric Constant: 1.2 to 1.8 @ 100 MHz, based on theoretical calculations. The dielectric constant of a composite will depend on the matrix material and volume loading of glass bubbles.

Scotchlite™ Glass Bubbles S Series

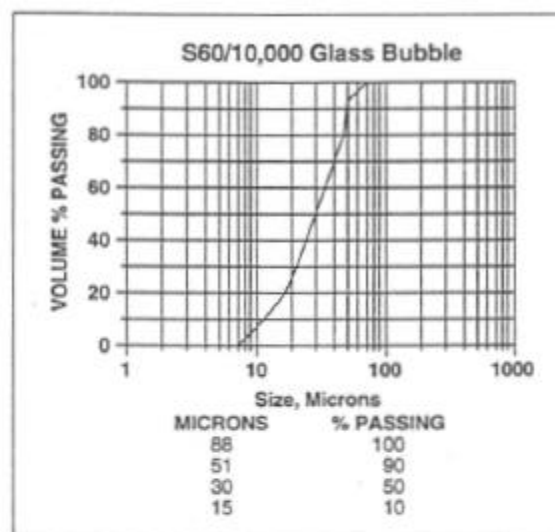
Typical Properties (*continued*)

Particle Size Distribution: (See Product Specifications, paragraph D for size specification)



Scotchlite™ Glass Bubbles S Series

Typical Properties (*continued*)



Scotchlite™ Glass Bubbles S Series

Product Specifications

This specification covers hollow, unicellular glass microspheres, hereafter referred to as Glass Bubbles. Glass Bubbles are composed of a water resistant and chemically stable soda-lime-borosilicate glass.

Requirements:

A representative sample of Glass Bubbles will conform to the following requirements:

A. Color and Appearance

Glass Bubbles will appear uniformly white to the unaided eye.

B. Isostatic Crush Strength:

<u>Product</u>	Test Pressure <u>psi</u>	Typical <u>% Survival</u>	Minimum <u>% Survival</u>
S15	300	90%	80%
S22	400	90%	80%
S32	2,000	90%	80%
S38	4,000	90%	80%
S60/10,000*	10,000	90%	80%

Test Method: 3M TM-2028

*Per ASTM D3102-78

C. Density:

<u>Product</u>	True Density (g/cc) <u>Typical</u>	Minimum	Maximum
S15	0.15	0.13	0.17
S22	0.22	0.19	0.25
S32	0.32	0.29	0.35
S38	0.38	0.35	0.41
S60/10,000	0.60	0.57	0.63

Test Method: ASTM D2840*

*Sampling – In order to obtain representative samples of Glass Bubbles for density measurement via ASTM D2840, use 3M's vacuum sampling procedure or equivalent to avoid breakage. 3M certified density values are obtained with continuous in-line sampling equipment which does not cause product breakage.

D. Size:

1. Hard Particles – no particles (e.g., glass slag, flow agent, etc.) greater than U.S. number 40 (420 microns) standard sieve will exist.

2. Oversize Particles –

For S15, S32, S38 and S60/10,000 Glass Bubbles:

When tested in accordance with ASTM D1214, using a 10 gram sample on a U.S. Number 140 standard sieve (105 microns), a maximum of three (3) percent by weight Glass Bubbles will be retained on the sieve.

Scotchlite™ Glass Bubbles S Series

Product Specifications (*continued*)

2. Oversize Particles – (*continued*)

For S22 Glass Bubble:

When tested in accordance with ASTM D1214, using a 10 gram sample on a U.S. Number 200 standard sieve (74 microns), a maximum of five (5) percent by weight Glass Bubbles will be retained on the sieve.

E. Alkalinity:

Maximum of 0.5 milliequivalents per gram

Test Method: ASTM D3100 (1982 edition)

F. Flotation:

<u>Product</u>	Floaters (% by bulk volume)	
	<u>Typical</u>	<u>Minimum</u>
S15	96%	90%
S22	96%	90%
S32	94%	90%
S38	94%	90%
S60/10,000	92%	90%

Test Method: 3M TM-588

G. Volatile Content:

Maximum of 0.5 percent by weight.

Test Method: 3M TM-587

H. Flow:

Scotchlite™ Glass Bubbles remain free flowing for at least one year from the date of shipment if stored in the original, unopened container in the minimum storage conditions of an unheated warehouse.

I. Packaging:

Glass Bubbles will be packaged in suitable containers to help prevent damage during normal handling and shipping. Each container will be labeled with:

1. Name of manufacturer
2. Type of Glass Bubbles
3. Lot number
4. Quantity in pounds

For further information on properties not covered in this specification, refer to Typical Properties.

Scotchlite™ Glass Bubbles S Series

Storage and Handling

To help ensure ease of storage and handling while maintaining free flowing properties, Scotchlite™ Glass Bubbles have been made from a chemically stable glass and are packaged in a heavy duty polyethylene bag within a cardboard container.

Storage:

Minimum storage conditions should be unopened cartons in an unheated warehouse.

Under high humidity conditions with the ambient temperature cycling over a wide range, moisture can be drawn into the bag as the temperature drops and the air contracts. The result may be moisture condensation within the bag. Extended exposure to these conditions may result in "caking" of the Glass Bubbles to various degrees. To minimize the potential for "caking" and prolong the storage life, the following suggestions are made:

1. Carefully re-tie opened bags immediately after use.
2. If the polyethylene bag is punctured during shipping or handling, use this bag as soon as possible, patch the hole, or insert the contents into an undamaged bag.
3. During humid summer months, store in the driest, coolest space available.
4. If good storage conditions are unavailable, carry a minimum inventory, and process on a first in/first out basis.

Handling:

Dusting problems that may occur while handling and processing can be minimized by the following procedures:

1. For eye protection wear chemical safety goggles. For respiratory system protection wear an appropriate NIOSH/MSHA approved respirator. (For additional information about personal protective equipment, refer to Material Safety Data Sheet.)
2. Appropriate ventilation in the work area.
3. Pneumatic conveyor systems have been used successfully to transport Glass Bubbles without dusting from shipping containers to batch mixing equipment. Static eliminators should be used help to prevent static charges.
Diaphragm pumps have been used successfully to convey Glass Bubbles. Vendors should be consulted for specific recommendations.

Glass Bubble Breakage:

Glass bubble breakage may occur if the product is improperly processed. To minimize breakage, avoid high shear processes such as high speed Cowles Dissolvers, point contact shear such as gear pumps or 3-roll mills, and processing pressures above the strength test pressure for each product.

Health and Safety Information

For product Health and Safety Information, refer to product label and Material Safety Data Sheet (MSDS) before using product.

Scotchlite™ Glass Bubbles S Series

Packaging Information

Large Box (50 cubic ft.)

Description: A single corrugated box with a plastic liner. Top enclosed with interlocking double cover banded. Bottom is normal box closure, entire box banded to wooden pallet.

Dimensions: Box I.D. of 48 in. x 42 in. x 44 in. overall load size is 48 $\frac{3}{4}$ in. x 42 $\frac{3}{4}$ in. x 50 in. including pallet. Pallet size is 42 in. x 48 in.

Small Box (10 cubic ft.)

Description: A single corrugated box with a plastic liner. All boxes are banded together and to the wooden pallet. 4 Boxes per pallet.

Dimensions: Each box I.D. is 22 in. x 19 in. x 39 in. Pallet size is 42 in. x 48 in.

Box Weights

<u>Product</u>	<u>Small Box</u>	<u>Large Box*</u>	<u>Truckload Large Box*</u>
S15	50 lb.	265 lb.	11,660 lb.
S22	60 lb.	385 lb.	16,940 lb.
S32	100 lb.	525 lb.	23,100 lb.
S38	100 lb.	680 lb.	29,920 lb.
S60/10,000	125 lb.	850 lb.	37,400 lb.

*Box weights may vary due to manufacturing tolerances on each product.

For Additional Information

To request additional product information or to arrange for sales assistance, call 612-733-0306. Address correspondence to: 3M Specialty Additives, 3M Center, Bldg. 220-8E-04, P.O. Box 3220, St. Paul, MN 55133-3220. Our FAX number is 612-736-4133. In Canada, phone: 1-519-451-2500. In Puerto Rico, phone: 809-750-3000.

Important Notice

The statements and technical information presented here are based on tests and data which 3M believes to be reliable, but the accuracy or completeness of such statements and technical information is not guaranteed. 3M MAKES NO WARRANTIES, EXPRESS OR IMPLIED, INCLUDING, BUT NOT LIMITED TO, ANY IMPLIED WARRANTY OF MERCHANTABILITY OR FITNESS FOR A PARTICULAR PURPOSE. User is responsible for determining whether the 3M product is fit for a particular purpose and suitable for user's method of application.

Limitation of Remedies and Liability

If the 3M product is proved to be defective, THE EXCLUSIVE REMEDY, AT 3M'S OPTION, SHALL BE TO REFUND THE PURCHASE PRICE OF OR TO REPAIR OR REPLACE THE DEFECTIVE 3M PRODUCT. 3M shall not otherwise be liable for loss or damages, whether direct, indirect, special, incidental, or consequential, regardless of the legal theory asserted, including negligence, warranty, or strict liability.



Specialty Additives

3M Center, Bldg. 220-8E-04
P.O. Box 3220
St. Paul, MN 55133-3220



Recycled Paper
40% pre-consumer
10% post-consumer

Printed in U.S.A.
©3M 1994 70-0704-5668-0

Appendix D

**Final Report on Glass Spheres in
Drilling Fluids**

MEI Report TR98-25

by

Bob Evans
MUDTECH LABORATORIES, INC.
October 1998

INTRODUCTION:

Mudtech Laboratories, Inc. was asked to evaluate the effect of LWSA on the rheology of several different fluid types. In addition, the effect of varying amounts of simulated drill solids was to be determined.

The fluid types to be tested were:

- PHPA Drilling Fluid
- Oil Base Drilling Fluid
- Synthetic Drilling Fluid
- 3% KCl Drilling Fluid
- CaCl_2 Brine
- CaBr_2 Brine
- ZnBr_2 Brine
- NaCl Brine

Each fluid was to be tested at 0%, 16%, 26%, & 36% by weight of the LWSA additive. Also the effects of 0%, 2%, 4%, 6%, 8%, & 10% by weight simulated drill solids was to be determined for each fluid at each concentration of LWSA additive. The test grid was as follows:

MUD TYPE	LWSA (%)	DRILL SOLIDS (%)					
		0	2	4	6	8	10
PHPA	0	*					
	16	*	*	*	*	*	*
	26	*	*	*	*	*	*
	36	*					
OIL BASE	0						
	16						
	26						
	36						
3% KCl	0						
	16						
	26	*					
	36						
CaCl_2	0						
	16						
	26						
	36						
CaBr_2	0						
	16						
	26						
	36						
ZnBr_2	0						
	16						
	26						
	36						
Synthetic Mud	0						
	16						
	26						
	36						
NaCl	0						
	16						
	26						
	36						

The cells with an asterisk in the above grid indicate tests that were conducted in phase one testing. We decided to recheck these data points since the base additives used in the phase one tests had been replaced. We wanted to ensure that the new data conformed to the phase one test data.

The properties tested were the 6-Speed Fann 35A rheology from which the Plastic Viscosity and Yield Point values were calculated, and the initial, 10 second, & 30 minute gel strengths. Additionally, since fluid loss is an important aspect of a drilling fluid, the API filtrate at 100 psi differential and for 30 minutes duration was determined for the water base fluids and the HPHT filtrate @ 250°F, 500 psi differential, and for 30 minutes duration was determined for the oil base and synthetic drilling fluids. Also the electrical stabilities were determined for the oil base and synthetic drilling fluids. Filtration rates were not conducted on the brine fluids.

The LWSA additive for the project was supplied by Maurer Engineering. The remainder of the materials were supplied by Mudtech Laboratories from our lab supplies.

RESULTS & DISCUSSION:

The tabular data is in Tables 1 to 32 (attached). Each of the fluids will be discussed below.

PHPA DRILLING FLUID:

The formulation for the PHPA drilling fluid was:

Houston Tap Water,bbl	1
API Bentonite,ppb	10
PHPA,ppb	1
Caustic Soda,ppb	0.25

Nothing unusual was noticed in the PHPA tests. As expected the plastic viscosities, yield points, and gel strengths increased with increasing concentrations of LWSA additive or simulated drill solids. At 16% LWSA additive, the rheological properties became unmanageable at 8% by volume of simulated drill solids. At 26% LWSA additive, the rheological properties became unmanageable at 8% by volume of simulated drilling solids. At 36% LWSA additive, the rheological properties became unmanageable at 6% by volume of simulated drill solids. The API filtration rates remained fairly constant with very little variation observed.

The PHPA data is presented in Tables 1 to 4.

OIL BASE DRILLING FLUID:

The formulation for the Oil Base drilling fluid was:

#2 Diesel,bbl	0.67
Organoclay,ppb	5
Primary Emulsifier,ppb	8
Secondary Emulsifier,ppb	5
Lime,ppb	5
30% CaCl ₂ ,bbl	0.22
Amine Lignite,ppb	8
Barite,ppb	150

The rheologies of the Oil Base drilling fluid increased as expected at each concentration of LWSA additive with increasing simulated drill solids concentrations; however, the rheologies did not increase correspondingly at all concentrations of LWSA additive. At 0%, 16%, and 26% of LWSA additive, each viscosity increased as expected (i.e. the viscosities at 26% LWSA additive was greater than the corresponding concentration of simulated drill solid concentration at 16% LWSA additive concentration. Likewise, 16% LWSA additive compared with 0% LWSA additive). At the 36% LWSA concentration, however, while the overall viscosity of the fluid increased, the yield points were lower than expected at the 8% & 10% simulated drill solids concentrations. We do not understand why this occurred. The electrical stabilities were dramatically lower at the 8% & 10% simulated drill solids concentration which could explain this, however, usually when electrical stabilities are low the yield point is high.

The Oil Mud data is presented in Tables 5 to 8.

3% KCl DRILLING FLUID:

The formulation for the 3% KCl drilling fluid was:

Houston Tap Water, bbl	1
API Bentonite, ppb	10
KCl, ppb	10.5
Xanthan Gum, ppb	1

Nothing unusual was noticed in the 3% KCl drilling fluid tests. Viscosities increased as expected with increased additions of either LWSA additive or simulated drill solids. The fluids containing 26% & 36% LWSA additive became very thick above 8% by volume simulated drill solids.

The 3% KCl drilling fluid data is presented in Tables 9 to 12.

BRINE FLUIDS:

The formulations for the brine fluids were as follows:

CaCl ₂ , BRINE		CaBr ₂ , BRINE	
11.7 ppg Brine, bbl	1	15.6 ppg Brine, bbl	1
HEC, ppb	0.5	HEC, ppb	0.5
ZnBr ₂ , BRINE		NaCl BRINE	
19.2 ppb Brine, bbl	1	10.0 ppg Brine	1
HEC, ppb	0.5	HEC, ppb	0.5

The NaCl, CaCl₂, and CaBr₂ Brines without LWSA additive, were virtually unaffected by increased simulated drill solids. This indicates that these brines have an inhibiting effect on the drill solids.

In the fluids that contained LWSA additive, the brines initially thinned when simulated drill solids were added and then thickened as the concentration of simulated drill solids increased. This behavior, which was duplicated in repeat tests, is unusual. We do not have an explanation for this. The LWSA additive should be inert in these brines; therefore, there should not be any chemical reactions occurring. It is possible that the addition of LWSA additive, which dramatically increases the volume of the system, reduced the concentration of HEC sufficiently to reduce the viscosity of the fluid until a concentration of simulated drill solids was attained that caused the viscosity to increase. Future testing should be designed to test this premise.

The ZnBr₂ Brine did not have the viscosity decrease seen in the other three (3) brines and behaved as expected. That is, the viscosity increased in a predictable manner when LWSA additive and/or simulated drill solids were added.

The CaCl₂ Brine, CaBr₂ Brine, and ZnBr₂ brine data are presented in Tables 13 to 24. The NaCl Brine data is presented in Tables 29 to 32.

SYNTHETIC DRILLING FLUID:

The formulation for the Synthetic drilling fluid was:

Polyalphaolefin, bbl	0.67
Organoclay, ppb	5
Primary Emulsifier, ppb	8
Secondary Emulsifier, ppb	5
Lime, ppb	5
30% CaCl ₂ , bbl	0.22
Amine Lignite, ppb	8
Barite, ppb	150

The synthetic drilling fluid, which was prepared using a C16/18 polyalphaolefin (PAO) as the base oil, performed similarly to the oil base mud except that the viscosities of the mud were slightly lower than for the oil base mud. This can be accounted for because the PAO has a lower viscosity than #2 diesel.

SUMMARY:

These tests show that LWSA additive can be used in the various fluids tested. The viscosities of the drilling fluids varied according to the amounts of either LWSA additive or simulated drill solids in predictable fashion. Viscosities increased with increasing concentrations of LWSA additive and also increasing amounts of simulated drill solids. The systems all had reasonable tolerance to the simulated drill solids, but did exhibit excessive viscosities in simulated drill solids concentrations above 8% by volume.

The brines tested, with the exception of ZnBr₂, exhibited unusual behavior in that the addition of simulated drill solids to the brines containing LWSA additive decreased the fluid viscosity at first before the viscosities began to increase.



5310 Milwee • Houston, Texas 77092 PH: 713-683-9716 Fax: 713-682-8147

LWDA FLUID RHEOLOGY TESTS
REPORT M98-3169
July 31, 1998

TABLE 1: PHPA FLUID WITH 0% B-38 BEADS

Rev Dust,ppb	0	18	36	54	72	90
Rev Dust,% by vol	0	2	4	6	8	10
600 rpm	26	29	39	61	83	110
300 rpm	15	17	25	39	56	77
200 rpm	10	12	17	31	45	63
100 rpm	7	8	12	23	31	45
6 rpm	1	2	3	6	10	15
3 rpm	0	1	2	4	8	13
PV	11	12	14	22	27	33
YP	4	5	11	17	29	44
10' Gel	1	1	2	4	6	14
10' Gel	2	2	3	6	12	77
30' Gel	3	4	7	15	37	181
API Filtrate	8.6	8.2	8.1	8.1	8.0	7.9

TABLE 2: PHPA FLUID WITH 16% B-38 BEADS

Rev Dust,ppb	0	18	36	54	72	90
Rev Dust,% by vol	0	2	4	6	8	10
600 rpm	32	39	54	78	114	167
300 rpm	19	23	35	54	81	115
200 rpm	13	16	26	41	63	93
100 rpm	8	11	14	24	40	69
6 rpm	2	3	5	9	14	24
3 rpm	1	2	4	7	13	21
PV	13	16	19	24	33	52
YP	6	7	16	30	48	63
10' Gel	1	2	3	5	8	25
10' Gel	2	2	5	11	61	257
30' Gel	4	5	9	23	117	OS
API Filtrate	7.0	6.9	6.9	6.7	6.6	6.6

TABLE 3: PHPA FLUID WITH 26% B-38 BEADS

Rev Dust,ppb	0	18	36	54	72	90
Rev Dust,% by vol	0	2	4	6	8	10
600 rpm	46	60	82	108	142	190
300 rpm	28	36	48	67	92	123
200 rpm	20	26	36	52	73	98
100 rpm	12	16	27	39	56	76
6 rpm	2	4	7	11	18	25
3 rpm	1	2	4	8	14	20
PV	18	24	34	41	50	67
YP	10	12	14	26	42	56
10' Gel	2	3	8	13	20	41
10' Gel	4	7	34	59	81	291
30' Gel	10	16	74	124	208	OS
API Filtrate	7.7	7.6	7.8	7.7	7.8	7.7

TABLE 4: PHPA FLUID WITH 36% B-38 BEADS

Rev Dust,ppb	0	18	36	54	72	90
Rev Dust,% by vol	0	2	4	6	8	10
600 rpm	69	88	118	150	191	245
300 rpm	41	54	74	98	126	160
200 rpm	29	38	52	70	91	116
100 rpm	15	23	36	51	68	88
6 rpm	3	4	7	11	16	23
3 rpm	2	3	5	8	13	18
PV	28	34	44	52	65	85
YP	13	20	30	46	61	75
10' Gel	2	4	10	19	30	56
10' Gel	4	8	41	79	164	OS
30' Gel	11	39	106	110	OS	OS
API Filtrate	7.8	7.8	7.9	7.8	7.9	7.8



5310 Milwee • Houston, Texas 77092 PH: 713-683-9716 Fax: 713-682-8147

LWDA FLUID RHEOLOGY TESTS

REPORT M98-3169

July 31, 1998

TABLE 5: OILMUD WITH 0% B-38 BEADS

Rev Dust,ppb	0	18	36	54	72	90
Rev Dust,% by vol	0	2	4	6	8	10
600 rpm	31	36	44	54	65	77
300 rpm	19	26	33	42	51	62
200 rpm	15	20	28	35	44	55
100 rpm	10	15	22	29	38	47
6 rpm	4	4	5	7	10	14
3 rpm	3	3	4	6	8	11
PV	12	10	11	12	14	15
YP	7	16	22	30	37	47
10" Gel	5	6	8	10	12	14
10' Gel	6	7	9	11	13	15
30' Gel	7	8	9	11	13	16
HPHT Filtrate	1.8	1.8	2.0	1.8	1.6	2.0
Electrical Stability	776	760	729	710	672	635

TABLE 6: OILMUD WITH 16% B-38 BEADS

Rev Dust,ppb	0	18	36	54	72	90
Rev Dust,% by vol	0	2	4	6	8	10
600 rpm	59	69	81	94	110	128
300 rpm	36	45	55	66	79	94
200 rpm	27	33	41	51	63	74
100 rpm	18	23	30	40	49	61
6 rpm	6	7	9	12	16	20
3 rpm	5	5	7	10	13	17
PV	23	24	26	28	31	34
YP	13	21	29	38	48	60
10" Gel	7	9	12	16	19	23
10' Gel	8	10	14	17	21	25
30' Gel	9	10	14	17	22	26
HPHT Filtrate	3.6	3.2	2.8	2.6	2.4	2.2
Electrical Stability	700	670	644	597	580	522

TABLE 7: OILMUD WITH 26% B-38 BEADS

Rev Dust,ppb	0	18	36	54	72	90
Rev Dust,% by vol	0	2	4	6	8	10
600 rpm	117	126	140	158	179	203
300 rpm	68	76	87	100	116	135
200 rpm	48	58	68	81	93	108
100 rpm	31	39	47	56	68	81
6 rpm	10	12	16	21	28	35
3 rpm	9	11	15	19	24	29
PV	49	50	53	58	63	68
YP	19	26	34	42	53	67
10" Gel	12	14	18	22	29	41
10' Gel	13	15	20	25	32	44
30' Gel	13	16	20	25	33	44
HPHT Filtrate	3.4	3.2	3.0	2.6	2.4	2.4
Electrical Stability	621	590	539	481	413	343

TABLE 8: OILMUD WITH 36% B-38 BEADS

Rev Dust,ppb	0	18	36	54	72	90
Rev Dust,% by vol	0	2	4	6	8	10
600 rpm	186	202	222	244	271	299
300 rpm	108	118	131	144	160	177
200 rpm	80	87	98	108	122	137
100 rpm	50	56	64	75	87	99
6 rpm	15	18	23	29	36	45
3 rpm	13	16	20	26	33	41
PV	78	84	91	100	111	122
YP	30	34	40	44	49	55
10" Gel	16	22	29	37	43	54
10' Gel	18	24	31	41	50	62
30' Gel	18	27	39	50	64	83
HPHT Filtrate	3.6	4.2	4.8	6.2	7.4	9.8
Electrical Stability	533	460	395	310	185	115



5310 Milwee • Houston, Texas 77092 PH: 713-683-9716 Fax: 713-682-8147

LWDA FLUID RHEOLOGY TESTS

REPORT M98-3169

July 31, 1998

TABLE 9: 3% KCl FLUID WITH 0% B-38 BEADS

Rev Dust,ppb	0	18	36	54	72	90
Rev Dust,% by vol	0	2	4	6	8	10
600 rpm	43	52	63	74	87	100
300 rpm	23	31	42	51	62	74
200 rpm	18	26	33	43	53	63
100 rpm	9	14	21	29	36	45
6 rpm	3	4	8	9	12	16
3 rpm	2	3	5	7	10	13
PV	20	21	21	23	25	26
YP	3	10	21	28	37	48
10' Gel	1	2	4	5	8	10
10' Gel	2	4	7	10	14	17
30' Gel	9	14	21	28	34	42
API Filtrate	89.6	71.5	58.2	48.9	37.4	32.2

TABLE 10: 3% KCl FLUID WITH 16% B-38 BEADS

Rev Dust,ppb	0	18	36	54	72	90
Rev Dust,% by vol	0	2	4	6	8	10
600 rpm	58	68	81	94	108	123
300 rpm	36	45	56	68	80	92
200 rpm	28	37	47	58	69	82
100 rpm	16	24	33	42	54	65
6 rpm	7	10	14	18	24	30
3 rpm	5	7	10	14	20	25
PV	22	23	25	26	28	31
YP	14	22	31	42	52	61
5	9	13	18	24	27	
10' Gel	8	16	23	33	43	50
30' Gel	28	40	54	65	81	93
API Filtrate	> 100	> 100	96.4	81.3	77.7	54.8

TABLE 11: 3% KCl FLUID WITH 26% B-38 BEADS

Rev Dust,ppb	0	18	36	54	72	90
Rev Dust,% by vol	0	2	4	6	8	10
600 rpm	71	84	99	116	135	154
300 rpm	46	58	70	85	101	117
200 rpm	37	47	59	71	84	103
100 rpm	22	32	42	53	67	79
6 rpm	11	15	21	28	34	42
3 rpm	9	13	17	21	28	34
PV	25	26	29	31	34	37
YP	21	32	41	54	67	80
10' Gel	9	19	27	39	48	57
10' Gel	13	24	36	48	64	77
30' Gel	42	56	73	91	106	129
API Filtrate	NC	NC	> 100	98.3	87.4	73.1

TABLE 12: 3% KCl FLUID WITH 36% B-38 BEADS

Rev Dust,ppb	0	18	36	54	72	90
Rev Dust,% by vol	0	2	4	6	8	10
600 rpm	85	107	131	157	186	221
300 rpm	57	72	90	109	130	152
200 rpm	46	59	73	90	106	124
100 rpm	29	41	52	67	83	99
6 rpm	16	24	30	39	48	59
3 rpm	13	19	26	33	41	49
PV	28	35	41	48	56	69
YP	29	37	49	61	74	83
10' Gel	13	27	41	54	71	86
10' Gel	19	33	48	66	75	106
30' Gel	59	77	99	123	157	188
API Filtrate	NC	NC	> 100	> 100	84.7	67.8



5310 Milwaukee • Houston, Texas 77092 PH: 713-683-9716 Fax: 713-682-8147

LWDA FLUID RHEOLOGY TESTS

REPORT M98-3169

July 31, 1998

TABLE 13: CaCl₂ FLUID WITH 0% B-38 BEADS

Rev Dust,ppb	0	18	36	54	72	90
Rev Dust,% by vol	0	2	4	6	8	10
600 rpm	26	32	39	46	54	62
300 rpm	13	17	22	28	34	40
200 rpm	9	12	17	21	26	31
100 rpm	5	7	10	13	17	21
6 rpm	1	2	3	5	7	9
3 rpm	1	1	2	2	4	6
PV	13	15	17	18	20	22
YP	0	2	5	10	14	18
10" Gel	1	2	2	3	5	8
10' Gel	1	2	3	4	6	10
30' Gel	1	3	5	7	10	15
API Filtrate	NC					

TABLE 14: CaCl₂ FLUID WITH 16% B-38 BEADS

Rev Dust,ppb	0	18	36	54	72	90
Rev Dust,% by vol	0	2	4	6	8	10
600 rpm	71	78	86	95	104	114
300 rpm	46	48	49	52	55	59
200 rpm	34	35	36	37	38	39
100 rpm	19	19	20	20	21	21
6 rpm	2	2	2	2	3	3
3 rpm	1	1	1	1	1	2
PV	25	30	37	43	49	55
YP	21	18	12	9	6	4
10" Gel	2	2	2	2	3	3
10' Gel	2	3	5	8	12	17
30' Gel	2	3	5	8	13	17
API Filtrate	NC					

TABLE 15: CaCl₂ FLUID WITH 26% B-38 BEADS

Rev Dust,ppb	0	18	36	54	72	90
Rev Dust,% by vol	0	2	4	6	8	10
600 rpm	126	144	163	185	210	236
300 rpm	82	89	98	107	116	127
200 rpm	60	64	68	74	81	86
100 rpm	33	34	38	40	45	50
6 rpm	3	4	4	4	6	7
3 rpm	1	1	1	2	4	5
PV	44	55	65	78	94	109
YP	38	34	33	29	22	18
10" Gel	1	1	2	3	4	5
10' Gel	2	3	5	8	11	16
30' Gel	2	4	5	9	12	16
API Filtrate	NC					

TABLE 16: CaCl₂ FLUID WITH 36% B-38 BEADS

Rev Dust,ppb	0	18	36	54	72	90
Rev Dust,% by vol	0	2	4	6	8	10
600 rpm	234	261	291	325	360	394
300 rpm	151	160	170	182	193	208
200 rpm	98	107	117	126	136	157
100 rpm	60	63	66	69	73	77
6 rpm	4	4	5	6	8	10
3 rpm	2	2	2	3	4	5
PV	83	101	121	143	167	186
YP	68	59	49	39	28	22
10" Gel	3	3	3	4	6	9
10' Gel	3	3	4	6	9	13
30' Gel	3	3	4	6	9	14
API Filtrate	NC					



5310 Milwee • Houston, Texas 77092 PH: 713-683-9716 Fax: 713-682-8147

LWDA FLUID RHEOLOGY TESTS
REPORT M98-3169
July 31, 1998

TABLE 17: CaBr₂ FLUID WITH 0% B-38 BEADS

Rev Dust,ppb	0	18	36	54	72	90
Rev Dust,% by vol	0	2	4	6	8	10
600 rpm	14	15	16	17	18	19
300 rpm	7	8	8	9	9	10
200 rpm	5	5	6	7	7	8
100 rpm	3	3	3	4	4	5
6 rpm	1	1	1	2	2	3
3 rpm	1	1	1	1	1	2
PV	7	7	8	8	9	9
YP	0	1	0	1	0	1
10" Gel	1	1	1	1	1	2
10' Gel	1	1	1	2	2	3
30' Gel	1	1	2	2	3	5
API Filtrate	NC					

TABLE 18: CaBr₂ FLUID WITH 16% B-38 BEADS

Rev Dust,ppb	0	18	36	54	72	90
Rev Dust,% by vol	0	2	4	6	8	10
600 rpm	50	52	54	57	61	65
300 rpm	26	28	30	33	36	39
200 rpm	18	20	22	25	28	31
100 rpm	10	12	14	16	19	22
6 rpm	1	2	4	6	9	11
3 rpm	1	1	3	5	8	10
PV	24	24	24	24	25	26
YP	2	4	6	9	11	13
10" Gel	1	1	1	2	3	4
10' Gel	2	2	3	3	4	5
30' Gel	3	4	5	6	7	8
API Filtrate	NC					

TABLE 19: CaBr₂ FLUID WITH 26% B-38 BEADS

Rev Dust,ppb	0	18	36	54	72	90
Rev Dust,% by vol	0	2	4	6	8	10
600 rpm	84	86	89	92	97	110
300 rpm	46	45	45	46	49	56
200 rpm	31	32	33	35	38	42
100 rpm	15	15	16	17	19	22
6 rpm	2	1	1	1	2	3
3 rpm	2	1	1	1	1	2
PV	38	41	44	46	48	54
YP	8	4	1	0	1	2
10" Gel	2	2	2	2	3	5
10' Gel	2	2	3	3	4	7
30' Gel	3	5	7	7	9	11
API Filtrate	NC					

TABLE 20: CaBr₂ FLUID WITH 36% B-38 BEADS

Rev Dust,ppb	0	18	36	54	72	90
Rev Dust,% by vol	0	2	4	6	8	10
600 rpm	123	130	137	144	151	159
300 rpm	66	68	70	74	77	81
200 rpm	45	47	49	53	57	60
100 rpm	23	24	26	27	29	32
6 rpm	2	2	2	2	3	3
3 rpm	1	1	1	2	2	2
PV	57	62	67	70	74	78
YP	9	6	3	4	3	3
10" Gel	2	2	3	3	5	7
10' Gel	3	3	4	5	8	10
30' Gel	8	9	11	13	16	19
API Filtrate	NC					



5310 Milwee • Houston, Texas 77092 PH: 713-683-9716 Fax: 713-682-8147

LWDA FLUID RHEOLOGY TESTS

REPORT M98-3169

July 31, 1998

TABLE 21: ZnBr₂ FLUID WITH 0% B-38 BEADS

Rev Dust,ppb	0	18	36	54	72	90
Rev Dust,% by vol	0	2	4	6	8	10
600 rpm	58	61	64	67	71	75
300 rpm	31	32	34	37	40	43
200 rpm	20	21	22	23	24	26
100 rpm	9	9	10	11	12	13
6 rpm	1	1	2	3	3	4
3 rpm	1	1	1	2	2	3
PV	27	29	30	30	31	32
YP	4	3	4	7	9	11
10" Gel	1	1	2	2	3	4
10' Gel	1	2	3	3	4	5
30' Gel	1	2	3	4	5	6
API Filtrate	NC					

TABLE 22: ZnBr₂ FLUID WITH 16% B-38 BEADS

Rev Dust,ppb	0	18	36	54	72	90
Rev Dust,% by vol	0	2	4	6	8	10
600 rpm	92	96	101	107	113	122
300 rpm	51	54	57	61	65	71
200 rpm	35	37	39	42	45	48
100 rpm	18	19	21	23	25	27
6 rpm	1	1	2	3	4	5
3 rpm	1	1	2	2	3	3
PV	41	42	44	46	48	51
YP	10	12	13	15	17	20
10" Gel	1	1	1	2	3	4
10' Gel	2	2	2	3	4	6
30' Gel	4	4	5	6	7	8
API Filtrate	NC					

TABLE 23: ZnBr₂ FLUID WITH 26% B-38 BEADS

Rev Dust,ppb	0	18	36	54	72	90
Rev Dust,% by vol	0	2	4	6	8	10
600 rpm	179	167	156	145	158	172
300 rpm	96	90	85	79	87	96
200 rpm	66	62	58	54	61	69
100 rpm	32	31	30	29	32	35
6 rpm	2	2	2	3	4	6
3 rpm	1	1	2	2	3	5
PV	83	77	71	66	71	76
YP	13	13	14	13	16	20
10" Gel	2	2	3	3	4	4
10' Gel	2	3	3	3	3	4
30' Gel	7	7	6	6	8	9
API Filtrate	NC					

TABLE 24: ZnBr₂ FLUID WITH 36% B-38 BEADS

Rev Dust,ppb	0	18	36	54	72	90
Rev Dust,% by vol	0	2	4	6	8	10
600 rpm	323	301	277	303	329	356
300 rpm	170	158	147	160	175	194
200 rpm	109	100	92	102	113	127
100 rpm	54	47	41	48	56	66
6 rpm	4	3	2	3	5	8
3 rpm	2	2	2	2	7	12
PV	153	143	130	143	154	162
YP	17	15	17	17	21	32
10" Gel	2	2	3	3	4	5
10' Gel	3	4	5	6	7	8
30' Gel	11	12	14	15	16	16
API Filtrate	NC					



5310 Milwee • Houston, Texas 77092 PH: 713-683-9716 Fax: 713-682-8147

LWDA FLUID RHEOLOGY TESTS

REPORT M98-3169

July 31, 1998

TABLE 25: SYNTHETIC FLUID WITH 0% B-38 BEADS

Rev Dust, ppb	0	18	36	54	72	90
Rev Dust, % by vol	0	2	4	6	8	10
600 rpm	27	32	38	46	56	68
300 rpm	17	20	24	30	39	50
200 rpm	12	14	17	21	27	36
100 rpm	8	9	11	14	18	24
6 rpm	2	2	3	4	5	7
3 rpm	1	1	2	3	3	4
PV	10	12	14	16	17	18
YP	7	8	10	14	22	32
10" Gel	5	6	8	9	11	12
10' Gel	5	7	9	11	13	14
30' Gel	6	8	10	12	15	17
HPHT Filtrate	2.2	2.4	2.0	2.2	1.8	2.0
Electrical Stability	697	677	655	632	599	583

TABLE 26: SYNTHETIC FLUID WITH 16% B-38 BEAD

Rev Dust, ppb	0	18	36	54	72	90
Rev Dust, % by vol	0	2	4	6	8	10
600 rpm	51	57	65	76	91	109
300 rpm	32	37	44	53	67	82
200 rpm	21	25	30	37	44	55
100 rpm	14	17	21	27	35	44
6 rpm	3	3	4	5	7	9
3 rpm	2	2	3	4	5	6
PV	19	20	21	23	24	27
YP	13	17	23	30	43	55
10" Gel	7	9	11	15	19	22
10' Gel	8	10	11	15	20	23
30' Gel	9	11	12	17	23	27
HPHT Filtrate	4.2	4.2	4.4	4.2	4.0	3.8
Electrical Stability	674	657	633	589	577	547

TABLE 27: SYNTHETIC FLUID WITH 26% B-38 BEADS

Rev Dust, ppb	0	18	36	54	72	90
Rev Dust, % by vol	0	2	4	6	8	10
600 rpm	101	110	121	134	152	174
300 rpm	61	67	75	85	98	116
200 rpm	38	43	49	58	68	83
100 rpm	24	27	31	37	45	59
6 rpm	5	6	8	10	13	17
3 rpm	3	3	4	5	7	11
PV	40	43	46	49	54	58
YP	21	24	29	36	44	58
10" Gel	10	11	16	20	28	43
10' Gel	12	13	19	24	32	48
30' Gel	13	14	19	25	32	50
HPHT Filtrate	4.6	4.4	4.2	4.4	4.8	5.4
Electrical Stability	522	516	496	482	439	402

TABLE 28: SYNTHETIC FLUID WITH 36% B-38 BEAD

Rev Dust, ppb	0	18	36	54	72	90
Rev Dust, % by vol	0	2	4	6	8	10
600 rpm	160	174	191	210	230	252
300 rpm	96	105	116	130	145	162
200 rpm	61	67	74	83	93	104
100 rpm	38	42	47	54	63	75
6 rpm	8	9	11	14	18	23
3 rpm	5	6	8	11	14	19
PV	64	69	75	80	85	90
YP	32	36	41	50	60	72
10" Gel	14	19	27	35	42	56
10' Gel	17	23	31	39	47	63
30' Gel	18	24	32	39	47	64
HPHT Filtrate	4.6	5.4	5.4	5.8	6.2	7.4
Electrical Stability	499	487	483	461	444	412



5310 Milwee • Houston, Texas 77092 PH: 713-683-9716 Fax: 713-682-8147

LWDA FLUID RHEOLOGY TESTS

REPORT M98-3169

July 31, 1998

TABLE 29: NaCl FLUID WITH 0% B-38 BEADS

Rev Dust,ppb	0	18	36	54	72	90
Rev Dust,% by vol	0	2	4	6	8	10
600 rpm	6	7	9	12	15	19
300 rpm	3	4	5	7	9	12
200 rpm	2	2	3	4	6	8
100 rpm	1	1	2	2	3	4
6 rpm	1	1	1	1	2	3
3 rpm	1	1	1	1	1	2
PV	3	3	4	5	6	7
YP	0	1	1	2	3	5
10" Gel	1	1	1	2	2	3
10' Gel	1	1	2	2	3	3
30' Gel	1	1	2	3	3	4
API Filtrate	NC					

TABLE 30: NaCl FLUID WITH 16% B-38 BEADS

Rev Dust,ppb	0	18	36	54	72	90
Rev Dust,% by vol	0	2	4	6	8	10
600 rpm	13	17	22	28	34	42
300 rpm	7	9	12	16	20	26
200 rpm	5	6	8	11	15	19
100 rpm	3	4	5	6	8	11
6 rpm	1	1	1	1	2	2
3 rpm	1	1	1	1	1	1
PV	6	8	10	12	14	16
YP	1	1	2	4	6	10
10" Gel	1	1	2	3	3	3
10' Gel	1	2	2	3	3	3
30' Gel	2	2	3	4	4	5
API Filtrate	NC					

TABLE 31: NaCl FLUID WITH 26% B-38 BEADS

Rev Dust,ppb	0	18	36	54	72	90
Rev Dust,% by vol	0	2	4	6	8	10
600 rpm	28	25	21	23	28	34
300 rpm	15	13	11	12	15	19
200 rpm	10	8	6	7	9	12
100 rpm	5	4	3	3	5	7
6 rpm	1	1	1	1	2	3
3 rpm	1	1	1	1	1	2
PV	13	12	10	11	13	15
YP	2	1	1	1	2	4
10" Gel	1	1	1	1	2	2
10' Gel	1	1	1	2	2	3
30' Gel	7	7	8	9	11	13
API Filtrate	NC					

TABLE 32: NaCl FLUID WITH 36% B-38 BEADS

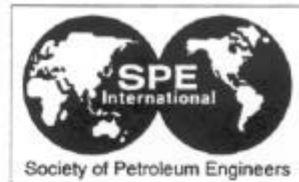
Rev Dust,ppb	0	18	36	54	72	90
Rev Dust,% by vol	0	2	4	6	8	10
600 rpm	93	59	37	49	68	95
300 rpm	52	35	24	30	41	58
200 rpm	28	21	15	19	26	35
100 rpm	14	11	8	10	13	18
6 rpm	2	2	3	4	6	8
3 rpm	1	1	2	3	4	5
PV	41	24	13	19	27	37
YP	11	11	11	11	14	21
10" Gel	2	2	2	2	2	2
10' Gel	4	6	7	8	8	8
30' Gel	17	16	15	16	18	22
API Filtrate	NC					

Appendix E
**SPE 38637: "Field Application of Lightweight Hollow Glass
Sphere Drilling Fluid"**

**SPE 72nd Annual Technical
Conference & Exhibition
October 1997**



SPE 38637



Field Application of LightWeight Hollow Glass Sphere Drilling Fluid

George H. Medley, Jr., SPE, Maurer Engineering Inc., Jerry E. Haston, Haston Petroleum Consultants, Richard L. Montgomery, 3M, I. Dylan Martindale, SPE, Mobil Oil Company, and John R. Duda, SPE, US Department of Energy

This paper was prepared for presentation at the 1997 SPE 72nd Annual Technical Conference & Exhibition held in San Antonio, Texas, October 5-8, 1997.

This paper was selected for presentation by an SPE Program Committee following review of information contained in an abstract submitted by the author(s). Contents of the paper have not been reviewed by the Society of Petroleum Engineers and are subject to correction by the author(s). The material, as presented, does not necessarily reflect any position of the Society of Petroleum Engineers, its officers, or members. Papers presented at SPE meetings are subject to publication review by Editorial Committees of the Society of Petroleum Engineers. Electronic reproduction, distribution, or storage of any part of this paper for commercial purposes without the written consent of the Society of Petroleum Engineers is prohibited. Permission to reproduce in print is restricted to an abstract of not more than 300 words; illustrations may not be copied. The abstract must contain conspicuous acknowledgment of where and by whom the paper was presented. Write Librarian, SPE, P.O. Box 633836, Richardson, TX 75083-3836, U.S.A., fax 972-952-9435.

Abstract

A new class of underbalanced drilling fluids being developed under U. S. Department of Energy sponsorship was recently successfully field tested. The fluid utilizes hollow glass spheres (HGS), also known as glass bubbles, to decrease the fluid density to below that of the base mud while maintaining incompressibility.

A previous paper, SPE 30500, described the rheological properties and laboratory behavior of HGS fluids. An HGS fluid was formulated in the field and used to drill two wells in Kern County, California in the fall of 1996 for a major operating company. Concentrations of up to 20% by volume were used to decrease the fluid density to 0.8 lb/gal (ppg) less than normally used in the field. The techniques employed to mix and maintain the mud, the rheological properties measured in the field, and a discussion of future applicability of HGS fluid are addressed here.

The field tests demonstrated that HGS drilling fluid can be easily and safely mixed under field operating conditions, is compatible with conventional drilling muds and rig equipment, and can be circulated through conventional mud motors, bits, and solids control equipment with little detrimental effect on either mud or equipment.

Potential benefits of using these fluids include higher penetration rates, decreased formation damage, and lost circulation mitigation. When used in place of aerated fluid they can eliminate compressor usage and allow the use of mud pulse MWD tools. These benefits improve drilling economics.

These and other recent advances in technology have spurred interest in underbalanced drilling to the highest level in 30 years. Industry-wide surveys indicate that more than 12% of wells

drilled in the United States in 1997 will intentionally employ underbalanced techniques.

Introduction

The U. S. Department of Energy (DOE) recognizes the benefits of advanced technology to the oil and gas industry. Consequently, DOE manages a portfolio of drilling related research, development, and demonstration projects designed to reduce cost and increase process efficiency. This program is implemented by the DOE's Federal Energy Technology Center and is a market-driven balance of near-, mid-, and long-term efforts. These drilling related projects support the department's ultimate goal of developing the nation's large natural gas resource base and maintaining market-responsive supplies at competitive prices.

Lightweight solid additives (LWSA) for drilling fluid density reduction were tested in the laboratory and in a test yard in drilling rig compatible equipment during 1994 and 1995. The Department of Energy (DOE) published a final report on this Phase I testing in the fourth quarter of 1995¹. The primary objective of the project since that time has been to test underbalanced drilling products in actual field operations.

The LWSA tested consists of hollow glass spheres (i.e. glass bubbles) manufactured in the United States and commonly used as a filler material for other lightweight products. The spheres have an average specific gravity of 0.37 and average collapse strength of 3,000 psi. The spheres average 50 microns in diameter. The goal of the DOE project is to use the glass bubbles to generate drilling fluids having densities less than that of the base fluids.

Much of the intangible cost of drilling wells is time sensitive, so techniques, which increase rate of penetration, are core to the DOE program. Underbalanced drilling products are investigated because of their potential for increasing drilling rate, as well as their potential to retain maximum well productivity by minimizing drilling induced formation damage. The LWSA fluids represent one such underbalanced drilling technology. A more comprehensive description of DOE drilling related research and development was provided in an earlier paper, SPE 30993².

Mobil Oil Company provided the first opportunity to test LWSA in a field operation in September 1996. The test wells were

located in the Midway-Sunset Field of Kern County, California.

Subject Wells

Mobil Oil Company gave final permission to perform the tests on up to four wells located in Kern Co., California. Two wells were actually tested with the LWSA. These wells were optimum for the initial field tests for the following reasons.

They were relatively shallow wells, allowing more than one well to be tested quickly using HGS having a collapse pressure of 3,000 psi. Material with a collapse pressure of 4,000 psi is available, but the lower strength material is less expensive. The original description of the wells indicated they would be approximately 1,200 ft deep; actual depths ranged to 1,780 ft.

The mud volume was very small. Initial indications were that only 200 barrels of mud would be required for each well. Again, less mud volume means fewer spheres, which in turn reduces cost.

The initial plan called for tests in 3-4 wells, but while drilling the first two a much larger volume of mud was required than originally anticipated. Rather than building only 200 barrels of fluid to drill each well, approximately 350-400 barrels were required. After the second well was successfully drilled all useful information had been gathered at this location, preempting the need for additional data collection.

Objectives

The overall objective of these field tests was to determine if a well could even be drilled using the LWSA in the drilling mud. This main objective can be further sub-divided more specifically to demonstrate:

1. The ability to safely and easily mix LWSA into drilling fluid under normal field conditions.
2. The compatibility of LWSA with conventional drilling fluids.
3. The durability of the LWSA during circulation downhole through conventional bits, mud-motors, and surface equipment (i.e. pumps and solids control equipment).
4. The ability to re-use or recycle the mud on more than one well.
5. The lack of detrimental effects on conventional drilling equipment.
6. The minimal environmental effect of the LWSA.

Pilot Testing

Pilot tests conducted by the mud company prior to the field tests demonstrated that LWSA additions of 10% by volume had very little effect on the rheology of the mud, as shown in Table 1.

The pilot test results demonstrated that no compatibility problems existed between the LWSA and the base mud, allowing the field tests to proceed.

General Procedures

The LWSA was added to the first subject well at concentra-

tions up to 10% by volume, and to the second well at concentrations up to 20% by volume. In both cases the LWSA performed better than expected. Attrition rate for the LWSA was less than 10%, exceeding expectations based on the manufacturer's specification that as much as 10% of the product may be "sinkers".

The original test plan called for the LWSA to be tested in vertical wells only, so the results would not be clouded by any detrimental effects of a mud motor on the LWSA. However, both wells were directional wells, and downhole mud motors were used to drill approximately one-third to one-half of each well.

Over 40 samples were taken from various points in the mud system during the drilling operations of these wells, with the samples being sent to a laboratory for analysis of the HGS content of each sample.

Mixing. Mixing the LWSA into the drilling mud was expected to be the most significant logistical problem. During yard testing, the product was added conventionally by dumping it into a normal mud hopper or by dumping it directly into the pit. However, the large volumes required for a full-scale field test precluded dumping the product because the packaging consisted of large boxes weighing approximately 640 pounds each.

The LWSA was mixed into the mud using the manufacturer's recommended procedure for similar products. This mixing system (Fig. 1) used a conventional double-diaphragm pump to transfer the glass bubbles from the package into the fluid. The diaphragm pump, also called a cellar pump or trash pump, is commonly found on most rigs. In fact, an identical pump was available on the test well rig.

The diaphragm pump was capable of transferring dry glass bubbles from the package to the mud pit at approximately 640 lbs per hour. The highest rate achieved was one 640-lb. box in 30 minutes. The transfer rate was slowed by two factors.

Normally, some air is injected into the LWSA directly at the pump suction point to "fluidize" the solid spheres and allow them to flow more readily into the suction hose. However, Mobil personnel requested that air not be injected because the drilling fluid used on the lease tends to foam and already contains too much air for efficient pumping. Fluidizing the spheres for other product mixtures normally causes no foaming. We estimated that each box of LWSA could be transferred to the pit in 5-10 minutes utilizing air fluidization.

Secondly, the air compression system available on the drilling rig was not capable of delivering sufficient pressure to the diaphragm pump when the rig hoisting system was in use. Consequently, the transfer pump had to be shut down when connections were made to the drill string. This slowed the average product transfer time, but was not detrimental to the process.

The initial mud volume was determined on site. The amount of spheres required to reach the desired volume percent was calculated (10% for the first well and 20% for the second), and mixing was begun. With the small volume of mud initially

built, one to two 640-lb. boxes of spheres were required. By the time this was added, enough additional mud had been built to require further LWSA additions. For both wells, the desired LWSA loading was reached after approximately three boxes of product were added (i.e., about 2.5 to 3 hours). At the rate the wells were drilled (about 60-80 feet per hour), product additions had to be made at the rate of about one box every 2-3 hours.

Environmental Concerns. The primary concern regarding environmental effects of the spheres, in particular while mixing them into the mud pit, was whether or not the LWSA would become airborne as dust because of its low specific gravity.

This concern was addressed by injecting the dry product through a hose lowered as deeply as possible into the conventional mud hopper on the mud pit system. Figure 2 shows the product exiting the pump through the hose placed in the hopper. No dust was produced while mixing the hollow glass spheres.

To further ensure that dust emissions were not a problem while using the LWSA, conventional dust masks were provided. The manufacturer also recommends that non-vented goggles be used while handling the product.

Results

General LWSA Mud Properties. The mud engineer normally controls the drilling fluid in the Midway-Sunset field by keeping the funnel viscosity (FV) of the mud in the 38-40 sec/qt. range. If the FV falls much below 38, additional gel (or bentonite) is added. If the FV gets much above 40, additional water is added or an attempt is made to "clean" the mud by dumping a sand trap from the mud pit system.

Figure 3 shows that the FV for the mud used in Well 1 varied from 34 to 44 sec/qt. This is a wider range than desired for the mud, but was acceptable.

The FV measured in Well 1 was essentially independent of the LWSA concentration as shown in Fig. 4. The FV measured with 13% by volume LWSA is about the same as that measured with only 3% LWSA.

Figures 5 and 6 show FV vs. depth and FV compared to LWSA content, respectively, for Well 2.

The FV was above the desired range of 38-40 sec/qt for most of Well 2, because the concentration of LWSA was higher in this well than in Well 1, reaching concentrations as high as 19% (Figure 5).

For fresh water-base muds, high solids content usually increases the FV. The LWSA content was higher in Well 2 than in Well 1 at all depths. However, near the bottom of Well 2, where the FV dropped to 38, the LWSA concentration was also lower, approaching levels used in Well 1.

In Well 2, increasing the volume percent of LWSA generally tended to increase the FV, as shown in Fig. 6.

Other significant fluid properties measured in the field included Plastic Viscosity (PV), in cp., Yield Point (YP), in lbs/100 SF, and API Fluid Loss (FL), in cc/30 min.

The API FL was relatively unaffected by the addition of LWSA to the mud. Measured API FL changed less than 1%

during the drilling of these wells. This agrees with the laboratory tests that showed API FL varied between 8.3 and 6.0 cc/30 min for any concentration of LWSA up to 40% by volume. These results were reported in SPE 30500.

Figures 7 and 8 show how the PV and YP changed while drilling deeper in both Wells 1 and 2.

Figure 7 shows that the PV increased from 12 to 15 as Well 1 was drilled, because the concentration of LWSA was increasing. The YP decreased from 10 to 7 as the well was drilled. Earlier laboratory work indicated that the YP would be expected to increase as the concentration of LWSA increased. However, the LWSA never exceeded 14% by volume in this well, which may be too small to demonstrate any definitive effect.

Figure 8 shows that PV decreased as Well 2 was deepened, while YP increased. This effect on PV was the opposite of what was expected, but measures taken to lower the FV (i.e., adding water) to the desired range also lowered PV.

The measured PVs and YPs for these two mud systems were within acceptable ranges for drilling fluids.

Maintaining LWSA Concentration. In general, LWSA concentration in the drilling fluid was determined based on the density of the fluid. As much as possible, all additions to, and subtractions from, the mud system were measured.

The pit volume was always known, since it was a compartmentalized steel tank. The mud engineer noted all dry product additions. A water meter was installed on the water inlet line to the mud pit system, and the initial meter reading was recorded.

The sand traps on the steel pit system were dumped periodically to control the FV as described above. These volumes were noted and accounted for in calculations of the volume percent of LWSA.

Since the pit system for this rig is relatively small (< 90 barrels), a small change in volume of any one constituent can make a large percentage change in the concentration of that or any other additive. For example, if 10 barrels of mud containing 10% by volume LWSA were lost from the pit on a drill string trip, and 10 barrels of water were added to the pit to make up the lost volume, the density of the fluid would increase nearly 0.1 ppg. At the same time, the overall volume percent of LWSA would decrease 11%. Figure 9 shows the mud pit system used for these tests.

The unknown parameters with the most impact besides unmeasured losses were the amount or volume of drill cuttings generated (i.e., hole size) and the amount of drill cuttings dumped into the sump by the solids control equipment. These volumes were inferred using history matching.

A spreadsheet was used to perform a volume balance. Parameters were varied until the predicted mud density matched typical or historical mud densities measured in this field. The matched values were then input into the spreadsheet and calculated volume percents of LWSA were compared to the known volumes being added to the mud.

The measured volume of LWSA added to the drilling fluid was used to calculate a theoretical mud weight (MW) in lbs/gal

(ppg). This result was compared to the actual measured MW to determine attrition of the LWSA. When the theoretical or calculated MW matches the measured MW, no hollow glass spheres are being lost in the system. Potential forms of LWSA attrition include breakage, loss downhole (either through loss of whole mud or through embedment into the wellbore wall), loss of whole mud at the surface, and loss through the solids control equipment.

Mud Weight (Fluid Density). Figure 10 shows that the calculated MW closely matched the measured mud weight at all depths in the first well, indicating minimal loss of LWSA.

Initially, the measured MWs were slightly higher than the calculated theoretical weights, indicating that some LWSA was being lost. Below 600 feet, however, measured MW was less than calculated MW. At a depth of 573 feet all drilling operations were shut down because of a steam blowout on a direct offset well, and the drilling location was evacuated. During the evacuation, the mud cleaner was inadvertently left on, and most of the LWSA drilling fluid in the surface system was thrown away to the sump, making it difficult to match predicted and measured values.

The calculated theoretical MW was less than the measured MW at the total depth for two reasons: First, an accurate water meter reading at total depth was not recorded, so the exact amount of water added to that point was unknown and had to be extrapolated. Secondly, at 1,421 ft the drill string was tripped out of the hole to lay down the mud motor. The fluid could not run through the motor as fast as the string was pulled, so some whole mud was lost from the pit system. As described above, any losses to the system can have a major effect on the mud properties because the overall system volume is relatively small.

Figure 11 shows calculated vs. measured MW for the second well. The agreement between measured and theoretical is excellent throughout most of the wellbore, indicating that no LWSA was being lost through attrition.

Near the bottom of the well, the measured mud weight was higher than the calculated value, indicating that some of the LWSA was being lost. Calculations show that as much as 17-32% of the LWSA was lost between 1,391 feet and total depth. Three phenomena explain this apparent LWSA loss:

1. The mud motor was tripped out of the well at that depth. Again, as on the first well, 10-20 barrels of whole mud may have been lost and rebuilt at a higher density.
2. The pits were diluted and the solids control equipment kept running even though mud was not circulating. This could have caused more fluid to be thrown into the sump than estimated. It is worth noting that the mud weight in the pits at the beginning of the trip out was 8.2 ppg, as was the mud weight when the motor reached the surface. However, when the new bit reached bottom after the trip, the mud weight had increased to 8.5 ppg. No circulation of the mud system occurred during this period, nor did any other action occur that could have damaged the spheres.

3. The model may not be a perfect match or some of the input parameters may not be exactly correct.

Volume Percent HGS. Figures 12 and 13 show how the volume percent of LWSA added to the mud compares to the volume percent of LWSA remaining in the mud for both wells. The volume of LWSA added was measured, and the volume remaining was calculated based on the measured mud weight. Figure 12 shows that the theoretical and actual volume percents of LWSA compare favorably through most of the wellbore in the first well.

Figure 13 shows that the theoretical volume percent of LWSA was nearly identical to the amount actually added from surface to near total depth for the second well.

Figures 12 and 13 show that the theoretical and actual values deviated below about 1,400 feet in both wells. Several factors can explain this deviation: 1) The trip to lay down the mud motor was made at 1,421 ft. in Well 1 and at 1,391 ft. in Well 2, resulting in unknown quantities of lightweight mud losses; 2) On Well 2, before and during the trip, the rig and pits were washed with an un-metered volume of water and soap. This rig wash ended up in the mud pits, changing the mud density.

Agreement in both parameters was closer in the second well. Comparison of the curves between the first and second well gives evidence of a strong learning curve on both wells in mixing the mud and measuring the data.

The evacuation of the rig on Well 1 not only resulted in lost drilling fluid, but also in lost continuity. Some drilling fluid was left in the wellbore (approximately 40 barrels), and the surface volume had to be rebuilt, resulting in a mixture of 40 barrels that theoretically contained 9.3% LWSA by volume and 85 barrels of mud on the surface that contained no LWSA.

Weight Percent HGS. The results of the volume percent concentration analysis were confirmed by a laboratory analysis of samples taken from the returns line, the pit, and the overflow and underflow from the solids control equipment. These samples were analyzed on the basis of weight percent. When conversion was made to volume percent the results were consistent with the on-site analysis.

For example, at a depth of 1,051 feet on Well No. 2 the concentration of glass bubbles in the mud was approximately 17% by volume, which corresponds to a concentration of about 4.2% by weight. Mud samples taken from the pit at that time had glass bubble concentrations of 3.8% by weight, indicating a loss of slightly less than 10% (well within manufacturer's specifications).

The glass bubble concentration in samples from the return line taken at the same time was 3.9% by weight, showing that the concentration of glass bubbles remained constant throughout the system.

Other measurements made on samples taken from the hydrocyclone underflow and the shale shaker overflow revealed glass bubble concentrations of 0.3-0.5% by weight. This

corresponds to a volume percent of 1-2%.

Effects of Solids Control Equipment. Extensive work was carried out to determine the effect of conventional solids control equipment on the LWSA, and vice versa. Earlier yard tests showed the most desirable solids control system for LWSA muds consists of a large mesh screen shale shaker (<100 mesh screen size) and a high quality mud cleaner with a capacity sufficient to process the entire mud volume.

The solids control system used on this drilling rig met that description. The shale shaker was maintained with a screen size of 40 to 60 mesh. A rented Krebs mud cleaner with six 4-inch hydrocyclones and a 160 mesh screen was used to drill all wells in the field. The mud cleaner screen was changed to 120 mesh at a depth of approximately 500 feet on the first well.

The shale shaker worked well throughout the tests, but several problems occurred with the mud cleaner.

Initially, underflow was only coming from two of the six cones. After the mud system was rebuilt at 600 feet on the first well and the cones cleaned, underflow came from all cones for the duration of the tests.

The hydrocyclone operation was not optimized. An indication of poor performance was the hydrostatic head measured across the cones. Solids control companies usually recommend a pressure head across cones of 75 to 90 feet. For the mud weight range generated with the LWSA (8.3-8.7 ppg), 75 feet of head translates to 32-41 psi. The pressure measured on the hydrocyclone was approximately 18 psi after the equipment was cleaned, corresponding to about 40 feet of head.

Because the formation being drilled had a tendency to disperse into the mud, the solids control equipment alone could not completely control the drilling fluid properties. So dilution of the mud with water and dumping of mud that was heavily contaminated with drill solids was a common practice on this rig. This "dump and dilute" procedure caused difficulty in keeping track of all additions and subtractions to and from the mud, causing more LWSA to be used per barrel than might otherwise have been required.

Economics

Three main factors, other than product cost, will ultimately determine whether or not the use of LWSA is feasible: 1) whether or not the Rate of Penetration (ROP) can be increased as a result of drilling with the lower density mud, 2) the ability to recycle whole mud containing LWSA, and 3) the ability to recover the LWSA and re-use it on additional wells.

Two other factors can make the use of LWSA worthwhile: 1) the mitigation of lost circulation and 2) a decrease in formation damage due to drilling underbalanced. These tests did not provide any real opportunity to investigate these factors.

Rate Of Penetration

When the subject wells for the field tests were first located, the operator stated that a faster rate of penetration (ROP) would be an important indicator of the applicability of lighter fluids on

these particular wells. However, after we arrived on site and discussed the aims of the test, the general consensus of those involved was that these wells would not provide the best test of increasing ROP.

The wells in question are very shallow wells that can typically be drilled in less than two days, with the ROP ranging from 50-100 feet/hour. One driller on the rig stated he could get any ROP we wanted and that his biggest constraints were the ability to handle the cuttings generated and connection time.

The ROP on Well 2 (where the LWSA concentration was twice that of the first well) was somewhat faster than on Well 1, but given the disparity in ROP from well to well historically, this could have been a coincidence. In deeper wells, with harder rock, the mud weight reduction produced by the LWSA should significantly increase drilling rates (i.e. 5 to 20 percent) if a true underbalance can be maintained.

Recycling of LWSA Mud. Even though economic success on the initial field tests was not of paramount importance, the best chance of making the initial tests economical would be to recycle the fluid on multiple wells.

Saving mud is a normal practice for oil-based drilling fluids due to their value. The same practice will be appropriate for the LWSA mud. Methods to separate the mud to capture the glass bubbles without the liquid phase of the mud can be devised. However, the cost savings would be trucking costs and storage tank volume. The cost of a complex separation apparatus may not be justified. For this case, where only two wells were to be drilled, the cost of a separation unit could not compete with the cost of simply storing the small volume of mud between wells.

The drilling mud used on Well 1 was stored off-site in an open-top, 500 barrel "Baker Tank" in the desert sun for two days. Only about 90-100 barrels of the final mud from Well 1 were salvaged, the rest being either left in the hole or lost to the sump when the casing was cemented in the well. In a deeper well, where a large volume of mud would be involved, about the same amount would have been lost, but more mud would be salvaged.

The final mud that was transported to storage weighed 9.1 ppg, which was higher than initially planned. The mud was heavier than desired because LWSA additions were stopped at approximately 1,400 feet due to the potential for a gas kick.

After a trip to lay down the mud motor, excess gas was noted after circulating bottoms up. The mud engineer believed the gas had a hydrocarbon odor and was afraid that the mud weight was too low and was allowing hydrocarbons to enter the wellbore downhole. The mud weight at that point was about 8.6 ppg, whereas normal mud weight for this lease at that depth is about 9.0-9.2 ppg.

Consequently, approximately 580 feet of hole were drilled with no additions of LWSA (i.e. about 33% of the total drilled). During this time, the mud weight was allowed to drift up as in a normal well. Total depth was reached at 1,780 feet with a mud weight of 9.1 ppg, and the mud was stored for re-use.

Further contamination from the Baker tank and the transport

trucks increased the mud weight to 9.2 ppg by the time the fluid reached the steel pits for the second well. This fluid contained an estimated 7.8% by volume LWSA, down from about 13% when additions of LWSA were halted at 1,400 ft.

The second well encountered a lost circulation zone at about 154 feet, even though our available information indicated no lost circulation was expected for any of the prospective test wells. The total volume of loss was unknown. Lost mud was replaced "on the fly" while drilling continued and while additions were being made to account for increasing hole depth. Estimated volume lost was about 30-40 barrels, further decreasing the already minimal savings potential of recycling the mud. The lost circulation was cured with the addition of conventional lost circulation material.

Recovery and Re-use of LWSA. Because of the condition of the solids control equipment, the limited space available on each location for necessary equipment, and because we elected to attempt whole mud recycling, no attempt was made during these tests to recover dry LWSA for re-addition to a future mud system.

General Observations

On Well 1 the bottom hole assembly was tripped out and run back to bottom with no reaming required. Typically, these holes must be reamed to bottom after tripping at total depth. This indicates decreased frictional drag in the hole due to the presence of the LWSA. This was expected because solid plastic and glass spheres are often used as mud additives to reduce friction in high angle and horizontal wells. This is also consistent with laboratory tests that showed the LWSA reduces casing wear 60-70 percent.

On Well 2, more reaming was required after trips, and more wall cake was circulated up than normal for the area, indicating that the wellbores in this field may require a higher mud weight to prevent shale sloughing. The LWSA test mud was the lowest weight mud ever run in this field to total depth.

The loss of large mud volumes on these wells during trips, due to the inexpensive rig operations typically performed, required much new mud to be built, decreasing the effectiveness of our test.

The mud remaining quiescent in the sand traps during trips built a thin layer of "cream" on top as the LWSA floated out of solution. The gel strength of this cream was very fragile and easily broken. Mud in the pit was kept moving utilizing jets to prevent LWSA floatation in the general mud system.

Analysis of the measurements made on the drilling fluid during the tests shows that the theoretical mud weight closely matched the measured mud weight. Accounting for all additions and subtractions to the mud system helped determine a theoretical mud weight at several points during the tests. These compared very favorably with measured data.

The LWSA performed better than expected. This was confirmed independently by two of the companies involved. Both companies performed calculations on the raw data collected during the test and arrived at this same conclusion.

Conclusions:

The field tests were very successful, demonstrating the following positive factors:

1. The LWSA can be easily and safely mixed into drilling fluid during field operations.
2. New mud containing LWSA can be built in the field.
3. The LWSA is compatible with conventional field drilling fluids.
4. The LWSA can be circulated through a conventional roller cone, insert bit with little or no destruction of the LWSA.
5. The LWSA can be circulated through a conventional downhole mud motor with little or no detrimental effect to the LWSA or the motor.
6. The overall survival rate of the LWSA was within an expected and acceptable range.
7. The environmental effect of using the LWSA was minimal.
8. The LWSA had no apparent detrimental effect on any of the conventional drilling rig equipment.
9. The drilling fluid system was very small (< 200 barrel active volume), allowing accurate monitoring and measurement of additions and deletions.
10. LWSA muds appear to be an economic alternative to aerated drilling fluid and should find increased use in the future.

Acknowledgements

We would like to thank Mike Davis, Chuck Duginski, and Don Ritter of Mobil Oil Company for providing the test wells; Roy Long and Al Yost of the Department of Energy for sponsoring the project; Tom Needham and Jim Clifford of Geo Drilling Fluids of Bakersfield, California for providing storage, transportation and sound mud engineering advice during the field tests; and Duane Jabbas of 3M for invaluable advice and help with adding HGS to the mud.

References

- Medley, George H. et al., 1995: Development and Testing of Underbalanced Drilling Products, Topical Report No. DOE/MC/31197-5129, published by the U. S. Department of Energy, September.
 Duda, John R. and Yost, A. B., 1995: "DOE/Fossil Energy's Drilling, Completion, and Stimulation RD&D: A Technologies/Products Overview," SPE 30993 presented at the SPE Eastern Regional Conference and Exhibition in Morgantown, WV, September 18-20.

TABLE 1 - Pilot Test Rheology

Sample Description	Initial Sample, No LWSA Added	Final Sample, 15 ppb (10% by Volume) LWSA
Mud Weight, ppg	8.9	8.25
Plastic Viscosity, cp.	17	24
Yield Point, lbs/100 SF	6	6
Apparent Viscosity, cp.	20	27
Gel Strength, 10 sec/10 min	3 / 4	4 / 4
API FL, cc/30 minutes	6.5	6.7

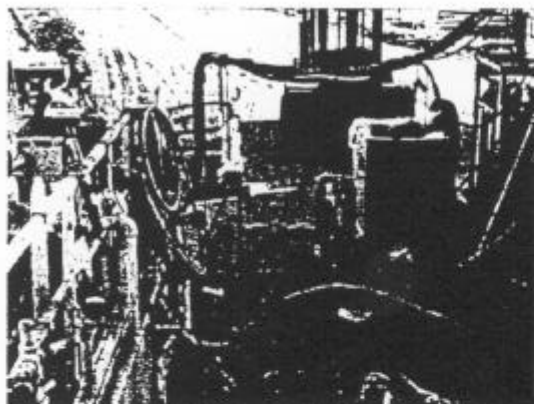


Fig. 1 - LWSA Mud Mixing System

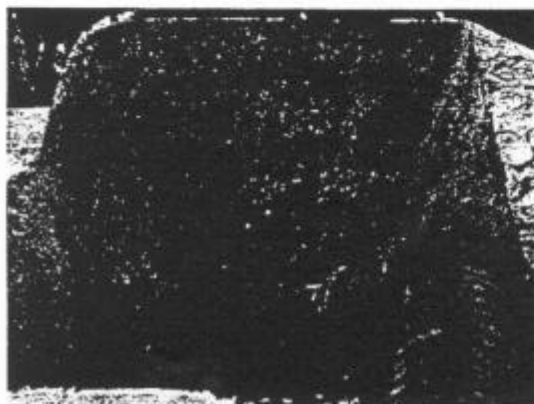


Fig. 2 - LWSA Injection Into Conventional Mud Mixing-Hopper

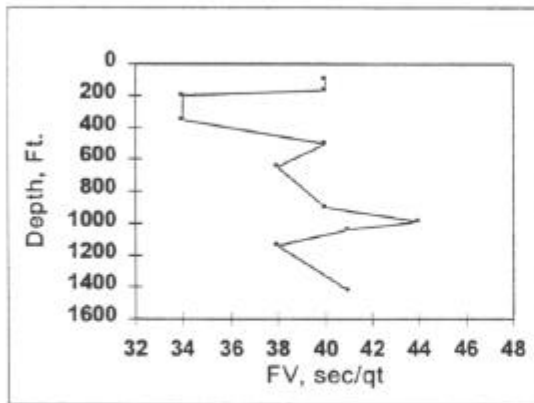


Fig. 3. Funnel Viscosity vs. Depth (Well 1)

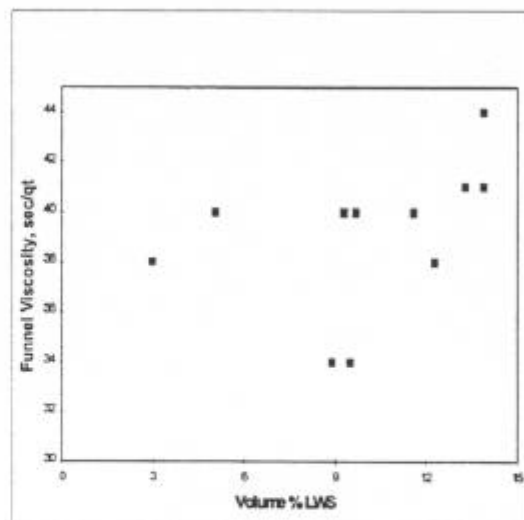


Fig. 4. - Funnel Viscosity vs. LWSA Concentration (Well 1)

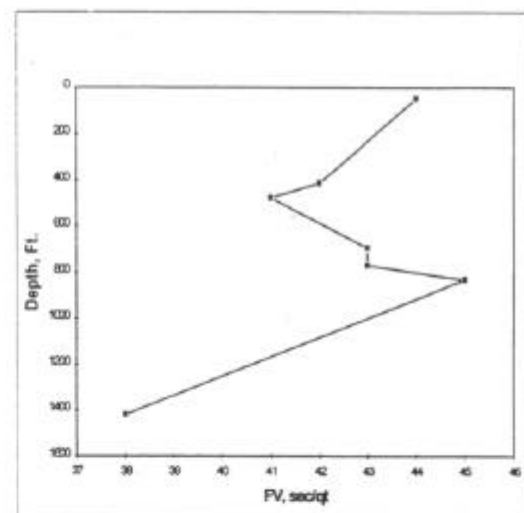


Fig. 5 - Funnel Viscosity vs. Depth (Well 2)

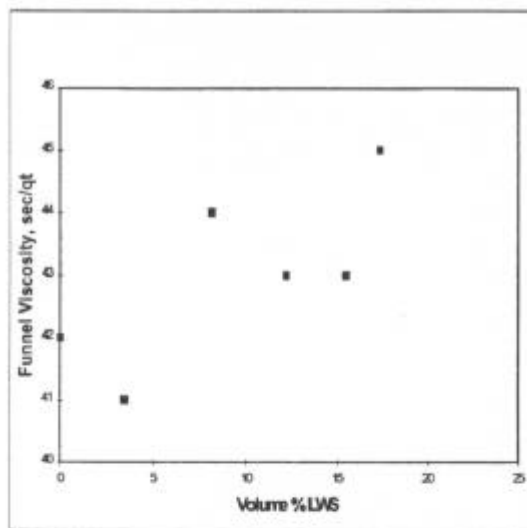


Fig. 6 - Funnel Viscosity vs. LWSA Concentration (Well 2)

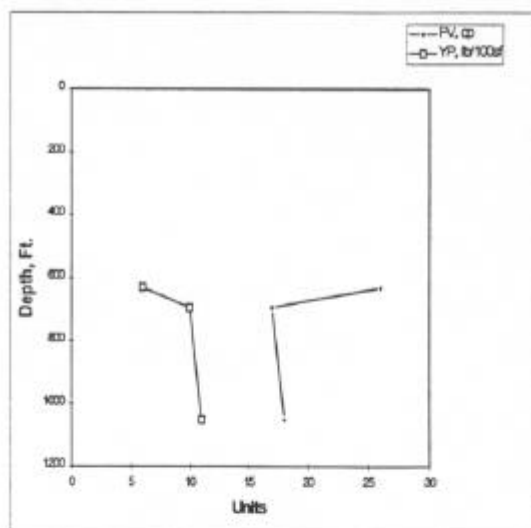


Fig. 8 - PV and YP Variation with Depth (Well 2)

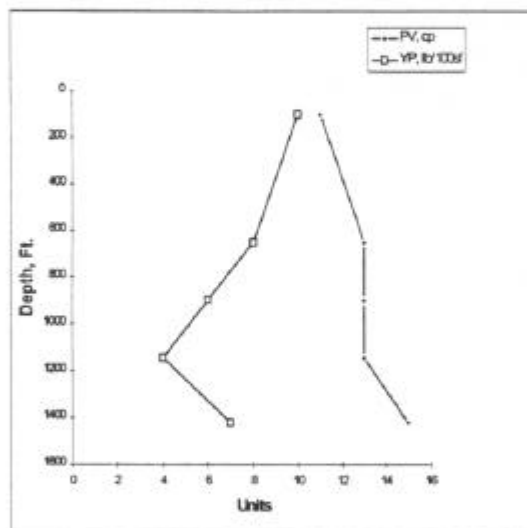


Fig. 7 - PV and YP Variation with Depth (Well 1)

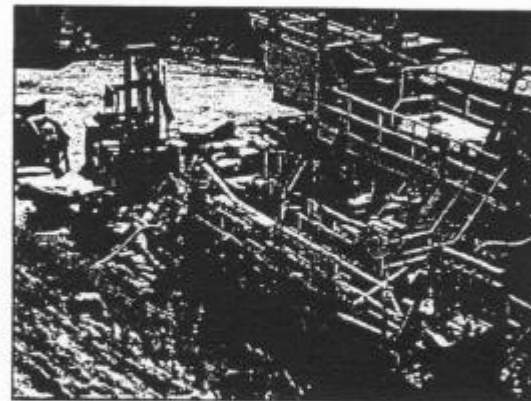


Fig. 9 - Golden State Drilling Co. Rig Mud Pit System

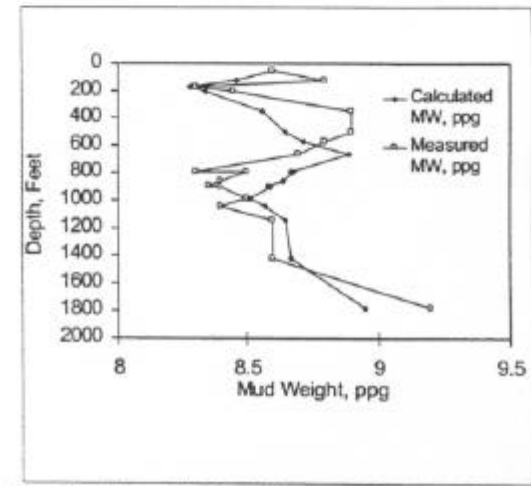


Fig. 10 - Theoretical and Measured Mud Weight (Well 1)

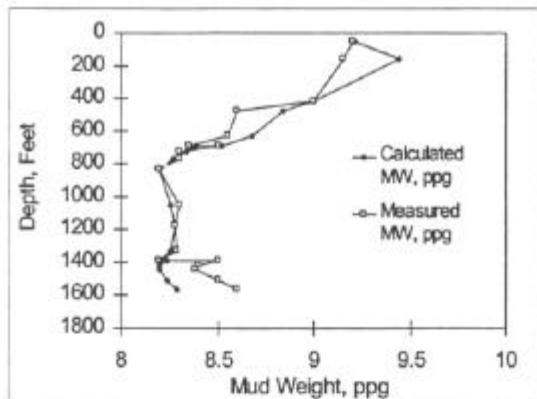


Fig. 11 - Theoretical and Measured Mud Weight (Well 2)

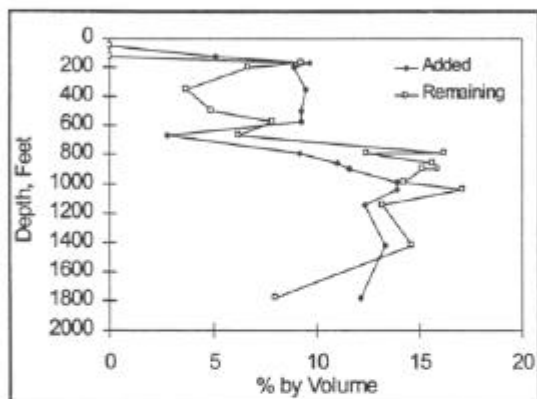


Fig. 12 - Theoretical vs. Actual Volume Percent LWSA (Well 1)

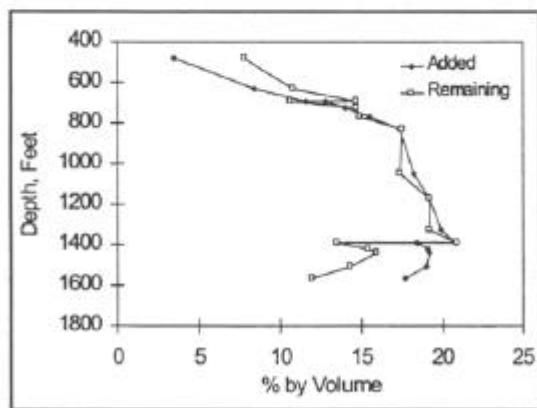


Fig. 13 - Theoretical vs. Actual Volume Percent LWSA (Well 2)

Appendix F

SPE 62899: "Field Application of Glass Bubbles as a Density-Reducing Agent"

**2000 SPE Annual Technical
Conference & Exhibition
October 2000**



SPE 62899

Field Application of Glass Bubbles as a Density-Reducing Agent

Manuel J. Arco, SPE, 3M, José G. Blanco, PDVSA-Intevep, Rosa L. Marquez, PDVSA-Intevep, Sandra M. Garavito, PDVSA, José G. Tovar, PDVSA, Antonio F. Farias, PDVSA E&P, and Jesus A. Capo, PDVSA E&P

Copyright 2000, Society of Petroleum Engineers Inc.

This paper was prepared for presentation at the 2000 SPE Annual Technical Conference and Exhibition held in Dallas, Texas, 1-4 October 2000.

This paper was selected for presentation by an SPE Program Committee following review of information contained in an abstract submitted by the author(s). Contents of the paper, as presented, have not been reviewed by the Society of Petroleum Engineers and are subject to correction by the author(s). The material, as presented, does not necessarily reflect any position of the Society of Petroleum Engineers, its officers, or members. Papers presented at SPE meetings are subject to publication review by Editorial Committees of the Society of Petroleum Engineers. Electronic reproduction, distribution, or storage of any part of this paper for commercial purposes without the written consent of the Society of Petroleum Engineers is prohibited. Permission to reproduce in print is restricted to an abstract of not more than 300 words; illustrations may not be copied. The abstract must contain conspicuous acknowledgment of where and by whom the paper was presented. Write Librarian, SPE, P.O. Box 833836, Richardson, TX 75083-3836, U.S.A., fax 01-972-952-9435.

Abstract

This communication describes preliminary results and observations of a successful application in a field environment that incorporated hollow glass spheres, also known as glass bubbles, as a density reducing agent in a drilling fluid. In this field application, a proprietary oil-in-water emulsion fluid developed by PDVSA-INTEVEP which contained hollow glass bubbles (3M) was used during the drilling of a producing interval. The oil-in-water emulsion provided a suitable fluid base, whereas the glass bubbles, by virtue of their low density, imparted a lower finished density than that of the corresponding base fluid. The density lowering capacity of the glass bubbles is proportional to the concentration of bubbles incorporated in the fluid.

The field trial substantiated that the fluid-glass bubble pair is stable, homogenous, and compatible through conventional mud motors, bits, surface cleaning equipment, and of such rheological and filtrate properties, as to lend itself to be used in low pressure reservoirs and in producing zones of high permeability.

During this field application, we were able to lower and maintain the density of the base fluid at 7.1 PPG. Additional oil production increase was observed relative to a vicinal well (vs. GF-134D) drilled with oil based fluids at an excessive overbalanced. This observation may suggest that damage to the producing zone has been avoided.

This technology is an alternative to the use of aerated fluids, with potential economic and technical advantages due to the elimination of surface compressing and air injection controller equipment, and to the simplification of operations required to avoid excessive overbalance during pipe trips.

Other potential benefits of using this low density fluid includes torque reduction as a result of higher lubricity, reduction in casing wear, higher penetration rates, decreased formation damage, lost control mitigation, and the use of mud pulse MWD tools. Glass bubbles are also a viable alternative to reduce the density of water based drilling fluids, oil and polymer-based fluids, and brines.

Laboratory tests were also carried out with conventional fluid systems to include water-based, 100% mineral oil and oil-in-water emulsions, with different concentrations of LITEDEN™ in order to evaluate the potential field use of such formulations as substitutes for aerated fluids in wells which might require lower density fluids. Several formulations for the systems mentioned above were developed with the purpose of achieving maximum density reduction without affecting filtrate control or rheological properties. Fluid densities as low as 5.5 and 6.0 ppg were obtained for corresponding 100% oil and O/W emulsions based fluids.

Introduction

In the last few years there has been an increasing necessity to drill deposits which have entered a partially depleted stage because of extended years of production. Excessive levels of overbalance pressure can increase fluid invasion. Differential sticking is a costly common problem associated with fluid invasion. In principle, loss of fluid allows the deposition of drilling fluid solids as a filter cake on the well bore. With further filter cake growth, the drill string and drill collars continued to be pulled against the side of the well bore. With time, mud filtrate flows further, building and accumulating solids around the tubulars, and preventing the pipe from moving.

The drilling of the above mentioned depleted deposits requires the use of lower density fluids with specific gravity less than 1 (8.33 ppg), such as mist, foam, and aerated or nitrified muds (Figure 1B). These fluids, in principle, would permit maximum extraction while minimizing damage to the producing formation from filtrate or solid invasion. However, there are limitations in the available fluids aimed to operate in a depleted reservoir.

Besides being driven by increased drilling, underbalanced drilling methodology has been put forth by the prospect of minimizing damage to underpressured hydrocarbon pools or

formations prone to loss circulation, and reservoirs that suffer irreversible damage due to rock-fluid or fluid-fluid compatibility problems.

Most underbalanced drilling operations in low pressure or depleted reservoirs are conducted, for the most part, using air, mist, or foam. And, although large projections for a steady future growth rate for controlled density drilling exist, operators may be reluctant to drill underbalanced with aerated fluids because of the difficulties normally associated with managing multi-phase, compressible fluids. Also, it is necessary to take into account other operation and logistic aspects when working with aerated and/or compressible fluids as they introduce increased operational complexity.

One important aspect of UBD is the availability of physical space for the location of the equipment in offshore environments. Another aspect is the cost associated with the rental of compressors to produce the *in situ* air or nitrogen. This rental cost can considerably increase the daily drilling cost in comparison with the use of other fluids.

Additionally, the use of a compressible fluid might be limited by the presence of dissolved oxygen, which in the presence of crude oil, and at formation pressure and temperature conditions, could produce fire or explosion. From a safety standpoint, the use of aerated fluids requires greater planning and security measures, as rig personnel may be unfamiliar with underbalanced drilling procedures.

The unsatisfactory separation of the gaseous phase from the liquid phase could cause surface mud losses. Also, if air is used in the aeration of the fluid, corrosion of the perforation circuit metallic components may present another limitation.

An alternative way to produce low density drilling fluids so as to obtain similar advantages as when using aerated compressible fluids consists of incorporating hollow glass bubbles into conventional drilling fluids (Figure 1A). In principle, this innovative additive can be added to virtually any type of existing mud system in order to reduce its weight. In other words, the low density drilling fluid is more or less independent of the nature of the liquid phase, and technically, could be made up of fresh water, brine, diesel or other.

Besides increased ROP and avoidance of drilling problems related to overbalanced drilling, low density drilling fluids (LDDF) containing glass bubbles may help reduce possible formation damages caused by the invasion of solids or of the filtrate, and improve the longevity of the drill bit. Elsewhere, LDDF based on glass bubbles, in combination with loss control materials, (LCM), have been used to eliminate drilling fluid losses through fractured reservoirs and lost circulation zones.

Glass bubbles based drilling fluids will allow underbalanced or near balanced drilling in low-pressure formations without the use of air or other gases. Another extremely attractive feature of these glass bubbles based fluids is the practicality of using existing standard mud handling equipment.

Glass Bubbles as a Density-Reducing Agent

Hollow, unicellular, soda-lime borosilicate glass bubbles are fairly unique materials. They are engineered fillers used in many industries like aerospace composites, automotive plastics and syntactic foam buoyancy modules when there is a need for weight reduction. Most of their applications are related to their capacity for weight reduction. They are chemically inert, other than in the presence of HF, have high water resistance, and high temperature and pressure resistance. With shell thickness between 0.5 to 2 microns, several glass bubble grades can tolerate high collapse pressures, some as high as 10,000 psi, making them usable in relatively deep wells, even beyond 10,000 ft depth.

Their particle size distribution range from 8 to 125 microns; however approximately 90% of bubbles fall in a range between 8 and 85 microns. For suitable drilling fluid grade glass bubbles, a typical particle size distribution (PSD) is:

D_{10} 15 microns
 D_{50} 40 microns
 D_{90} 75 microns
 D_{100} 85 microns

Field Handling Glass Bubbles. Understanding handling principles for materials that are less than 100 microns and with low bulk density is important in implementing successful field usage. Glass bubbles are slightly more challenging than free flowing coarse granules or pellets. Improperly handled, their size, shape, density, and PSD can become a nuisance dusty environment, especially indoors at a fluid plant.

Glass bubbles material properties dictate handling. At a rig site, they can be unloaded from their boxes either manually, by gravity feeding into a compounding hopper, or mechanically, by using a pneumatic conveying system. Personnel should wear safety goggles before unloading by either method.

Ideally, a vacuum conveying system that utilizes either a transfer pump or the ubiquitous venturi funnel found at most rig sites are convenient ways to unload glass bubbles from their boxes. A preferred transfer pump type is a double diaphragm, or butterfly pump. Both of these systems incorporate the use of an attached wand at the pick up point.

The concept of using the venturi system at rig site to unload glass bubble boxes has been successfully field-tested. An adapter (Figure 3A) was fabricated utilizing a steel plate with an 80 mm ball valve mounted to an 80 mm pipe which was raised 30 cm away from the venturi to avoid splashing.

To this extension pipe, a non-transparent hose with a wand at its end was attached (Figure 3B.) By a wand, we mean an 80-mm stainless steel or plastic pipe with a concentric 5-mm tube vented to the atmosphere at the top of the wand through the side of the 80-mm pipe. This vacuum wand works very well in supplying fluidized glass bubbles to the venturi. This set-up has been successfully used to empty a 680 pounds box in 12 minutes.

Field Results from Directional Well GF-136D

In drilling an area with sub-normal pressures like the reservoirs in the Guafita field, it is convenient to use a drilling system with specific characteristics like low density, good rheological properties, good cutting transport and suspension capabilities, and with a plugging agent which will prevent migrationn of fluids toward the formation. The drilling fluid system INTEFLOW®-2000 takes into account all the above considerations.

INTEFLOW® is a drilling, completion and workover fluid, designed and developed by PDVSA-INTEVEP for specific use in low pressure zones like previously described. This fluid has been used with optimal results in the completion and rehabilitation work of more than 100 wells by PDVSA-South/East/West, and in the drilling of more than 20 horizontal wells.

This work addresses the addition of LITEDEN™, a density reducing glass bubbles agent, to INTEFLOW®-2000 drilling fluid, for the purpose of generating the same advantages that are reached when using aerated fluid with densities between 5.7 and 7.0 ppg.

The application of LITEDEN™ in well GF-136D in Guafita evolved because of the necessity to minimize the problems of differential sticking which is a very frequent occurrence in the area, and which has been observed when using commercial fluid systems which cause invasion of liquid and non-desirable solids as a result of using muds with densities above 8.33 ppg.

Background on the application of LITEDEN™. Previously, during drilling of well GF-135H in Guafita, the reducing density agent LITEDEN™ was used, with good results, during the pumping of a pill for the purpose of reducing the hydrostatic column on the formation. The density of INTEFLOW®-2000 system was lowered from 7.3 to 6.2 ppg. In Figure 2 we show the density vs. pore pressure reached by adding LITEDEN™ to INTEFLOW®-2000.

Objective of drilling GF-136D. The purpose of the drilling was to drain the hydrocarbon accumulation of G8 and G9 in the Guafita formation. In this section, we briefly describe the technical drilling proposal, using data provided by the Barinas district drilling department, and previous experiences with GF-135H, GF-132H and GF-134D wells.

Initial Data of the Guafita Crudes. For the processing of the technical proposal, the data evaluated by PDVSA for crude physical and chemical properties (Table 1), and analysis SARA (Table 2) was used. In Table 3, we present the general characteristics of sands G-7, G-8, G-9, and G-10, along with mineralogical characterization and theoretical permeability values for GF-134D.

Geological Information. The Guafita field is located 43 Km. southwest of Guasdualito, in El Amparo municipality, Paez district, Apure State. The field is separated from Colombian hydrocarbon fields Cano Limon, La Yuca and Mata Negra, by the Rio Arauca.

Geologically, the field is located to the extreme north of the Meta river basin, which itself, is part of a series of sub-Andean pericratonic sedimentary basins, adjacent to the Andes mountain range.

The Guafita structure is an anticline of slight slope, whose axis has an approximate North 45° East direction. This axis is cut by a zone of faults that crosses the field and divides it in two blocks which have been denominated Guafita Norte and Guafita Sur.

The Norte denominated block has a $\pm 1^\circ$ gradient to the northwest and it is cut by a normal fault of smaller magnitude, with an east-west course, which further divides Norte block in two segments, giving rise to two reservoirs defined by different oil-water contacts and estimated at different depths. This location principal objectives is the Tertiary Age accumulated deposit,G8 (0001), of the Guafita Formation, which is located towards the southwestern flank of the South segment, limited to the south and to the north by the Guafita-Cano Limon faults, and the inferred one, which repectively separates it from the G9 (0002) deposit.

The recipient rock is a sandy package identified as G-8 and G-9 with an average porosity of 25.8 %, a hydrocarbon saturation of 78 % and an average permeability of 5000 millidarcies. In Table 3, we present the general characteristics of sands G-7, G-8, G-9, and G-10, along with mineralogical characterization and theoretical permeability values for GF-134. These sands (G-8) are further characterized with particle size distribution analysis as shown in Figure 4. In Table 4 we also present the mineralogical characterization of GF-134D rock.

In Table 5 we show the grain size statistical data for the G-8 sand. In Figure 6, we show a typical pore throat diameter distribution for well GF-134D sand core, G-8, at 7319-7414' depth. The pore throat morphology from this sand typically has a very disperse distribution, with pore throat values ranging between 10 and 90 μm . Typical D_{50} pore throat value is 35 μm . In Table 6 and Table 7, we introduce core petrophysical data corresponding to the reservoir G-8 and G-9 sands for wells GF-134D and GF-26.

The analysis of the pore throat size distribution, which served as the basis for the selection of plugging material, was made by characterizing wall samples from neighboring GF-26 and GF-134D wells. Figure 5 and Figure 6 present respective pore throat size distribution for G-8 sand.

Drilling Fluid Technical Proposal

A technical proposal was made to use the INTEFLOW®2000 fluid system. This fluid is designed for usage as a drilling/completion/workover fluid in low-pressure zones without causing damage to the producing formation while enhancing production.

INTEFLOW®2000 behaves as a pseudoplastic, exhibitiing lower viscosities at high shear rates while maintainig adequate suspension properties to carry cuttings out of the wellbore. The fluid shows good filtration control values and lubricity. LITEDEN™ is added to INTEFLOW®2000 to reduce the

density of the system and to help avoid possible differential sticking problems.

During the trial, we had access to equipment for measuring the population of drop sizes in the drilling emulsion (Figure 8). These measurements are important as fluid rheological properties and fluid stability can be directly related. The recommended liquid particle distribution should have 90% of the drops below a diameter of 10μ . This technique is very fast and also allows one to track the amount of undesirable solids in the system.

To insure control of undesirable solids, it is necessary that the solids control equipment operate continuously with a minimum efficiency of 85%, including the high and low RPM centrifuges, which would be operated intermittently as needed, to optimize fluid cleaning. During the drilling operations of this trial, contract personnel were in charge of insuring the efficient operation of solids control equipment. The specific details of recommended solids control equipment can be found in Table 12.

For the purpose of avoiding increases in the rheology, fluid dilution was planned to be made solely with fresh mud in the necessary proportion to maintain the CIC value below an equivalent of 5 lpb.

INTEFLOW®/LITEDEN™ Composition.

INTEFLOW®: It is a mixture of biodegradable liquid surfactants. It is used in conjunction with diesel, or another oil, and water to form an emulsion.

VISCOSIFIER: It is used to maintain the emulsion rheological properties. It must be stable to high temperatures. Commonly, either xanthan gum rubber or a polymer of low to medium molecular weight is used.

FILTRATE CONTROLLER: It is used to control filtrate; a starch stable to high temperatures is generally used.

BIOCIDE: It is used to prevent the growth of bacteria in the fluid that may reduce the concentration of surfactant and polymer, and affect the stability of the fluid.

MONOETHANOLAMINE (MEA): A solution used to maintain the alkalinity of the system.

POTASSIUM CHLORIDE (KCl): This salt provides a source of potassium ions to inhibit the swelling of clays and their dispersions.

LITEDEN™: Hollow glass bubbles and a density reducing agent. It can lower fluid density by as much as 1-2 ppg, and may prevent fluid invasion in permeable zones. It may also reduce or mitigate pipe sticking due to differential pressure. Figure 7A shows a particle size distribution for LITEDEN™ 4000 and Figure 7B illustrates LITEDEN™ 4000 collapse profile (reduction in volume) as a function of applied pressure. Table 8 highlights typical parameters for LITEDEN™ 4000.

System formulation and rheological properties. On the basis of the results obtained during the evaluation of the different Guafita sands, and taking into account the capability of the density reduction additive, we proposed a fluid of density of 7.0-7.1 ppg. Table 10 shows the list of ingredients

that make up the formulation of the system INTEFLOW®, and Table 11 outlines the formulation properties. To achieve a density of 7.1 ppg with an INTEFLOW®/LITEDEN™ emulsion, (O/W = 66/34), it is necessary to have a concentration of LITEDEN™ approximateley equal to 7-8 lpb.

General recommendations for solids control equipment.

The plan was to operate the solids control equipment at an efficiency of 85 %. In Table 12, we list the recommended equipment for solids control during drilling.

Volumetric Circuit. Table 9 shows estimated INTEFLOW®-LITEDEN™ fluid volumes needed for drilling the GF-136D producing interval (7" casing+ $6^{1/8}$ " hole.)

Summary of Drilling Operations During LITEDEN™ Usage.

We outline a timetable of activities carried out during the drilling of GF-136D with the INTEFLOW®2000-LITEDEN™ system:

1. After seating the 7 " liner, we addressed the $6^{1/8}$ production interval section beginning by washing and removal of residual cement. For this purpose, we utilized INTEFLOW®/LITEDEN™ at an initial density of 7.1 ppg to perforate through the shoe.
2. We pumped 20 barrels of a high rheology pill to insure effective cleaning of the 7 " liner.
3. Table 13 shows the initial properties of a sample of the fluid taken from rig CPV-8 active tank.
4. Table 14 shows the fluid system properties throughout the extent of the payzone drilling, and in Figure 8, we show the low-density fluid overall particle size distribution. This data gives valuable information to the mud engineer in terms of fluid quality control during drilling.

In Figure 9, a summary of the behavior of drilling in the producing hole interval is shown, where it is possible to observe the pore pressure and the density of the fluid as a function of the depth of the producing interval.

After drilling an estimated 210 feet, we circulated and conditioned the fluid at a density of 7.3 ppg. At this point we observed an inflow of crude oil. The well was observed statically for 15 minutes. We began circulation again and we had additional inflow of crude. Because of crude inflow, and to stabilize the hole, the decision was made to increase the density of the fluid to 7.5 ppg. Afterwards, drilling and section extension continued without interruption.

Once the drilling of the pay zone was finished, we proceeded to take density, gamma ray, and caliper logs in the interval between 7227 to 7569 feet, and also to run RFT to determine reservoir and formation pressures. Logs were of good quality. Caliper log showed an in-gauge hole indicating that the fluid did not cause any alterations of the drilled hole.

Conclusions

- We validated that a fluid prepared with the density reducing agent, LITEDEN™, was stable, homogenous and had useful rheological and filtrate properties when

- used in high permeability, low pressure producing zones.
- We were able to lower the density of an emulsion drilling fluid to 7.1 ppg by adding LITEDEN™ to the base fluid.
- Field mixing of INTEFLOW®/LITEDEN™ was easily accomplished. Fluid behave similarly to conventional fluids.
- Conventional solids control equipment can be utilized on this type of fluid. Fluid was compatible with field operating conditions.
- During drilling of GF-136D, we did not experience any differential sticking, a situation that has been typical of previous wells in the Guafita area.
- After drilling, a hole in-gauge was observed, suggesting that the fluid, altogether with the hydraulics, fulfilled the well drilling plan.
- Improved productivity, above comparable vicinal wells drilled with oil-based fluids at excessive overbalance, was observed.

Acknowledgements

The authors would like to thank several organizations for permission to publish this paper. These include PDVSA-Intevep, PDVSA, PDVSA Exploration and Production, and 3M.

References

- Medley, George H. et. al., 1995: Development and Testing of Underbalanced Drilling Products, Topical Report No. DOE/MC/31197-5129, published by the U. S. Department of Energy, September.
- Medley, George H. et. al.; "Field Application of LightWeight Hollow Glass Spheres Drilling Fluids," paper SPE 38637 presented at SPE 72nd Annual Technical Conference and Exhibition, San Antonio, Texas. 5-8 de Octubre, 1997.
- Medley, George H. et. al.; "Use of Hollow Glass Spheres for Underbalanced Drilling Fluids," paper SPE 30500 presented at SPE Annual Technical Conference and Exhibition, Dallas, Texas. 22-25 October, 1995.
- Blanco, J.; Quintero, L. "An oil-in-water well servicing fluid used in oil well drilling comprises a mineral oil or biodegradable oil emulsion stabilised with a mixture of e.g an anionic alkali metal sulphonate and a non-ionic ethoxylated alkyl phenol surfactant," Patent No. US 5921933. 1998.
- Quintero, L.; Blanco, J.; Guimerans, R.; Rojas, E.;: "Formulation, Stability, and Formation Damage of Gasoil in water Emulsions. Used as Drilling and Completion Fluids." Paper SPE 37290 presented at the 1997 SPE International Symposium on Oilfield Chemistry Conference and Exhibition, Houston, Texas. 18-21 February, 1997.

Metric Conversion Factors

$$\text{cP} \times 1.0 \times 10^{-3} = \text{Pa}$$

$$\text{ft} \times 3.048 \times 10^{-1} = \text{m}$$

$$\text{ft}^2 \times 9.290 \times 10^{-4} = \text{m}^2$$

$$\text{ft}^3 \times 2.831 \times 10^{-2} = \text{m}^3$$

$$\text{md} \times 9.869 \times 10^{-23} = \mu\text{m}^2$$

$$\text{psi} \times 6.894 \times 10^{-5} = \text{kPa}$$

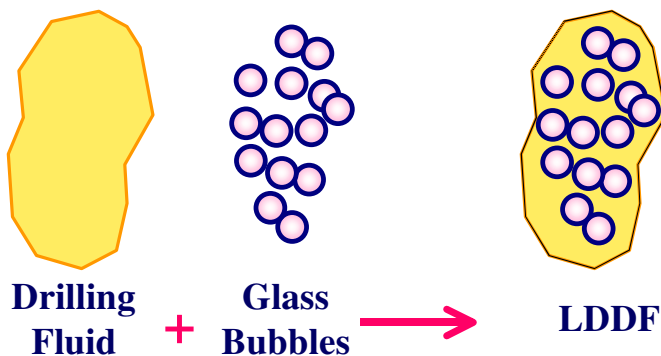


Figure 1A - Conceptual Low Density Drilling Fluid Using Glass

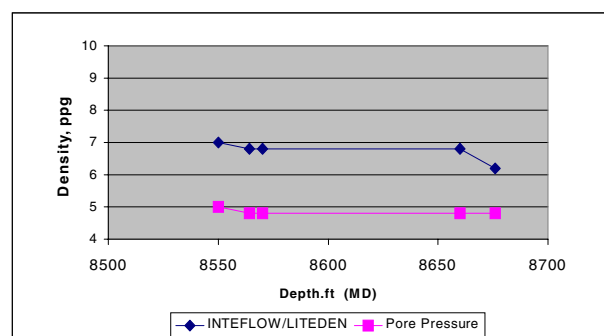


Figure 2 – Achieved Density During Drilling of Well GF-135H

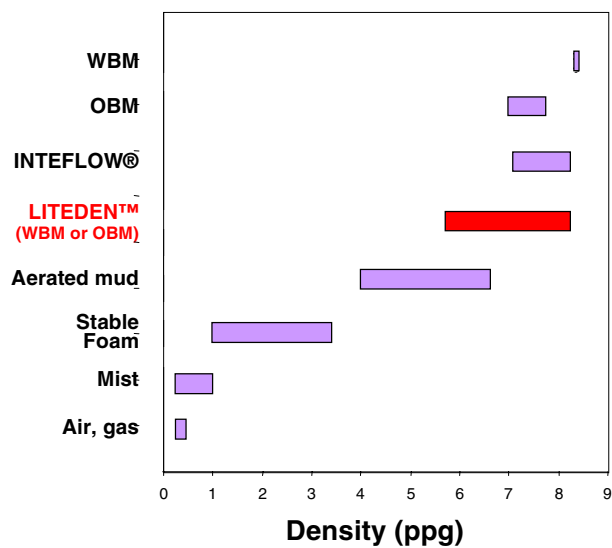


Figure 1B – Density of Some Drilling Fluids.

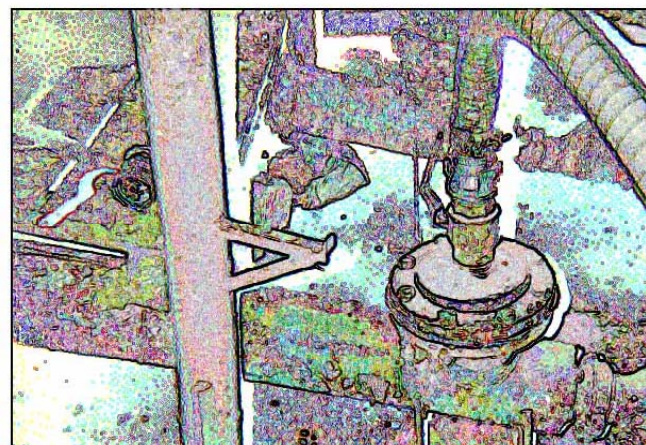


Figure 3A–Venturi funnel adapter

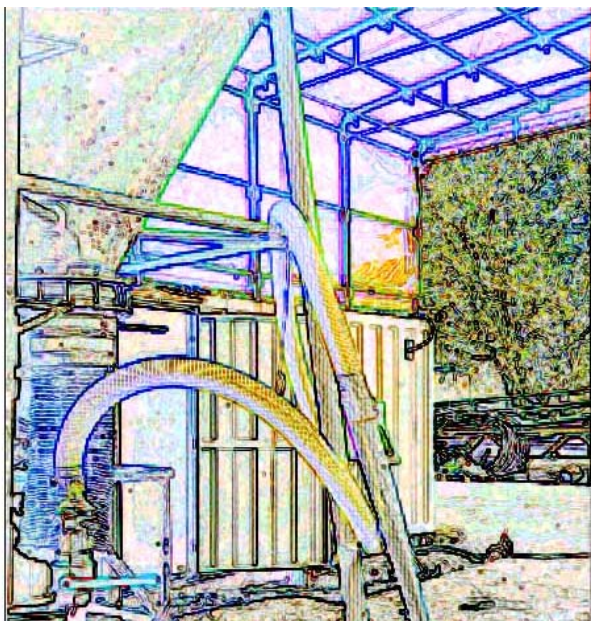


Figure 3B – Vacuum Wand and Flexible Hose Attachment

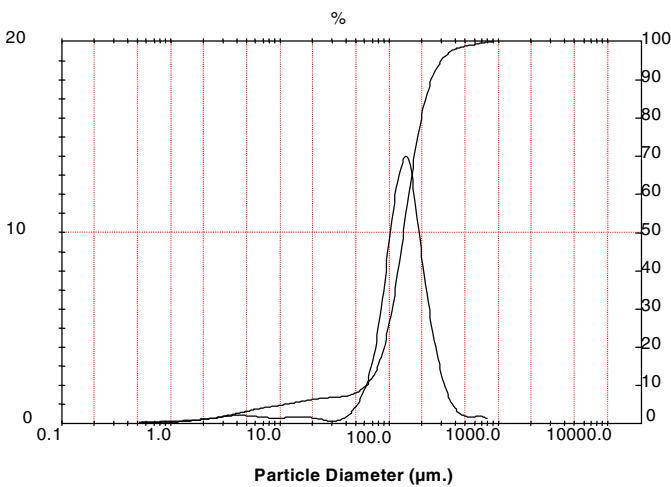


Figure 4 – Particle Size Distribution for G-8

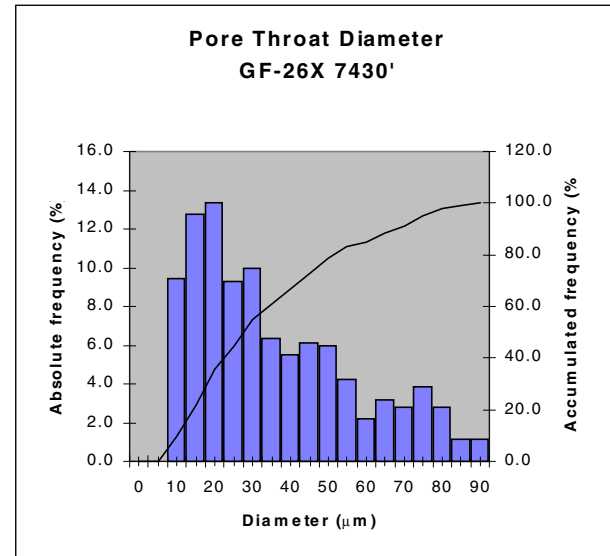


Figure 5 – Typical Micrograph G-9 Sand Sample at 7319-7414' Depth

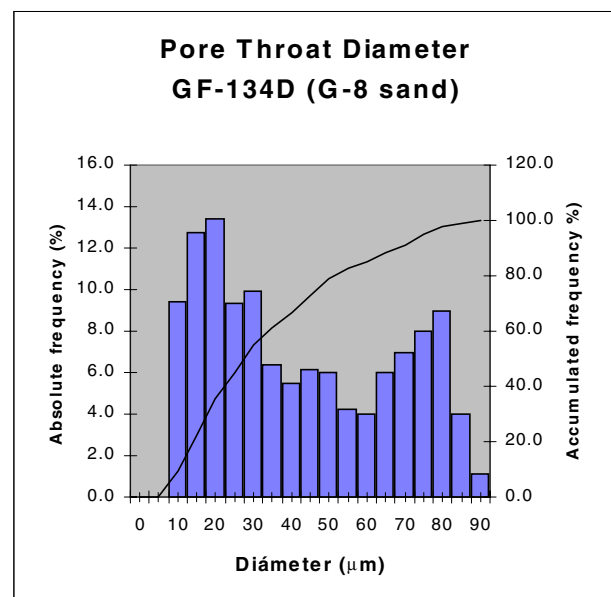


Figure 6 - Typical Micrograph G-8 Sand Sample at 7319-7414' Depth

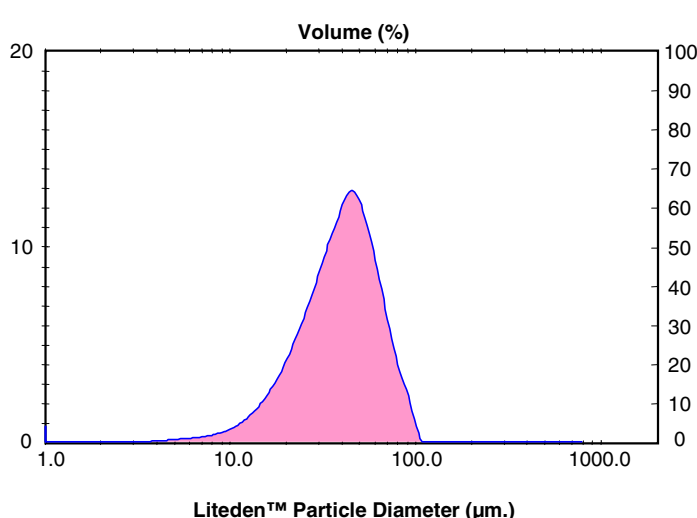


Figure 7A - Liteden™ Particle Size Distribution

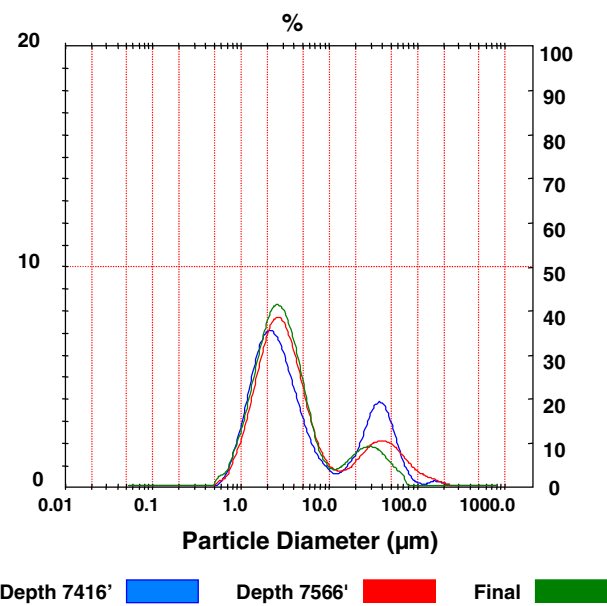


Figure 8– Stages of PSD for In-Use Fluid in Well GF-136D.

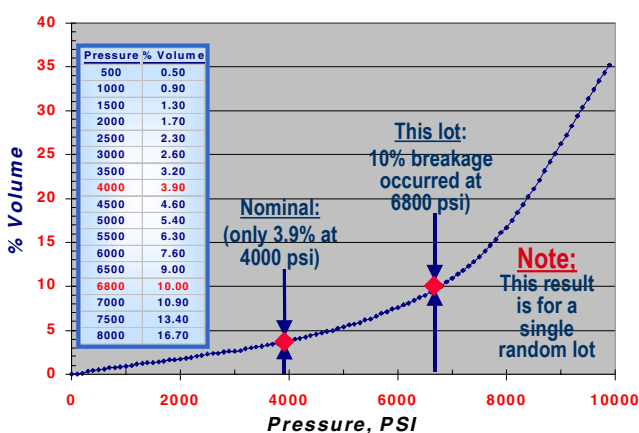
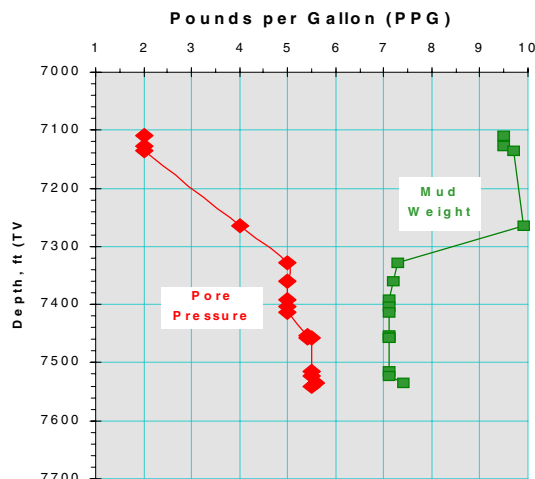
Figure 7B -Pressure Collapse Profile for Liteden $\rho = 0.38 \text{ g/cc}$ 

Figure 9 - Pore Pressure and Fluid Density vs. Producing Interval Depth.

**Table 1 - Physical/Chemical Characteristics
of Guafita Crude**

Guafita Crude	Properties
°API	29.6
Water. %	40
Acidity, meq KOH per g of crude	0.865
Viscosity at 100 °F. cp	52

Table 3 - Target sands characterization

Sample #	Depth, ft	Depth, TVD, ft	Press., psi	Formation
25	7796	7110	767	G - 7 / 2
24	7814	7127	773	G - 7 / 2
23	7824	7136	776	G - 7 / 2
22	7961	7254	-	G - 7 / 3
21	7964	7257	1440	G - 7 / 3
20	7970	7262	1441	G - 7 / 3
19	8037	7319	1832	G - 8
18	8046	7329	1835	G - 8
17	8056	7336	1838	G - 8
16	8076	7355	1846	G - 8
15	8082	7359	1848	G - 8
14	8102	7375	1874	G - 8
13	8108	7381	1876	G - 8
12	8120	7392	1914	G - 8
11	8128	7399	1915	G - 8
10	8134	7404	1917	G - 8
9	8140	7411	1918	G - 8
8	8144	7414	1920	G - 8
7	8192	7454	2101	G - 9
6	8198	7458	2103	G - 9
5	8206	7466	2105	G - 9
4	8264	7515	2145	G - 10
3	8273	7524	2148	G - 10
2	8287	7534	2156	G - 10
1	8294	7540	2159	G - 10

Table 2 - Analysis SARA Guafita crudes

Sample	Sand	Depth	API	Saturated	Aromatics	Resins	Asphaltene
GF-5X	G7	7295	29,5	52,94	31,56	10,29	5,21
GF-21	G8	6119	29,8	55,44	31,37	10,37	2,82
GF-29	G9	7448	29,5	53,46	33,15	11,12	2,27
GF-29	G9	7533	29,5	53,36	31,46	12,67	2,5
GF-13X	G10	7647	30,3	53,12	31,25	11,57	3,67

**Table 4 - Mineralogical Characterization
of GF-134D Rock**

Depth	Quartz	Clay	Pirite	Siderite
7421	75	19	4	2

Table 7 - Petrophysical Data GF-26 Nucleus

Well	Sand	Depth, ft	Water Content, %	Porosity, %	Ka, md
GF-26	G-9	7426	29-35	26	2013

Table 6 - Petrophysical Data GF-134D Nucleus

Sample	Sand	Depth, ft	Porosity, %	Vp, cc	Ka, md
1		8077	37	19.7	7083
2	G-8	8132	35.2	19.9	327
3	Clay-Lutite	7992		3	

Table 8. Liteden 4000 Typical Parameters

Property	Value
Specific gravity, g/cc	0.38
Collapse pressure, psi	4000
Average particle size, micron	36
Thermal stability, (°C)	600
Alkalinity, meq/g	Máx. 0,5
Dielectric constant @ 100 MHz	1.2 -1.8

Table 5 - Grain size statistical data, G-8

Result: Analysis Table								
ID: arena G-8 (8132')	Run No: 3		Measured: 27/8/99 09:55					
File: SANDRA	Rec. No: 212		Analysed: 27/8/99 09:55					
Path: C:\SIZERS\DATA\			Source: Analysed					
Range: 300 mm	Beam: 14.30 mm	Sampler: MS7	Obs': 30.9 %					
Presentation: 3KHF	Analysis: Polydisperse		Residual: 0.681 %					
Modifications: None								
Conc. = 0.0387 %Vol	Density = 1.000 g/cm^3		S.S.A.= 0.1664 m^2/g					
Distribution: Volume	D[4, 3] = 149.67 um		D[3, 2] = 36.05 um					
D(v, 0.1) = 61.81 um	D(v, 0.5) = 135.93 um		D(v, 0.9) = 244.72 um					
Span = 1.346E+00	Uniformity = 4.555E-01							
Size (um)	Volume Under%	Size (um)	Volume Under%	Size (um)	Volume Under%	Size (um)	Volume Under%	
0.49	0.00	3.60	2.34	26.20	6.75	190.80	78.03	
0.58	0.03	4.19	2.77	30.53	6.89	222.28	86.25	
0.67	0.10	4.88	3.20	35.56	7.04	258.95	91.77	
0.78	0.19	5.69	3.60	41.43	7.31	301.68	95.16	
0.91	0.29	6.63	3.97	48.27	7.88	351.46	97.07	
1.06	0.42	7.72	4.30	56.23	8.95	409.45	98.09	
1.24	0.56	9.00	4.61	65.51	10.84	477.01	98.64	
1.44	0.72	10.48	4.91	76.32	14.11	555.71	99.01	
1.68	0.89	12.21	5.23	88.91	19.60	647.41	99.37	
1.95	1.10	14.22	5.57	103.58	28.11	754.23	99.74	
2.28	1.33	16.57	5.92	120.67	39.64	878.67	100.00	
2.65	1.61	19.31	6.26	140.58	53.06			
3.09	1.95	22.49	6.54	163.77	66.82			

**Table 9 - Estimated Fluid Volumes
Needed to Drill GF-136**

Circuit	Total, barrels
Surface tank	688
7" casing	298
6 1/8" hole	46
Total Volume Interval III (directional section)	1032

Table 10 - Components Used in Formulation of INTEFLOW®-2000

INTEFLOW®	It is a mixture of biodegradable liquid surfactants. It is used in conjunction with diesel, or another oil, and water to form an emulsion.
VISCOSIFIER	It is used to maintain the emulsion rheological properties. It must be stable to high temperatures. Commonly, either xantham gum rubber or a polymer of low to medium molecular weight is used
FILTRATE CONTROLLER	It is used to control filtrate; a starch stable to high temperatures is generally used.
BIOCIDE	It is used to prevent the growth of bacteria in the fluid that may reduce the concentration of surfactant and polymer, and affect the stability of the fluid.
MONOETHANOLAMINE (MEA)	A solution used to maintain the alkalinity of the system.
LITEDEN	Hollow glass bubbles and a density reducing agent. It can lower fluid density by as much as 1-2 ppg, and may prevent fluid invasion in permeable zones. It may also reduce or eliminate pipe sticking due to differential pressure. Figure 7 shows particle si
POTASSIUM CHLORIDE (KCl)	This salt provides a source of potassium ions to inhibit the swelling of clays and their dispersions.

Table 11 - INTEFLOW®/LITEDEN Fluid Properties

Property	Value
Density, ppg	7.0 – 7.1
FV, s/qt	40-60
PV, cP	25-30
YP, lbs/100 ft ² :	15-20
Gel, lbs/100 ft ²	8/9
6 and 3 RPM readings	8/6
pH	9.0-11.0
Filtrate, cc/30 min.	<4

Table 12 – Recommended Solids Control Equipment.

Description	Qty.	GPM max.	Mesh	Notes
			180	Continued mesh inspection
Lineal shaker	3	600	180	Efficiency checks
			180	Efficiency checks
2-12" cones Desander 10-4" cones Desilter Vibrator	1	600	200 mesh	Operate intermittently with a pressure between 36 and 40 psi. Continued mesh inspection
High RPM centrifuge	1	50	3000 RPM	Operate intermittently to free
Low RPM centrifuge	1	50	1800 RPM	fluid from very fine solids

Tabla 13 - INTEFLOW/LITEDEN Properties Prior to Commencing Drilling

Sample taken at 7227 ft.	Inlet	Inlet	Inlet
Density, ppg	7.4	7.3	7.1
FV, sec	55	65	68
VP, cp	21	25	24
YP, lb/100 ft ²	15	15	12
API filtrate, cc/30min	1.5	1.5	1.5
Oil, from retort, %	64	65	66
Oil/water ratio	64/36	65/35	66/34

Table 14 - INTEFLOW/LITEDEN Properties During Drilling of GF-136D

Sample	Inlet	Inlet	Inlet	Final
Depth, ft	7371	7416	7566	Tank 1
Density, ppg	7.3	7.1	7.1	7.5
Temperature, °F	90	94	100	87
FV, sec/qt	45	68	67	45
Gel, 10 min, lb/100 ft ²	6	5	3	5
PV, cp	25	24	22	15
YP, lb/100 ft ²	15	12	7	10
pH	10.2	10..2	10,5	10,6
Solids, %	4	6	7	5
Oil/water ratio, %	66/34	66/34	65/32	56/44
API filtrate, cc/30min	4.5	3.5	4,5	1,5

Appendix G

The Potential Use of Hollow Glass Spheres in Dual Density Drilling

by

**Liliana Vera and Hans Juvkam-Wold
Texas A&M University
December 2000**

THE POTENTIAL USE OF HOLLOW GLASS SPHERES IN DUAL DENSITY DRILLING

By

Liliana Vera and Hans Juvkam-Wold

Texas A&M University

December 2000

Contents

- Dual Density Drilling – what is it?
- Static Wellbore Pressure Profiles
- Pressure Profiles while Circulating
- Hydraulics Calculations
- U-Tubing
- Transition from single to dual density

Dual Density Drilling – what is it?

Dual Density Drilling is a process that allows the use of higher mud weights in the wellbore, below the mudline, with a resulting reduced annulus pressure at the mudline. The reduction in wellhead pressure can be achieved by pumping the mud from the seafloor up to the surface, by using gas lift to assist in returning the mud to the surface, or, as proposed in this report, by injecting low-density, hollow glass spheres into the return mud in the marine riser at or near the mudline.

The primary benefits of dual density drilling are:

- A reduction in the number of casing strings required
- Increased probability of reaching total depth
- A larger diameter production string
- Lower cost
- Safer drilling operations in that larger kick and trip tolerances can be achieved
- A positive riser margin can be maintained at all times if the wellhead pressure is maintained at seawater hydrostatic pressure.

Figure 1 demonstrates the basic concepts of dual density drilling using hollow glass spheres. Heavy mud is circulated down the drillpipe, through the bit and up the wellbore annulus to the mudline. At this point hollow glass spheres (HGS) are injected into the marine riser to reduce the density of the return mud to a value approaching that of the density of seawater.

Static Wellbore Pressure Profiles

The green line in **Fig. 1** shows the static annulus pressure under conventional drilling conditions. The pressure increases linearly with depth from the surface to the bottom of the hole. The blue line shows the static pressure in the annulus

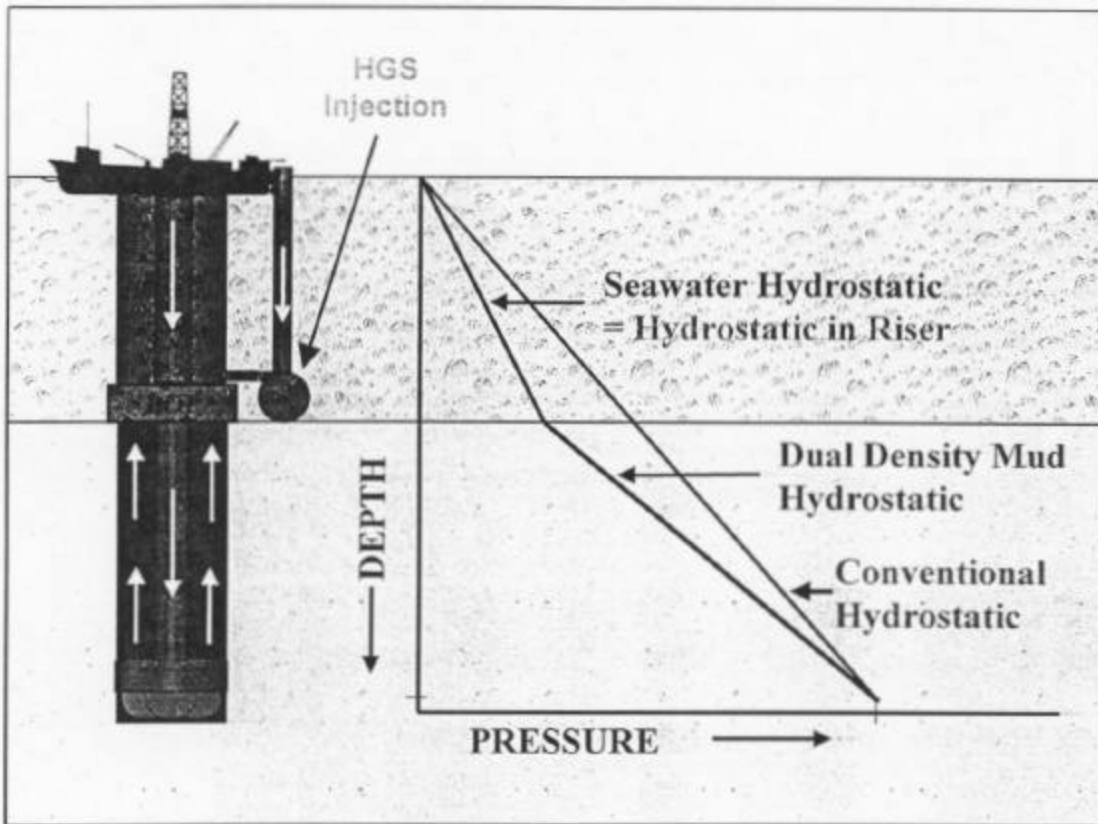


Fig. 1 – Dual Density Drilling Concept - Static Annular Pressure Profiles.

under dual density drilling. It may be seen that the pressure in the annulus is the same at the bottom of the hole, but is lower everywhere else in the case of dual density drilling. In the most common configuration of dual density drilling the pressure at the top of the annulus is equal to seawater hydrostatic pressure. When hollow gas spheres are used to achieve this configuration, the hydrostatic pressures inside and outside the marine riser are equal at all depths.

Figure 2 shows the static wellbore pressures in dual density drilling. Pressures inside and outside the drillstring, below the mudline are equal. The pressure inside the drillpipe, as shown in red, continues linearly above the mudline, and reaches zero (atmospheric pressure) at a point indicated as "Static Fluid Level in the Drillpipe." This point is defined by the hydrostatic head in the drillpipe, above the mudline, being equal hydrostatic head in the seawater column.

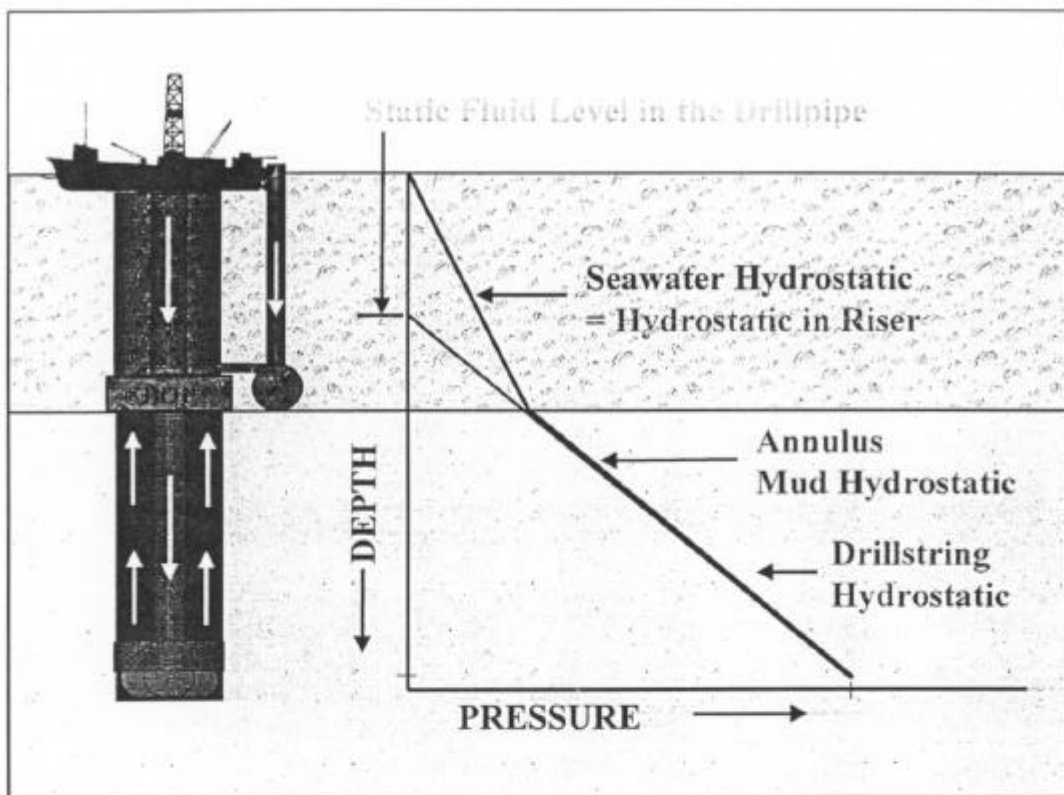


Fig. 2 – Static pressure profiles in dual density drilling.

Pressure Profiles while Circulating

A typical pressure profile while circulating is shown in Fig. 3. The bottomhole pressure increases slightly above the static pressure because of friction in the annulus, below the mudline. This annular friction also causes the pressure in the drillstring to increase by the same amount. The pressure drop across the bit and the friction in the drillstring further increase the pressures everywhere in the drillstring as shown. There is also a slight increase in pressure at the mudline because of friction inside the marine riser. This change is only a few psi for a large-diameter riser.

The pressure drop across the bit is indicated as ΔP_{BIT} in Fig. 3. If the circulation rate is decreased then the standpipe pressure will decrease. This is because of reduced friction pressure and reduced pressure drop across the bit. At some

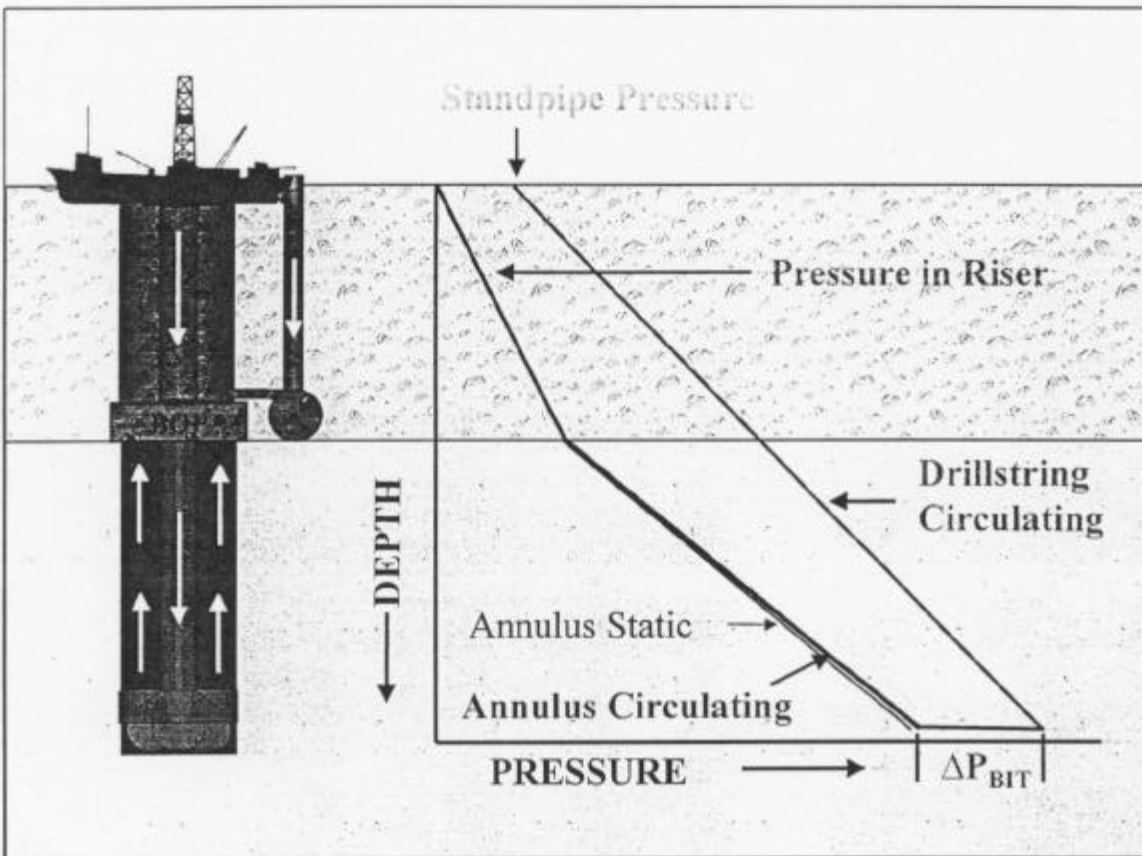


Fig. 3 – Circulating pressure profiles in dual density drilling.

point, if the circulation rate is reduced sufficiently, the standpipe pressure will drop to zero. This may occur at a rate of several hundred gallons per minute, depending on mud rheological properties, wellbore geometry, water depth, concentration of hollow glass spheres and nozzle flow area. Further decreases in circulation rate will cause the fluid level in the drillpipe to drop, and, as the circulation rate approaches zero, the wellbore pressure profile will approach the static profile shown in Fig. 2.

More examples of pressure profiles are shown in subsequent sections.

Hydraulics

Hydraulics calculations in dual-density drilling differ from those in the conventional case because we are now dealing with two mud systems in the annulus. The static pressure gradient in the marine riser, from the surface to the seafloor, is the same as the seawater pressure gradient, whereas a heavy mud pressure gradient is applied from sea floor to total depth. The required mud density below the mudline (ρ_{mud}) depends on the well depth (D), the water depth (D_w), the density of the seawater (ρ_{sw}) and the desired bottomhole pressure (BHP). This mud density can be determined through the following equation:

$$\rho_{mud} = \frac{BHP - 0.052\rho_{sw}D_w}{0.052(D - D_w)} \quad \dots \dots \dots \text{Equation 1}$$

Circulating pressures in the wellbore can be calculated using any of the conventional rheological models. **Figure 4** shows pressure profiles for a 19.17 ppg mud for various concentrations of hollow glass spheres. Pressure inside the drill string increases with depth mainly because of hydrostatic pressure increase. Pressure loss across the bit is present only when circulating. The Power-law model was used in hydraulics calculations for these pressure profiles.

Four different HGS concentrations, 0%, 36%, 50% and 66% are considered; 66% is the concentration required to reach seawater density for this very heavy mud. In general, increasing spheres concentration reduces pressure at the sea floor level. For instance, at 0% the pressure at this level is 9,971 psi, with 66% it is reduced to that of seawater hydrostatic pressure; meaning a reduction in pressure of about 5,500 psi. Note how an increase in spheres concentration decreases the pressure, not only in the riser, but everywhere in the system.

Hollow glass spheres mud behaves similarly to conventional mud; viscosity increases with the addition of solids, likewise does frictional pressure loss. **Figure 5** illustrates this fact. Only the annular sector where the HGS fluid is circulating is considered.

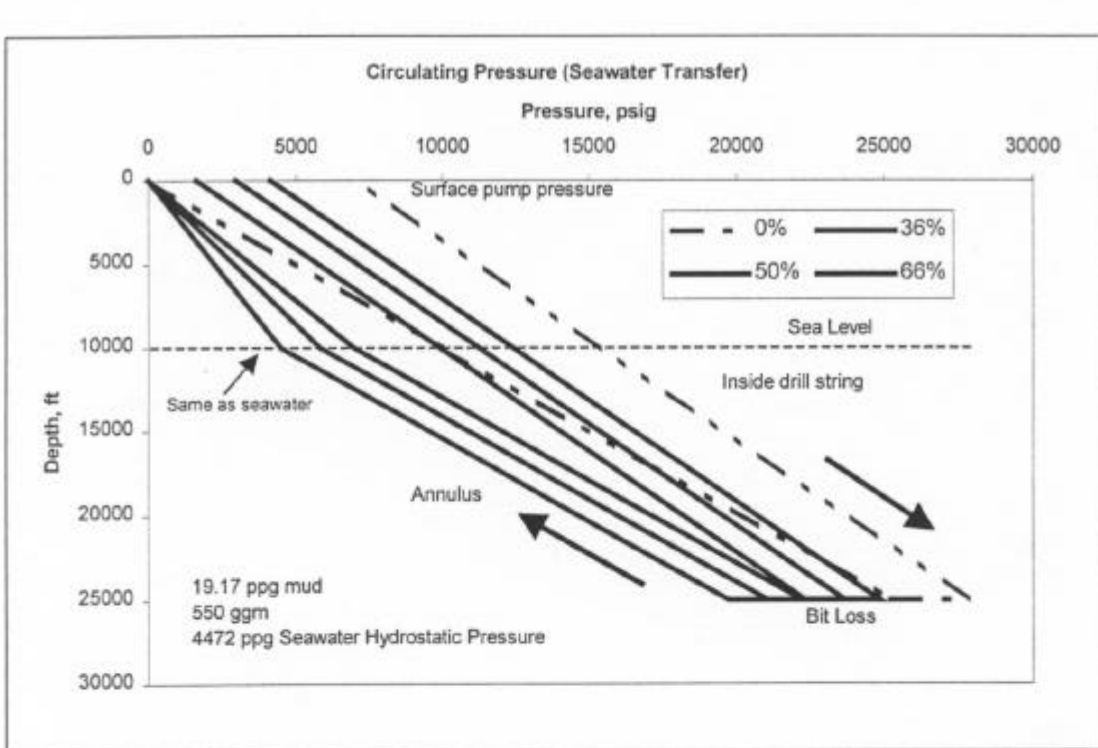


Fig. 4 – Circulating Pressure, 19.17 ppg and 10,000 ft of Water Depth.

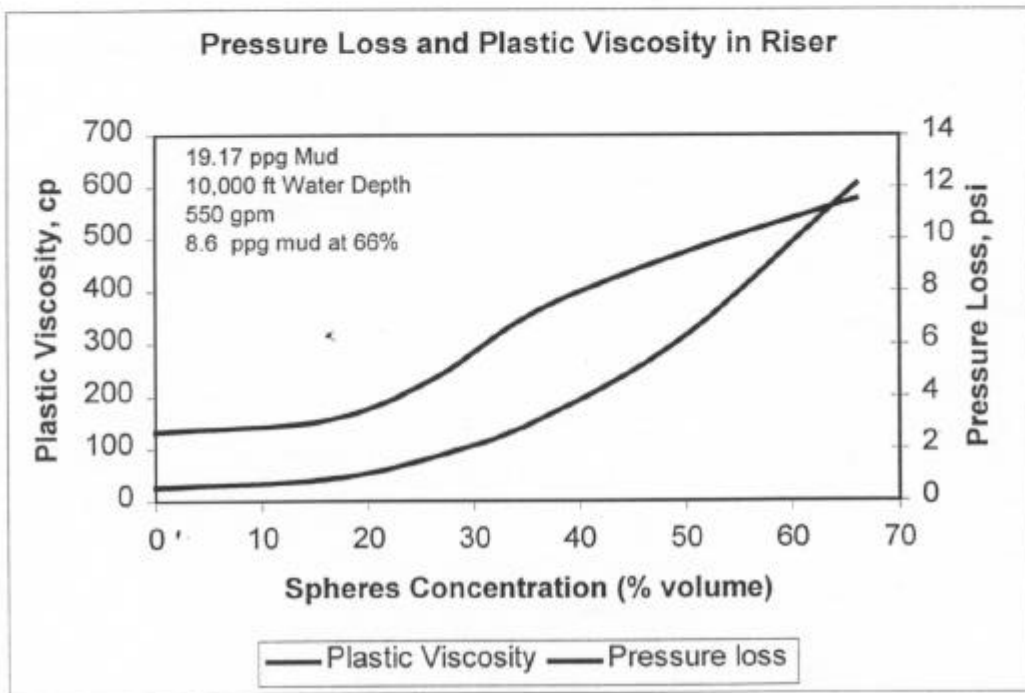


Fig. 5 – Pressure Loss and Plastic Viscosity in Riser.

Note that a significant pressure loss in the riser is not achieved. Increasing the viscosity from 27 to 605 cp results in an increase in friction of only 9 psi for a 19.17 ppg mud. Further research is required in this area since viscosity also affects HGS separation from de mud. This operation has to be carried out every time the mud returns to the surface in order to be able to pump the heavier mud to the bottom of the well and the spheres to the bottom of the riser.

U-Tubing Effects

In dual density drilling the effective hydrostatic pressure inside the drill string is higher than that in the annulus. For this reason, every time the surface pump is shut down, the mud level inside the drill string will drop by free fall or u-tube effects until equilibrium is reached. Free fall occurs during pipe connections, before pipe trips out of the hole, or any other time the rig pump is stopped.

Figure 6 shows the wellbore as a U-tube, and demonstrates the condition after u-tubing is complete and hydrostatic equilibrium has been established.

The maximum drop in fluid level inside the drillpipe (h_{max}), depends on the mud density (ρ_{mud}), the seawater density (ρ_{sw}) and the water depth (D_w). If the pressure at the sea floor level is kept equal to seawater hydrostatic pressure, then the maximum mud level drop (h_{max}) can be calculated according from the following equation:

$$h_{max} = D_w \frac{(\rho_{mud} - \rho_{sw})}{\rho_{mud}} \quad \dots \dots \dots \text{Equation 2}$$

Figure 7 shows the effect of mud density on maximum mud level drop. For this case, both systems consider seawater density at the sea floor. Larger mud level drops will result at higher mud densities, and longer times are required to reach equilibrium. Longer times are also required to fill up the drillpipe after circulation is reestablished. In **Fig. 7**, free-fall occurs until equilibrium is reached (Points A

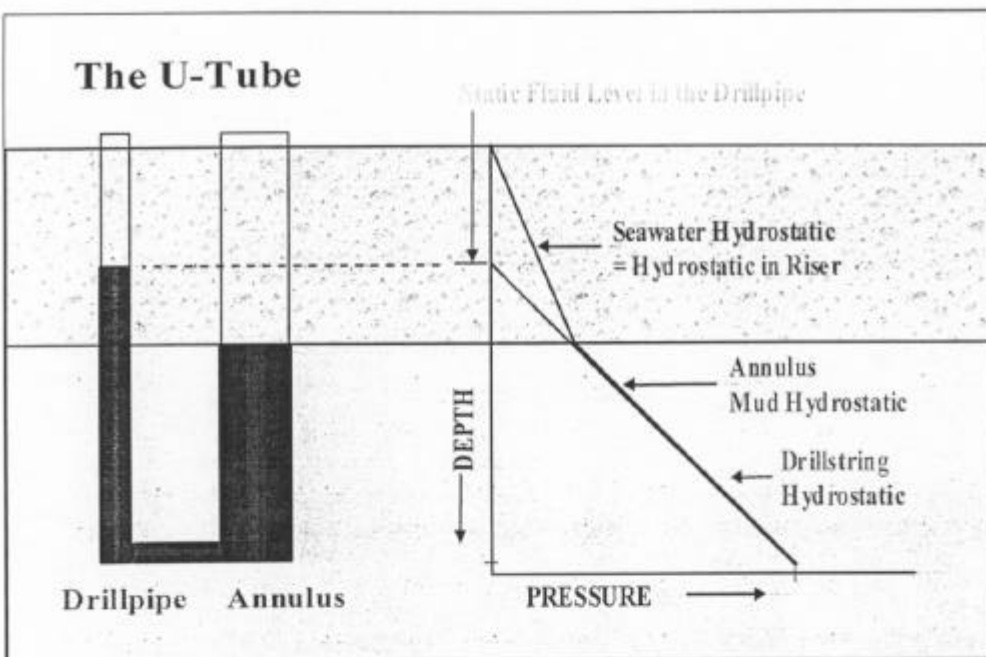


Fig. 6 – At equilibrium the hydrostatic head due to mud in the drillpipe is balanced against the the seawater hydrostatic head in the water column.

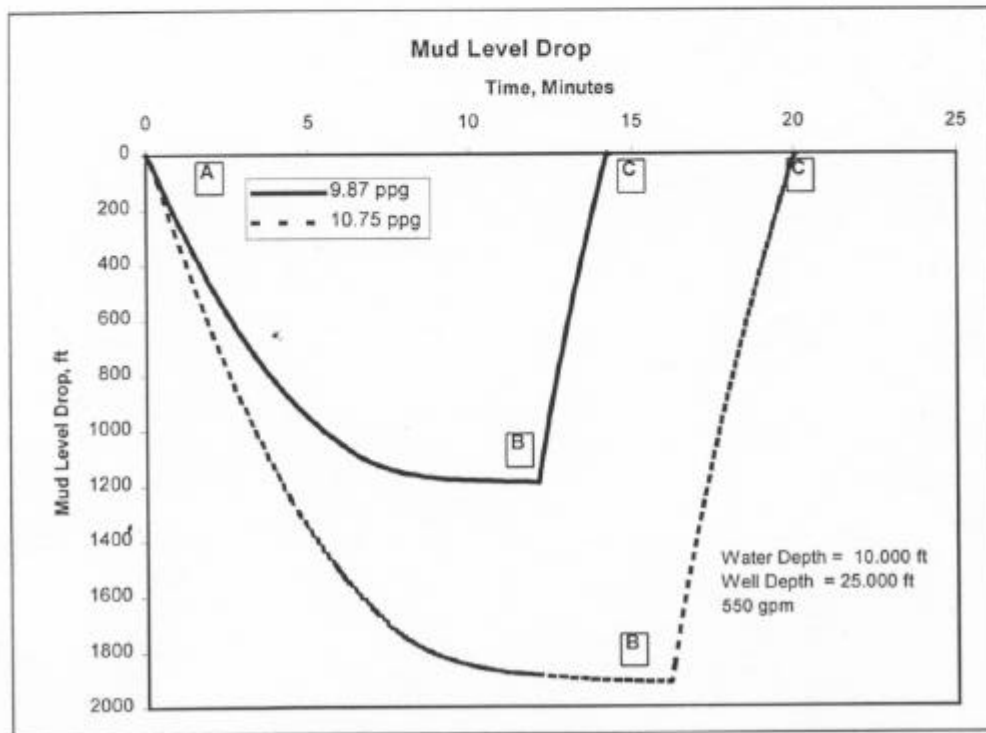


Fig. 7 – Drop in mud level vs. time when circulation stops and restarts.

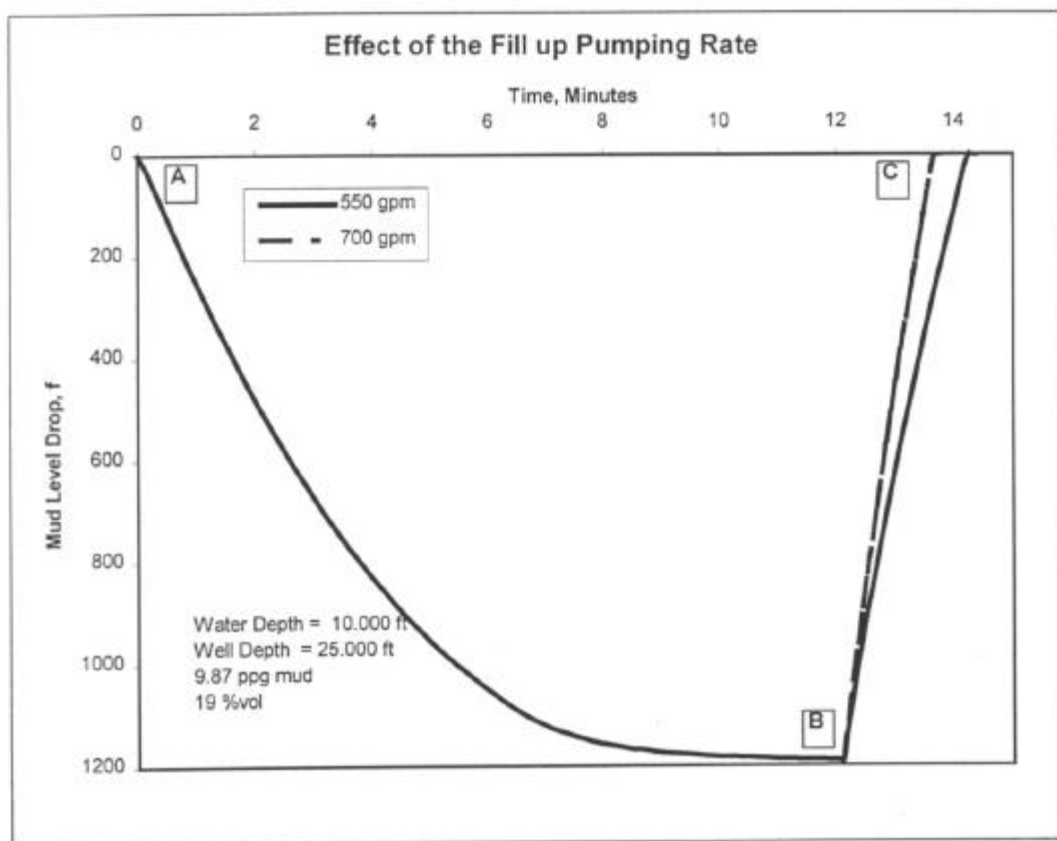


Fig. 8 – Effect of the Fill up Pumping Rate

to B). When the pump is shut down the u-tubing rate is highest, but then the rate gradually decreases and eventually becomes zero. At point B the pump is restarted and drillpipe fill-up occurs between points B and C.

The total time required to fill up the drillpipe is also a function of the mud pumping rate. In Fig. 8, two pumping rates are considered, 550 gpm and 700 gpm. Fill-up occurs between points B and C. The mud density for these cases is 9.87 ppg, the sphere concentration required to reach seawater pressure at the mudline is 19% and the maximum fluid level drop is 1,200 ft, approximately.

Mud density also influences the u-tubing rate vs. time after the pump is shut down. Figure 9 shows a plot of flow rate vs. time. Two mud densities, 9.87 and 10.75 ppg. are considered. It takes longer time to complete the whole

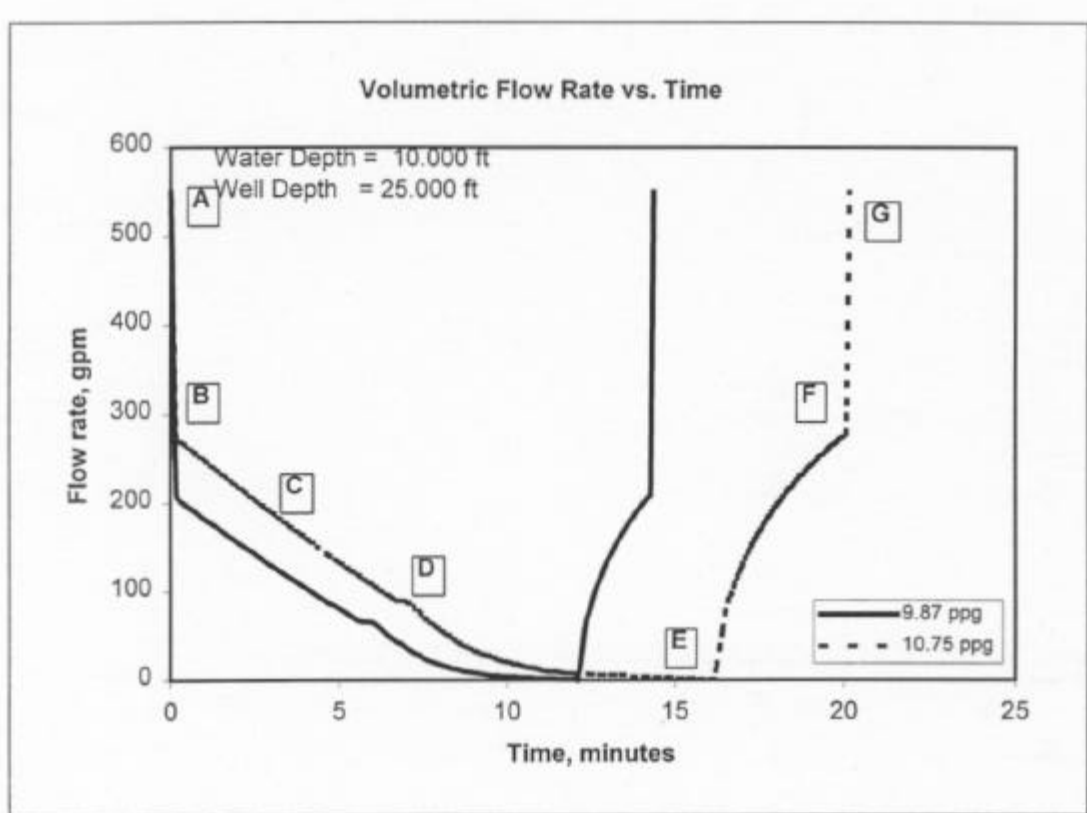


Fig. 9 – Volumetric Flow Rate Vs. Time (Two mud densities are considered).

process for the denser fluid. Additionally, several stages can be differentiated in this plot. Point A represents the initial pumping rate, before the rig pump is shut down. From A to B the fluid rapidly slows down. Point B indicates zero standpipe pressure, which means a maximum free fall rate for the system under consideration. From this point onward, the flow rate decreases more or less linearly until the flow condition changes from turbulent to laminar flow inside the drill pipe (Point D). After that it decreases gradually and finally reaches zero when equilibrium is established (Point E).

From Point E to G, the fill-up part is depicted. Note how the return rate converges to the maximum free fall rate, Point F. Hence, in order to fill up the drillpipe completely, the rig pump circulation rate must be higher than the maximum free fall rate. Higher rig pump circulation rates means shorter times to fill up the pipe (see Fig. 10).

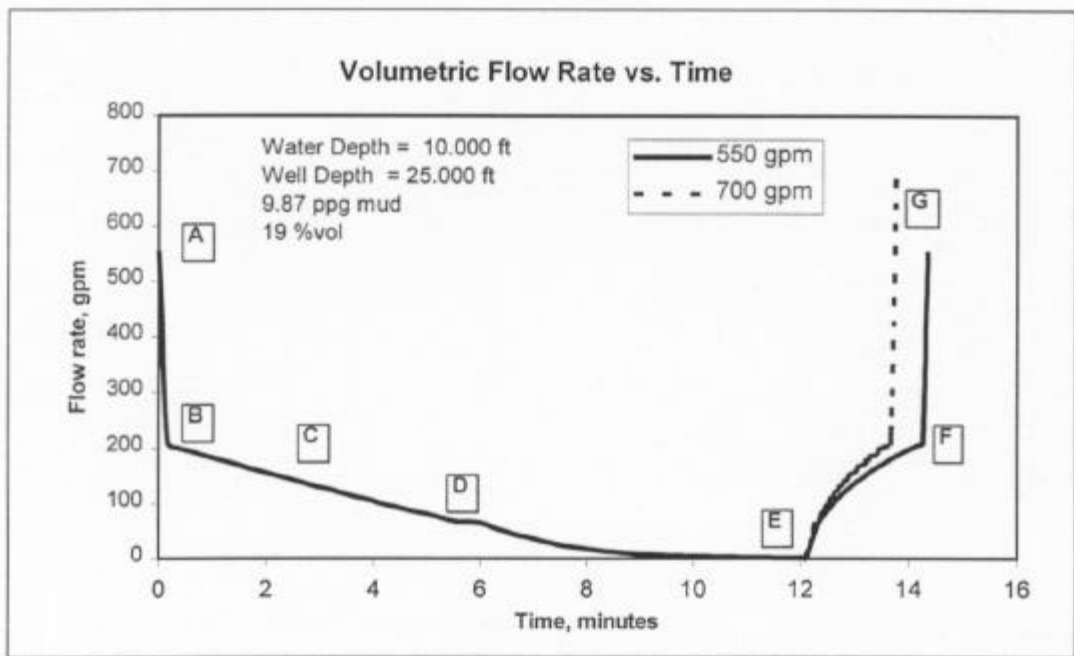


Fig. 10 – Volumetric Flow Rate Vs. Time for two different pumping rates.

The u-tubing effect is also important during pipe connections. Similar plots to those presented above have been generated to analyze mud level drop, pumping rate and pit gain. Two cases have been considered, a connection that last two minutes and one that last five minutes. The results are shown in **Fig. 11**. From Points A to B the mud level drop occurs. For the two cases considered, a two-minute connection and a five-minute connection, the curves follow the same trajectory from A to B. For the fill-up part (going from B to C) the curves are almost parallel. Of course, it takes longer to fill up the pipe when the connection has lasts longer. The mud density for this example is 9.87 ppg and the spheres concentration needed to reach seawater density is 19%.

During a connection, or other temporary pump shutdown, the flow rate profile does not show all the stages described in **Fig. 9**. It can be seen, for example, that the rate does not go to zero. Whether we reach laminar flow or not depends on the time the connection lasts. In general, the curves follow the

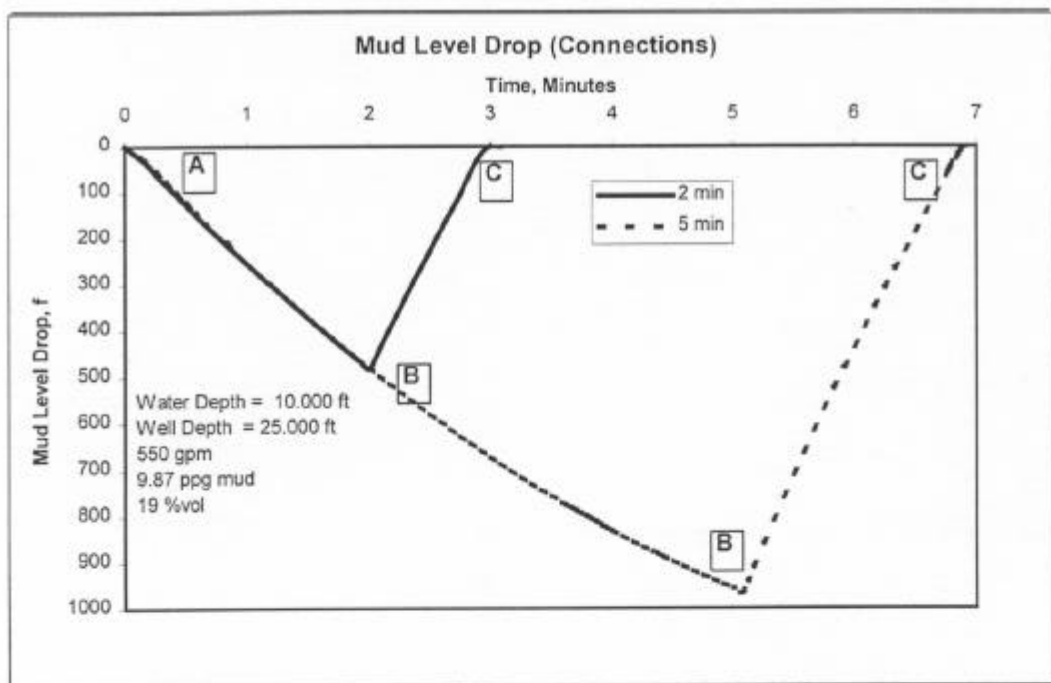


Fig. 11 – Fluid level drop vs. time during connections.

same behavior, as seen in Fig. 12. In this case the rate drop goes from Point A to Point B, while the fill-up takes place between Points B and C.

Figure 13 presents the pit gain during the connections. From A to B the pit gain due to u-tubing occurs as all the mud that u-tubes out of the drillpipe shows up as pit gain. From B to C, we have the pit losses due to drillpipe fill-up. Ideally, the volume gained is equal to the volume lost.

Other factors than the ones discussed above also influence u-tubing rates, such as mud viscosity, drillpipe ID, nozzles size and well depth below the mudline.

In the above discussion it was assumed that drilling was already being performed using hollow glass spheres. In most cases it was also assumed that the density of the return mud was reduced all the way to seawater density. It should be noted that considerable benefit from the use of dual density drilling can be achieved by partial reduction in the mud density. It is not always

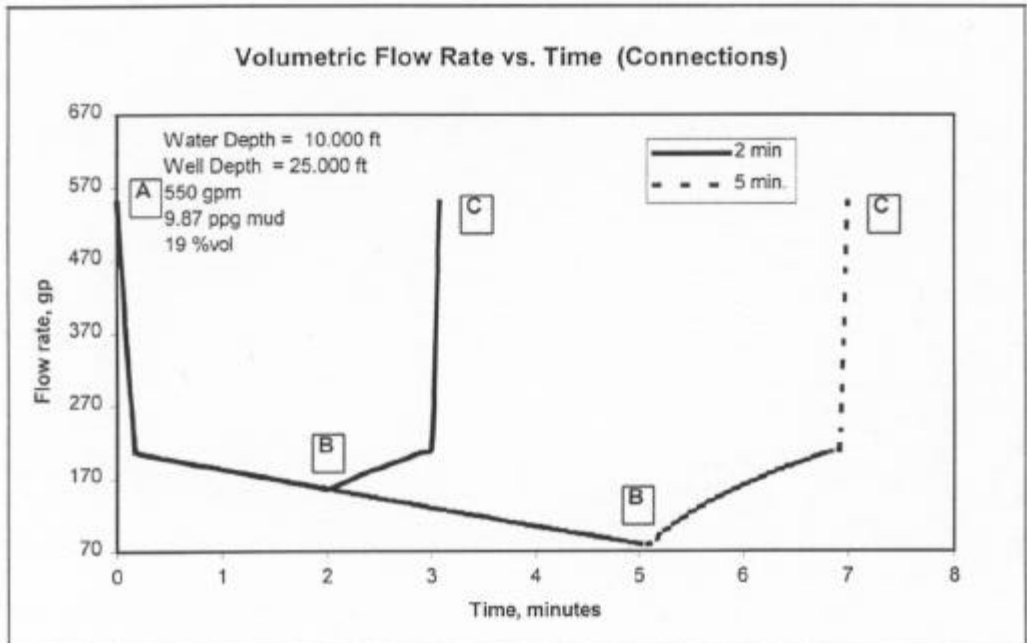


Fig. 12 – Flow Rate Vs. Time (Connections).

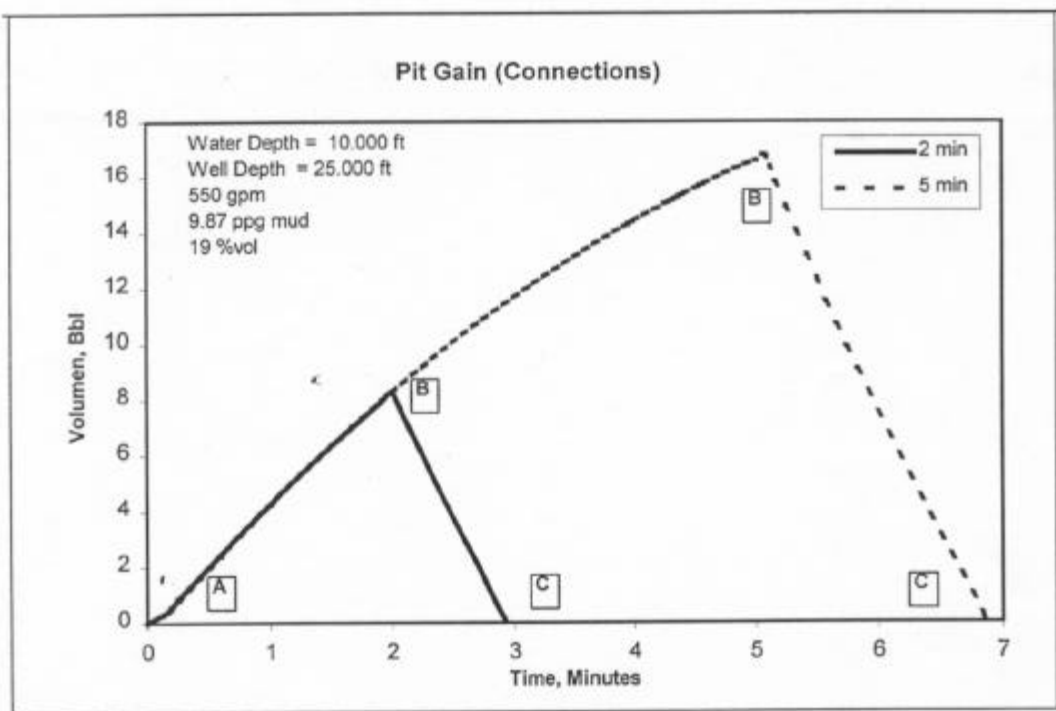


Fig. 13 – Pit Gain and loss during connections.

practical, or even necessary, to reduce the density all the way to seawater density.

The transition from drilling conventionally to switching to dual density drilling is considered in the next section.

Transition From Single to Dual Density

The transition from conventional drilling to dual density drilling is fairly straightforward from a hydraulics point of view. The pressure in the riser will decrease gradually at a rate that depends on a number of factors. **Figure 14** shows the projected reduction in pressure at the mudline when drilling with 14 ppg mud and circulating at 500 gpm. Assumed water depth is 10,000 ft, riser ID is 20 in, drillpipe OD is 6 5/8 in. Concentrations of HGS from 20% to 50 % are considered. It takes three to four hours to fill the riser with the lower density mud. If the mud circulation rate is doubled, the time to fill the riser, of course, is cut in half.

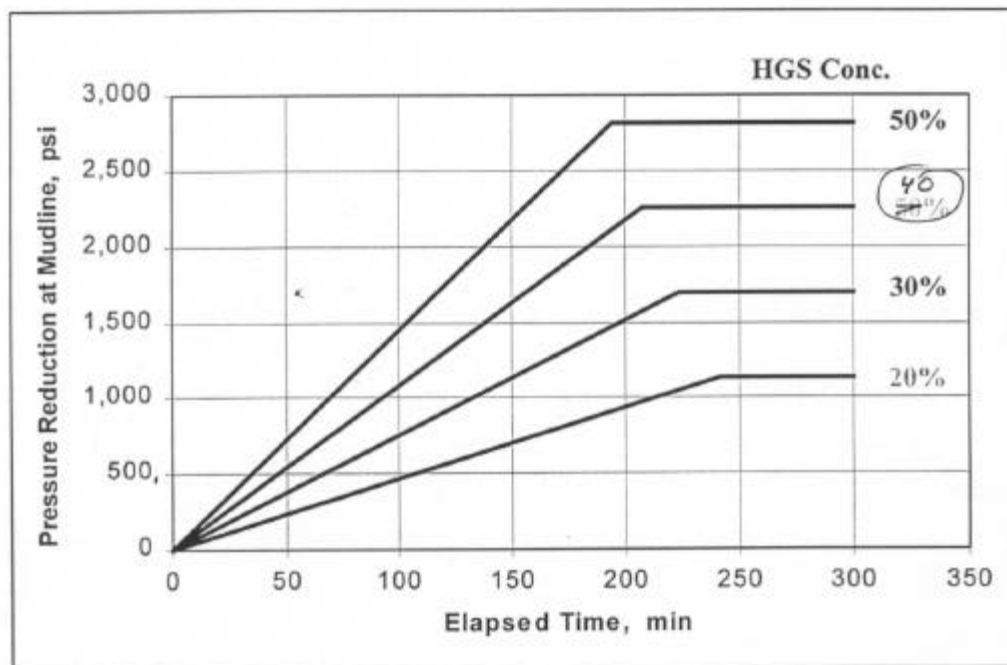


Fig. 14 – Reduction in pressure at the mudline while the riser is filling up with hollow glass spheres.

Appendix H

Impact of Hollow Glass Spheres on Wettability

by

Cementing Solutions, Inc.
Houston, Texas

Appendix H

Impact of Hollow Glass Spheres on Wettability Cementing Solutions, Inc. Houston, Texas

EXPERIMENT NO. 1

Two synthetic drilling fluids were prepared with conventional products (viscosifiers and weighting materials). One mud was tested as is and the other included 16% high-strength HGS. Both fluids were conditioned and placed in the wettability testing device and allowed to set static for 1 minute. (This device is a modified rotational viscometer that measures the film thickness of the fluid on a static sleeve.) The mud was then removed and a seawater solution placed in the fluid cup. Rotation was initiated at 300 rpm at 80°F and the relative film thickness was measured. **Figure 1** shows the data collected. Relative film thickness was used because we did not have a good calibration standard for thickness. The data indicate that drilling mud with HGS was more difficult to remove with a seawater flush than a drilling mud without HGS.

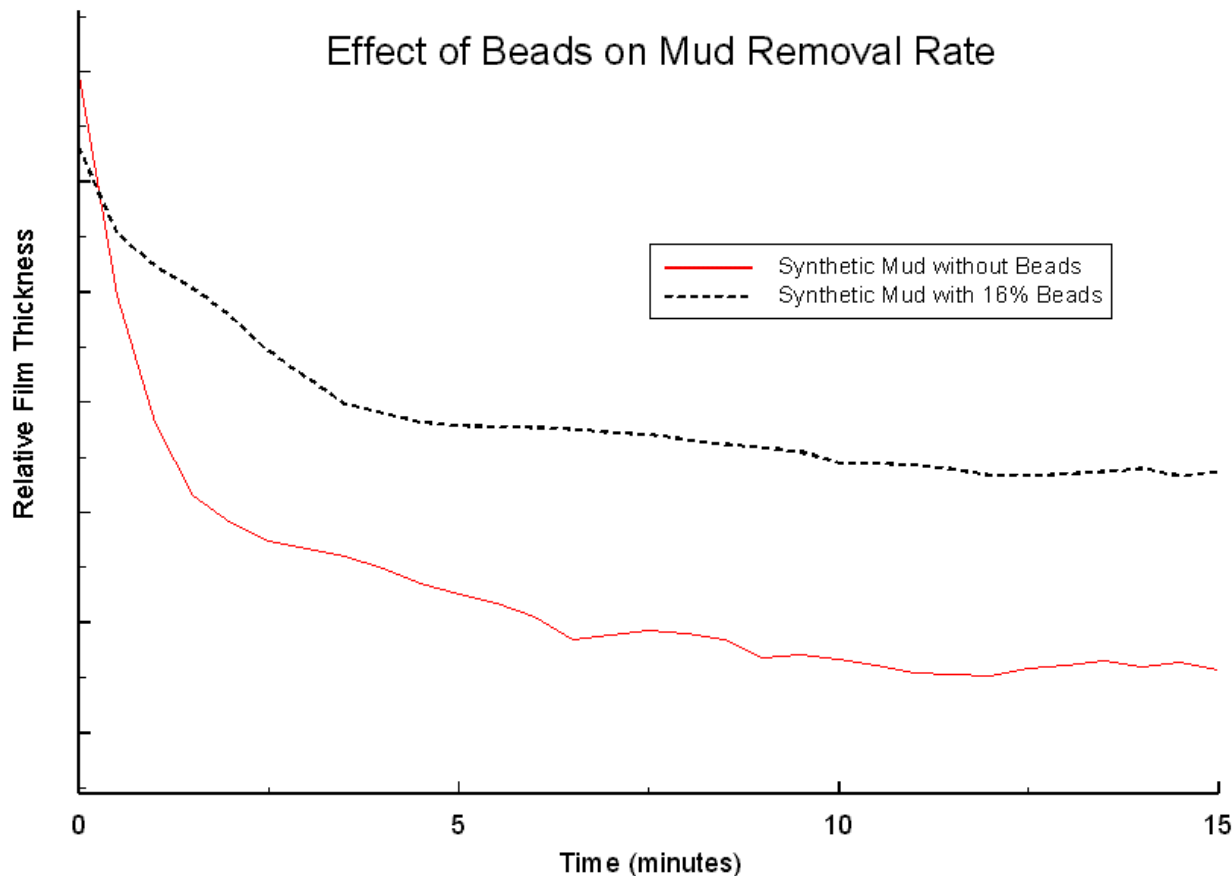


Figure 1. Removal of Mud Containing HGS

EXPERIMENT NO. 2

Drilling mud without HGS was used in this experiment. Two spacers were designed. Both spacers consisted of salt water, mixing aid, and spacer mix. The second spacer also included 16% by volume HGS. The mud was placed on the testing sleeve and bob for 5 minutes to allow the mud film to form (in a static condition). The mud was replaced with the appropriate spacer. The rotational viscometer was run at 300 rpm and the film thickness measured with time (see **Figure 2**). These results indicated that spacer with HGS cleaned the synthetic mud faster and better than spacer without HGS.

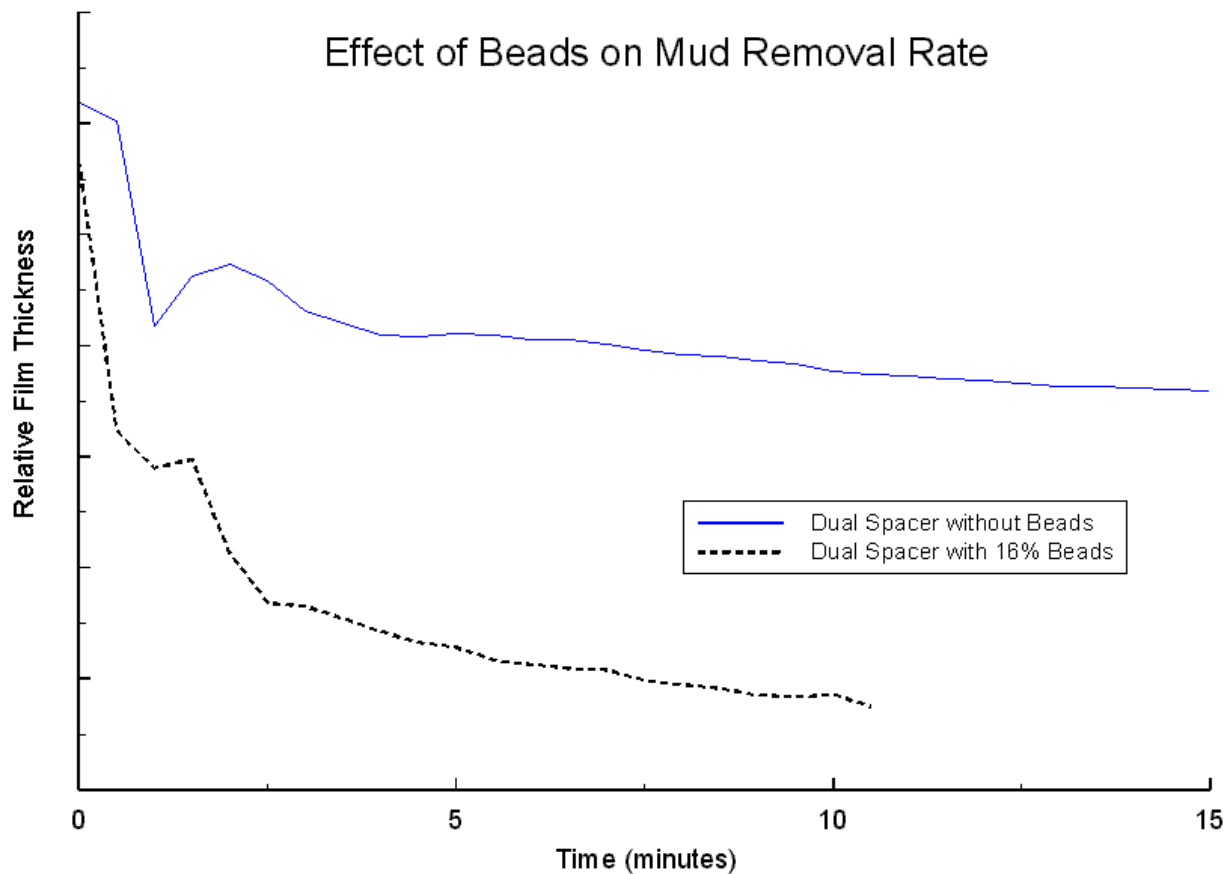


Figure 2. Mud Removal by Spacer Containing HGS

ELECTRONICS

The electronics use a high frequency signal to measure the complex impedance between two electrodes in a conductive solution. Experiments demonstrate that an oil film thickness on the electrodes produces changes in complex impedance. The electronic hardware measures the current and relative phase of the current across two electrodes from which the film is being removed. The electronics diagram is shown in **Figure 3**.

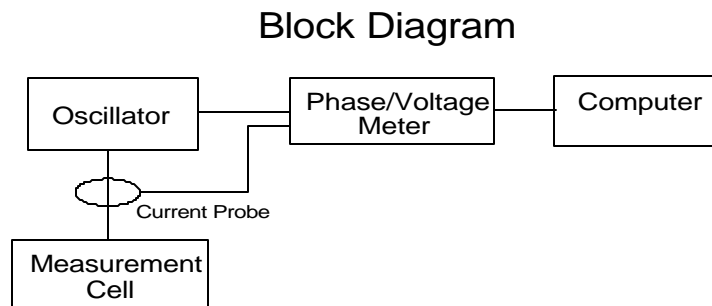


Figure 3. Electronics for Measuring Film Thickness

CHANDLER WETTABILITY TEST APPARATUS

The experimental cell is clamped onto the stationary housing of a rotational viscometer. A locking sleeve is first placed on the viscometer; then the lower part of the device is threaded onto the sleeve. This causes the sleeve to tighten onto the viscometer. The fluid level rises to the two holes in the rotating sleeve. Rotation of the sleeve causes shear fluid forces between the inner sleeve and the electrodes 1 and 2. This shear causes the oil on the surfaces to be removed over time. The inner sleeve is made from a non-conducting material so that the sleeve is not a part of the current path. Experimental design was to make the amount of oil on the surface of the sleeve have minimal effect on the measurement. The electrodes are made from a steel which simulates the well casing. The area behind the electrodes is made from an insulator. Wires from the electrodes pass up into a pair of holes, then out from this assembly into a small chamber holding a transformer. The transformer converts the low impedance of the cell into a higher impedance of around 100 ohms. A coaxial cable connects to the electronics which are used to provide a voltage signal and a current signal to a laboratory voltage phase meter. Output of this meter is then digitized and saved in a computer file for later processing. A real-time approximate thickness is always available to monitor the progress of the experiment. The cable connecting the meter to the cell introduces some phase shift. This is calibrated for accurate measurements.

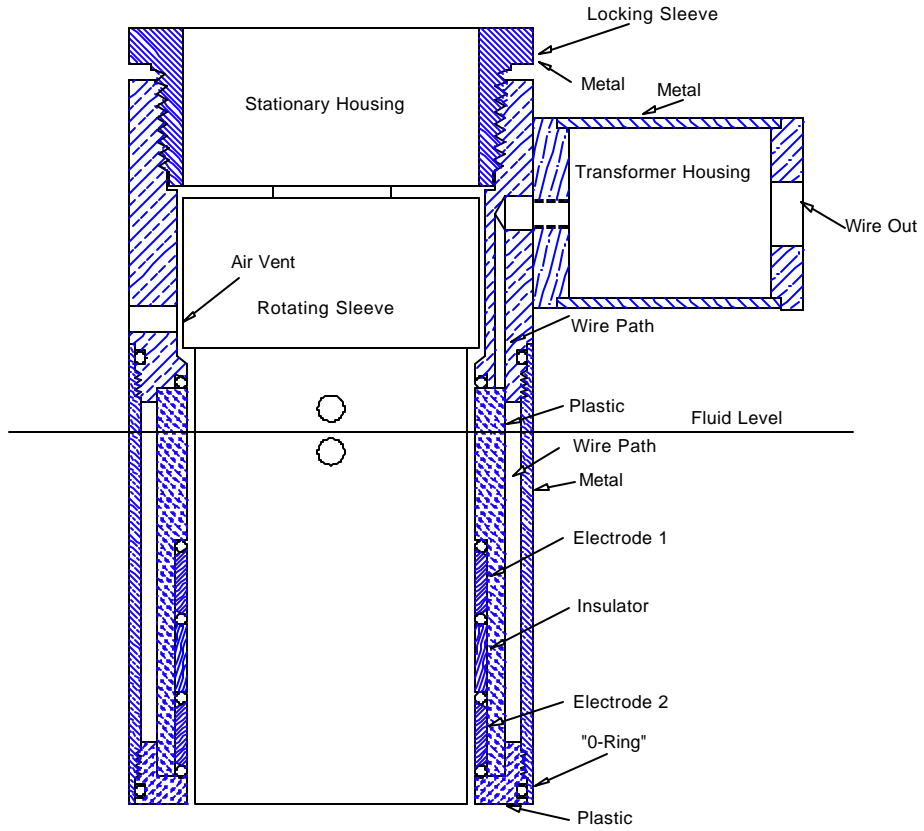


Figure 4. Wettability Cell

The electrical impedance appears as a resistor in parallel with a capacitor when there is oil present on the surface of the electrode. When the plastic sleeve is in the cell, the resistive term and the phase are strongly related to film thickness. The frequency for the measurement signal ranges from 10 kHz to 1MHz. The frequency typically is 400 kHz.

This cell is calibrated by two methods. The first is to measure various resistors ranging from 1 ohm to 5000 ohms across the electrodes. The second is to measure a salt solution while gradually increasing the amount of salt in the solution. The data are recorded and a formula is fit to the data to obtain true phase measurements. True phase is then used to compute the film thickness from a calibration equation developed from actual film thickness measurements.

The measurement is simply to coat the inner surface of the cell below the fluid level with mud. Once the cell is assembled onto the rotational viscometer, the clean-up fluid is placed in a cup and moved up to bring the fluid to the proper level relative to the cell. The rotation is started and the data are recorded.